MENDEL UNIVERSITY IN BRNO
FACULTY OF AGRISCIENCES

PhD thesis

Brno 2016   **MSc. MIGUEL ÁNGEL MERLOS RODRIGO**

Mendel University in Brno
Faculty of AgriSciences
Department of Chemistry and Biochemistry

_____

Matrix assisted laser desorption ionization for characterization of higher molecular thiols in biological samples

PhD thesis
Branch of study: 4106V017 Agricultural Chemistry

Thesis supervisors: Candidate:
RNDr. Ondrej Zitka, Ph.D.   MSc. Miguel Ángel Merlos Rodrigo

Specialist supervisor:
Mgr. Zbyněk Heger, Ph.D.
Ing. Pavlína Adam, Ph.D.

Brno 2016

PROHLÁŠENÍ

Prohlašuji, že disertační práce na téma "Matrix assisted laser desorption ionization for characterization of higher molecular thiols in biological samples" je samostatným autorským dílem podle Autorského zákona. Nositelem majetkového autorského práva je pracoviště a univerzita.

Výsledky práce shrnuté v této závěrečné práci byly financovány z veřejných prostředků z Evropských fondů a státního rozpočtu České republiky. Vzniklé dílo jako celek je chráněno autorským zákonem. Užití tohoto díla pro další šíření a využívání je vázáno na uzavřenou výhradní licenční smlouvu.

Podle § 12 autorského zákona platí, že autorské dílo lze užít jen se svolením autora. Základní informace o práci jsou přístupné všem žadatelům a jsou plně k dispozici (abstrakt). V případě zájmu o využití díla pro další užití (výuka, prezentace, konference, komerční účely) je zapotřebí se řídit licenčními podmínkami.

Licenční podmínky jsou dány licenční smlouvou, kde na jedné straně je pracoviště vzniku díla a děkana nebo rektora univerzity (nositel majetkového autorského práva) a na druhé straně je žadatel o využití výsledku. Realizátor závěrečné práce podléhá licenčním podmínkám, pokud jeho práci chce použít pro jiné účely než ukončení studia. Užití § 29 zákona užití pro osobní potřebu citace není dotčeno.

Disertační práce a výsledky v ní prezentované jsou dílem vypracovaným v Laboratoři metalomiky a nanotechnologií působící na půdě Agronomické fakulty Mendelovy univerzity v Brně a mohou být použity k dalšímu prezentování případně ke komerčním účelům jen se souhlasem vedoucího disertační práce a děkana. V opačném případě se jedná o porušení zákona.

dne …………………………………….

podpis…………………………………….

Tato práce vznikla v rámci CEITEC - Středoevropského technologického institutu s pomocí výzkumné infrastruktury financované projektem CZ.1.05/1.1.00/02.0068 z Evropského fondu regionálního rozvoje.

Acknowledgements

I would like to express my gratitude to all the people who have supported and helped me through my PhD work.

I would like to thank to Professor **Vojtech Adam** and **Rene Kizek** for accepting me into the group and giving me the opportunity for gaining more knowledge and professional experience.

I would like to thank to **Ondrej Zitka** for a valuable advices, help, support and professional guidance in processing of thesis.

I would like to thank to all my colleagues (past and present members of the group) from Department of Chemistry and Biochemistry (DCB), their cooperation and professionalism. I want to give "special" thanks to my inseparable and best friend **Ana Jimenez**, for her patience and for her support.

I would like to thank to **My Family**, who from so far away, they have always helped me.

"As fate would have you left and you did not be with me, but nobody can tear my memories of my heart". **Mommy**†, thank you very much for helped me from so far away, in heaven, in the glory or wherever you are.

"All our science, measured against reality, is primitive and childlike and yet it is the most precious thing we have."

Albert Einstein

Anotace

Mezi nejlépe charakterizované kov-vázající ligandy v buňkách patří fytochelatiny (PC) a metalothioneiny (MT). PC a MT jsou rozdílné třídy molekul, které jsou bohaté na obsah cysteinů. PC jsou enzymaticky syntetizované peptidy, zatímco MT jsou geneticky kódované polypeptidy. Pro analýzu PC, MT a komplexů těžkých kovů bylo v rozdílných studiích využito několik analytických metod. V současné době je metoda, spojující matricí asistovanou laserovou desorpci/ionizaci s hmotnostním analyzátorem doby letu (MALDI-TOF MS), známá pro její snadnou obsluhu a pro využívání levných matric a chemikálií pro přípravu vzorků. Mnohem důležitější ale je, že je tuto metodu lze plně automatizovat. V této studii jsme určili vhodné podmínky pro charakterizaci fytochelatinu PC2 a komplexu Cd-PC2 pomocí MALDI-TOF MS. Dále byly exprimovány geny lidských metalothioneinů *MT2A* a *MT3* klonováním v heterologních organismech (*Escherichia coli*). Dále byl izolován MT2 protein z králičích jater. MT byly purifikovány pomocí rychlé proteinové kapalinové chromatografie (FPLC). Předkládaná práce demonstruje využití MALDI-TOF MS pro charakterizaci různých isoforem MT. Bylo využito také elektrochemických metod pro potvrzení vzniku thiolových komplexů s kovovými ionty. Navíc byl navržen snadno použitelný nástroj pro izolaci MT, využívající jednoduchou a plně automatizovanou elektrochemickou detekční techniku.

Klíčová slova: fytochelatin, metalothionein, MALDI-TOF, těžké kovy, homeostáze kovů, rakovina

Annotation

Among the heavy metal-binding ligands in cells the phytochelatins (PCs) and metallothioneins (MTs) are the best characterized. PCs and MTs are different classes of cysteine-rich, heavy metal-binding molecules. PCs are enzymatically synthesized peptides, whereas MTs are gene-encoded polypeptides. Several analytical methods have been used to analyze PCs, MTs and complexes of metal in different studies. Today, matrix-assisted laser desorption/ionization time-of-flight mass spectrometry (MALDI-TOF MS) is renowned for its extreme ease of operation and requirement of inexpensive matrices for preparation of sample; more importantly, the instrumentation is capable to be fully automated. In this study, the optimal condition for the characterization of PC2 and Cd-PC2 complex by MALDI-TOF MS was determined. The human *MT2A* and *MT3* genes were expressed in heterologous organisms (*Escherichia coli*) by cloning. Further, MT2 protein was isolated from rabbit liver. MTs were purified by fast protein liquid chromatography (FPLC). The present study demonstrates analytical approaches of employing MALDI-TOF MS for characterization MTs. Other electrochemical methods were used for confirmation of thiols complexes with metal. Moreover, easy-to-use instruments for MTs isolation, coupled with simple analytical detection method in fully automatic mode, providing prototype for the construction of sensor was designed.

Key words: Phytochelatin, metallothionein, MALDI-TOF, heavy metal, metal homeostasis, cancer.

CONTENTS

1   Introduction

The plants and animals have adapted numerous ways to maintain metal homeostasis while mitigating detrimental effects of excess metals ions, including the metal-chelating metallothioneins (MTs) and phytochelatins (PCs). PCs have been shown to play an important role in the detoxification of certain heavy metals in both plants and animals. Metals at the toxic levels have the capability to interact with several vital cellular biomolecules such as nuclear proteins and DNA, leading to excessive augmentation of reactive oxygen species (ROS). In addition, these metals generate ROS which in turn can cause neurotoxicity, hepatotoxicity and nephrotoxicity in humans and animals. Notably, higher plants, algae, certain yeasts and animals are equipped with a repertoire of mechanisms to counteract metal-toxicity. The key elements of these are chelation of metals by forming PCs and MTs. Although presence of genes encoding PCs was confirmed in a few animal species, their function in these organisms was not satisfactorily elucidated. Some studies revealed that PCs in animal species are closely linked with detoxification processes in similar way as in plants. MTs have many important and crucial functions. The most important of them includes detoxification of essential as well as non-essential heavy metal ions. These proteins have been isolated and studied in a wide variety of organisms, including prokaryotes, plants, invertebrates and vertebrates. A number of studies have demonstrated the presence or enhanced synthesis of MTs in rapidly proliferating normal cells, regenerating cells and cancer cells. MTs overexpression has been revealed in variety of human tumors. Positive correlation between MTs overexpression and aggressive biological behaviour as well as poorer prognosis have been found in many of them (e.g. for carcinomas of urinary and digestive tract, breast cancers, lung carcinomas, squamous cell carcinomas of oral cavity and larynx as well as malignant melanoma). Several analytical methods have been used to analyze PCs, MTs and complexes of metal. Today, matrix-assisted laser desorption/ionization time-of-flight mass spectrometry (MALDI-TOF MS) is renowned for its extreme ease of operation and requirement of inexpensive matrices for preparation of sample; more importantly, the instrumentation is capable to be fully automated and thus it makes providing the screening of a large number of samples possible in addition to very short time due to advanced laser technology and counting operations.

2 Aims

- Summarization of the literature about PCs and MTs characteristics, structure, isoforms and their roles in homeostasis and pathology diseases.

- Literature analysis devoted to MALDI-TOF MS as an analytical technology for analysis PCs and MTs in biological system.

- Characterization of PCs, MTs, Cd-PC complexes by MALDI-TOF MS.

- Isolation, cloning and expression of mammalian MTs in heterologous organism (*Echerichia coli*) and characterization by MALDI-TOF MS.

3   Literary overview

The concept of phytoremediation of contaminated soils has been increasingly supported by research in recent years. The identification of PC synthase genes from plants and other organisms is a significant breakthrough that will lead to a better understanding of the regulation of a critical step in PC biosynthesis. Many studies showed the mechanisms of chelation of metals-PC in plants in recent years. Chelation and sequestration of metals by particular ligands are also mechanisms used by plants to deal with metal stress. The two best-characterized metal-binding ligands in plant cells are the PC and MTs. While the role played by PC synthase enzymes and PC in animals still remains to be fully explored, there is increasing evidence that PC synthase genes are likely to be found in many important animal groups and that PC may well turn out to be important players in metal ion detoxification in many of these species. A subject of interest in the future will definitely be to whether different animal species coordinate PC and MTs responses to potentially toxic elements, and if this is different for different metal ions.

3. 1. Phytochelatin

3.1.1. Structure and biosynthesis of phytochelatin

Anthropogenic impacts have caused more and more hazardous metals/metalloids (hereafter termed as „metal/s") releasing to environment. Increasing emissions of metals such as Cd, Hg, and As into the environment pose an acute problem for all organisms. Metals, unlike organic contaminants, are not degradable and but remain persistent in soils [1-3]. Once taken up, these metals can bring severe toxic consequences in cells due to their chemical similarity to replace metals necessary for the effective functioning of the cell. Nevertheless, metals at toxic levels have the capability to interact with several vital cellular biomolecules such as nuclear proteins and DNA, leading to excessive augmentation of ROS [4-6]. In addition, these metals generate ROS, which in turn can cause neurotoxicity, hepatotoxicity and nephrotoxicity in humans and animals [7]. Notably, higher plants, algae, certain yeasts and animals are equipped with a repertoire of mechanisms to counteract metal-toxicity. The key elements of these are chelation of

metals by forming PCs and related cysteine-rich polypeptides [8, 9]. PCs are produced from glutamine, cysteine and glycine due to PC synthases known as γ-glutamylcysteine (γ-Glu-Cys) dipeptidyl transpeptidases [10]. PCs have been identified in a wide variety of plant species, microorganisms and invertebrates. They are structurally related to glutathione (GSH) and were presumed to be the products of a biosynthetic pathway. Numerous physiological, biochemical and genetic studies have confirmed that GSH is the substrate for PC biosynthesis [11, 12]. The general structure of PCs is (γ -Glu-Cys)n-Gly, with increasing repetitions of the dipeptide Glu-Cys, where n can range from 2 to 11, but is typically no more than 5 [13]. Except glycine, also other amino acid residues can be found on *C*-terminal end of (γ-Glu-Cys)$_n$ peptides. In **Figure 1**, we show the general structure of PC and steps for synthesized from GSH through a PC synthase in response to high concentrations of toxic metals. Originally thought to be plant-specific, PC and PC synthases have now been reported in a few fungal taxa, such as the yeast *Schizosaccharomyces* sp. and the mycorrhizalascomycete *Tuber melanosporum* [14, 15], and invertebrates belonging to the nematodes, annelids or plathyhelminths [15-22]. In the light of recent literature, the PCs role and modulation are overviewed separately in metal/metalloid-exposed plants and animals/humans; major methods for the determination of PCs and the bioassays for enzymes involved in PC-synthesis are discussed; the connection of PCs with bionanoparticles is evaluated; and finally, major aspects so far unexplored in the present context are highlighted.
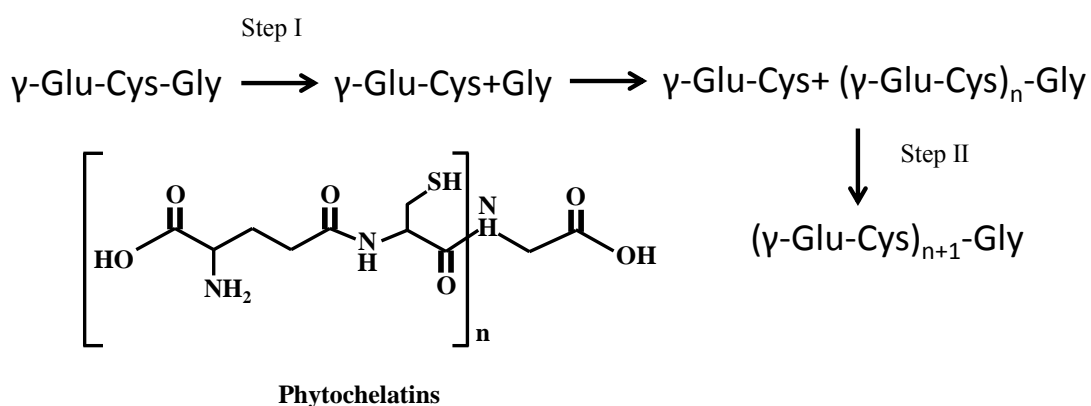
Figure 1.The general structure of PCs and steps for synthesized from glutathione (GSH) through a PC synthase in response to high concentrations of toxic metals.

3.1.2. Phytochelatins in metal/metalloid-exposed plants

Contamination with metals can be considered as one of the most critical threats to soil and water resources as well as to human health [23, 24]. Contamination of soils with toxic metals has often resulted from human activities, especially those related to accelerated rate of industrialization, intensive agriculture, and extensive mining. Metals belong to group of non-biodegradable, persistent inorganic chemicals with cytotoxic, genotoxic, and mutagenic effects on humans or animals and plants through influencing and tainting food chains, soil, irrigation or potable water and aquifers [6, 25, 26]. Chelation and sequestration of metals by particular ligands are also mechanisms used by plants to deal with metal stress. The two best-characterized metal-binding ligands in plant cells are the PCs and metallothioneins [27-31].

In the **Figure 2** is shown the scheme of heavy metal detoxification by PCs in a plant cell. PC, which has a higher affinity for Cd, is formed by the polymerization of 2– gamma-glutamylcysteine (11γ-EC) moieties via PC synthase. Several studies confirm that in plants both GSH and PC synthesis increases after exposure to Cd and other metals [10, 23, 32-38]. In the **Figure 3**, the general functions of the PC and model of complex between Cd^{2+} ion and one molecule of PC are shown.
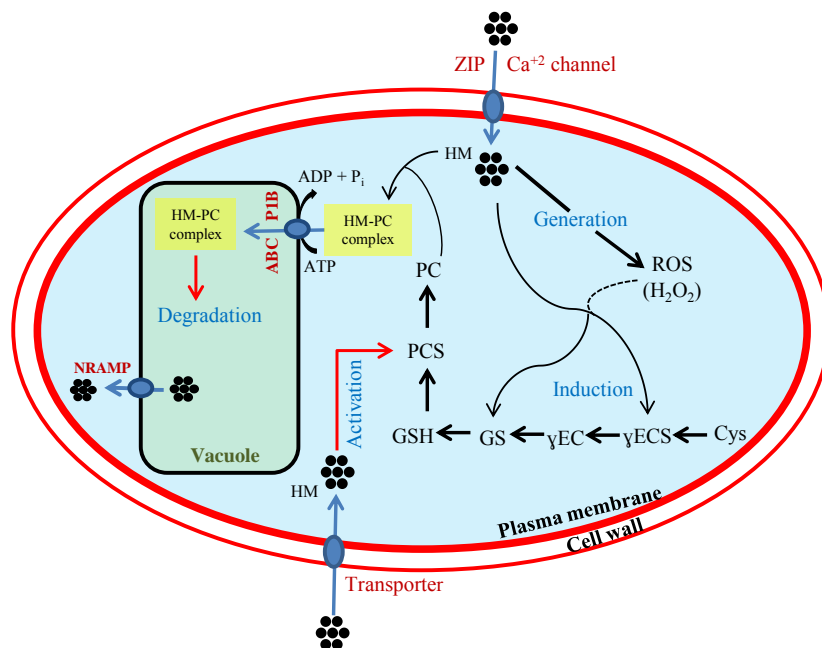
Figure 2. A scheme of heavy metal (HM) detoxification by phytochelatins (PC) in a plant cell. HM activate phytochelatin synthase (PCS), which forms the HM-PC complex with metals ions. This complex is consequently transported through tonoplast to vacuole by ATP-binding-cassette and P1B-ATPase transporter (ABC-P1B). HM chelation by ligands such as PC occurs in the cytosol. Induction of PC synthesis by HM and a large flux of GSH is achieved by increased activities of GSH metabolic enzymes, γ-ECS and GS. It is possible that the enzyme activation is not a direct effect of HM, but due to H_2O_2 produced as a result of HM-treatment. Transport of HM into the plasma membrane (ZIP). Transport of HM in the vacuole (NRAMP: natural resistance associated macrophage protein). Heavy metals are shown as black dots [39].

Gonzalez-Mendoza *et al.* showed that PC synthase gene (in coordination with the expression of *MT* gene) is present in *Avicennia germinans* leaves, and that its expression increases in response to metal-exposure, which supports the hypothesis that PC synthase and MT are part of the metal-tolerance mechanisms in this species. In addition, they found that *A. germinans* has the ability to express both genes (*AvMT2* and *AvPCS*) as a coordinated response mechanism to avoid the toxics effects caused by non-essential metals. However, for essential metals such as Cu^{2+}, the results showed that *AvPCS* was the most active gene involved in the regulation of this metal in the leaves [40]. Recent study showed that *Lunularia cruciata* compartmentalizes Cd^{2+} in the vacuoles of the photosynthetic parenchyma by means of a PC-mediated detoxification strategy, and possesses a PC synthase that is activated by Cd and homeostatic concentrations of Fe^{2+} and Zn^{2+}. *Arabidopsis thaliana* PC synthase displays a higher and broader response to several metals (such as Cd^{2+}, Fe^{2+}, Zn^{2+}, Cu^{2+}, Hg^{2+}, Pb^{2+}, As^{3+}) than *L. cruciata* PC synthase [35].
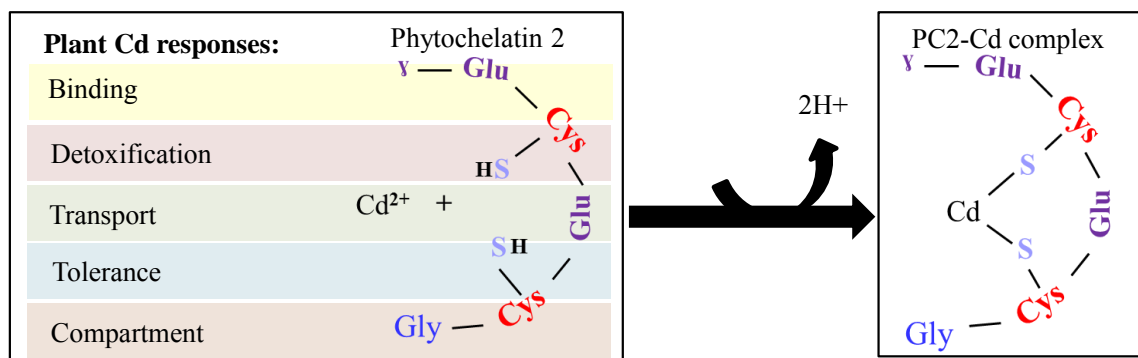
Figure 3. The general functions of PCs and the model of complex between cadmium (Cd^{+2}) ion and one molecules of PC2. Cys, cysteine; Glu, glutamic acid; Gly, glycine; S, sulfur.

Naturally, hyperaccumulating plants do not overproduce PCs as part of their mechanism against toxic metals. This appears to be an inducible rather than a constitutive mechanism, observed especially in metal non-tolerant plants [41]. Some reports have argued against the roles of PC in some metal-tolerant plants based on the effects of buthionine-S-sulfoximine and PCs/metal concentrations [42]. Several studies on plants overexpressing γ-glutamyl-cysteine synthetase or transgenic plants expressing bacterial γ-glutamyl-cysteine synthetase evaluated its effect on metal tolerance based on the assumption that higher levels of GSH and PCs will lead to more efficient metal-sequestration [43]. *Bacopa monnieri*, a wetland macrophyte is well known for its accumulation potential of metals and metal tolerance and thus is suitable in phytoremediation. Aquatic plants respond to metal stress by increased production of PC as well as other antioxidants. The accumulation potential of *B. monnieri* for various metals warrants its evaluation for metal tolerance and detoxification mechanism for its suitability in phytoremediation [44]. *Arabidopsis thaliana* showed that Cd is immediately scavenged by thiols in root cells, particularly by PC, at the expense of GSH. At the same time, a redox signal is suggested to be generated by a decreased GSH pool in combination with an altered GSH:GSSG (reduced glutathione:oxidised glutathione) ratio in order to increase the antioxidant capacity [45]. Overexpression of PCs synthesis in *Arabidopsis* led to 20-100 times more biomass on 250 and 300 μM arsenate than in the wild type. Also, the accumulation of thiol-peptides was ten times higher than after the exposure to Cd and arsenic, compared to the wild type. Gamma-glutamyl cysteine, which is a substrate for PC synthesis, increased rapidly after arsenate or Cd-exposure. Overexpression of this gene can be useful for phytoremediation [46]. Additionally, legumes are also capable of synthesizing homo-PCs in response to metal stress. Citrus plants were also able to synthesize PC in response to metal-intoxication [47]. In wheat, PC–metal complexes have been reported to accumulate in the vacuole. Retention of Cd in the root cell vacuoles might influence the symplastic radial Cd transport to the xylem and further transport to the shoot, resulting in genotypic differences in grain Cd accumulation [48].

3.1.3. Phytochelatins in animals

PCs peptides have been widely described and characterized in plants, yeasts, algae, fungi and bacteria, as well as in nematodes and trematodes [21]. PC synthase genes are also present in animal species from several different phyla. PCs synthesis appears not to be transcriptionally regulated an animal [49]. Originally thought to be found only in plants and yeast, PC synthase genes have since been found in species that span almost the whole animal tree of life.

Fuctional of PCs in Animal

Biochemical studies have also shown that these PC synthase genes are functional: the *Caenorhabditis elegans* PC synthase produces PCs when it is expressed in an appropriate host, and knocking out the gene increases the sensitivity of *C. elegans* to cadmium [50]. Several studies have since measured PCs by direct biochemical analysis of *C. elegans* tissue extracts and found that cadmium exposure did indeed increase PCs levels in *C. elegans*. PC2, PC3 and PC4 have all been found, with PC2 the highest concentration [22, 51, 52]. Therefore, these studies showed that PCs production plays a major role in protecting *C. elegans* against cadmium toxicity. PC2 and PC3 were increased in autochthonous *Lumbricus rubellus* populations sampled from contaminated sites [49].

The yeast (for example, *S. pombe*) possesses an ATP-binding cassette (ABC) transporter, Hmt1, which was originally thought to play a possible role in translocation of PCs–metal complexes to the vacuole. However, while knocking out the *C. elegans* HMT-1 (CeHMT-1) increases sensitivity to cadmium, the increase is greater than could be explained by a lack of PCS alone [53].

It is important to say that MTs are widely established as a key metal detoxification system in animals, even though they certainly have many other biological functions as well. As yet, there is very little known about how MTs and PCs may complement each other for dealing with toxic metals [49].

3.1.4. Methods for determining phytochelatins and phytochelatin synthase enzyme

3.1.4.1 Determination of phytochelatins

In this chapter, an overview of the methods used for determination of PC is given, comprising a broad range of electrochemical as well as spectrometric methods, which have been optimized and even hyphenated with different separation methods to detect PC. Recently, Wood *et al.*, showed the analytical methodology for quantification of PC and their metal(loid) complexes [54]. The classical approach to the analysis of PC is reversed phase (RP) high performance liquid chromatography (HPLC) with post-column derivatization of the sulfhydryl groups and spectrophotometric detection, but the detection is not specific for PC. An analytical technique able to detect compounds specifically is for example mass spectrometry. Independent studies showed a sensitive method for determination of PCs by HPLC with fluorescence detection [55, 56]. A simple sensitive method for the identification, sequencing and quantitative determination of PCs in plants by electrospray tandem mass spectrometry (ESI MS-MS) was shown in different studies [57, 58]. Other study has shown the combination of three processes for identification of PC: (1) simple sample preparation including thiol reduction, (2) rapid and high resolution separation using ultra-performance liquid chromatography (UPLC), and (3) specific and sensitive ESI-MS/MS using multi-reaction mode (MRM) for detection of transitions in alga"s extract [59]. In other studies, *in vitro* formed Cd-PC2 complexes were characterized using ion exchange chromatography (IEC), flow injection analysis/HPLC with CoulArray or Coulochem electrochemical detector and MALDI-TOF MS [60, 61]. Zitka *et al.* optimized HPLC coupled with electrochemical detector for determination of PC2 [62]. Many studies showed the determination of cysteine, reduced and oxidized glutathione, and PC in different species of plants using HPLC with electrochemical detection [63, 64].

3.1.4.2. Bioassays for phytochelatin synthase activity

Methods for identification and quantification of PC synthase are multidisciplinary, among themselves, comprising a broad range of molecular biology, electrochemical and spectrometric methods. HPLC coupled with electrochemical detector has been suggested as a new tool for determination of the PC synthase activity. The optimized procedure was subsequently used for studying PC synthase activity in the tobacco BY-2 cells treated with different concentrations of Cd^{2+} ions and the results were in good agreement with Nakazawa *et al* [65]. Other study in animal showed that HPLC system coupled to a single quadrupole LC–MS equipped with electrospray ionization (ESI) was sensitive method for PC synthase activity [21]. A highly sensitive assay for PC synthase activity was devised, in which the dequenching of Cu(I)-bathocuproinedisulfonate complexes was used in the detection system of a reversed-phase HPLC. The presented assay method is a sensitive tool that can be used to investigate this issue and would allow the determination of PC synthase activity using 10–100-fold less protein [66]. Electrochemical methods, such as differential pulse voltammetry and HPLC with electrochemical detection, were used for determination of Pt(IV) content, glutathione levels, PC synthase activity in maize and pea plants treated with various doses of Pt(IV) [67].

Other methods are necessary for identification and characterization of PC synthase, for example a novel technology of molecular biology. Xu *et al.* showed a study that represents the first transcriptome-based analysis of miRNAs and their targets responsive to Cd stress in radish roots. Furthermore, a few target transcripts including PC synthase 1, iron transporter protein, and ABC transporter protein were involved in plant response to Cd stress [68]. In 2009, Amaro *et al* reported the identification and characterization of a cDNA encoding a PC synthase homologous sequence from the ciliated protozoan *T. thermophila*, the first to be described in ciliates. A quantitative real-time PCR (qRT-PCR) expression analysis of PC synthase has been carried out under different metal stress conditions. Several experimental evidences suggest that this enzyme is biosynthetically inactive in PC formation, which makes it the first pseudo-PC synthase described in eukaryotes [69].

3.1.5. Phytochelatins in connection with bionanoparticles

The connection of nanoparticles and PC has two faces; on the one hand, the biosynthesis of nanoparticles, on the second hand, the protection of stress caused by the damage of any harmful nanoparticles. An *in vitro* study showed the enzyme mediated synthesis of CdS nanocrystals by immobilized PC synthase, which converts glutathione into the metal-binding peptide PC. Formation of CdS nanocrystals was observed upon the addition of $CdCl_2$ and Na_2S with PC as the capping agent [70]. This study helps in designing a rational enzymatic strategy for the synthesis of nanoparticles of different chemical compositions, shapes and sizes. Also, an enzymatic synthesis route to peptide-capped gold nanoparticles was developed. Gold nanoparticles were synthesized *in vitro* using alpha-NADPH-dependent sulfite reductase and PC [71]. The microbiological production of inorganic nanoparticles is an interesting and promising alternative to the known physical and chemical production methods. Extensive studies revealed the potential of bacteria, actinomycetes, algae, yeasts, and fungi for biosynthesis of nanoparticles [72]. Few studies discussed a possible synthesis of nanoparticles by algae, particularly *Phaeodactylum tricornutum* exposed to Cd forms Cd–PC complexes in which sulfide ions (S^{2-}) can be incorporated to stabilize PC-coated CdS nanocrystallites [73, 74]. Metal is immobilized by an intracellular detoxification mechanism. *Krumov et al* showed that Cd is associated to a protein fraction between 25 and 67 kDa which corresponds to the theoretical molecular weight of CdS nanoparticles of 35 kDa coated with PC determined by size exclusion chromatography [75]. However, any exposure to nanoparticles may pose a risk to human health and to the environment, depending on the type of nanoparticles and their concentration [76]. Zinc oxide nanoparticles (ZnONPs) are used in large quantities by the cosmetic, food and textile industries. The harmful effects of ZnONPs are driven by their physicochemical properties and the resulting physical damage caused by the aggregation and agglomeration of nanoparticles. PC synthase may confer protection against zinc oxide nanoparticle induced toxicity in *Caenorhabditis elegans* [77]. Effect of magnetic nanoparticles on tobacco BY-2 cell suspension culture showed induced PC biosynthesis. These trends were observable for almost all monitored PCs: PC2, PC3 and PC5 [78].

3.2 Metallothionein

Mammalian MTs belong to a group of intracellular and low molecular weight proteins (app. 6 kDa), which were discovered in 1957 when *Margoshes and Valee* isolated them from horse renal cortex tissue [79-82]. MTs have been implicated in a number of functions, including toxic metal detoxification, as a metal chaperone and in metal ion homeostasis [83]. These proteins have been isolated and studied in a wide range of organisms, including prokaryotes, plants, invertebrates and vertebrates [84]. These intracellular proteins are characterized by their unusual high cysteine content (30%) and lack of aromatic amino acids. Because of their rich thiol content, MTs bind a number of trace metals including cadmium, mercury, platinum and silver, and also protect cells and tissues against heavy metal toxicity. Additionally, MTs belong among the most abundant intracellular aspects for biologically essential metals, zinc and copper [85].

3.2.1. Structure of Metallothionein

A metal-free protein or apo-MT appears to possess a predominantly disordered structure. However, upon binding of metal ions a well-defined protein fold develops. MTs are single-chain proteins with amino acid number oscillating between app. 20 and more than 100 residues according to the type of organism. Almost one third of this number is cysteine occurring in conserved sequences cys-x-cys, cys-xy- cys and cys-cys where *x* and *y* represent other amino acid. Divalent metal ions bonded to sulfhydryl groups of cysteines are creating tetrahedral configuration of thiolate clusters [86]. Binding capacity of MT is seven and twelve atoms for divalent and monovalent ions, respectively. MT"s tertiary structure consists of two domains: more stable α (*C*-terminal) domain, containing four ion binding sites, and β (N-terminal) domain capable to incorporate three ions (**Figure 5**) [87]. Rigby *et al.* demonstrated the migration of the eleven cysteinyl sulphurs in α domain and the nine cysteinyl sulphurs in the β domain to the outside of the protein while the polypeptide backbone adopted a random coil conformation. This cysteinyl sulphur inversion is necessary for metal scavenging in the surrounding environment under the formation of more stable and proteolytically

protected metal-bound MT [88]. The model of mammalian MTs with marked cysteine moieties is shown in **Figure 6**.
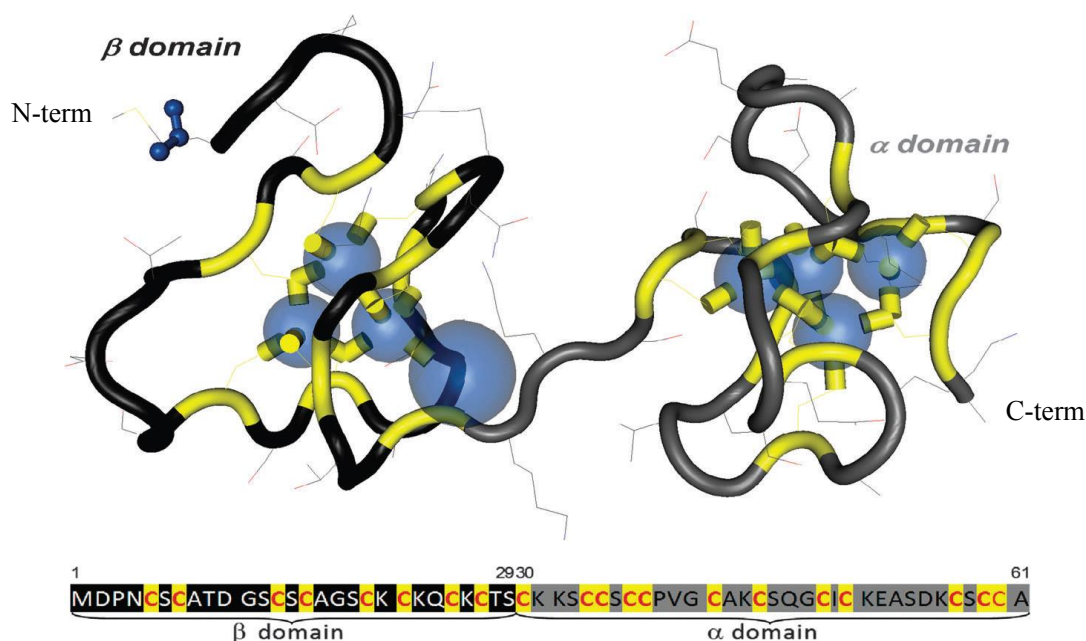
Figure 5. MTs tertiary structure with two domains (α and β) and amino acid sequence [84].
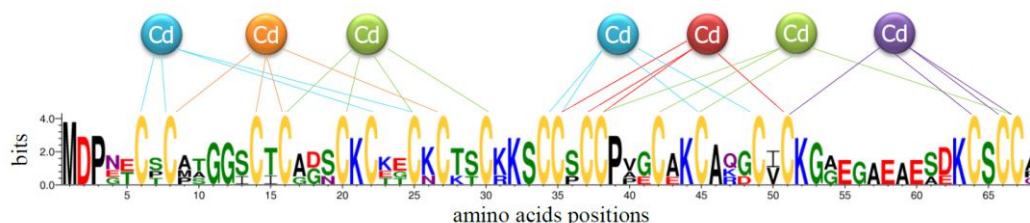
Figure 6. Signatures for complete sequences of mammalian MTs. 125 MT sequences were used for the proposition of this model. Cysteine moieties are yellow marked. MTs metal-binding properties are well-evident [88].

3.2.2. Metallothionein isoforms and regulation genes

MTs are a family of proteins with Mr around 6000, comprised of MT-1, MT-2, MT-3 and MT-4 classes with multiple isoforms within each class. MT-1 and MT-2 are ubiquitously expressed and are stress inducible. MT-1 isoform inducibility is reported to depend on the embryonic germ layer from which a tumor is derived. In human, MTs are encoded by a family of genes consisting of 10 functional MT isoforms and the encoded

proteins are conventionally subdivided into four groups: MT-1, MT-2, MT-3 and MT-4 proteins. The **Figure 7** shows the alignment of amino acid sequences of the four human MT isoforms. While a single *MT-2A* gene encodes MT-2 protein, MT-1 protein comprises many subtypes encoded by a set of *MT-1* genes (*MT-1A*, *MT-1B*, *MT-1E*, *MT-1F*, *MT-1G*, *MT-1H* and *MT-1X*), accounting for the micro-heterogeneity of the MT-1 protein [89]. Different MT genes in humans possibly play different functional roles during development or under various physiological conditions.

```
MT-1H   MDPN-CSCEA GGSCACAGSC KCKKCKCTSC KKSCCSCCPL GCAKCAQGCI CKGA------ SEKCSCCA
MT-2A   MDPN-CSCAA GDSCTCAGSC KCKECKCTSC KKSCCSCCPV GCAKCAQGCI CKGA------ SDKCSCCA
MT-3    MDPETCPCPS GGSCTCADSC KCEGCKCTSC KKSCCSCCPA ECEKCAKDCV CKGGEAAEAE AEKCSCCQ
MT-4    MDPRECVCMS GGICMCGDNC KCTTCNCKTC WKSCCPCCPP GCAKCARGCI CKGG------ SDKCSCCP
```

Figure 7. Alignment of amino acid sequences of the four human MT isoforms using ClustalW (http://www.ebi.ac.uk/Tools/msa/clustalw2/). The conserved cysteine residues are highlighted. The numbering is that of the human MT-3 sequence [90].

In mammals, MT-1 and MT-2 isoforms are expressed at all stages of development in many cell types of all organs. MT-1 and MT-2 are inducible by a variety of stress conditions and compounds, including glucocorticoids, cytokines, reactive oxygen species and metal ions. The most potent inducers of MT-1 and MT-2 biosynthesis are metal ions such as zinc and cadmium. Not all MTs are regulated as a transcription factor. Certain organisms have neither metal-responsive elements (MREs) within the promoter region or MTF as transcription factor. There remains an elusive transcriptional activation of MTs [91].

The MTs promoter has other response elements that up-regulate transcription including the glucocorticoid response elements (GREs), elements activated by signal transducers and activators of transcription (STAT) proteins through cytokine signaling and the antioxidant (or electrophile) response elements (ARE) activated in response to redox status.

MTs are able to scavenge ROS, thus, their involvement in ROS-mediated diseases may be considered, especially in the light of the possible single-nucleotide polymorphism and changes in MTs transcription induction [92]. The second mechanism of the involvement of MT in pathogenesis is based on the regulation of zinc(II) ions that affect zinc-regulated gene expression. This fact was shown by Mazzatti *et al.* in the study focused on the zinc-dependent transcription of pro-inflammatory cytokines and

alterations in metabolic regulatory pathways [38] or by Bellomo *et al.*, who demonstrated regulation of cytosolic zinc levels, ZiP and MT gene expression by glucose in primary pancreatic islet beta cells [39].

The ubiquitously expressed MT-1 and MT-2 family members have been extensively studied and are widely recognized for their ability to attenuate heavy metal induced toxicity through binding and sequestering metals [93, 94]. The promoter regions of MT-1 and MT-2 genes contain several metal and glucocorticoid responsive elements (MREs and GREs) as well as elements involved in basal level transcription. The transcription factor MTF-1 (metal-responsive transcription factor 1), which is essential for basal expression and induction by metals, binds to a promoter proximal MREs. This protein is composed of six zinc fingers that are responsible for DNA binding [95].

The *MT-1* and *MT-2* genes are expressed in many tissues, and at a particularly high level in liver and kidney. MT-1 and MT-2 are present in all cells throughout the body. They regulate copper and zinc, are involved in cell transcription, detoxify heavy metals, play a role in immune function, and are involved in a variety of gastrointestinal tract functions. Exposure of the RWPE-1 cells to either Cd^{2+} or Zn^{2+} was shown to resulted in the rapid induction of the MT-1/2 protein with eventual accumulations easily exceeding 10 % of total cell protein. Similarly, exposure of the human prostate epithelial cell line to either Cd^{2+} or Zn^{2+} resulted in the increased accumulation of MT-1E, MT-1X and MT-2A mRNAs; however, the initial increase in MT-1/2 protein appeared before the increase in MT mRNA suggesting a possible component of posttranscriptional regulation [96].

MT-3 represents an unique metalloprotein called also neuronal-growth inhibitory factor, which inhibits outgrowth of neuronal cells [97]. MT-3 is located primarily in the central nervous system with small amounts present in the pancreas and intestines. It plays a major role in the development, organization and programmed death of brain cells [85].

MT-4 is found in the skin and upper gastrointestinal tract. They help regulate stomach acidic pH, taste and texture discrimination of the tongue and help protect against sunburn and other skin traumas.

3.2.3. General roles of Metallothionein

MTs have many important and crucial functions. **Figure 8** shows the main functions of MTs in an organism [86]. The most important of them includes detoxification of essential as well as non-essential heavy metal ions. Expression of MTs is sensitively and strictly regulated by the oxidative state induced in mitochondrial respiration. Some of MTs actions have therapeutic possibilities in treatment of acute as well as chronic diseases, where oxidative stress plays a crucial role. MTs are supposed to participate in some pathological processes, such as carcinogenesis as well as emergence of radioresistance or chemoresistance [84].
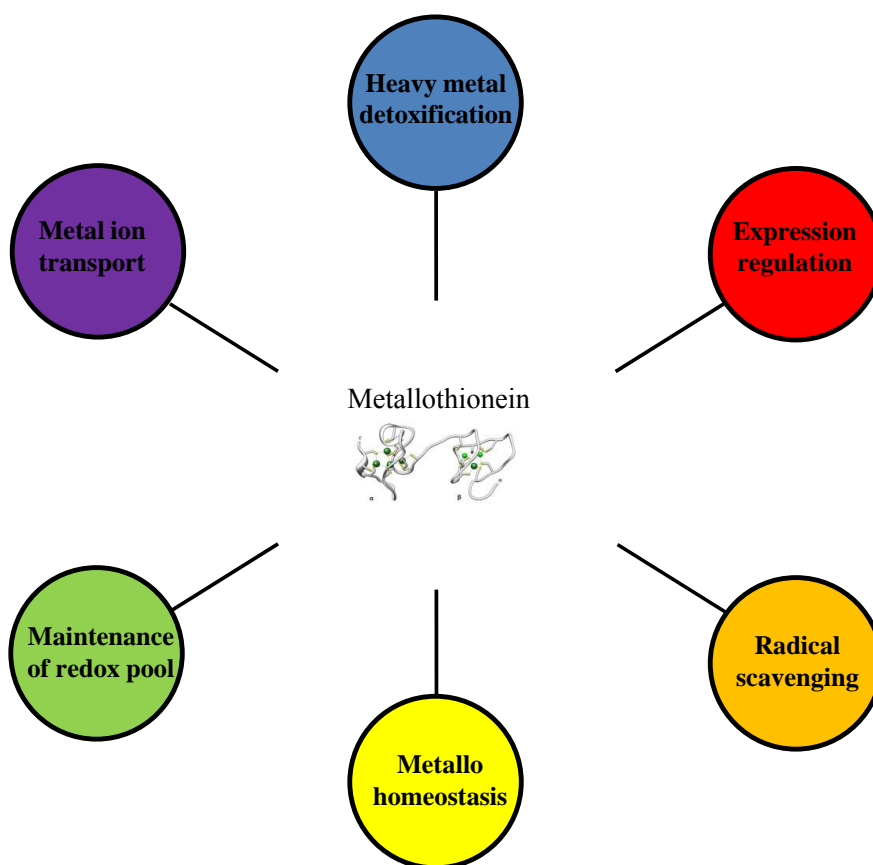
Figure 8. Main functions of MTs in an organism. MTs participate mainly in maintaining of metal ions homeostasis, toxic metal ions detoxification and metal ions transport. Adapted from [86].

3.2.3.1. MTs in cancer diseases

A number of studies have demonstrated the presence or enhanced synthesis of MTs in rapidly proliferating normal cells, regenerating cells and cancer cells. MTs have been shown to protect cells against the cytotoxic effects of electrophilic anticancer drugs. The enhanced expression of MTs in cells induces the antiapoptotic effects and a lack of MTs in MT-null cells increases the susceptibility to apoptotic cell death after exposure to certain anticancer drugs [98]. MTs have also been shown to be involved in the development of resistance to anticancer drug cisplatin, one of the most widely used chemotherapeutic metal-based drugs [99]. The increase in cellular content of MTs was considered as a fact that MTs can be possible biomarkers of resistance to treatment with cisplatin [100, 101]. MTs overexpression has been revealed in a variety of human tumors. Positive correlation between MTs overexpression and aggressive biological behaviour as well as poorer prognosis has been found in many of them (e.g. in carcinomas of urinary and digestive tract, breast cancers, lung carcinomas, squamous cell carcinomas of oral cavity and larynx as well as malignant melanoma) [102-108]. Knocking down MT-1X by siRNA could sensitize cells to cisplatin through increased apoptosis of cancer cells and inhibition of cell proliferation. The study suggests that inhibitors of MT-1X may have potential therapeutic application in inducing apoptosis in oral squamous cell carcinoma. These findings may help in the development of better cancer chemotherapy strategies [109]. Moreover, MTs might be involved in the protection against *Helicobacter pylori* induced-gastric chronic inflammation associated with gastric carcinogenesis [110]. p53, p21, BAX, c-kit, and MTs may have different roles in the pathogenesis of ovarian tumors. p53 and MTs may be helpful in the typing the borderline and malignant ovarian tumors [111, 112]. Different studies have shown that MT has important functions in hematopoietic cells; these studies also considered possible role of MTs in these cells. MT has been reported to be involved in the differentiation and proliferation of hematopoietic cells [113, 114], and prevention of apoptosis [115]. The MT-1A, E, X and MT-2A isoforms have been revealed to play an important function in prostate cancer. It has been shown that MT-1 and MT-2 isoforms may be related to the proliferative activity of breast, colon and prostate human cancers [116, 117]. Five isoforms of MT were overexpressed in non-small cell lung cancer (NSCLC); overexpression of the MT-1F and MT-2A isoforms predicted patient‟s poor

prognosis. Both these isoforms might be involved in progression of this type of cancer; this fact has been confirmed by the correlation analysis of up-regulated MT-1F expression, size of primary tumor and rate of grade of malignancy [118]. Connection between zinc and MTs in central nervous system is still studied. In the central nervous system, zinc is released along with glutamate during neurotransmission and, in excess, can promote neuronal death. Experimental studies have shown that metallothioneins 1/2 (MT-1/2), which chelate free zinc, can affect seizures and reduce neuronal death after status epilepticus [119]. MTs have role in the pathogenesis of autoimmune diseases. The expression of MTs 1 and 2 and the concentrations of Zn and Cu in the tissues of brain, spinal cord (SC) and liver during the periods of attacks and remissions in chronic relapsing experimental autoimmune encephalomyelitis (CR-EAE) have been estimated to have a role in the disorders of central nervous system. This data, obtained by clinical assessment, immunohistochemistry and inductively coupled plasma (ICP) spectrometry, showed that MTs 1 and 2 were markedly up-regulated in the subarachnoid regions and perivascular space in astrocytes, microglia and spinal neurons; copper in the liver was significantly increased. During the second doses a new overexpression of MTs was found in the cerebellum, in sulcus hippocampi, in spinal neurons and particularly in hepatocytes around the central vein; concentration of Cu was significantly increased in the brain [120].

3.2.3.2. MTs role in oxidative stress

The most critical advance in MTs research is a demonstration of the redox regulation of Zn-S interaction and the coupling of zinc and redox metabolism. The cluster structure of Zn-MT provides a chemical basis by which the cysteine ligand can induce oxidoreductive properties which constitutes a MT redox cycle [121]. It is clear that MTs are induced by oxidative stress. Thus, one of the most important MTs functions consists of cell protection against free radicals. The potential antioxidant role of MTs in the nucleus may be more significant than a role in the cytosol. The protective role of MT, however, requires that the protein redistributes between nuclear and cytoplasmic compartments. Since MT is more efficient than GSH in protecting DNA from hydroxyl radical attack, this could indicate that MT is a more important nuclear antioxidant than GSH. The presence of MT in the nucleus may be important to protect DNA from

damage induced by oxidative stress because the nucleus does not contain antioxidant enzymes such as superoxide dismutase, catalase and peroxidase [122]. Studies using a cell-free system have demonstrated the ability of MT as a free radical scavenger [123]. Iszard *et al.* showed the effect of several MTs inducers on oxidative stress defense mechanisms in rats [124]. Studies using cultured cells and intact animal models have provided further evidence supporting the antioxidant function of MTs [125, 126]. Also, MTs are potent antioxidants that protects kidney against oxidative damage [127]. Ogra *et al.* suggested that MT can scavenge NO using the sulfhydryl groups of cysteines in its molecule to form nitrosothiol, thereby reducing nuclear and cytoplasmic damage by NO [128]. Inhibition of superoxide generation and associated nitrosative damage is involved in MTs prevention of diabetic cardiomyopathy [129]. A review has proven that the antioxidant property of MT enhances in a presence of zinc. The zinc redox-dependent functions of MT are important for the regulation of physiological processes that depend on zinc and the pathological processes in which oxidative stress mobilizes zinc. The decrease of zinc availability from MT suggests that the mutant MT is either less reactive towards nitric oxide or it is in an oxidized state and does not bind sufficient amounts of zinc [130, 131].

3.2.3.3. Other MT roles in pathology

MT is a protein involved in numerous key processes. MTs have the important role in cell death in the injured brain [132, 133]. MT by interaction with other proteins fulfills its function, resulting in different effects in the body. Interaction of MT with ferritin, which causes a redox reaction, resulting in the reduction of Fe^{3+} stored in ferritin and a release of harmful Fe^{2+}, was observed. Possibly in the future MT will become a therapeutic agent, which will result in a breakthrough in the field of pharmacy and medicine [134]. The expression of MT-3 has been found to be downregulated or altered [135-137] and changes in normal homeostasis of essential transition metals such as zinc and copper have been implicated as possible etiological factors in neurodegenerative diseases [137, 138].

In particular, MT is induced by inflammatory stress; its roles in inflammation are implied. Also, MT expression in various organs/tissues can be enhanced by

inflammatory stimuli, implicating in inflammatory diseases. Through a genetic approach, MT has been shown to protect against various types of (including lipopolysaccharide related, allergic, and oxidative) inflammatory conditions in mice, implicating MT-induction/enhancement and/or zinc supplementation to induce/enhance MT as possible therapeutic options for inflammatory diseases, although additional research is needed to conclude its clinical utility [139].

Pressure and volume overload produce distinct forms of cardiac hypertrophy. Gene expression profiled in rat hearts subjected to pressure overload showed that MT was one of the genes with the highest level of up-regulation [140].

In conclusion, the most widely expressed isoforms in mammals, MT-1 and MT-2, are rapidly induced in the liver by a wide range of metals, drugs and inflammatory mediators. In the gut and pancreas, MT responds mainly to Zn status. A brain isoform, MT-3, has a specific neuronal growth inhibitory activity, while MT-1 and MT-2 have more diverse functions related to their thiolate cluster structure. These include involvement in Zn homeostasis, protection against heavy metal (especially Cd) and oxidant damage, and metabolic regulation via Zn donation, sequestration and/or redox control [141].

3.2.4. Expression of human MTs in *Escherichia coli*

MTs are potential candidates for medicine development and application [142, 143]. The importance of inflammation, hormone response, anti-apoptotic and zinc-dependent transcription factor function, and zinc regulation in cellular resistance to toxins, coupled with understanding of how MTs influences them, sets the stage for rational therapeutic targeting of MT to enhance cancer treatment while sparing normal tissues [84, 134, 144].

The increased MTs expression by virtue of transient or stable transfection of heterologous MTs expression vectors and in vitro observation of direct of MTs can help to know the specific function in the organisms. Bacterial expression systems for heterologous protein production are attractive because of their ability to grow rapidly and at high density on inexpensive substrates, their often well-characterized genetics and the availability of an increasingly large number of cloning vectors and mutant host strains [145]. *Escherichia coli* is the most widely used bacterial vehicle to produce heterologous proteins [146]. *E. coli* is one of the organisms of choice for the production of recombinant proteins. Its use as a cell factory is well-established and it has become the most popular expression platform. For this reason, there are many molecular tools and protocols at hand for the high-level production of heterologous proteins, such as a vast catalog of expression plasmids, a great number of engineered strains and many cultivation strategies [147]. Odawara *et al* showed a genetic approach to investigate the physiological roles of human MT-2. It was demonstrated that human MT-2 functioned for cadmium detoxification in *E. coli* [148]. Also, Adam *et al* showed that *E. coli* expressing human *MT-3* gene were used like model organisms for studying of metals influence to MTs expression [149].

3.2.5. Analytical technology for analays of MTs: MALDI TOF MS

^{113}Cd and ^{1}H nuclear magnetic resonance, electron paramagnetic resonance, Raman spectroscopy, circular dichroism, Mossbauer spectroscopy and techniques based on absorption and diffraction of X-rays have been utilized for structural analysis of MTs [150, 151]. Due to the absence of aromatic amino acids in MTs primary structure the UV-VIS spectrometric methods are applicable for apo-MT analysis only in deep UV range (below 220 nm), however metal-MT can be determined at wavelengths between 250-800 nm due to the MT-metal bond [150]. Immunochemical methods

(immunoassays) are based on the interaction of antigen and antibody and include: a) enzyme-linked immunosorbent assay (ELISA), b) radioimmunoassay (RIA), c) fluorescence immunoassay (FIA), and d) Western blotting. Polyclonal as well as monoclonal antibodies can be employed for all mentioned immunoassays of MTs [86, 152-159]. Monitoring of MT-mRNA is commonly carried with quantitative reverse transcription polymerase chain reaction (qRT-PCR) or microarrays. Advantage of this approach is distinguishing MT isoforms; however the fact that mRNA amount could not match with protein concentration, is a concern [156, 159-167]. Other important methods for separation and/or detection of MT are sodium dodecyl sulphate polyacrylamide gel electrophoresis (SDS-PAGE), capillary electrophoresis and chromatography [168-174]. Electrochemical and voltammetric methods as Brdicka reaction have been also used [175-178].

Mass spectrometry represents, in coupling with electrospray ionization (ESI), matrix assisted laser desorption/ionization (MALDI) and inductively coupled plasma (ICP) ionization techniques, the most important techniques in metallomics deserving special attention.

Andon *et al.* established a method for the separation and characterization of rabbit liver MT"s subisoforms by capillary electrophoresis coupled to electrospray ionization time-of-flight mass spectrometry (CE-ESI-TOF MS). The analysis described here revealed the presence of the apothioneins MT-1a, MT-1d, and MT-1e, belonging to MT-1 sample, and MT-2a, MT-2b, and MT-2c belonging to MT-2. Similar results were found when MALDI-TOF experiments were performed; they enabled to identify all the sequenced rabbit liver MTs as apo-MT-forms, as in the CE-ESI-TOF MS coupling [179]. Other study verified that the sub-isoforms of MT in rabbit liver have a different apparent molecular mass under different conditions. This experiment predicted that there probably exist a stable peptide structure of MT-2 using MALDI-TOF MS to study the sub-isoforms of MTs and get their exact primary structure [180]. Moreover, two-dimensional gel electrophoresis (2-DGE), MALDI-TOF MS, the peptide mass fingerprinting (PMF) map, and bioinformatic analysis used for studying differentially expressed proteins between multidrug resistant cells HL-60/DOX and drug sensitive cells HL-60 of acute myeloblastic leukemia were potential methods for identification of proteins in these cells. The results revealed presence of MTs only in HL-60 cells [181].

MALDI-TOF MS acts as one of the most comprehensive and versatile tools for research in proteomics [182]. Wang *et al.* have shown a simple and rapid method for identification of MTs isoforms in cultured human prostate cells (RWPE-1 cell line) by MALDI-TOF/TOF mass spectrometry [183] and they demonstrated that MS method allows correlation between expression of isoform-specific proteins and expression of isoform-specific mRNA by providing information about expression of MTs isoforms in a rapid fashion. The lack of publications is well evident in the area of MALDI analysis of MTs in cancer. For example, MALDI imaging of cancer tissue could be very beneficial to confirm hypotheses about possible connection of MTs with matrix metalloproteinases (MMPs), due to presence of zinc ions in peripheral tumour tissue [184].

The MALDI-TOF MS was used for comparative study focused on interactions of cisplatin and ruthenium arene anticancer complexes with MTs. The results showed that the novel ruthenium arene anticancer complexes are much less reactive with thiol-rich MTs, which overexpression in the cancer tissues is closely connected with increased resistance to cisplatin. This finding may be helpful to better understand the distinct pharmacological profile of ruthenium arene anticancer complexes, such as reduced toxicity and no cross-resistance to cisplatin [102]. Platinum(II) complexes have been demonstrated to form covalent bonds with sulphur-donating ligands (in MTs, GSH and other sulphur-containing biomolecules) or coordination bonds with nitrogen-donating ligands (such as histidine and guanine). Moreover, it has been demonstrated that the Terpyridine platinum(II) (TP-Pt(II)) complex formed a covalent bond with the active-site cysteine residue in two other types of cysteine protease by using MALDI-TOF MS. This results showed unequivocally that TP-Pt(II) complexes can selectively bind into the active site of most of cysteine proteases and can be useful in the design of new platinum(II) compounds with promising anti-cancer, anti-parasitic or anti-viral activities [185].

3.2.6. Optimization of MALDI-TOF method for detection of MTs in cancer

3.2.6.1 Matrix

Researchers have discussed the importance of choosing the matrix, conditions of crystallization of the matrix and analyte, concentration of matrix, and the use of matrix additives for different proteins and peptides. The matrix consists of small organic compounds, which show strong resonance absorption at the applied laser wavelength. Pulsed laser systems are used to enable an explosive disintegration of a laser-light-excited matrix-analyte volume, and thus subsequent desorption with ionization. In the most of the studies reviewed, 2,5-dihydroxybenzoic acid (2,5-DHB) and α-cyano-4-hydroxycinnamic acid (CHCA) were the constituents of matrix used for appropriate determination of MTs [186, 187]. CHCA is commonly used for peptides with the lower molecular mass range. This matrix is insoluble in water and well soluble in organic solvents [186]. It is considered as a hard matrix, which means that the molecules of analyte get a lot of internal energy during desorption and ionization. Therefore, the main advantage of CHCA in the measurement of peptides is its ability to form small homogenous crystals. Since geometry in homogeneity relates directly to decreased resolution in the MALDI analysis, CHCA usually yielded good resolution. 2,5-DHB is the matrix of choice for the preparation of glycoproteins, peptides and proteins. Unlike CHCA, it is soluble in water as well as organic solvents [187]. The main disadvantage of 2,5-DHB is the creation of big needle-shaped crystals. The main advantage of 2,5-DHB for MALDI-TOF MS protein analysis is the fact that this matrix is more tolerant towards contamination with salts and/or detergents in comparison with other matrices. In a few published studies focused on the determination of MTs in cancer tissues by MALDI-TOF MS, both 2,5-DHB and CHCA were used for detection and the samples of MTs were prepared in TFA and ACN in different concentrations (50% ACN containing 0.1% TFA or 30% ACN with 0.1% TFA) for obtain better signal [186].

3.2.6.2 Influence of interfering compounds on the signal

MALDI-TOF MS analysis of proteins yields a lot of information that instruments with lower resolution cannot deliver, but only by using proper sample preparation techniques. MS analysis is commonly impaired by common contaminants like fatty acids and salts that are ordinarily used to increase solubilisation of proteins. Nevertheless, these components interfere with the proteins and they affect the ability to ionize them efficiently for mass spectrometry analysis of MT. There are different methods for the removal of contaminants from the samples; these methods allow efficient solubilisation of protein without interfering with formation of MALDI-TOF matrix crystal or ionization of protein, and the signal of MT in MALDI-TOF is more intense and well defined. The undigested (intact) MT samples or samples of MT digested by trypsin usually can be enriched and desalted with ZipTip micropipette tips that are packed with a bed of C18 material, according to the manufacturer's instructions [177, 183]. CHCA has been widely used as a matrix to facilitate the ionization of proteins and peptides in MALDI-TOF MS. However, sodium and potassium ions induce creation of CHCA adducts. These elements are commonly present in solvents and buffers and are released from many plastics that are used for preparation and storage of samples. Matrix adducts are ubiquitous in MALDI-TOF mass spectra, and are evident particularly at low concentrations of analysed sample. Thus, detection of an analyte in very low concentration as well as low molecular weight analytes often becomes problematic. To treat these unfavourable conditions, matrix additives can be used to scavenge or exchange metal ions. In one study, reduced matrix adducts were observed in mass spectra by adding ammonium monobasic phosphate ($NH_4H_2PO_4$) or ammonium dibasic citrate [$(NH_4)_2C_6H_6O_7$] to the matrix/sample [188, 189]. An increase in the intensity and the signal-to-noise ratio of peaks (signals) of peptide in MALDI-TOF MS was another observed benefit of the addition of ammonium monobasic phosphate to samples. Combining both of the approaches, addition of ammonium salts into the CHCA matrix followed by one post-crystallization washing step with ammonium buffer provided a substantial improvement of the sensitivity of MALDI-MS detection compared to unwashed sample spots. This method of preparation of sample is necessary to improve quality of spectra obtained and is essential for successful searching in databases for subnanomolar concentrations of protein digests [188].

3.2.6.3 Quantification of MTs by MALDI-TOF MS

Several research groups have applied MALDI-TOF MS in relative quantitative measurements of MT. At the same time, the non-quantitative character of this method has been widely reported. Szajli *et al.* conducted experiments to test the reliability of this technique of quantitation using the statistical method of the inverse confidence limit calculation for the first time in this context. The relationship between relative intensities of known amounts of standard peptides and their concentration ratios was investigated. They found that the concentration ratios determined by the relative intensity measurements were highly inaccurate and strongly influenced by the molecular milieu of the sample analyzed. Thus, they emphasize the necessity to use the sample itself for calibration and recommend performing a similar statistical analysis to demonstrate reliability for every system where MALDI-TOF MS is used for quantitative measurements [190]. Mirgorodskaya *et al.* have developed a method for quantification of proteins and peptides in very low, picomolar and sub-picomolar, concentrations using MALDI-TOF MS with internal ^{18}O-labeled standards. Mathematical algorithm that uses the isotopic patterns of the substance, the internal standard, and the substance/internal standard mixture for accurate quantitation of the substance has been developed. A great advantage of the proposed method consists in the absence of limitation in molecular weight for the quantitation of proteins and the possibility of quantitation without previous fractionation of proteins and peptides [191]. Even though MALDI is a powerful technique for mass spectrometry of peptides and proteins, it is not quite useful for their quantification. This is one of the most outstanding problems in the quantitative proteomics. The main difficulty lies in the poor reproducibility of MALDI spectra. Park *et al.* showed a novel method to quantify any analyte amenable to MALDI-TOF MS [192]. This method is based on the previous observations that the reaction quotient for the matrix-to-peptide proton transfer evaluated in temperature-selected MALDI was nearly constant regardless of the peptide concentration in the solid sample. This implied a direct proportionality between the relative abundance of an analyte ion in a temperature-selected MALDI spectrum and the concentration of the corresponding neutral in the solid sample. This relation has been confirmed by calibration curves obtained for some peptides. Another characteristic of the relation is that it persists even when other analytes are present. This has been demonstrated for mixtures that contained

peptides and proteins. This and the fact that the method does not require the addition of internal standards allow rapid and inexpensive quantification of any analyte amenable to MALDI [192].

3.3. Book chapter

Participation in the work of the author M.A. Merlos Rodrigo literature research 40% and manuscript preparation 40%.

PCs have been identified in a wide variety of plant species, microorganisms and invertebrates. They are structurally related to GSH and were presumed to be the products of a biosynthetic pathway. Numerous physiological, biochemical and genetic studies have confirmed that GSH is the substrate for PC biosynthesis. In the light of recent literature, the PCs" role and modulation are overviewed separately in metal-exposed plants and animals/humans and major methods for the determination of PCs and the bioassays for enzymes involved in PC synthesis are discussed hereunder. Additionally, connection of PCs with bionanoparticles is evaluated, and finally, major aspects so far unexplored in the present context are briefly highlighted.

Role of Phytochelatins in Redox Caused Stress in Plants and Animals

Miguel Angel Merlos Rodrigo, Naser A. Anjum, Zbynek Heger, Ondrej Zitka, Adam Vojtech, Eduarda Pereira and Rene Kizek

Additional information is available at the end of the chapter

Abstract

Varied environmental compartments (such as soil and water) potentially contaminated with different metals/metalloids can impact the health of both plants and animals/humans. Trace amounts of Cu, Mn, Mo, Ni and Zn are beneficial for higher plants, whereas, Cr, Cu, Co, Mn, Mo, Se, V and Zn are known as the micronutrient metal/metalloids for animals/humans. However, elevated levels of the metals/metalloids can cause severe toxic consequences in both plants and animals/humans. Common in plants and animals/humans, phytochelatins (PCs), the principal non-protein, S-rich, thiolate peptides, protect (through different mechanisms) cellular functions and metal/metalloid homeostasis by performing their chelation and/or detoxification. With the major aim of broadening the current knowledge on the subject, this chapter (a) overviews PCs' role and modulation separately in metal/metalloid-exposed plants and animals/humans; (b) discusses major methods for determination of PCs and bioassays for enzymes involved in PC synthesis; (c) evaluates the connection of PCs with bionanoparticles; and finally (d) highlights so far unexplored aspects in the present context.

Keywords: Phytochelatin, metal, glutathione, stress

1. Introduction

Anthropogenic activities have caused the release of a wide range of hazardous metals/metalloids (hereafter termed as 'metal/s') into the environment. In particular, increasing emissions of metals such as Cd, Hg and As into the environment pose an acute problem for all organisms. Metals, unlike organic contaminants, are not degradable and remain persistent in soils [1–3]. Once taken up, these metals can bring severe toxic consequences in cells due to their chemical similarity to replace the metals necessary for cellular functions. Nevertheless,

metals at toxic levels have the capability to interact with several vital cellular biomolecules such as nuclear proteins and DNA, leading to excessive augmentation of reactive oxygen species (ROS) [4–6]. In addition, these metals generate ROS which in turn can cause neurotoxicity, hepatotoxicity and nephrotoxicity in humans and animals [7, 8]. Notably, higher plants, algae, certain yeasts and animals are equipped with a repertoire of mechanisms to counteract metal toxicity. The key elements of these are chelation of metals by forming phytochelatins (PCs) and related cysteine-rich polypeptides [9–11]. PCs are produced from glutamine, cysteine and glycine and the process is catalysed by PC synthases known as γ-glutamylcysteine (γ-Glu-Cys) dipeptidyl transpeptidases [12, 11]. PCs have been identified in a wide variety of plant species, microorganisms and invertebrates. They are structurally related to glutathione (GSH) and were presumed to be the products of a biosynthetic pathway. Numerous physiological, biochemical and genetic studies have confirmed that GSH is the substrate for PC biosynthesis [13, 14]. The general structure of PCs is (γ-Glu-Cys)n-Gly, with increasing repetitions of the dipeptide Glu-Cys, where n can range from 2 to 11 but is typically no more than 5 [15]. Except glycine, other amino acid residues can be found on the C-terminal end of (γ-Glu-Cys)n peptides. In Figure 1, we show the general structure of PC and the major steps involved in its synthesis from GSH through PC synthase in response to high concentrations of toxic metals. Originally thought to be plant-specific, PC and PC synthases have now been reported in a few fungal taxa, such as the yeast *Schizosaccharomyces* sp. and the mycorrhizal ascomycete *Tuber melanosporum* [16, 17] and invertebrates belonging to the nematodes, annelids or plathyhelminths [18, 19, 4, 1, 20, 17, 21–24].

In the light of recent literature, the PCs' role and modulation are overviewed separately in metal-exposed plants and animals/humans and major methods for the determination of PCs and the bioassays for enzymes involved in PC synthesis are discussed hereunder. Additionally, connection of PCs with bionanoparticles is evaluated, and finally, major aspects so far unexplored in the present context are briefly highlighted.
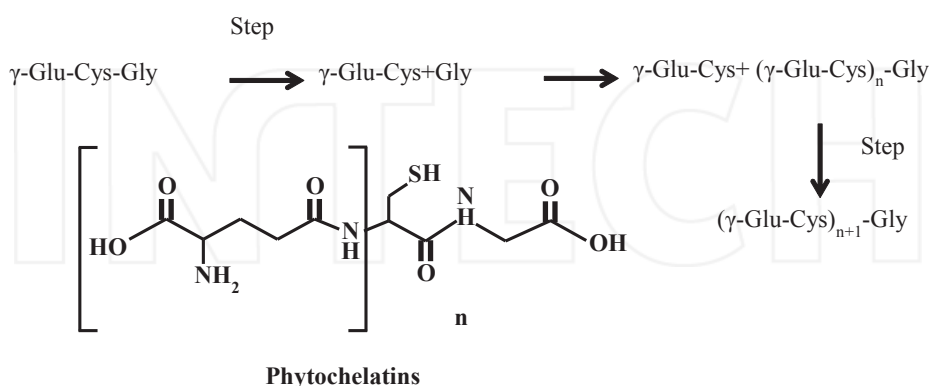
Figure 1. General structure of phytochelatins (PCs) and the major steps involved in its synthesis from glutathione (GSH) through a PC synthase in response to high concentrations of toxic metals.

2. Phytochelatins in metal/metalloid-exposed plants

Contamination by metals can be considered as one of the most critical threats to soil and water resources as well as to human health [25, 26]. In fact, the contamination of soils with toxic metals has often resulted from human activities, especially those related to accelerated rate of industrialization, intensive agriculture and extensive mining. Metal belongs to group of non-biodegradable, persistent inorganic chemical having cytotoxic, genotoxic and mutagenic effects on humans or animals and plants through influencing and tainting food chains, soil, irrigation or potable water and aquifers [27, 28, 6]. Chelation and sequestration of metals by particular ligands are the major mechanisms employed by plants to deal with metal stress. The two best-characterized metal-binding ligands in plant cells are the PC and metallothioneins (MTs) [29–33, 6, 34].

Figure 2 shows the scheme of metal-detoxification by PCs in a plant cell. PC, which has a higher affinity for Cd, is formed by the polymerization of 2–11 γ-EC moieties via PC synthase. Several studies confirm that in plants, both GSH and PC synthesis are increased after exposure to Cd and other metals [12, 35–41]. In Figure 3, we show both general functions of the PC and a model of complex between Cd^{+2} ion and one molecule of PC.

Gonzalez-Mendoza et al. showed that PC synthase gene (in coordination with the expression of metallothionein gene) is present in *Avicennia germinans* leaves, and that their expression increases in response to metal exposure, which supports the hypothesis that PC synthase and metallothionein are part of the metal-tolerance mechanisms in this species. In addition, these authors found that *A. germinans* has the ability to express both genes (*AvMT2* and *AvPCS*) as a coordinated response mechanism to avoid the toxic effects caused by non-essential metals. However, for essential metals such as Cu^{2+}, the results showed that *AvPCS* was the most active gene involved in the regulation of this metal in the leaves [42]. Recent study showed that *Lunularia cruciata* compartmentalizes Cd^{+2} in the vacuoles of the photosynthetic parenchyma by means of a PC-mediated detoxification strategy, and possesses a PC synthase that is activated by Cd and homeostatic concentrations of Fe(II) and Zn. *Arabidopsis thaliana* PC synthase displays a higher and broader response to several metals (such as Cd, Fe(II), Zn, Cu, Hg, Pb, As(III)) than *L. cruciata* PC synthase [35].

Naturally hyperaccumulating plants do not overproduce PCs as a part of their mechanism against toxic metals. This appears to be an inducible rather than a constitutive mechanism, observed especially in metal non-tolerant plants [43]. Some reports have argued against the roles of PC in some metal-tolerant plants based on the effects of buthionine-S-sulphoximine and PCs/metal concentrations [44]. Several studies on plants overexpressing γ-glutamyl-cysteine synthetase or transgenic plants expressing bacterial γ-glutamyl-cysteine synthetase evaluated its effect on metal tolerance based on the assumption that higher levels of GSH and PCs will lead to more efficient metal sequestration [45]. *Bacopa monnieri*, a wetland macrophyte, is well known for its accumulation potential of metals and metal tolerance and thus is suitable for phytoremediation. Aquatic plants respond to metal stress by increasing the production of PC as well as other antioxidants. The accumulation potential of *B. monnieri* for various metals warrants its evaluation for metal tolerance and detoxification mechanism and for its suitability
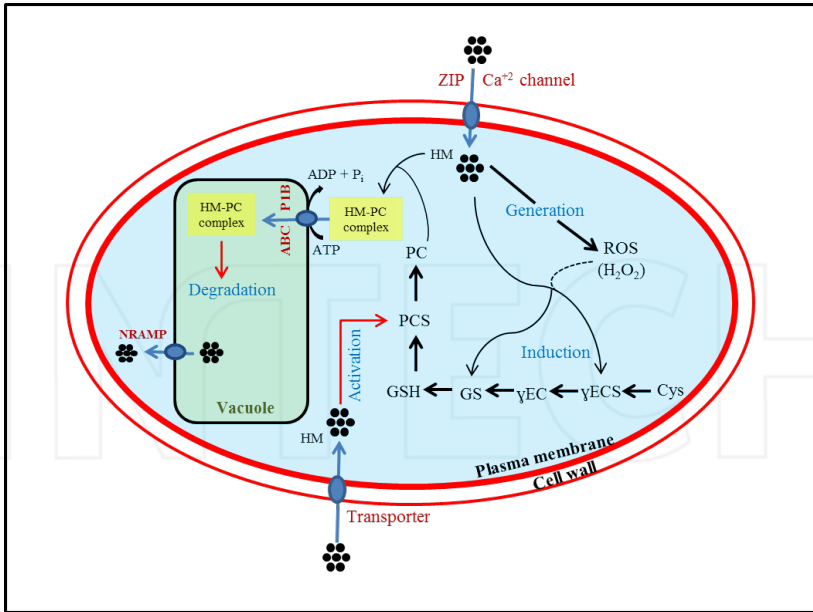
Figure 2. The scheme of heavy metal (HM) detoxification by phytochelatins (PC) in a plant cell. HM activates phyto-chelatin synthase (PCS) and the HM–PC complexes are established. These complexes are consequently transported through tonoplast to vacuole by ATP-binding-cassette and P1B-ATPase transporter (ABC-P1B). HM is chelated in the cytosol by ligands such as PC. Induction of PC synthesis by HM and a large flux of GSH is further achieved by in-creased activity of the GSH metabolic enzymes, γ-ECS and GS. It is possible that the enzyme activation is not directed through effects of HM but due to H2O2 produced as a result of HM-presence. Transport of HM through the plasma membrane (ZIP). Vacuolar transport of HM (NRAMP: natural resistance associated macrophage protein). Heavy met-als are shown as black dots. Figure adapted and modified from [26].
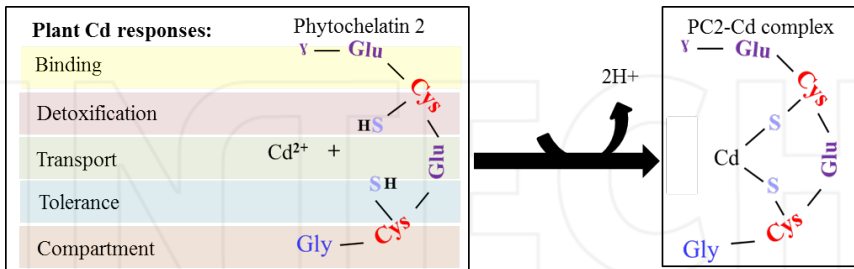
Figure 3. General functions of phytochelatins (PCs) and the model of complex between cadmium (Cd^{+2}) ion and one molecule of PC2. Cys, cysteine; Glu, glutamic acid; Gly, glycine; S, sulphur.

in phytoremediation [38]. In a study on *Arabidopsis thaliana* showed that Cd is immediately scavenged by thiols in root cells, in particular PC, at the expense of GSH. At the same time, a redox signal is suggested to be generated by a decreased GSH pool in combination with an

altered GSH:GSSG ratio in order to increase the antioxidant capacity [46]. Overexpression of PCs synthetase in Arabidopsis led to 20–100 times more biomass on 250 and 300 μM arsenate than in the wild type. Also, the accumulation of thiol-peptides was 10 times higher after the exposure to Cd and arsenic, compared to the wild type. Gamma-glutamyl cysteine, which is a substrate for PC synthesis, increased rapidly after arsenate or Cd-exposure. Overexpression of PC synthase gene can be useful for phytoremediation [47]. Additionally, legumes are also capable of synthesizing homo-PCs in response to metal stress [45]. Citrus plants were also reported to synthesize PC in response to metal intoxication [48]. In wheat (*Triticum aestivum*), PC–metal complexes have been reported to accumulate in the vacuole. Retention of Cd in the root cell vacuoles might influence the symplastic radial Cd transport to the xylem and further transport to the shoot, resulting in genotypic differences in grain Cd accumulation [49].

3. Phytochelatins in metal/metalloid-exposed animals

As mentioned also above, PC proteins have been broadly described and characterized in plants, yeasts, algae, fungi and bacteria [22]. However, PC synthase genes are also present in animal species from several phyla. PC synthesis appears not to be transcriptionally regulated in animals [50]. Nevertheless, originally thought to be found only in plants and yeast, PC synthase genes have since been found in species that span almost the whole animal tree of life. Notably, PC synthase genes are found in species from several other metazoan phyla, including Annelida, Cnidaria, Echinodermata, Chordata and Mollusca (both Gastropoda and Bivalvia classes) [51, 52].

Several phyla of the Metazoa contain one or more species harbouring PC synthase homologous sequences: the Cnidaria (*Hydra magnipapillata*), the Chordata (*Molgula tectiformis*, as well the model chordate *Ciona intestinalis*), the Echinodermata (*Strongylocentrotus purpuratus*), the Annelida (*Lumbricus rubellus*) and the Platyhelminthes (*Schistosoma japonicum* and *Schistosoma mansoni*) [53, 51]. Biochemical studies have also shown that these PC synthase genes are functional. The *Caenorhabditis elegans* PC synthase produces PC when it is expressed in an appropriate host, and knocking out the gene increases the sensitivity of *C. elegans* to Cd [54]. Several studies have since measured PC by direct biochemical analysis of *C. elegans* tissue extracts, and found that Cd exposure did indeed increase PC levels in *C. elegans*. PC2, PC3 and PC4 have all been found, with PC2 in the highest concentration [55, 20, 56]. Therefore, these studies concluded that PCs production can play a major role in protecting *C. elegans* against Cd toxicity. PC2 and PC3 were increased in autochthonous *Lumbricus rubellus* populations sampled from contaminated sites [50]. The yeast (for example, *S. pombe*) possesses an ATP-binding cassette (ABC) transporter, Hmt1, which was originally thought to play a possible role in translocation of PCs–metal complexes to the vacuole. However, while knocking out the *C. elegans* HMT-1 (CeHMT-1) increases the sensitivity to Cd; the increase is greater than could be explained by a lack of PC synthase alone [57]. It is important to say that MTs are another widely established metal-binding ligand and a key metal detoxification system in animals. Additionally, MTs have many other important biological functions

as well. Nevertheless, little is known about how MTs and PCs may complement each other for dealing with toxic metals [50].

The activation and function of PC synthase in animals came into light from studies on the nematode *C. elegans* [58], the flatworm *Schistosoma mansoni* [19, 59, 21], and Cionidae *Ciona intestinalis* [60]. The occurrence of PC synthase in animals suggests the occurrence, in these organisms, of a stress oxidative and metal detoxification system based on a class of molecules which was considered as the privilege of plants. The PC synthase gene has a wide phylogenetic distribution and can be found in species that cover almost all of the animal tree of life. But even though some members of particular taxonomic groups may contain PC synthase genes, there are also many species without these genes. Ron Elran et al. reported the regulation of GSH cycle genes in *Nematostella vectensis*, and an interesting finding was that PC synthase 1, which synthesizes the non-ribosomal formation of metal-binding PC, was upregulated after Hg and Cu treatments [15]. Phylogenetic analyses supported the hypothesis that PC synthase evolved independently in plants, cyanobacteria and green algae. Among the sequenced metazoan genomes, only a few contain a PC synthase gene. However, the reason for the scattered distribution of these genes remains unclear, considering that metazoans with PC synthase genes in their genomes do not share any physiological, behavioural or ecological features [60]. Just how (and if) PC in invertebrates complement the function of MTs remains to be elucidated, and the temporal, spatial and metal specificity of the two systems are still unknown [6].

4. Methods for the assays of phytochelatins and phytochelatin synthase enzyme

4.1. Determination of phytochelatins

We briefly discuss herein different methods for the detection and quantification of PC. Additionally, we are giving an overview of the methods used for determination of PC, comprising a broad range of electrochemical as well as spectrometric methods, which have been optimized and even hyphenated with different separation methods to detect PC. Recently, Wood et al. showed the analytical methodology for quantification of PC and their metal(loid) complexes [61]. The classical approach to the analysis of PC is reversed phase HPLC with post-column derivatization of the sulphydryl groups and spectrophotometric detection, but the detection is not specific to PC. The use of an analytical technique is able to detect compounds, specifically mass spectrometry. Independent studies showed a sensitive method for determining PCs by HPLC with fluorescence detection [62, 63]. A simple sensitive method for the identification, sequencing and quantitative determination of PCs in plants by electrospray tandem mass spectrometry (ESI MS-MS) was showed for different studies [64, 65]. Other study showed the combination of three processes for identification PC: (1) easy sample preparation including thiol reduction, (2) rapid and high-resolution separation using ultra-performance liquid chromatography (UPLC) and (3) specific and sensitive ESI-MS/MS detection using multi-reaction mode (MRM) transitions in alga's extract [66].

Nevertheless, in vitro formed Cd–PC2 complexes were characterized using ion exchange chromatography (IEC), flow injection analysis/high-performance liquid chromatography with CoulArray or Coulochem electrochemical detector and matrix-assisted laser desorption/ionization time-of-flight (MALDI-TOF) mass spectrometry [67, 68]. Zitka et al. optimized high-performance liquid chromatography coupled with electrochemical detector for determination of PC2 [69]. Many studies showed the determination of cysteine, reduced and oxidized glutathione and PC in different species of plants using high-performance liquid chromatography with electrochemical detection [70, 71].

### 4.2. Bioassays for phytochelatin synthase activity

The methods for identification and quantification of PC synthase are multidisciplinary, among themselves, comprising a broad range of molecular biology, electrochemical and spectrometric methods. HPLC coupled with electrochemical detector has been suggested as a new tool for the determination of PC synthase activity. The optimized procedure was subsequently used for studying PC synthase activity in the tobacco BY-2 cells treated with different concentrations of Cd(II) ions and the results were in good agreement with Nakazawa et al. [72]. Other study in animals showed that HPLC-LC system coupled to a single quadrupole LC–MS equipped with ESI was a sensitive method for PC synthase activity [22]. A highly sensitive assay for PC synthase activity was devised, where, the dequenching of Cu(I)-bathocuproinedisulphonate complexes was used in the detection system of a reversed-phase high-performance liquid chromatography. The present assay method is a sensitive tool that can be used to investigate this issue and would allow for the determination of PC synthase activity using 10–100-fold less protein [73]. Electrochemical methods such as differential pulse voltammetry and high-performance liquid chromatography with electrochemical detection were used for determination of Pt(IV) content, GSH levels, PC synthase activity in maize (*Zea mays*) and pea (*Pisum sativum*) plants treated with various doses of Pt(IV) [74].

Other methods required for the identification and characterization of PC synthase are, for example, the novel technology of molecular biology. Xu et al. showed a study that represents the first transcriptome-based analysis of miRNAs and their targets responsive to Cd stress in radish (*Raphanus sativus*) roots. Furthermore, a few target transcripts including PC synthase 1 (PCS1), iron transporter protein and ABC transporter protein were involved in plant response to Cd stress [75]. In 2009, Amaro et al. reported the identification and characterization of a cDNA encoding a PC synthase homologous sequence from the ciliated protozoan *T. thermophila*, the first to be described in ciliates. A quantitative real-time PCR (qRT-PCR) expression analysis of PC synthase been carried out under different metal stress conditions. Several experimental evidences suggest that this enzyme is biosynthetically inactive in PC formation, which makes it the first pseudo-PC synthase to be described in eukaryotes [76].

5. Phytochelatins in connection with bionanoparticles

The connection of nanoparticles and PC has two faces: on one hand, the biosynthesis of nanoparticles and on the other hand, the protection of stress caused by the damage of any

harmful nanoparticles. An *in vitro* study showed the enzyme-mediated synthesis of CdS nanocrystals by immobilized PC synthase, which converts GSH into the metal-binding peptide PC. Formation of CdS nanocrystals were observed upon the addition of CdCl2 and Na2S with PC as the capping agent [77]. This study is expected to help in designing a rational enzymatic strategy for the synthesis of nanoparticles of different chemical compositions, shapes and sizes. Also, an enzymatic synthesis route to peptide-capped gold nanoparticles was developed. Gold nanoparticles were synthesized using alpha-NADPH-dependent sulphite reductase and PC in vitro [78]. In Figure 4, we show the general structure of nanocrystal with cross-linked, PC-like coating (Figure modified from [79]). The microbiological production of inorganic nano-particles is an interesting and promising alternative to the known physical and chemical production methods. Extensive studies revealed the potential of bacteria, actinomycetes, algae, yeasts and fungi for biosynthesis of nanoparticles [80]. Few studies have discussed the possible synthesis of nanoparticles by algae. Particularly, *Phaeodactylum tricornutum* exposed to Cd, forms Cd–PC complexes, where sulphide ions (S^{2-}) can be incorporated to stabilize PC-coated CdS nanocrystallites [81, 82]. Metal is immobilized by an intracellular detoxification mecha-nism. Krumov et al. showed that Cd is associated to a protein fraction between 25 and 67 kDa which correspond to the theoretical molecular weight of CdS nanoparticles of 35 kDa coated with PC by size exclusion chromatography [83]. However, contingent to their types and concentrations, any nanoparticles can pose a risk to human health and to the environment [84]. Zinc oxide nanoparticles (ZnONPs) are used in large quantities by the cosmetic, food and textile industries. The harmful effects of ZnONPs are driven by their physicochemical properties and the resulting physical damage caused by the aggregation and agglomeration of nanoparticles. PC synthase may confer protection against ZnONPs-induced toxicity in *Caenorhabditis elegans* [24]. Effect of magnetic nanoparticles on tobacco BY-2 cell suspension culture showed induced PC biosynthesis. These trends were observable for almost all moni-tored PCs: PC2, PC3 and PC5 [85].
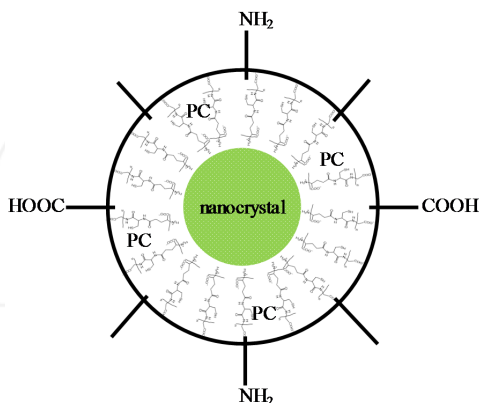
Figure 4. Nanocrystal with crosslinked, phytochelatin (PC)-like coating, an effective strategy to make QDs as small with a crosslinked peptide sheath by mimicking PC-coated heavy metal nanoclusters. Figure adapted and modified from [79].

6. Conclusions

The concept of phytoremediation of contaminated soils has been increasingly supported by research in recent years. The identification of PC synthase genes from plants and other organisms is a significant breakthrough that will lead to a better understanding of the regulation of a critical step in PC biosynthesis. Many studies showed the mechanisms of chelation of metals–PC in plants in recent years. Chelation and sequestration of metals by particular ligands are also mechanisms used by plants to deal with metal stress. The two best-characterized metal-binding ligands in plant cells are the PCs and MTs. While the role played by PC synthase enzymes and PCs in animals still remains to be fully explored, there is increasing evidence that PC synthase genes are likely to be found in many important animal groups and that PCs may well turn out to be important players in metal ion detoxification in many of these species. It will be of interest in the future to see whether different animal species coordinate PC and MT responses to potentially toxic elements and if this is different for different metal ions.

Acknowledgements

Author details

Miguel Angel Merlos Rodrigo[1,2], Naser A. Anjum[3], Zbynek Heger[1], Ondrej Zitka[1,2],
Adam Vojtech[1,2], Eduarda Pereira[3] and Rene Kizek[1,2*]

*Address all correspondence to: kizek@sci.muni.cz

1 Department of Chemistry and Biochemistry, Laboratory of Metallomics and Nanotechnologies, Mendel University in Brno, Brno, Czech Republic

2 Central European Institute of Technology, Brno University of Technology, Brno, Czech Republic

3 CESAM-Centre for Environmental and Marine Studies & Department of Chemistry, University of Aveiro, Aveiro, Portugal

References

[1]   Shi W-y, Shao H-b, Li H, Shao M-a, Du S. Progress in the remediation of hazardous heavy metal-polluted soils by natural zeolite. J Hazard Mater 2009;170:1–6.

[2]   Wu G, Kang HB, Zhang XY, Shao HB, Chu LY, Ruan CJ. A critical review on the bio‐removal of hazardous heavy metals from contaminated soils: issues, progress, eco‐environmental concerns and opportunities. J Hazard Mater 2010;174:1–8.

[3]   Vodyanitskii YN. Contamination of soils with heavy metals and metalloids and its ecological hazard (analytic review). Eurasian Soil Sci 2013;46:793–801.

[4]   Sharma SS, Dietz K-J. The relationship between metal toxicity and cellular redox im‐balance. Trend Plant Sci 2009;14:43–50.

[5]   Yadav SK. Heavy metals toxicity in plants: an overview on the role of glutathione and phytochelatins in heavy metal stress tolerance of plants. S Afr J Bot 2010;76:167–79.

[6]   Emamverdian A, Ding Y, Mokhberdoran F, Xie Y. Heavy metal stress and some mechanisms of plant defense response. Sci World J 2015;2015:1–18.

[7]   Harris GK, Shi X. Signaling by carcinogenic metals and metal-induced reactive oxy‐gen species. Mutat Res-Fundament Molecul Mechan Mutagen 2003;533:183–200.

[8]   Valko M, Morris H, Cronin MTD. Metals, toxicity and oxidative stress. Curr Med Chem 2005;12:1161–208.

[9]   Cobbett C, Goldsbrough P. Phytochelatins and metallothioneins: Roles in heavy met‐al detoxification and homeostasis. Ann Rev Plant Biol 2002;53:159–82.

[10] Tan W-N, Li Z-A, Zou B. Molecular mechanisms of plant tolerance to heavy metals. Zhiwu Shengtai Xuebao 2006;30:703–12.

[11] Rea PA. Phytochelatin synthase: of a protease a peptide polymerase made. Physiol Plant 2012;145:154–64.

[12] Mendoza-Cozatl DG, Butko E, Springer F, Torpey JW, Komives EA, Kehr J, Schroed‐er JI. Identification of high levels of phytochelatins, glutathione and cadmium in the phloem sap of Brassica napus. A role for thiol-peptides in the long-distance transport of cadmium and the effect of cadmium on iron translocation. Plant J 2008;54:249–59.

[13] Zenk MH. Heavy metal detoxification in higher plants - a review. Gene 1996;179:21–30.

[14] Rauser WE. Structure and function of metal chelators produced by plants - the case for organic acids, amino acids, phytin, and metallothioneins. Cell Biochem Biophys 1999;31:19–48.

[15] Pivato M, Fabrega-Prats M, Masi A. Low-molecular-weight thiols in plants: Functional and analytical implications. Arch Biochem Biophys 2014;560:83–99.

[16] Clemens S, Kim EJ, Neumann D, Schroeder JI. Tolerance to toxic metals by a gene family of phytochelatin synthases from plants and yeast. Embo J 1999;18:3325–33.

[17] Bolchi A, Ruotolo R, Marchini G, Vurro E, di Toppi LS, Kohler A, Tisserant E, Martin F, Ottonello S. Genome-wide inventory of metal homeostasis-related gene products including a functional phytochelatin synthase in the hypogeous mycorrhizal fungus Tuber melanosporum. Fungal Genet Biol 2011;48:573–84.

[18] Vatamaniuk OK, Bucher EA, Ward JT, Rea PA. A new pathway for heavy metal detoxification in animals - phytochelatin synthase is required for cadmium tolerance in Caenorhabditis elegans. J Biol Chem 2001;276:20817–20.

[19] Brulle F, Cocquerelle C, Wamalah AN, Morgan AJ, Kille P, Lepretre A, Vandenbuicke F. cDNA cloning and expression analysis of Eisenia fetida (Annelida : Oligochaeta) phytochelatin synthase under cadmium exposure. Ecotoxicol Environment Safety 2008;71:47–55.

[20] Schwartz MS, Benci JL, Selote DS, Sharma AK, Chen AGY, Dang H, Fares H, Vatamaniuk OK. Detoxification of multiple heavy metals by a half-molecule ABC transporter, HMT-1, and Coelomocytes of Caenorhabditis elegans. Plos One 2010;5.

[21] Ray D, Williams DL. Characterization of the phytochelatin synthase of Schistosoma mansoni. Plos Neglect Trop Dis 2011;5.

[22] Rigouin C, Vermeire JJ, Nylin E, Williams DL. Characterization of the phytochelatin synthase from the human parasitic nematode Ancylostoma ceylanicum. Molecul Biochem Parasitol 2013;191:1–6.

[23] Elran R, Raam M, Kraus R, Brekhman V, Sher N, Plaschkes I, Chalifa-Caspi V, Lotan T. Early and late response of Nematostella vectensis transcriptome to heavy metals. Molecul Ecol 2014;23:4722–36.

[24] Polak N, Read DS, Jurkschat K, Matzke M, Kelly FJ, Spurgeon DJ, Sturzenbaum SR. Metalloproteins and phytochelatin synthase may confer protection against zinc oxide nanoparticle induced toxicity in Caenorhabditis elegans. Compar Biochem Physiol C-Toxicol Pharmacol 2014;160:75–85.

[25] Yoon J, Cao X, Zhou Q, Ma LQ. Accumulation of Pb, Cu, and Zn in native plants growing on a contaminated Florida site. Sci Total Environ 2006;368:456–64.

[26] Anjum NA, Hasanuzzaman M, Hossein MA, Thangavel P, Roychoudhury A, Gill SS, Rodrigo MAM, Adam V, Fujita M, Kizek R, Duarte AC, Pereira E, Ahmed I. Jacks of metal/metalloid chelation trade in plants-an overview. Front Plant Sci 2015; 6:192. doi:10.3389/fpls. 2015.00192.

[27] Flora SJS, Mittal M, Mehta A. Heavy metal induced oxidative stress & its possible reversal by chelation therapy. Ind J Med Res 2008;128:501–23.

[28] Rascio N, Navari-Izzo F. Heavy metal hyperaccumulating plants: How and why do they do it? And what makes them so interesting? Plant Sci 2011;180:169–81.

[29] Raab A, Feldmann J, Meharg AA. The nature of arsenic-phytochelatin complexes in Holcus lanatus and Pteris cretica. Plant Physiol 2004;134:1113–22.

[30] Pagani MA, Tomas M, Carrillo J, Bofill R, Capdevila M, Atrian S, Andreo CS. The response of the different soybean metallothionein isoforms to cadmium intoxication. J Inorg Biochem 2012;117:306–15.

[31] Gupta DK, Huang HG, Corpas FJ. Lead tolerance in plants: strategies for phytoremediation. Environ Sci Pollut Res 2013;20:2150–61.

[32] Kim Y-O, Jung S, Kim K, Bae H-J. Role of pCeMT, a putative metallothionein from Colocasia esculenta, in response to metal stress. Plant Physiol Biochem 2013;64:25–32.

[33] Bashir H, Ibrahim MM, Bagheri R, Ahmad J, Arif IA, Baig MA, Qureshi MI. Influence of sulfur and cadmium on antioxidants, phytochelatins and growth in Indian mustard. AoB Plants 2015;7.

[34] Shahpiri A, Soleimanifard I, Asadollahi MA. Functional characterization of a type 3 metallothionein isoform (OsMTI-3a) from rice. Int J Biol Macromolecul 2015;73:154–9.

[35] Degola F, De Benedictis M, Petraglia A, Massimi A, Fattorini L, Sorbo S, Basile A, di Toppi LS. A Cd/Fe/Zn-responsive phytochelatin synthase is constitutively present in the ancient liverwort Lunularia cruciata (L.) Dumort. Plant Cell Physiol 2014;55:1884–91.

[36] Fischer S, Kuehnlenz T, Thieme M, Schmidt H, Clemens S. Analysis of plant Pb tolerance at realistic submicromolar concentrations demonstrates the role of phytochelatin synthesis for Pb detoxification. Environ Sci Technol 2014;48:7552–9.

[37] Garcia JD, Mendoza-Cozatl DG, Moreno-Sanchez R. An uncommon phytochelatin synthase gives hints on how to improve their catalytic efficiency on heavy metal hyperaccumulator organisms. Protein Sci 2014;23:185–6.

[38] Kuhnlenz T, Schmidt H, Uraguchi S, Clemens S. Arabidopsis thaliana phytochelatin synthase 2 is constitutively active in vivo and can rescue the growth defect of the PCS1-deficient cad1-3 mutant on Cd-contaminated soil. J Experiment Bot 2014;65:4241–53.

[39] Castro AV, de Almeida A-AF, Pirovani CP, Reis GSM, Almeida NM, Mangabeira PAO. Morphological, biochemical, molecular and ultrastructural changes induced by Cd toxicity in seedlings of Theobroma cacao L. Ecotoxicol Environment Safety 2015;115:174–86.

[40] Hazama K, Nagata S, Fujimori T, Yanagisawa S, Yoneyama T. Concentrations of metals and potential metal-binding compounds and speciation of Cd, Zn and Cu in

phloem and xylem saps from castor bean plants (Ricinus communis) treated with four levels of cadmium. Physiol Plant 2015;154:243–55.

[41] Lee BD, Hwang S. Tobacco phytochelatin synthase (NtPCS1) plays important roles in cadmium and arsenic tolerance and in early plant development in tobacco. Plant Biotechnol Rep 2015;9:107–14.

[42] Gonzalez-Mendoza D, Moreno AQ, Zapata-Perez O. Coordinated responses of phytochelatin synthase and metallothionein genes in black mangrove, Avicennia germinans, exposed to cadmium and copper. Aquatic Toxicol 2007;83:306–14.

[43] Freeman J, Gustin J, Salt D. Constitutively elevated salicylic acid signals glutathione mediated Ni tolerance in Thlaspi Ni hyperaccumulators. Plant Biol (Rockville) 2005;2005:111–2.

[44] Schat H, Llugany M, Vooijs R, Hartley-Whitaker J, Bleeker PM. The role of phytochelatins in constitutive and adaptive heavy metal tolerances in hyperaccumulator and non-hyperaccumulator metallophytes. J Experiment Bot 2002;53:2381–92.

[45] Zagorchev L, Seal CE, Kranner I, Odjakova M. A central role for thiols in plant tolerance to abiotic stress. Int J Molecul Sci 2013;14:7405–32.

[46] Jozefczak M, Keunen E, Schat H, Bliek M, Hernandez LE, Carleer R, Remans T, Bohler S, Vangronsveld J, Cuypers A. Differential response of Arabidopsis leaves and roots to cadmium: glutathione-related chelating capacity vs antioxidant capacity. Plant Physiol Biochem 2014;83:1–9.

[47] Li YJ, Dhankher OP, Carreira L, Lee D, Chen A, Schroeder JI, Balish RS, Meagher RB. Overexpression of phytochelatin synthase in Arabidopsis leads to enhanced arsenic tolerance and cadmium hypersensitivity (vol 45, pg 1787, 2004). Plant Cell Physiol 2005;46:387.

[48] Lopez-Climent MF, Arbona V, Perez-Clemente RM, Zandalinas SI, Gomez-Cadenas A. Effect of cadmium and calcium treatments on phytochelatin and glutathione levels in citrus plants. Plant Biol 2014;16:79–87.

[49] Stolt JP, Sneller FEC, Bryngelsson T, Lundborg T, Schat H. Phytochelatin and cadmium accumulation in wheat. Environment Experiment Bot 2003;49:21–8.

[50] Liebeke M, Garcia-Perez I, Anderson CJ, Lawlor AJ, Bennett MH, Morris CA, Kille P, Svendsen C, Spurgeon DJ, Bundy JG. Earthworms produce phytochelatins in response to arsenic. Plos One 2013;8.

[51] Clemens S. Evolution and function of phytochelatin synthases. J Plant Physiol 2006;163:319–32.

[52] Clemens S, Persoh D. Multi-tasking phytochelatin synthases. Plant Sci 2009;177:266–71.

[53] Vatamaniuk OK, Bucher EA, Ward JT, Rea PA. Worms take the 'phyto' out of 'phyto-chelatins'. Trend Biotechnol 2002;20:61–4.

[54] Bundy JG, Kille P. Metabolites and metals in Metazoa - what role do phytochelatins play in animals? Metallomics 2014;6:1576–82.

[55] Cui Y, McBride SJ, Boyd WA, Alper S, Freedman JH. Toxicogenomic analysis of Caenorhabditis elegans reveals novel genes and pathways involved in the resistance to cadmium toxicity. Genome Biol 2007;8.

[56] Hall J, Haas KL, Freedman JH. Role of MTL-1, MTL-2, and CDR-1 in mediating cadmium sensitivity in Caenorhabditis elegans. Toxicol Sci 2012;128:418–26.

[57] Vatamaniuk OK, Bucher EA, Sundaram MV, Rea PA. CeHMT-1, a putative phytochelatin transporter, is required for cadmium tolerance in Caenorhabditis elegans. J Biol Chem 2005;280:23684–90.

[58] Hughes SL, Bundy JG, Want EJ, Kille P, Sturzenbaum SR. The metabolomic responses of Caenorhabditis elegans to cadmium are largely independent of metallothionein status, but dominated by changes in cystathionine and phytochelatins. J Proteome Res 2009;8:3512–9.

[59] Bernard F, Brulle F, Douay F, Lemiere S, Demuynck S, Vandenbulcke F. Metallic trace element body burdens and gene expression analysis of biomarker candidates in Eisenia fetida, using an 'exposure/depuration' experimental scheme with field soils. Ecotoxicol Environ Safety 2010;73:1034–45.

[60] Franchi N, Piccinni E, Ferro D, Basso G, Spolaore B, Santovito G, Ballarin L. Characterization and transcription studies of a phytochelatin synthase gene from the solitary tunicate Ciona intestinalis exposed to cadmium. Aquatic Toxicol 2014;152:47–56.

[61] Wood BA, Feldmann J. Quantification of phytochelatins and their metal(loid) complexes: critical assessment of current analytical methodology. Anal Bioanal Chem 2012;402:3299–309.

[62] Kawakami SK, Gledhill M, Achterberg EP. Determination of phytochelatins and glutathione in phytoplankton from natural waters using HPLC with fluorescence detection. Trac-Trend Anal Chem 2006;25:133–142.

[63] Ju XH, Tang SR, Jia Y, Guo JK, Ding YZ, Song ZG, Zhao YJ. Determination and characterization of cysteine, glutathione and phytochelatins (PC2-6) in Lolium perenne L. exposed to Cd stress under ambient and elevated carbon dioxide using HPLC with fluorescence detection. J Chromatography B-Anal Technol Biomed Life Sci 2011;879:1717–24.

[64] Vacchina V, Chassaigne H, Oven M, Zenk MH, Lobinski R. Characterisation and determination of phytochelatins in plant extracts by electrospray tandem mass spectrometry. Analyst 1999;124:1425–30.

[65] Baralkiewicz D, Kozka M, Piechalak A, Tomaszewska B, Sobczak P. Determination of cadmium and lead species and phytochelatins in pea (Pisum sativum) by HPLC-ICP-MS and HPLC-ESI-MSn. Talanta 2009;79:493–8.

[66] Braeutigam A, Wesenberg D, Preud'homme H, Schaumloeffel D. Rapid and simple UPLC-MS/MS method for precise phytochelatin quantification in alga extracts. Anal Bioanal Chem 2010;398:877–83.

[67] Rodrigo MAM, Cernei N, Kominkova M, Zitka O, Beklova M, Zehnalek J, Kizek R, Adam V. Ion exchange chromatography and mass spectrometric methods for analysis of cadmium-phytochelatin (II) complexes. Int J Environ Res Public Health 2013;10:1304–11.

[68] Rodrigo MAM, Zitka O, Kominkova M, Adam V, Beklova M, Kizek R. Analysis of cadmium-phytochelatins 2 complexes using flow injection analysis coupled with electrochemical detection mass spectrometry. Int J Electrochem Sci 2013;8:4409–21.

[69] Zitka O, Skutkova H, Krystofova O, Sobrova P, Adam V, Zehnalek J, Havel L, Beklova M, Hubalek J, Provaznik I, Kizek R. Rapid and ultrasensitive method for determination of phytochelatin(2) using high performance liquid chromatography with electrochemical detection. Int J Electrochem Sci 2011;6:1367–81.

[70] Zitka O, Stejskal K, Kleckerova A, Adam V, Beklova M, Horna A, Supalkova V, Havel L, Kizek R. Utilizing electrochemical techniques for detection of biological samples. Chemicke Listy 2007;101:225–31.

[71] Skladanka J, Adam V, Zitka O, Krystofova O, Beklova M, Kizek R, Havlicek Z, Slama P, Nawrath A. Investigation into the effect of molds in grasses on their content of low molecular mass thiols. Int J Environ Res Public Health 2012;9:3789–805.

[72] Nakazawa R, Kato H, Kameda Y, Takenaga H. Optimum assay conditions of the activity of phytochelatin synthase from tobacco cells. Biol Plant 2002;45:311–3.

[73] Ogawa S, Yoshidomi T, Shirabe T, Yoshimura E. HPLC method for the determination of phytochelatin synthase activity specific for soft metal ion chelators. J Inorg Biochem 2010;104:442–5.

[74] Mikulaskova H, Merlos MAR, Zitka O, Kominkova M, Hynek D, Adam V, Beklova M, Kizek R. Employment of electrochemical methods for assessment of the maize (Zea mays L.) and pea (Pisum sativum L.) response to treatment with platinum(IV). Int J Electrochem Sci 2013;8:4505–19.

[75] Xu L, Wang Y, Zhai LL, Xu YY, Wang LJ, Zhu XW, Gong YQ, Yu RG, Limera C, Liu LW. Genome-wide identification and characterization of cadmium-responsive microRNAs and their target genes in radish (Raphanus sativus L.) roots. J Experiment Bot 2013;64:4271–87.

[76] Amaro F, Ruotolo R, Martin-Gonzalez A, Faccini A, Ottonello S, Gutierrez JC. A pseudo-phytochelatin synthase in the ciliated protozoan Tetrahymena thermophila. Compar Biochem Physiol C-Toxicol Pharmacol 2009;149:598–604.

[77] Liu F, Kang SH, Lee Y-I, Choa Y-h, Mulchandani A, Myung NV, Chen W. Enzyme mediated synthesis of phytochelatin-capped CdS nanocrystals. Appl Phys Lett 2010;97.

[78] Kumar SA, Abyaneh MK, Gosavi SW, Kulkarni SK, Ahmad A, Khan MI. Sulfite reductase-mediated synthesis of gold nanoparticles capped with phytochelatin. Biotechnol Appl Biochem 2007;47:191–5.

[79] Zheng Y, Yang Z, Li Y, Ying JY. From glutathione capping to a crosslinked, phytochelatin-like coating of quantum dots. Adv Mater 2008;20:3410–5.

[80] Krumov N, Perner-Nochta I, Oder S, Gotchev V, Angelov A, Posten C. Production of inorganic nanoparticles by microorganisms. Chem Eng Technol 2009;32:1026–35.

[81] Morelli E, Cruz BH, Somovigo S, Scarano G. Speciation of cadmium - gamma-glutamyl peptides complexes in cells of the marine microalga Phaeodactylum tricornutum. Plant Sci 2002;163:807–13.

[82] Gioacchino Scarano EM. Properties of phytochelatin-coated CdS nanochrystallites formed in a marine phytoplanktonic alga. Plant Sci 2003;165: 803–10.

[83] Krumov N, Oder S, Perner-Nochta I, Angelov A, Posten C. Accumulation of CdS nanoparticles by yeasts in a fed-batch bioprocess. J Biotechnol 2007;132:481–86.

[84] Nowack B, Brouwer C, Geertsma RE, Heugens EHW, Ross BL, Toufektsian M-C, Wijnhoven SWP, Aitken RJ. Analysis of the occupational, consumer and environmental exposure to engineered nanomaterials used in 10 technology sectors. Nanotoxicology 2013;7:1152–6.

[85] Krystofova O, Sochor J, Zitka O, Babula P, Kudrle V, Adam V, Kizek R. Effect of magnetic nanoparticles on tobacco BY-2 cell suspension culture. Int J Environ Res Public Health 2013;10:47–71.

3.4. Review I

NASER A. ANJUM , MIRZA HASANUZZAMAN, MOHAMMAD A. HOSSAIN, PALANISWAMY THANGAVEL, ARYADEEP ROYCHOUDHURY, SARVAJEET S. GILL, **MIGUEL A. MERLOS RODRIGO**, VOJTECH ADAM, MASAYUKI FUJITA, RENE KIZEK, ARMANDO C. DUARTE, EDUARDA PEREIRA AND IQBAL AHMAD (2015). Jacks of metal/metalloid chelation trade in plants−an overview. *Front. Plant Sci*. http://dx.doi.org/10.3389/fpls.2015.00192

Participation in the work of the author M.A. Merlos Rodrigo literature research 20% and manuscript preparation 20%.

Plants have been credibly reported to avoid the damaging effects of metal toxicity, using strategies or mechanism involving: the binding of heavy metals to cell wall and immobilization exclusion of the plasma membrane, expression of more general stress response mechanisms such as stress proteins (heat shock proteins), and metal-chelation and -compartmentalization. In particular, chelation is the most widespread intracellular mechanism for the maintenance of low concentrations and detoxification of free metals in plant cytoplasm that can be performed by thiol compounds (which contain sulfhydryl/thiol groups; such as a tripeptide glutathione, GSH, γ-Glu-Cys-Gly; phytochelatins, PCs; metallothioneins, MTs), and also by non-thiol compounds (such as organic acids, and amino acids). This paper presents an appraisal of recent reports on both thiol (PCs and MTs) and non-thiol compounds in an effort to shed light on the significance of these compounds in plant-metal tolerance, as well as to provide scientific clues for the advancement of metal-phytoextraction strategies.

Jacks of metal/metalloid chelation trade in plants—an overview

Naser A. Anjum[1], Mirza Hasanuzzaman[2]*, Mohammad A. Hossain[3], Palaniswamy Thangavel[4], Aryadeep Roychoudhury[5], Sarvajeet S. Gill[6], Miguel A. Merlos Rodrigo[7,8], Vojtěch Adam[7,8], Masayuki Fujita[9], Rene Kizek[7,8], Armando C. Duarte[1], Eduarda Pereira[1] and Iqbal Ahmad[1,10]

[1] Centre for Environmental and Marine Studies and Department of Chemistry, University of Aveiro, Aveiro, Portugal, [2] Department of Agronomy, Faculty of Agriculture, Sher-e-Bangla Agricultural University, Dhaka, Bangladesh, [3] Department of Genetics and Plant Breeding, Bangladesh Agricultural University, Mymensingh, Bangladesh, [4] Department of Environmental Science, School of Life Sciences, Periyar University, Salem, India, [5] Post Graduate Department of Biotechnology, St. Xavier's College (Autonomous), Kolkata, India, [6] Stress Physiology and Molecular Biology Lab, Centre for Biotechnology, Maharshi Dayanand University, Rohtak, India, [7] Central European Institute of Technology, Brno University of Technology, Brno, Czech Republic, [8] Department of Chemistry and Biochemistry, Mendel University in Brno, Brno, Czech Republic, [9] Laboratory of Plant Stress Responses, Faculty of Agriculture, Kagawa University, Miki-cho, Japan, [10] Centre for Environmental and Marine Studies and Department of Biology, University of Aveiro, Aveiro, Portugal

Varied environmental compartments including soils are being contaminated by a myriad toxic metal(loid)s (hereafter termed as "metal/s") mainly through anthropogenic activities. These metals may contaminate food chain and bring irreparable consequences in human. Plant-based approach (phytoremediation) stands second to none among bioremediation technologies meant for sustainable cleanup of soils/sites with metal-contamination. In turn, the capacity of plants to tolerate potential consequences caused by the extracted/accumulated metals decides the effectiveness and success of phytoremediation system. Chelation is among the potential mechanisms that largely govern metal-tolerance in plant cells by maintaining low concentrations of free metals in cytoplasm. Metal-chelation can be performed by compounds of both thiol origin (such as GSH, glutathione; PCs, phytochelatins; MTs, metallothioneins) and non-thiol origin (such as histidine, nicotianamine, organic acids). This paper presents an appraisal of recent reports on both thiol and non-thiol compounds in an effort to shed light on the significance of these compounds in plant-metal tolerance, as well as to provide scientific clues for the advancement of metal-phytoextraction strategies.

Keywords: metal/metalloids, plant tolerance, chelation, thiol compounds, glutathione, organic acid, metallothioneins, phytochelatins

Introduction

Metal(loid)s and their Chelation Strategies in Plants

The Earth's crust harbors varying levels of different metals/metalloids (hereafter termed as "metal/s"). Though at optimum level, many metals (such as Cu, Fe, Mn, Ni, Zn) are essential for plant cells; however, the supra-optimum concentrations of these metals and even low concentrations of other metals such as Ag, Al, As, Cd, Cr, Cs, Hg, Pb, Sr, and U exhibit phytotoxicity. Thus, higher concentrations of all metals that have potential to cause detrimental

consequences in human or environments can be considered as "contaminant" (reviewed by Anjum et al., 2015). Nevertheless, the inception of industrialization, metalliferous mining and smelting, sewage sludge treatment, warfare, and military training, waste disposal sites and indiscriminate agricultural fertilizer use have caused significant addition of previous toxic metals to soils (Padmavathiamma and Li, 2007; Hassan and Aarts, 2011; Alloway, 2013). Though, it remained technically a challenge for the global scientific community, the cleanup of metal-contaminated soils has been widely advocated to minimize their impact on human and environmental health (reviewed by Ali et al., 2013). In this context, compared to different physical, chemical and biological approaches employed for this purpose, plant and associated microbes based approach (phytoremediation) stands outstanding in terms its novelty, cost-effective, efficiency, environment- and eco-friendly, *in situ* applicability, and natural (solar-driven) (Mench et al., 2009; Hassan and Aarts, 2011; Anjum et al., 2012a; Ali et al., 2013). Basically, the phytoremediation approach is based on a number of strategies including: (a) phytoextraction, (b) rhizofiltration (phytofiltration), and (c) phytostabilization. Notably, plant types growing on contaminated or metalliferous soils were evidenced to develop metal-hyperaccumulation potential (reviewed by Baker and Whiting, 2002). Metal-hyperaccumulation, a process technically termed as phytoextraction, is a striking phenomenon exhibited by <0.2% of angiosperms, where a direct accumulation of metals into aboveground organs with subsequent removal/ processing of these plant-organs is possible. Nevertheless, metal-hyperaccumulators can exhibit extraordinarily high amounts of metals in their above-ground tissues to levels far exceeding those present in the soil or in non-accumulating plant species growing nearby (reviewed by Hassan and Aarts, 2011; Rascio and Navari-Izzo, 2011; Gill et al., 2012).

Understanding physiological and molecular defense strategies adopted by both hyperaccumulator and non-hyperaccumulator plants to cope with metal stress either during accumulation, degradation or elimination of metal pollutants in contaminated soils are of the utmost significance in phytoremediation studies. In particular, plant tolerance to potential toxicity caused by tissue-/organ-metal loads (during metal-hyperaccumulation/extraction) largely decides the efficiency and success of a metal remediation system (Vangronsveld et al., 2009; Maestri et al., 2010; Hassan and Aarts, 2011; Anjum et al., 2014a,b,c). Processes such as exclusion, compartmentalization, complexation, and the synthesis of metal-binding proteins and/or metal ion chelation are included in the list of defense strategies evidenced in plants under metal stress (Clemens, 2001; Méjáre and Bülow, 2001; reviewed by Hassan and Aarts, 2011). Plants have been credibly reported to avoid the damaging effects of metal toxicity, using strategies or mechanism involving: the binding of heavy metals to cell wall and immobilization (Mari and Lebrun, 2006; Kanneganti and Gupta, 2008; Bolan et al., 2014), exclusion of the plasma membrane (Lee et al., 2005; Arrivault et al., 2006), expression of more general stress response mechanisms such as stress proteins (heat shock proteins) (Song et al., 2012), and metal-chelation and -compartmentalization (Lal, 2010; Jozefczak et al., 2012; Seth et al., 2012; Lv et al., 2013). In

particular, chelation is the most widespread intracellular mechanism for the maintenance of low concentrations and detoxification of free metals in plant cytoplasm that can be performed by thiol compounds (which contain sulfhydryl/thiol groups; such as a tripeptide glutathione, GSH, γ-Glu-Cys-Gly; phytochelatins, PCs; metallothioneins, MTs), and also by non-thiol compounds (such as organic acids, and amino acids) (Clemens, 2001; Méjáre and Bülow, 2001; Lal, 2010; Hassan and Aarts, 2011; Anjum et al., 2012b, 2014b,d; Jozefczak et al., 2012; Seth et al., 2012; Lv et al., 2013) (**Figure 1**).

Based on recent reports, this paper discusses the basic physiology/molecular biology of metal-chelation by GSH, PCs, MTs, organic acids, amino acids—considered herein as jacks of metal-chelation trade in plants.

Thiol-Compounds and Metal(loid)-Chelation

Thiol compounds such as GSH, PCs, and MTs contain sulfhydryl (–SH) groups for binding a variety of metals (reviewed by Seth et al., 2012). GSH, a tripeptide (γ-Glu-Cys-Gly) with a wide distribution (0.5–10 mM) in plant cell compartments (namely cytosol, endoplasmic reticulum, vacuole, and mitochondria) is a major –SH compound. Apart from performing key roles in cellular redox homeostasis and the antioxidant defense, GSH is involved in the chelation and detoxification of free metal (reviewed by Anjum et al., 2010, 2012a, 2014d; Seth et al., 2012). The role of GSH in metal-chelation lies behind its significance as a precursor for the synthesis of phytochelatins (PCs, family of peptides structurally related to GSH) in metal-exposed plants (Clemens, 2006; Srivalli and Khanna-Chopra, 2008). The other important –SH compound, MTs [sulfur(S)-containing, cysteine (Cys)-rich, short, low molecular weight (4–8 kDa) gene-encoded polypeptides] have been reported to bind varied metals through the –SH of their Cys-residues (Cobbett and Goldsbrough, 2002; Verbruggen et al., 2009). Therefore, GSH, PCs, and MTs stand second to none in terms of their role in metal-chelation in plants (**Figure 1**; **Table 1**). GSH is briefly overviewed hereunder before discussing other –SH compounds and S-donor ligands—PCs and MTs in detail.

GSH is recognized as an antioxidant that plays a key role in the defense mechanism of plants (Anjum et al., 2010, 2012a, 2014d; Seth et al., 2012; Nahar et al., 2015). Notably, since GSH is also an essential component in the synthesis of metal-binding peptides such as PCs, GSH has been the major metabolic/biochemical modulator of of PCs (Hall, 2002; Guo et al., 2012). The ability to maintain a high GSH level is therefore considered as an essential intrinsic feature, enabling the reduction of oxidative damage caused by accumulated metals in these species. Some metal-tolerant plants, e.g., *Thlaspi goesingense*, *Thlaspi oxyceras*, *Thlaspi rosulare*, and *Holcus lanatus* have a constitutively high GSH content, unlike e.g., *Silene vulgaris* or *Pteris vittata* (Ernst et al., 2008). The higher levels of GSH and Cys were also found in Cd-resistant mutant of *Chlamydomonas reinhardtii* than the wild type (Hu et al., 2001), Cu-resistant alga *Stichococcus minor* (Kalinowska and Pawlik-Skowrónska, 2010) and 276-4d strains
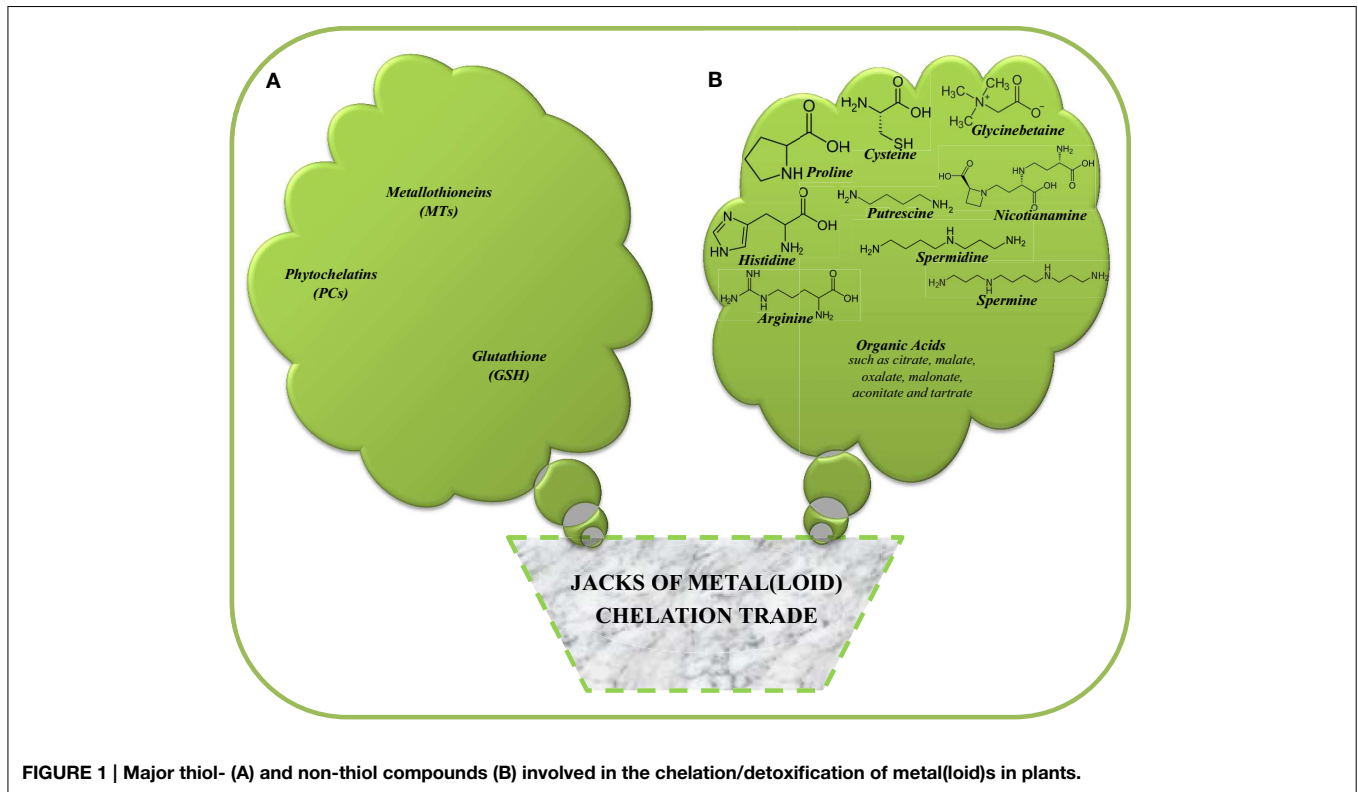
FIGURE 1 | Major thiol- (A) and non-thiol compounds (B) involved in the chelation/detoxification of metal(loid)s in plants.

of *Desmodesmus armatus* (Pokora et al., 2014). Cys could act as a defense mechanism not only for participating in PC biosynthesis but also directly as metal-chelator. Cys content was higher in freshwater microalga *Chlamydomonas moewusii* than that of GSH when Cd was present in the medium. Further, the amount of GSH decreased only slightly with the increase in the PC levels. This would suggest that the intracellular GSH was consumed during the PC biosynthesis and replaced quickly by new synthesis from the S of the medium (Mera et al., 2014). Estrella-Gómez et al. (2012) showed that *Salvinia minima* plants responded to Pb exposure by increasing the concentration of GSH, the activity of glutathione synthase (GS) and the expression levels of the SmGS gene. Similarly, GSH and glutathione reductase (GR) levels were also increased when tomato *(Lycopersicon esculentum)* plants are exposed to arsenite in which the activity of GR is essential for recharging the cells of GSH and the time of increased synthesis of PCs (Marmiroli et al., 2014). On the other hand, since Glu and Cys are important precursors in GSH biosynthesis, it is somewhat surprising that proteins involved in Gln and Cys synthesis were less abundant upon long term Cd-exposure (Dupae et al., 2014). Cd-accrued PCs-induction can cause elevation in the consumption of GSH as a result of utilization of GSH [and also the γ-GluCys (γ-EC) moiety from GSH by transpeptidation] in the production of PCs (Mendoza-Cózatl et al., 2008). In contrast, elevation in GSH pool, reported in some metal-exposed plants has been considered as a strategy to detoxify/tolerate metals(Cd)-accrued consequences either by direct binding or by synthesis of PCs (Cánovas et al., 2004; Thangavel et al., 2007;

reviewed by Anjum et al., 2012b). Although the concentrations of GSH in ectomycorrhizal fungus are even in millimolar range (Schützendübel and Polle, 2002; Courbot et al., 2004) and GSH readily binds both to Cd and Zn (Feretti et al., 2007), it may provide a fast protection against the metal ion transients entering the cytoplasm.

Phytochelatins
Overview
Phytochelatins [PCs; γ-glutamyl (Glu)-cysteinyl (Cys)]$_n$–X, where $n = 2$–11 and X is glycine (Gly), serine, β-alanine, glutamate or glutamine] are the principal non-protein, metal-binding (and metal-dotoxifying), S-rich, thiolate peptides (Cobbett and Goldsbrough, 2002). However, in iso-PCs (isoforms of PCs), the terminal amino acid consists of serine, glutamic acid, glutamine, or β-alanine (in the case of the homo-PCs, present in many legumes) (Oven et al., 2002). In fact, PCs are non-ribosomal peptides and are synthesized enzymatically (not by translation of mRNA owing to the presence of γ-carboxamide linkage between Glu and Cys) in response to varied metals from GSH by phytochelatin synthase (PCS), which is a γ-Glu-Cys dipeptidyl transpeptidase (E.C.2.3.2.15) (Vatamaniuk et al., 2004). Both GSH and hGSH can be the substrates for the synthesis of homo-PCs in Cd-exposed legume (Oven et al., 2002). Nevertheless, though, the amino acids Cys, Glu, and Gly constitute PCs (Zenk, 1996), PC variants without C-terminal Gly-residues can also be found (Oven et al., 2002). The occurrence of PC synthesis in metal-exposed plants was reported to follow

TABLE 1 | Summary of representative studies on metal(loid)-tolerance in plants *via* expression of genes related with major thiol and non-thiol compounds.

Plant species	Gene inducing agent	Gene overexpressed	Defensive effects	Tolerance gained	References
Raphanus sativus L.	Exogenous Spd (1 mM) under Cr stress	*RsADC* and *RsSPDS*	Increased biosynthesis of Put and Spd	Cr (VI) stress	Choudhary et al., 2012b
Arabidopsis	Induced by Pb stress	*At3g02470*	This gene encodes *S*-adenosylmethionine decarboxylase, an enzymes of PA biosynthesis pathway	Pb tolerance	Liu et al., 2009
Raphanus sativus	Exogenous Spd (1 mM) under Cu stress	*RsCOPT1* and *RsCOPT2*	Decrease of Cu uptake	Cu tolerance	Choudhary et al., 2012a
		RsHMA5	Decrease of Cu assimilation		
		RsMT1C and *RsCCH1*	Cu detoxification by regulating the levels of metallothionenins and Cu chaperones		
		RsADC1, *RsADC2*, and *RsSAMDC*	Regulated Put metabolism		
		RsSPDS1 and *RsPAO2*	Regulated Spd metabolism		
		RsSPDS3, *RsPAO2*, and *RsPAO4*	Regulated Spm metabolism		
		RsCYP79B3, *RsYUC1*, and *RsYUC3*	Regulated IAA metabolism		
		RsABA3, *RsNCED*, *RsAAO3*, and *RsCYP707A3*	Regulated ABA metabolism		
Arabidopsis halleri	Zn (25, 50 μM)	*At5g19530*	Induction of Spm/Spd synthase family protein	Zn tolerance	Sharma and Dietz, 2006
		At5g04610	Induction of Spd synthase-related/Put aminopropyltransferase-related		
Arabidopsis thaliana	Cs (2 mM)	*At5g19530*	Induction of Spm/Spd synthase family protein	Cs tolerance	Sharma and Dietz, 2006
		At1g80600	Induction of acetylornithine aminotransferase, mitochondrial, putative/acetylornithine transaminase, putative/AOTA		
		At5g46180	Induction of Orn aminotransferase, putative/Orn-oxo-acid aminotransferase		
Arabidopsis thaliana	Pb(NO$_3$)$_2$ (25, 50 ppm)	*At5g19530*	Induced Spm/Spd synthase family protein	Pb tolerance	Sharma and Dietz, 2006
		At1g23820	Induced Spd synthase 1 (SPDSYN1)/Put aminopropyltransferase 1		
Nicotiana tobacum	150 μM CdCl$_2$	*TaMT3*	Increased the ability of ROS cleaning-up	Cd tolerance	Zhou et al., 2014

(Continued)

59

TABLE 1 | Continued

Plant species	Gene inducing agent	Gene overexpressed	Defensive effects	Tolerance gained	References
Arabidopsis thaliana	As exposure	*S1ptTECS*	Strong induction of GSH1 protein expression in the shoots	As tolerance	Li et al., 2006
Arabidopsis thaliana	Cd exposure	*S1ptTECS*	Three- to five-fold increase in γ-EC related peptides	Cd tolerance	Li et al., 2005
Populus canescens	0.01–0.1 mM $ZnSO_4$	*GSH1*	Levels of GSH and PCs are maintained by GSH1 in these transgenics	Zn tolerance	Bittsánszkya et al., 2005
Arabidopsis thaliana	As exposure	*arsC*	Specific reduction of arsenate to arsenite in that easily trapped by thiols such as GSH and PCs	As tolerance	Dhankher et al., 2002
Avicennia germinans	Low concentration of Cd and Cu	*AvPCS*	Strong ROS scavenging activity in addition to high metal-binding capacity	Cd and Cu detoxification	Gonzalez-Mendoza et al., 2007
Pyrus communis	500 μM $CuSO_4$	*MdSPDS1*	Alteration of polyamine titers in pear and reduction of Cu accumulation	Cu tolerance	Wen et al., 2008
Arabidopsis thaliana	Cu exposure	*MT1 and MT2*	Highest levels of non-protein thiols	Cu tolerance	Murphy and Taiz, 1995
Saccharum spp.	500 μM $CdCl_2$ or 100 μM $CuCl_2$	*ScMT2-1-3*	Enhanced Cu and Cd detoxification	Cu and Cd tolerance	Guo et al., 2013
Alyssum lesbiacum	30 μM $NiSO_4$	*ATP-PRT*	Many-fold increase in the pool of free His without affecting the concentration of any other amino acid	Ni tolerance	Ingle et al., 2005
Arabidopsis halleri	10 μM $ZnSO_4$	*NICOTIANAMINE SYNTHASEs*	Enhanced nicotianamine synthesis and subsequent binding of a variety of transition metals.	Zn tolerance	Haydon et al., 2012
Arabidopsis halleri	10 μM $ZnSO_4$	*NAS2*	Elevated nicotianamine levels and subcellular compartmentalization of a metal chelator in balancing the transport processes of Zn	Zn tolerance	Deinlein et al., 2012
Nicotiana tabacum	600 and 1000 mM of $NiCl_2$	*AtNAS1*	Ten-fold elevated levels of NA in comparison with wild type which led to an enhanced tolerance against up to 1 mM Ni	Increased Ni tolerance	Douchkov et al., 2005

different hierarchical levels from algae to higher plants including trees (Thangavel et al., 2007; Minocha et al., 2008). In earlier studies, PC production and the enzyme PCS were not found in land plants or bryophytes including liverworts, mosses, and hornworts (Bruns et al., 2001; Kopriva et al., 2007). *Microsterias denticulata* is the only charophytic algae where the synthesis of PCs has until now been definitely detected (Volland et al., 2014). Recently, the PC-synthesis capability and the presence of constitutive and functional PCS were considered as ancestral (plesiomorphic) characters for basal land plants including bryophytes, charophytes, and lycophytes (Petraglia et al., 2014). A lower amount of PC produced under Cd stress (36 and 72 μM of Cd for 72 h) in all the bryophyte lineages and in the lycophyte *Selaginella denticulata*previous was suggested due to lower PCS activity as compared to angiosperms. Notably, potential

toxicity of accumulated metals can be decreased as a result of the formation and subsequent sequestration of "metal-PC complexes" in vacuoles *via* transport across the tonoplast (Cobbett and Goldsbrough, 2002). Nevertheless, when expressed in an appropriate host the *Caenorhabditis elegans* PCS gene that control PCs production; however, knocking out the gene can increase the sensitivity of *C. elegans* to Cd (Vatamaniuk et al., 2001). Considering the previous roles of PCs as well as due to their significant role in the induction in plants under metal-exposure, the "status of PCs in plants" has been advocated as one of the major indicators of metal pollution (Dago et al., 2014).

Metal(loid)-Specificity and -Chelation Mechanisms

Synthesis of PCs can be plant-specific and/or metal-specific. Depending on the metal type, Hg, Cd, As, Ag, and Fe have been

reported as strong inducers of PCs while Pb and Zn are weak inducers and Cu and Ni are moderate inducers (Zenk, 1996). Among metals, Cd has been detected as a strong inducer of PCs in various plant species (Ortega-Villasante et al., 2005; Clemens, 2006; Rellán-Álvarez et al., 2006; Thangavel et al., 2007; Sobrino-Plata et al., 2009; Gill et al., 2012; Guo et al., 2012; Dago et al., 2014). Compared to Zn (Thangavel et al., 2007) and Hg (Ortega-Villasante et al., 2005; Rellán-Álvarez et al., 2006; Sobrino-Plata et al., 2009) Cd was observed as a major PC-inducer. Opposite to GSH, which was more concentrated in Hg-exposed *Hordeum vulgare* aerial parts than in *H. vulgare* roots, longer-chain PCs (such as PC3, PC4, and PC5) were more abundant in *H. vulgare* roots than in aerial parts of *H. vulgare* and were increased with increase in phytoavailable Hg in soils (Dago et al., 2014). Moreover, the decreased concentrations of smaller thiols such as GSH and PC2 with increasing phytoavailable Hg in soils can be due to use of both GSH and PC2 as substrates for the synthesis of the said longer-chain PCs. Pb and Cd exposure can cause the production of PC2 and PC4, respectively, in *Phaeodactylum tricornutum* cells (Morelli and Scarano, 2001). Among different chains of PC synthesis (PC2–PC5), PC3 and PC4 were the major PCs exhibited in Cd-exposed microalga *C. moewusii* (Mera et al., 2014). Similarly, PC3 was the major peptide in both the 276-4d and B1-76 strains of green alga *Desmodesmus armatus* under 93 μM Cd (Pokora et al., 2014). However, the other PC-oligomers (PC2, PC4 and unidentified P1, P2, and P3) were also higher in B1-76 strain in the first-phase of cell cycle. The unidentified thiol P1, found in green alga *Stichococcus bacillaris* may represent γ-Glu-Cys as the precursor of GSH and PC synthesis (Pawlik-Skowrónska, 2002). The remaining two unidentified non-protein thiols P2 and P3 were also found in the freshwater green alga *Stigeoclonium tenue* that differed from each other in one γ-Glu-Cys unit and contained an additional Cys-residue which was resistant to a mixture of heavy metals (Pawlik-Skowrónska, 2003). Although a linear relationship between Cd and PC production was previously observed in numerous algal species (Gekeler et al., 1988), the amount of synthesized PC after Cd-exposure may not reflect exactly the level of Cd-accumulation (Ahner et al., 1995; Nishikawa et al., 2006). Further, the mechanism underlying the Cd-efficiency for PC synthesis-activation remained unproven. PCs can also function as important chelators of Zn ions (Tennstedt et al., 2009). Song et al. (2014) suggested that essential metal ions, such as Zn(II), Cu(II), and Mn(II), can be transported into vacuoles as forms of "PC2-metal complexes" through the putative ABC transporter(s). However, the efficiency and speed of free Zn^{2+} chelation in the cytoplasm was higher in Cd/Zn hyperaccumulator *Arabidopsis halleri* than in *Arabidopsis thaliana* and these results are helpful to identify the metal sensitivity of the plants in terms of changes in the plasma membrane potential of root cortical cells (Ovečka and Takáč, 2014).

As highlighted also above that the –SH group of the Cys-residues help PCs to bind and generate strong "PC-metal complexes" in high metal-exposed plants. Subsequently, the "PC-metal complexes" are sequestered into vacuoles (via ABC type transporters, Verbruggen et al., 2009 or a group of organic solute transporters, Solanki and Dhankhar, 2011) for detoxification.

Several studies have provided a strong evidence for the formation of Pb-PC complex and its role in Pb tolerance in plants (Zhang et al., 2008; Andra et al., 2010; Fernández et al., 2012). Spisso et al. (2014) also found Hg-PC complexes especially Hg-PC2, Hg-PC3, and Hg-PC4 in *Vitis vinifera* under 100 mg L^{-1} of Hg-exposure. The PC-As (III) complexation in rice leaves was reported to reduce translocation of As from leaves to grains (Duan et al., 2011). The chelation of Cd with PCs in the cytoplasm and compartmentalization of the PC-Cd complexes in the vacuole are generally considered as a "first line" of defense mechanism against Cd phytotoxicity (Inouhe, 2005). The PC-Cd complexes are up to 1000 times less toxic to many enzymatic proteins than the free Cd ions (Solt et al., 2003). The increase in the cytosolic pH of aquatic macrophyte *Elodea canadensis* after Cd addition could contribute to symplasmic Cd detoxification through PC-Cd complex formation (Tariq Javed et al., 2014), because PC-Cd complex stability increases with a rise in pH (Dorcak and Krezel, 2003). Further, such increase in cytosolic pH also activates vacuolar transporters as reported for *Saccharomyces cerevisiae* (Park et al., 2012). Mendoza-Cózatl et al. (2008) identified high concentrations of PCs, GSH, and Cd in the phloem sap of *Brassica napus* and suggested that, along with the xylem, the phloem is a channel for long-distance source-to-sink transport of Cd-PC and Cd-GSH complexes.

In contrast to the facts discussed above, overexpression of PCS gene does not always have beneficial effects on heavy metal tolerance. The heterologous overexpression of *Triticum aestivum TaPCS1* in rice increased Cd sensitivity and significantly increased Cd accumulation in shoots but not in roots (Wang et al., 2012). On the contrary, expression of *CdPCS1* from aquatic macrophyte *Ceratophyllum demersum* in tobacco (*Nicotiana tabacum*), *Escherichia coli* (Shukla et al., 2012) or *Arabidopsis* (Shukla et al., 2013) enhanced PC synthesis as well as Cd and As accumulation. As observed in the previous studies mentioned earlier in this section, higher level of PC accumulation was also detected in roots of cucumber (*Cucumis sativus*) plants treated with 25 or 50 μM Cd, individually or simultaneously with selenium (Se) (Hawrylak-Nowak et al., 2014). PC4 and PC2 were predominant in individual Cd-exposed cucumber roots and leaves, respectively. However, a reduction of PCs accumulation was observed only in roots of cucumber when Cd-exposed plants with Se addition; whereas no change in GSH and PC contents in leaves (Hawrylak-Nowak et al., 2014). Because Se interferes with S metabolism and can replace S in the S-amino acids which results into the production of the corresponding Se-amino acids (seleno-Cys and selenomethionine), their subsequent incorporation into enzymatic proteins may affect catalytic activity (Ellis and Salt, 2003). The catalytic moiety of PCS enzyme contains the active Cys. Moreover, the C-terminal domain of PCs from different species shows low sequence conservation, but shares a common feature in that they all contain multiple Cys residues that bind Cd ions with high affinity and high capacity (Wang et al., 2009). Thus, the replacement of Cys by seleno-Cys in the PCs probably may affect the biosynthesis and accumulation of PCs in the plant tissues (Hawrylak-Nowak et al., 2014).

Metallothioneins

Overview

Another important metal chelator –SH compound and S-donor ligand, metallothioneins (MTs) are products of mRNA translation, characterized as low mass weight (4–14 kDa) Cys-rich metal-binding proteins, and are widely distributed in both prokaryotic and eukaryotic organisms (Cobbett and Goldsbrough, 2002). Margoshes and Vallee (1957) for the first time characterized MTs from horse kidneys as Cd-binding proteins. Based on sequence similarities and phylogenetic relationships plant MTs are divided into four subfamilies, type 1–4 (Freisinger, 2008; Hassinen et al., 2011). Type 1 and 2 sequences contain two Cys-rich domains separated by a central Cys-free spacer. In type 1 sequences the Cys residues are exclusively arranged in Cys-Xaa-Cys motifs (Xaa represents another amino acid) in both the N- and C-terminus, while type 2 have Cys-Cys, Cys-Xaa-Xaa-Cys, and Cys-Xaa-Cys sequences in the N-terminal domain and Cys-Xaa-Cys in the C-terminal domain. Each type of MT genes displays a distinct spatial and temporal expression pattern (Cobbett and Goldsbrough, 2002; Hassinen et al., 2011). Based on structural models, it can be assumed that the MT molecule is composed of two binding domains, α and β, which are composed of Cys-clusters. Covalent binding of metal atoms involves sulfhydryl cysteine residues. The N-terminal part of the peptide is designated as β-domain and has three binding sites for divalent ions, and the C-terminal part (the α-domain) has the ability to bind four divalent metal ions (Ruttkay-Nedecky et al., 2013).

Metal(loid)-Specificity and -Chelation Mechanisms

MTs exhibit their high affinity for both essential and non-essential metals, where MTs can provide thiols for metal chelation in their reduced state. High affinity of MTs for metals provides not only a mechanism for protection against the toxicity of different metals (such as Cd) but it is also significant for the maintenance of homeostasis of some essential metals such as Zn and Cu ions. A general structure for plant MT has been proposed for *Triticum durum* MT type I. This protein forms dimers or higher oligomers and adopts an extended conformation containing both α-helix and β-sheet structures. This model proposes an overall dumbbell shape similar to that reported for mammalian MTs (Bilecen et al., 2005), in agreement with dynamic data obtained on *Fucus vesiculosus* MTs (Merrifield et al., 2006). The involvement of peptide donor groups (S-thiol and N-imidazole) and non-protein ligands (as sulfide anions) in metal chelation, as well as secondary structure elements, was demonstrated. The protein accommodates up to six Cd^{2+} together with four S^{2-}; while, less than four Zn^{2+} could bind the protein (Zimeri et al., 2005). The combination of high thermodynamic but low kinetic stability is one of the main features of the metal-MT complexes, which bind the metals very tightly but a part of the metal ions is easily exchanged for other proteins (Hassinen et al., 2011). The MT superfamily combines a large variety of small Cys-rich proteins that have the ability to coordinate various transition metal ions, including Zn^{2+}, Cd^{2+}, and Cu^+ (Freisinger, 2011). Metal ions can also be coordinated through His residues, but the impact of this ligand on the metal binding properties and function of MTs is not clear (Blindauer, 2008).

There exists inconsistency in the literature available on major stimuli capable of MTs induction/expression in plants. Though abiotic stresses such as drought, salinity, heat, cold light, wounding and senescence can modulate MT gene expression in plants (references cited in Sekhar et al., 2011), among metals, Cu, Cd, Pb, and Zn can strongly induce the plant MT gene expression (reviewed by Mehes-Smith et al., 2013). Cu-induced expression of a Type 1 MT gene in *Arabidopsis*. Guo et al. (2003) were the first to describe the expression of the complete MT gene family in *Arabidopsis* and their responses to Cu treatment. In non-accumulator plants, like *A. thaliana*, *MT1a* and *MT1b* are expressed at high levels in roots during exposure to Cd, Cu, and Zn (Maestri et al., 2010). In *Thlaspi caerulescens*, the levels of MT1mRNA were found in leaves constitutively higher than in roots; the levels increased with exposure to Cu. The primary sequence of the type 3 MT of *T. caerulescens* displays modifications that are proposed to increase its Cu-binding properties when compared to the non-hyperaccumulator, *A. thaliana* ortholog. *A. halleri* and *T. caerulescens* have a constitutively high expression of *MT2*. The expression of *MT3* genes increases during leaf aging and upon exposure to Cu in non-accumulator plants (Roosens et al., 2004). *MT4* is highly expressed in seeds of *A. thaliana*. It plays a role in metal homeostasis during seed development and seed germination rather than in metal decontamination (Roosens et al., 2004; Maestri et al., 2010). The analysis of the expression of *MT2a* in *A. thaliana*, a non-Pb tolerant species, showed that were specifically over-expressed in roots by Pb-treatment (Auguy et al., 2013). MTs are extremely diverse in plants and *T. caerulescens* seems to be an excellent model to understand the adaptive significance of this phenomenon. MT1, MT2, and MT3-related cDNAs were isolated in *T. caerulescens* and both *TcMT1*- and *TcMT3*-deduced protein sequences display modifications in their Cys domains when compared to their homologs in *A. thaliana*. Functional tests in yeast indicated that such modifications may alter the metal chelation of the plant MT proteins. Roosens et al. (2005) showed that the drastic decrease in the Cys number of domain 1 of *TcMT1* is associated with a lower tolerance to Cd and Zn of the yeast expressing *TcMT1* when compared to *AtMT1*. Ectopic expression of MT1 and MT2 (from *Brassica campestris*) in *A. thaliana* enhanced the tolerance to Cd and Cu and increased the Cu concentration in the shoots of the transgenic plants. Transgenic *Arabidopsis* accumulated less reactive oxygen species (ROS) than wild-type plants. *BcMT1* and *BcMT2* increased Cd and Cu tolerance in transgenic *Arabidopsis*, and decreased production of Cd- and Cu-induced ROS, thereby protecting plants from oxidative damage (Lv et al., 2013). The expression levels of the genes *MT2a*, *MT2b*, and *MT3* showed to be much higher in *T. caerulescens* than in non-metallophyte, non-hyperaccumulating reference species, as shown by microarray analyses. The expression of *MT2a* and *MT2b* in the roots is much higher in *T. caerulescens* than in *A. thaliana* (van de Mortel et al., 2006). Various MTs involved for As detoxification in *Oryza sativa* was also reported (Gautam et al., 2012). The authors have also shown that 11 class I MT genes in rice genome that are expressed differently during the growth and development

(Gautam et al., 2012) which is influenced on Cu and Cd tolerance in plants (Zhou and Goldsbrough, 1994). *Arabidopsis* plants over-expressing pigeon pea *CcMT1* were more tolerant to Cu and Cd (Sekhar et al., 2011), while the garlic MTs *AsMT2b* and the *Colocasia esculenta* protein CeMT2b simultaneously confer Cd tolerance and promote Cd accumulation (Zhang et al., 2006). MT-like protein has also been found in *Chlorella vulgaris* capable of detoxifying Cd and Zn toxicities (Huang et al., 2009a). Recently, Zn ($100\,\mu M\,L^{-1}$) was reported cause a higher induction of Zn-MT-like proteins (1.65-fold than control) in *C. vulgaris* (Yang et al., 2014). In a recent study by Nath et al. (2014), *MT1* and *MT2* has strongly expressed in *O. sativa* during 5 days of As (V) exposure. The ability of MTs to bind and sequester with metals/metalloids depends upon the distribution and organization of Cys residues and their regulated expression during stress is a major option for metal detoxification and homeostasis (Usha et al., 2009; Singh et al., 2011; Gautam et al., 2012).

Non-Thiol Compounds and Metal(loid)-Chelation

A number of non-thiol compounds such as organic acid (OAs, including citrate, malate, oxalate, malonate, aconitate, and tartrate) and amino acids and their derivatives (including glycinebetaine/betaine; proline, Pro; histidine, His; cysteine, Cys; arginine, Arg; glutamate, Glu; nicotianamine, NA) in isolation and/or in coordination with thiol compounds have been credibly evidenced to contribute to metal-chelation in plants (Hall, 2002; Sharma and Dietz, 2006; Jakkeral and Kajjidoni, 2011) (**Figure 2**). Hereunder follows an appraisal of recent studies on chelation of metals in plants considering the mentioned above major non-thiol compounds.
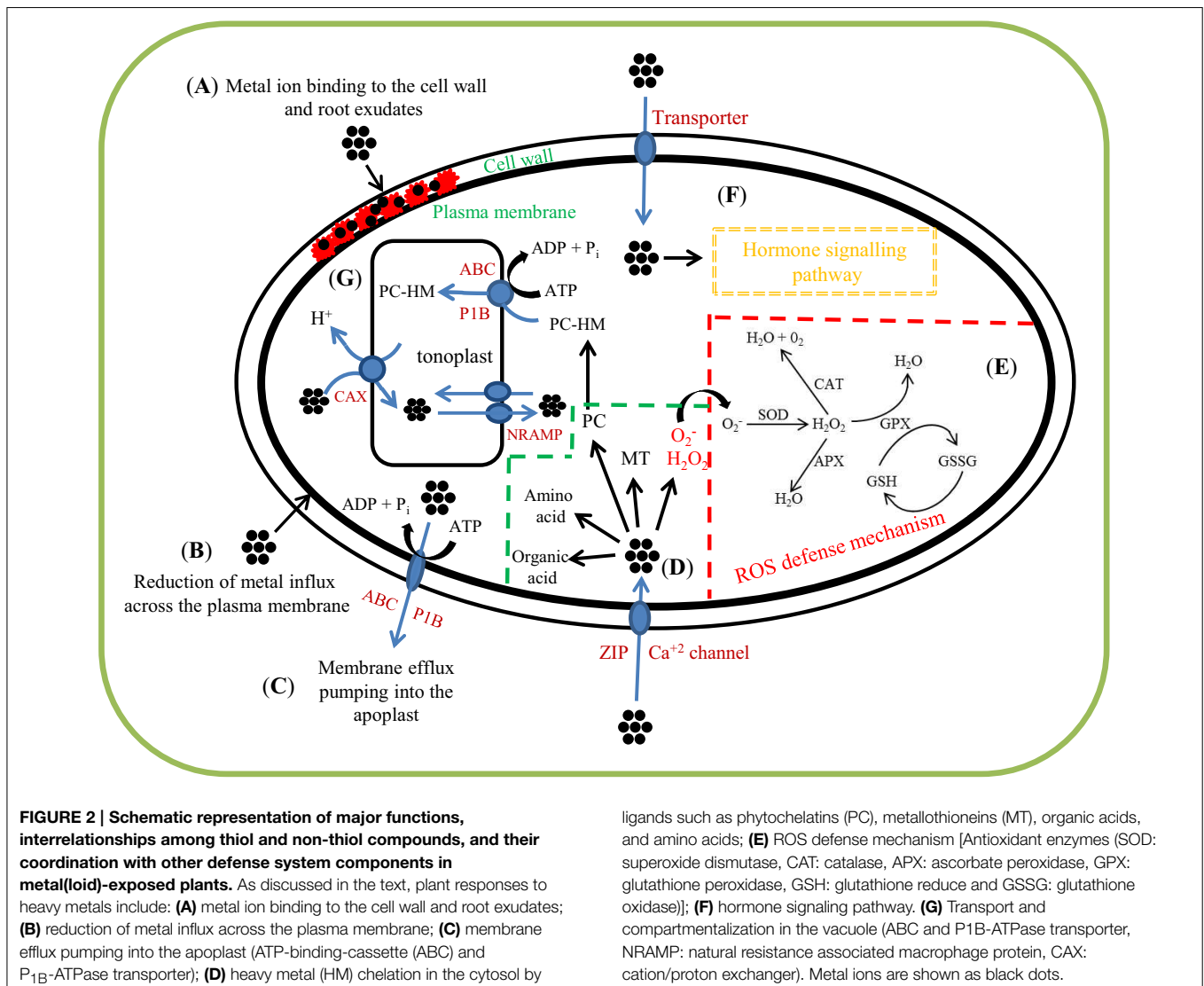
Organic Acids
Overview
Organic acid (OAs) such as citrate, malate, oxalate, malonate, aconitate, and tartrate are low molecular weight weak-acidic compounds, possess at least one carboxyl group, and are termed as oxygen-donor metal ligands. Some of these compounds are present in all plant cells as intermediates of the tricarboxylic acid cycle (TCA), the main respiratory pathway involved in the oxidation of pyruvate (Trejo-Tellez et al., 2012). OAs potentially perform multiple functions in the rhizosphere. Contingent to the number of carboxylic groups and dissociation properties, OAs can carry varying negative charge, thereby allowing the complexation of metal cation in solution and displacement of anions from the soil-matrix (Jakkeral and Kajjidoni, 2011). Present in considerable amounts, citrate belongs to the key metabolites in plant cells. Lemons, wild strawberries and spinach leaves contain from 8 to 15% citrate, based on dry weight (Popova and Pinheiro de Carvalho, 1998). Metabolism of citrate in plants is carried out by several metabolic pathways located in different cellular compartments. Citrate has been extensively reported to be involved in carbon metabolism (as an intermediate) and plant-tolerance to varied stresses of abiotic (metals, nutrient deficiencies) and biotic (plant-microbe interactions operating at the rhizosphere) types (reviewed by Trejo-Tellez et al., 2012).

Oxalate, C2 dicarboxilic acid anion is one of the strong OAs and a common constituents of plants. Though oxalate can be found in relatively small amounts in plants, it can be accumulated at high levels in several plants species (called extreme oxalate accumulators; can exhibit >3–18% oxalate based on their dry weight) from the families Caryophyllaceae, Chenopodiaceae, and Polygonaceae (Massey, 2003). Since oxalate can combine with various plant ions to from soluble or insoluble compounds, oxalate has been suggested to balance the excess of various inorganic cations (such as K^+, Na^+, NH_4^+, Ca^{++}, and Mg^{++}) over anions (such as NO_3^-, Cl^-, $H_2PO_4^-$, and SO_4^{2-}) (reviewed by Çalişkan, 2000). The role of oxalic acid in Al-tolerance has been well-documented (Furukawa et al., 2007; Liu et al., 2009; Maron et al., 2010; Yokosho et al., 2010). The dicarboxylic acid malate (an intermediate of the TCA cycle), an important plant metabolite, can be present in all cell types, and accumulated in plants to the levels up to 350 mM concentration. Malate in plants is involved in photosynthesis (C3, C4, and CAM plants), respiration and energy metabolism, fatty acid oxidation, stomatal, and pulvinual movement, lignin biosynthesis, nitrogen fixation, amino acid biosynthesis, ion balance, P- and Fe-uptake, and Al-tolerance (reviewed by Finkemeier and Sweetlove, 2009).

Metal(loid)-Specificity and -Chelation Mechanisms
Metal-complexation with OAs has been argued to have potential role in the long distance xylem transport of heavy metals (Rascio and Navari-Izzo, 2011). Among the various OAs studied in plants, citrate has a high capacity to chelate metal ions and has been well-documented in the case of Fe and Al (Clemens, 2001; Singh and Chauhan, 2011). However, other metals such as Zn, Co, Ni, and Cd also exhibit their strong affinity for citrate. Cd-citrate complexes were evidenced in the xylem sap of *Arabidopsis hallerii* (Ueno et al., 2008). Involvement of citrate was evidenced in Cu-exclusion mechanisms in non-accumulators (reviewed by Mehes-Smith et al., 2013) and Ni-exclusion (Hall, 2002). The role of Ni-complexation with citric acid in Ni-uptake and hyperaccumulation has been reported (Boominathan and Doran, 2003). Although exudation of OAs is common Al-tolerance mechanism in different plant species, there are species-specific peculiarities worth noting (Simões et al., 2012). In general, citrate has the maximum ability followed by malate and oxalate to alleviate Al-toxicity (Singh and Chauhan, 2011). The mechanism of Al-tolerance in *Sorghum bicolor*, *Glycine max*, *Zea mays*, and *Hordeum vulgare* involves mainly citrate exudation/release (Furukawa et al., 2007; Maron et al., 2010). Similarly, citrate exudation has also been found to contribute to Al-tolerance in *T. aestivum*, *Arabidopsis*, and rye (Liu et al., 2009; Yokosho et al., 2010). In *O. sativa*, citrate exudation (Yokosho et al., 2011) as well as symplastic mechanisms are likely to contribute to the extreme Al-tolerance in this species (Huang et al., 2009b). A correlation between citric acid exudation and Al-tolerance was detected by Miyasaka et al. (1991) in *Phaseolus vulgaris*. Co-occurrence of different Al-tolerance mechanisms has also been reported in some species. In *Z. mays*, root oxalate (Kidd et al., 2001) and citrate (Piñeros et al., 2002) exudation are likely involved in Al-tolerance. However, Piñeros et al. (2005) observed

63

FIGURE 2 | Schematic representation of major functions, interrelationships among thiol and non-thiol compounds, and their coordination with other defense system components in metal(loid)-exposed plants. As discussed in the text, plant responses to heavy metals include: **(A)** metal ion binding to the cell wall and root exudates; **(B)** reduction of metal influx across the plasma membrane; **(C)** membrane efflux pumping into the apoplast (ATP-binding-cassette (ABC) and P_{1B}-ATPase transporter); **(D)** heavy metal (HM) chelation in the cytosol by ligands such as phytochelatins (PC), metallothioneins (MT), organic acids, and amino acids; **(E)** ROS defense mechanism [Antioxidant enzymes (SOD: superoxide dismutase, CAT: catalase, APX: ascorbate peroxidase, GPX: glutathione peroxidase, GSH: glutathione reduce and GSSG: glutathione oxidase)]; **(F)** hormone signaling pathway. **(G)** Transport and compartmentalization in the vacuole (ABC and P1B-ATPase transporter, NRAMP: natural resistance associated macrophage protein, CAX: cation/proton exchanger). Metal ions are shown as black dots.

a low correlation between citrate exudation and Al tolerance in *Z. mays*, suggesting that this species has other complementary mechanisms enabling them to tolerate Al stress. Exposure of cells of the Co-hyperaccumulator *Crotalaria cobalticola* and non-accumulators *Raufolia serpentina*, and *Silene cucubalus* to Co-ions resulted in an increase of citrate, indicating the involvement OA in the complexation of metal ions (Oven et al., 2002). The Al-activated mechanism of malate exudation is well-described in a number of plants including *B. napus* (Ligaba et al., 2006), *A. thaliana* (Hoekenga et al., 2006), *T. aestivum* (Sasaki et al., 2004), and rye (*Secale cereale*) (Collins et al., 2008). Recently, Zhu et al. (2011) showed that Cd-induced oxalate secretion from root apex is associated with Cd exclusion and resistance in *L. esculentum*.

Considering mechanisms underlying OAs-assisted metal-chelation, OAs confer metal-tolerance by transporting metals through the xylem and sequestrating ions in the vacuole, but they have multiple additional roles in the cell (reviewed by Fernie and Martinoia, 2009; Finkemeier and Sweetlove, 2009; Yang

et al., 2013). Mechanism of metal-tolerance and detoxification in plants can be divided into two categories: external exclusion and internal tolerance. In the external detoxification process, organic acids excreted from plant roots may form stable metal–ligand complexes with metal ion and change their mobility and bioavailability, thus preventing the metal ions from entering plants or avoiding their accumulation in the sensitive sites of roots. In internal metal-detoxification, OAs may chelate with metal in the cytosol, where the ions can be transformed into a non-toxic or less toxic form (Clemens, 2001; Hall, 2002). The chelation of metals with ligands, such as OAs, amino acids and thiols facilitates the movements of heavy metals from roots to shoots (Zacchini et al., 2009). The xylem cell wall has a high cation exchange capability, thus the movement of metal cations is severely retarded when the metals are not chelated by ligands. OAs are involved in the translocation of Cd in the species *Brassica juncea* (Salt et al., 1999). OA-mediated Al stress tolerance has been well-studied in plants (Ma et al., 2001; Singh and Chauhan, 2011; Delhaize et al., 2012).

Amino Acids and their Derivatives

Overview

Due to metal-binding capacity, amino acids and their derivatives may be deployed in response to metal-toxicity and in conferring to plants resistance to toxic levels of metal ions (Manara, 2012). However, a clear correlation between metal accumulation and the production of these compounds has not been established yet. Some of the amino acids, e.g., glycinebetaine (betaine), proline (Pro), histidine (His), cysteine (Cys), arginine (Arg), glutamate (Glu), nicotianamine (NA), and the polyamines (spermidine, Spd; spermine, Spm; putrescine, Put), are synthesized in the small (milimollar range) amount in response to metal stress (**Figure 1**). Thus, in many cases, nitrogen (N) metabolism is vital to the response of plants to metals (Sharma and Dietz, 2006). Based on several studies on different plants, chelation of metals by previous compounds and subsequent compartmentalization of the complexes formed with varied metals are well-established mechanisms for the detoxification of and tolerance to excess metals in plants (Hall, 2002; Sharma and Dietz, 2006).

Betaines are quaternary ammonium compounds (QACs) which contain a carboxylic acid group. They may be generally regarded as fully N-methylated amino or imino acids. There are several kinds of betaine among which glycine betaine (GB) is the most common. GB, also called as original betaine (N,N,N-trimethylglycine) was first discovered from *Beta vulgaris* which is later found to be distributed in microorganisms, plants and animals. It is one of the most abundant quaternary ammonium compounds those are accumulated in plants during dehydration-promoting conditions (Ashraf and Foolad, 2007). The role of GB as a significant osmoprotectant, ROS-scavenger, and metal-chelator has been reported in metal-exposed plants (Sharma and Dietz, 2006; Theriappan et al., 2011; Asgher et al., 2013; Kumchai et al., 2013; Gill et al., 2014). The other non-proteinogenic amino acid nicotianamine (NA) is ubiquitous in higher plants, and is considered as a key element in plant metal chelation and homeostasis (Takahashi et al., 2003; Rellán-Álvarez et al., 2008). The first step of NA biosynthesis is the formation of *S*-adenosylmethionine (SAM) from methionine by the action of *S*-adenosylmethionine synthetase (SAMS) (Mori et al., 2007). Arginine (Arg) is the most functionally diverse amino acid in living cells. Thus, role of Arg has come into light due to its multiple metabolic fates. Apart from serving as a constituent of proteins, Arg is a precursor for biosynthesis of other substances like polyamines (PAs), agmatine and Pro, Glu and nitric oxide (NO) those play vital role in metal stress tolerance (Liu et al., 2006; Nasibi et al., 2013). Arg biosynthesis in plant occurs through ornithine (Orn) which comes from few steps conversion of Glu involving five enzymes (Verma and Zhang, 1999). These compounds including NA, PAs, Pro, Glu, and NO play vital role in metal chelation and detoxification in plants (Hasanuzzaman and Fujita, 2013; Hasanuzzaman et al., 2013, 2014).

PAs are ubiquitous low molecular weight polycationic aliphatic amines have roles in plant growth, development and senescence. Diamine Put $[NH_2(CH_2)_4NH_2]$, triamine Spd $[NH_2(CH_2)_3NH(CH_2)_4NH_2]$, tetramine Spm $[NH_2(CH_2)_3NH(CH_2)_4NH(CH_2)_3NH_2]$ are most common PAs in higher plants which exist as soluble conjugated, and insoluble

bound forms and differential forms of PAs function differently (Lefevre et al., 2001). Some other PAs homospermidine, 1,3-diaminopropane, cadaverine, and canavalmine also common in some plants, animals, algae, and bacteria (Valero et al., 2002). Diversified properties of PAs including acid neutralizing, antioxidant properties, membrane and cell wall stabilizing abilities make those potent protectants against environmental stresses (Zhao and Yang, 2008). Both endogenous PAs and exogenous application of PAs confer tolerance against different stresses including metals (Groppa et al., 2003; Wang et al., 2007; Hasanuzzaman et al., 2014).

Metal(loid)-Specificity and -Chelation Mechanisms

Literature is scarce on the specificity of amino acids and their derivatives to varied metals. However, plants exposed to varied metals (such as Cd, Cu, Ni, and Zn) can accumulate and synthesize different N-containing metabolites including Pro, amino acids, and oligopeptides, betaine, PAs, and NA. Pro and His have metal-binding, antioxidant, and signaling functions and can be accumulated in plants in response to different metals including As, Cd, Cu, Hg, and Ni (Kerkeb and Krämer, 2003; Sharma and Dietz, 2006; Irtelli et al., 2009; Richau and Schat, 2009; Richau et al., 2009; Theriappan et al., 2011; Ahmad and Gupta, 2013; Anjum et al., 2014b; Gill et al., 2014). NA and His/Pro were among the most important Cu-chelators in xylem sap of *Brassica carinata* under conditions of Cu deficiency and excess, respectively (Irtelli et al., 2009). Elevated accumulation of NA was evident different plants exposed to a number of metals such as Cd, Cu, Fe, Ni, and Zn (Takahashi et al., 2003; Vacchina et al., 2003; Kim et al., 2005; Irtelli et al., 2009; Kawachi et al., 2009; reviewed by Hassan and Aarts, 2011 and Mehes-Smith et al., 2013). In fact, the presence of six functional groups in NA allows its octahedral coordination and an optimal structure ideal for chelation of metal ions (Rellán-Álvarez et al., 2008). Notably, the pK of the resulting "metal-NA complexes" as well as the pH of the solution (with most metals being chelated at neutral or basic pH values) were considered to significantly control the ability of NA to chelate metals (Rellán-Álvarez et al., 2008). Apart from acting as an antioxidant, PAs function mainly as signaling molecule and can activate metal detoxification mechanisms (Sharma and Dietz, 2006). PAs are strongly supported to stabilize and protect membrane from toxic effects of metal ions specially the redox active metals (Sharma and Dietz, 2006). As a cation PAs can mimic and compete for the binding with Mg^{2+} and Ca^{2+} on receptors, membranes and enzymes. Polyamines bind cations including Cu, Fe that protects cell. The roles of PAs as metal chelators are contradictory. But some other N-containing compounds like porphyrins and chlorophylls strongly bound Cu, Fe, Co, and Ni by forming complexes. Presences of complex groups in same molecule regulate chelation effects. That is why complexes of PAs with high number of N-groups supposed to enhance chelation mechanism (Løvaas, 1997).

Amino acids and their derivatives exhibit their affinity to different metals, play vital role in their chelation and subsequently confer metal stress tolerance in plants. However, potential mechanisms underlying amino acids and their derivatives-assisted metal-chelation are not so conclusive in the literature. Both Pro

65

and GB are potential osmoprotectants and they are mostly studied in plants grown under salinity and drought stress. However, role of Pro and GB in osmoprotection, ROS-scavenging, and metal-chelation has also been studied in many metal-exposed plants (Sharma and Dietz, 2006; Theriappan et al., 2011; Asgher et al., 2013; Kumchai et al., 2013; Gill et al., 2014). In addition, involvement of the elevated level of Pro in regulation of expression of genes of PCS, metallothionine-2 (MT-2), glutathione reductase (GR), and glutathione synthetase (GS) was recently reported in As-exposed plants (Ahmad and Gupta, 2013). Though Pro and GB do not take part directly in metal-chelation, they stabilize native state of proteins by regulating their water and hence these osmoprotectants (especially Pro) help in maintaining the conformational characteristics and integrity of proteins (Paleg et al., 1981). It may happen due to the capacity of Pro to increase surface tension of water and thus can force water-protein interfaces into contact. This promotes proteins to maintain more native/folded configuration (Arakawa and Timasheff, 1985). Among the amino acids Pro accumulation is generally the highest under metal exposure which may be more than 20-fold in some species like *S. vulgaris* (Sharma and Dietz, 2006). However, their accumulation also varied depending on the metals where the plants were grown. Increased level of Pro was observed in *B. oleracea* in presence of Cd and Hg as reported by Theriappan et al. (2011). The role of Pro in the chelation of metals was reviewed by Sharma and Dietz (2006). One of the important role of Pro is the enhancement of endogenous GSH level from which PCs are synthesized, where the metal binds to the constitutively expressed enzyme PC synthase (PCS), thereby activating it to catalyze the conversion of GSH to PC (Zenk, 1996). Pro-mediated enzyme-protection can be possible via Pro-assisted reduction of free metal ion activity as a result of "metal(Zn/Cd)-Pro-complex" formation (Sharma et al., 1998).

Metal stress tolerance is enhanced by PAs as a result of their multiple roles such as the regulation of endogenous hormones (including IAA; abscisic acid, ABA) and antioxidants or ROS-scavengers (Groppa et al., 2007; Wang et al., 2007; Zhao et al., 2008; Choudhary et al., 2012a). Additionally, a number of PA-gene-expressing transgenic plants have been developed exhibiting enhanced metal-tolerance (**Table 1**). However, a direct role of PAs in metal-chelation has been least explored. To this end, Put-mediated activation of long-distance Ni-transport within the plant was argued to enhance plant-Ni tolerance (Shevyakova et al., 2011). Spd-induced mitigation of Cr-toxicity was related with reduced Cr-uptake and enhanced titers of PCs (Choudhary et al., 2012b). Put was reported to exhibit a selective effect on ion flux in Cd and Pb exposed plant leaves (Lakra et al., 2006). In many studies, NA was found to play a vital role in Cu-complexation in plants (Takahashi et al., 2003; Kim et al., 2005; Irtelli et al., 2009). Role of NA in the intracellular delivery of metals (and also plant reproductive development) has been reported (Takahashi et al., 2003). In Ni-hyperaccumulator, *T. caerulescens*, NA was found to chelate Ni in the xylem as a response to toxic levels of external Ni, and eventually provide Ni-tolerance (Vacchina et al., 2003). Additionally, NA was reported to perform the chelation and transportation of Fe and few divalent metal ions like Zn, Ni, and Cu in plants (reviewed by Hassan and Aarts,

2011). High levels of Zn, Cd, Cu, Fe, and/or Ni can significantly induce the expression of NA synthase genes (responsible for the synthesis of NA by trimerization of S-adenosylmethionine) (reviewed by Hassan and Aarts, 2011; Mehes-Smith et al., 2013). Over-expression of the *T. caerulescens* NAS3 gene in the Ni-excluder *A. thaliana* was reported to improve its Ni-tolerance and Ni-accumulation in their aerial organs (Pianelli et al., 2005). Similarly, overexpression of the NAS3 gene led to increased accumulation of Fe, Zn, and Cu in *O. sativa* (Kawachi et al., 2009).

Histidine (His) is a major N-donor ligand important for metal chelation in (metal hyperaccumulator) plants. Having carboxyl, amino, and imidazole groups as major structural components, His has been considered as a versatile chelator of metals (such as Ni) in plants (Callahan et al., 2006). Metal-chelation role of free His has been extensively reported in plants exposed to varied metals including Ni (Kerkeb and Krämer, 2003; Richau and Schat, 2009; Richau et al., 2009). Nevertheless, the role of elevated free root cell-His in reduced Ni-vacuolar sequestration and enhanced Ni-xylem loading was evidenced (Richau et al., 2009; Richau and Schat, 2009). To this end, higher free His concentration in roots but less Ni-in root vacuoles were evidenced in *T. caerulescens* (Ni-hyperaccumulator) when compared to *Thlaspi arvense* (non-Ni hyperaccumulator) (Richau et al., 2009). It was advocated that the His-Ni complexes were much less taken up by vacuoles than free Ni ions. Further, an inhibited vacuolar sequestration of "His-Ni complexes" in *T. caerulescens* roots was argued as a result of a higher increase in free His therein (hence an enhanced His-mediated Ni-xylem loading) compared to free Ni in non-Ni-hyperaccumulator *T. arvense* (Richau and Schat, 2009; Richau et al., 2009). In Ni-exposed *Alyssum lesbiacum* and *B. juncea*, Ni uptake was not highly correlated with His uptake but the release of Ni into the xylem was associated with a concomitant release of His from an increased root free His pool (Kerkeb and Krämer, 2003). However, in *Alyssum montanum* (and also in *B. juncea*), these authors evidenced a role of exogenously applied His in conferring enhanced Ni-tolerance possibly as a result of enhanced Ni-flux into the xylem. Enhanced tolerance to excess Ni in transgenic *A. thaliana* overexpressing *StHisG* (*Salmonella typhimurium* ATP phosphoribosyl transferase enzyme) was argued due to the accumulation of about 10-fold higher His level (vs. wild type) (Wycisk et al., 2004). A comprehensive study on the composition of amino acids under Cu stress was done by Irtelli et al. (2009). Among the amino acids His/Pro was found to be the most important Cu chelator in xylem sap of *B. carinata* under Cu toxicity. However, the accumulation of amino acids was dependent on the dose of Cu applied to plants. When *B. carinata* was treated with $5\,\mu M$ $CuSO_4$, the accumulation of His, threonine, Gln, glycine, Pro, and methionine was 140, 22, 7, 23, 6, and $13\,\mu M$, respectively which could make about 67, 42, 45, 52, 60, and 33% complexation of $0.94\,\mu mol$ Cu under a pH of 5.8 (Irtelli et al., 2009). For every case, the accumulation of amino acids was pH dependent. More importantly, in the absence of His, Pro was found to play a very important role in Cu binding and the role of other amino acids (threonine, Gln, glycine, and methionine were negligible in presence of His and Pro (Irtelli et al., 2009). Although other amino acids such as NA was not

efficiently involved in the response to excess of Cu but it participates in Cu-transport to the shoots in conditions of deficiency (Irtelli et al., 2009). An amino acid derivative namely 2-amino-3-(8-hydroxyquinolin-3-yl)propanoic acid (HQ-Ala) was reported to form highly stable complexes with most transition metal ions via its metal ion chelating group 8-hydroxyquinoline Lee et al. (2009). Cys can also perform a direct chelation of metals (such as Cd) by synthesizing methionine and GSH/PCs that in turn can sequester metals and provide a higher antioxidant defense in plants (Dominguez-Solis et al., 2004).

Conclusions and Future Prospects

Plant tolerance to metal-load-accrued impacts largely decides the efficiency and success of a metal-remediation system (Vangronsveld et al., 2009; Maestri et al., 2010; Anjum et al., 2014a,b,c). Hence, a sound knowledge is essential on the compounds that help plants to keep a tight control over concentrations of free metal(loid)s in cytoplasm. Considering recent reports, this paper attempted to present an orchestrated overview of both thiol- and non-thiol compounds that play significant roles in metal-chelation and maintain low concentrations of free metal(loid)s in cytoplasm. PCs and MTs are among the best characterized –SH compounds that strongly interact with metals, chelate them, reduce their concentrations in cytosol, and finally limit their potential toxicity (Cobbett and Goldsbrough, 2002; Solanki and Dhankhar, 2011; Hossain and Komatsu, 2013). To the other, OAs such as citrate, malate, oxalate, malonate, aconitate, and tartrate, and amino acids and their derivatives including GB, Pro, His, and NA are among non-GSH associated compounds and have also been extensively evidenced to contribute to metal-chelation in plants (Hall, 2002; Sharma and

Dietz, 2006; Jakkeral and Kajjidoni, 2011). Both thiol- and non-thiol compounds are functionally related, and may coordinate with other defense system components in order to chelate and/or detoxify and tolerate potential metal impact in plants (**Figure 2**). The reports appraised herein evidenced extensive studies on thiol-compounds in particular context with metal-tolerance in plants; in contrast, reports on non-thiol compounds is rare. Nevertheless, the literature reviewed herein points toward the need of more molecular-genetic studies in order to get more insights into synthesis pathways, metal-specificity, and biological and non-biological factors responsible for the induction/expression of, and potential coordination among mechanisms underlying thiol- and non-thiol compounds-assisted metal-chelation. Together, the suggested studies will help to develop at large scale the transgenic plants with exceptional capacity to extract, chelate different metals and avert their potential toxic consequences.

References

Ahmad, M. A., and Gupta, M. (2013). Exposure *of Brassica juncea* (L) to arsenic species in hydroponic medium: comparative analysis in accumulation and biochemical and transcriptional alterations. *Environ. Sci. Pollut. Res.* 20, 8141–8150. doi: 10.1007/s11356-013-1632-y

Ahner, B. A., Kong, S., and Morel, F. M. M. (1995). Phytochelatin production in marine algae. 1. An interspecies comparison. *Limnol. Ocenogr.* 40, 649–657. doi: 10.4319/lo.1995.40.4.0649

Ali, H., Khan, E., and Sajad, M. A. (2013). Phytoremediation of heavy metals–concepts and applications. *Chemosphere* 91, 869–881. doi: 10.1016/j.chemosphere.2013.01.075

Alloway, B. (2013). "Heavy metals and metalloids as micronutrients for plants and animals," in *Heavy Metals in Soils*, ed B. J. Alloway (Dordrecht: Springer), 195–209.

Andra, S. S., Datta, R., Sarkar, D., Makris, K. C., Mullens, C. P., Sahi, S. V., et al. (2010). Synthesis of phytochelatins in vetiver grass upon lead exposure in the presence of phosphorus. *Plant Soil* 326, 171–185. doi: 10.1007/s11104-009-9992-2

Anjum, N. A., Ahamd, I., Mohmood, I., Pacheco, M., Duarte, A. C., Pereira, E., et al. (2012b). Modulation of glutathione and its related enzymes in plants' responses to toxic metals and metalloids–a review. *Environ. Exp. Bot.* 75, 307–324. doi: 10.1016/j.envexpbot.2011.07.002

Anjum, N. A., Aref, I. M., Duarte, A. C., Pereira, E., Ahmad, I., and Iqbal, M. (2014d). Glutathione and proline can coordinately make plants withstand the

joint attack of metal(loid) and salinity stresses. *Front. Plant Sci.* 5:662. doi: 10.3389/fpls.2014.00662

Anjum, N. A., Gill, S. S., and Gill, R. (2014b). *Plant Adaptation to Environmental Change: Significance of Amino Acids and their Derivatives, 1st Edn.* Wallingford, UK: CABI.

Anjum, N. A., Israr, M., Duarte, A. C., Pereira, M. E., and Ahmad, I. (2014c). *Halimione portulacoides* (L.) physiological/biochemical characterization for its adaptive responses to environmental mercury exposure. *Environ. Res.* 131, 39–49. doi: 10.1016/j.envres.2014.02.008

Anjum, N. A., Pereira, M. E., Ahmad, I., Duarte, A. C., Umar, S., and Khan, N. A. (2012a). *Phytotechnologies: Remediation of Environmental Contaminants*. Boca Raton, FL: CRC Press.

Anjum, N. A., Singh, H. P., Khan, M. I. R., Masood, A., Per, T. S., Negi, A. et al. (2015). Too much is bad – an appraisal of phytotoxicity of elevated plant-beneficial heavy metal ions. *Environ. Sci. Pollut. Res.* 22, 3361–3382. doi: 10.1007/s11356-014-3849-9

Anjum, N. A., Umar, S., and Chan, M. T. (2010). *Ascorbate-Glutathione Pathway and Stress Tolerance in Plants*. Dordrecht: Springer. doi: 10.1007/978-90-481-9404-9

Anjum, N. A., Umar, S., and Iqbal, M. (2014a). Assessment of cadmium accumulation, toxicity, and tolerance in Brassicaceae and Fabaceae plants – implications for phytoremediation. *Environ. Sci. Pollut. Res.* 21, 10286–10293. doi: 10.1007/s11356-014-2889-5

Arakawa, T., and Timasheff, S. N. (1985). The stabilization of proteins by osmolytes. *Biophys. J.* 47, 411–414. doi: 10.1016/S0006-3495(85)83932-1

Arrivault, S., Senger, T., and Kramer, U. (2006). The *Arabidopsis* metal tolerance protein AtMTP3 maintains metal homeostasis by mediating Zn exclusion from the shoot under Fe deficiency and Zn oversupply. *Plant J.* 46, 861–879. doi: 10.1111/j.1365-313X.2006.02746.x

Asgher, M., Khan, M. I. R., Iqbal, N., Masood, A., and Khan, N. A. (2013). Cadmium tolerance in mustard cultivars: dependence on proline accumulation and nitrogen assimilation. *J. Funct. Environ. Bot.* 3, 30–42. doi: 10.5958/j.2231-1750.3.1.005

Ashraf, M., and Foolad, M. R. (2007). Roles of glycine betaine and proline in improving plant abiotic stress resistance. *Environ. Exp. Bot.* 59, 206–216. doi: 10.1016/j.envexpbot.2005.12.006

Auguy, F., Fahr, M., Moulin, P., Brugel, A., Laplaze, L., El Mzibri, M., et al. (2013). Lead tolerance and accumulation in *Hirschfeldia incana*, a Mediterranean Brassicaceae from metalliferous mine spoils. *PLoS ONE* 8:e61932. doi: 10.1371/journal.pone.0061932

Baker, A. J. M., and Whiting, S. N. (2002). In search of the Holy Grail: a further step in understanding metal hyperaccumulation. *New Phytol.* 155, 1–4. doi: 10.1046/j.1469-8137.2002.00449_1.x

Bilecen, K., Ozturk, U. H., Duru, A. D., Sutlu, T., Petoukhov, M. V., Svergun, D. I., et al. (2005). *Triticum durum* metallothionein–Isolation of the gene and structural characterization of the protein using solution scattering and molecular modeling. *J. Biol. Chem.* 280, 13701–13711. doi: 10.1074/jbc.M412984200

Blindauer, C. A. (2008). Metallothioneins with unusual residues: histidines as modulators of zinc affinity and reactivity. *J. Inorg. Biochem.* 102, 507–521. doi: 10.1016/j.jinorgbio.2007.10.032

Bolan, N., Kunhikrishnan, A., Thangarajan, R., Kumpiene, J., Park, J., Makino, T., et al. (2014). Remediation of heavy metal (loid) s contaminated soils – to mobilize or to immobilize? *J. Hazard. Mater.* 266, 141–166. doi: 10.1016/j.jhazmat.2013.12.018

Boominathan, R., and Doran, P. M. (2003). Organic acid complexation, heavy metal distribution and the effect of ATPase inhibition in hairy roots of hyperaccumulator plant species. *J. Biotechnol.* 101, 131–146. doi: 10.1016/S0168-1656(02)00320-6

Bruns, I., Sutter, K., Menge, S., Neumann, D., and Krauss, G. J. (2001). Cadmium lets increase the glutathione pool in bryophytes. *J. Plant Physiol.* 158, 79–89. doi: 10.1078/0176-1617-00071

Bittsánszkya, A., Kfmives, T., Gullner, G., Gyulai, G., Kiss, J., Heszky, L., et al. (2005). Ability of transgenic poplars with elevated glutathione content to tolerate zinc(2+) stress. *Environ. Int.* 31, 251–254. doi: 10.1016/j.envint.2004.10.001

Çalişkan, M. (2000). The metabolism of oxalic acid. *Turk. J. Zool.* 24, 103–106.

Callahan, D. L., Baker, A. J. M., Kolev, S. D., and Wedd, A. G. (2006). Metal ion ligands in hyperaccumulating plants. *J. Biol. Inorg. Chem.* 11, 2–12. doi: 10.1007/s00775-005-0056-7

Cánovas, D., Vooijs, R., Schat, H., and De Lorenzo, V. (2004). The role of thiol species in the hypertolerance of *Aspergillus* sp. P37 to arsenic. *J. Biol. Chem.* 279, 51234–51240. doi: 10.1074/jbc.M408622200

Choudhary, S. P., Kanwar, M., Bhardwaj, R., Yu, J. Q., and Tran, L. S. P. (2012b). Chromium stress mitigation by polyamine-brassinosteroid application involves phytohormonal and physiological strategies in *Raphanus sativus* L. *PLoS ONE* 7:e33210. doi: 10.1371/journal.pone.0033210

Choudhary, S. P., Oral, H. V., Bhardwaj, R., Yu, J. Q., and Tran, L. S. P. (2012a). Interaction of brassinosteroids and polyamines enhances copper stress tolerance in *Raphanus sativus*. *J. Exp. Bot.* 63, 5659–5675. doi: 10.1093/jxb/ers219

Clemens, S. (2001). Molecular mechanisms of plant metal tolerance and homeostasis. *Planta* 212, 475–486. doi: 10.1007/s004250000458

Clemens, S. (2006). Evolution and function of phytochelatin synthases. *J. Plant Physiol.* 163, 319–332. doi: 10.1016/j.jplph.2005.11.010

Cobbett, C., and Goldsbrough, P. (2002). Phytochelatins and metallothioneins: roles in heavy metal detoxification and homeostasis. *Annu. Rev. Plant Biol.* 53, 159–182. doi: 10.1146/annurev.arplant.53.100301.135154

Collins, N. C., Shirley, N. J., Saeed, M., Pallotta, M., and Gustafson, J. P. (2008). An ALMT1 gene cluster controlling aluminum tolerance at the Alt4 locus of rye (*Secale cereale* L.). *Genetics* 179, 669–682. doi: 10.1534/genetics.107.083451

Courbot, M., Diez, L., Ruotola, R., Chalot, M., and Leroy, P. (2004). Cadmium-responsive thiols in the ectomycorrhizal fungus *Paxillus involutus*. *Appl. Environ. Microbiol.* 70, 7413–7417. doi: 10.1128/AEM.70.12.7413-7417.2004

Dago, A., González, I., Ariño, C., Díaz-Cruz, J. M., and Esteban, M. (2014). Chemometrics applied to the analysis of induced phytochelatins in *Hordeum vulgare* plants stressed with various toxic non-essential metals and metalloids. *Talanta* 118, 201–209. doi: 10.1016/j.talanta.2013.09.058

Deinlein, U., Weber, M., Schmidt, H., Rensch, S., Trampczynska, A., Hansen, T. H., et al. (2012). Elevated nicotianamine levels in *Arabidopsis halleri* roots play a key role in Zn hyperaccumulation. *Plant Cell* 24, 708–723. doi: 10.1105/tpc.111.095000

Delhaize, E., Ma, J. F., and Ryan, P. R. (2012). Transcriptional regulation of aluminium tolerance genes. *Trend Plant Sci.* 17, 341–348. doi: 10.1016/j.tplants.2012.02.008

Dhankher, O. P., Li, Y., Rosen, B. P., Shi, J., Salt, D., Senecoff, J. F., et al. (2002). Engineering tolerance and hyperaccumulation of arsenic in plants by combining arsenate reductase and -glutamylcysteine synthetase expression. *Nat. Biotechnol.* 20, 1140–1145. doi: 10.1038/nbt747

Dominguez-Solis, J. R., Lopez-Martin, M. C., Ager, M. C., Ynsa, M. D., Romero, L. C., and Gotor, C. (2004). Increased cysteine availability is essential for cadmium tolerance and accumulation in *Arabidopsis thaliana*. *Plant Biotechnol. J.* 2, 469–476. doi: 10.1111/j.1467-7652.2004.00092.x

Dorcak, V., and Krezel, A. (2003). Correlation of acide-base chemistry of phytochelatin PC2 with its coordination properties towards the toxic metal ion Cd (II). *Dalton. Trans.* 11, 2253–2259. doi: 10.1039/b301357j

Douchkov, D., Gryczka, C., Stephan, U. W., Hell, R., and Bäumlein, H. (2005). Ectopic expression of nicotianamine synthase genes results in improved iron accumulation and increased nickel tolerance in transgenic tobacco. *Plant Cell Environ.* 28, 365–374. doi: 10.1111/j.1365-3040.2005.01273.x

Duan, G. L., Hu, Y., Lui, W. J., Kneer, R., Zhao, F. J., and Zhu, Y. G. (2011). Evidence for a role of phytochelatins in regulating arsenic accumulation in rice grains. *Environ. Exp. Bot.* 71, 416–421. doi: 10.1016/j.envexpbot.2011.02.016

Dupae, J., Bohler, S., Noben, J. P., Carpentier, S., Vangronsveld, J., and Cuypers, A. (2014). Problems inherent to a meta-analysis of proteomics data: a case study on the plants' response to Cd in different cultivation conditions. *J. Proteomics* 108, 30–54. doi: 10.1016/j.jprot.2014.04.029

Ellis, D. R., and Salt, D. E. (2003). Plants, selenium and human health. *Curr. Opin. Plant Biol.* 6, 273–279. doi: 10.1016/S1369-5266(03)00030-X

Ernst, W. H. O., Krauss, G. J., Verkleij, J. A. C., and Wesenberg, D. (2008). Interaction of heavy metals with the sulphur metabolism in angiosperms from an ecological point of view. *Plant Cell Environ.* 31, 123–143. doi: 10.1111/j.1365-3040.2007.01746.x

Estrella-Gómez, N. E., Sauri-Duch, E., Zapata-Pérez, O., and Santamaría, J. M. (2012). Glutathione plays a role in protecting leaves of *Salvinia minima* from Pb^{2+} damage associated with changes in the expression of *SmGS* genes and increased activity of GS. *Environ. Exp. Bot.* 75, 188–194. doi: 10.1016/j.envexpbot.2011.09.001

Feretti, L., Elviri, L., Pelinghelli, M. A., Prediery, G., and Tegoni, M. (2007). Glutathione and N-acetylcysteinylglycine: protonation and $Zn2^+$ complexation. *J. Inorg. Biochem.* 101, 1442–1456. doi: 10.1016/j.jinorgbio.2007.06.020

Fernández, R., Bertrand, A., García, J. I., Tamés, R. S., and González, A. (2012). Lead accumulation and synthesis of non-protein thiolic peptides in selected clones of *Melilotus alba* and *Melilotus officinalis*. *Environ. Exp. Bot.* 78, 18–24. doi: 10.1016/j.envexpbot.2011.12.016

Fernie, A. R., and Martinoia, E. (2009). Malate. Jack of all trades or master of a few? *Photochemistry* 70, 828–832. doi: 10.1016/j.phytochem.2009.04.023

Finkemeier, I., and Sweetlove, L. J. (2009). The role of malate in plant homeostasis. *Biol. Rep.* 1:47. doi: 10.3410/B1-47

Freisinger, E. (2008). Plant MTs-long neglected members of the metallothionein superfamily. *Dalton. Trans.* 47, 6663–6675 doi: 10.1039/b809789e

Freisinger, E. (2011). Structural features specific to plant metallothioneins. *J. Biol. Inorg. Chem.* 16, 1035–1045. doi: 10.1007/s00775-011-0801-z

Furukawa, J., Yamaji, N., Wang, H., Mitani, N., Murata, Y., Sato, K., et al. (2007). An aluminum-activated citrate transporter in barley. *Plant Cell Physiol.* 48, 1081–1091. doi: 10.1093/pcp/pcm091

Gautam, N., Verma, P. K., Verma, S., Tripathi, R. D., Trivedi, P. K., Adhikari, B., et al. (2012). Genome-wide identification of rice class I metallothionein gene: tissue expression patterns and induction in response to heavy metal stress. *Funct. Integr. Genomics* 12, 635–647. doi: 10.1007/s10142-012-0297-9

68

Gekeler, W., Grill, E., Winnacker, E. L., and Zenk, M. H. (1988). Algae sequester heavy metals via synthesis of phytochelatin complexes. *Arch. Microbiol.* 150, 197–202. doi: 10.1007/BF00425162

Gill, S. S., Anjum, N. A., Ahmad, I., Pacheco, M., Duarte, A. C., Umar, S., et al. (2012). "Metal hyperaccumulation and tolerance in Alyssum, *Arabidopsis* and *Thlaspi*," in *The Plant Family Brassicaceae: Contribution Towards Phytoremediation*, eds N. A. Anjum, I. Ahmad, E. Pereira, A. C. Duarte, S. Umar, and N. A. Khan (Dordrecht: Springer), 99–137.

Gill, S. S., Gill, R., and Anjum, N. A. (2014). "Target osmoprotectants for abiotic stress tolerance in crop plants – glycine betaine and proline," in *Plant Adaptation to Environmental Change: Significance of Amino Acids and Their Derivatives*, eds N. A. Anjum, S. S. Gill, and R. Gill (Wallingford, CT: CAB International), 97–108.

Gonzalez-Mendoza, D., Moreno, A. Q., and Zapata-Perez, O. (2007). Coordinated responses of phytochelatin synthase and metallothionein genes in black mangrove, *Avicennia germinans*, exposed to cadmium and copper. *Aqu. Toxicol.* 83, 306–314. doi: 10.1016/j.aquatox.2007.05.005

Groppa, M. D., Benavides, M. P., and Tomaro, M. L. (2003). Polyamine metabolism in sunflower and wheat leaf discs under cadmium or copper stress. *Plant Sci.* 161, 481–488. doi: 10.1016/S0168-9452(01)00432-0

Groppa, M. D., Ianuzzo, M. P., Tomaro, M. L., and Benavides, M. P. (2007). Polyamine metabolism in sunflower plants under long-term cadmium or copper stress. *Amino Acids* 32, 265–275. doi: 10.1007/s00726-006-0343-9

Guo, J., Xu, L., Su, Y., Wang, H., Gao, S., Xu, J., et al. (2013). ScMT2-1-3, a metallothionein gene of sugarcane, plays an important role in the regulation of heavy metal tolerance/accumulation. *BioMed. Res. Int.* 2013:904769. doi: 10.1155/2013/904769

Guo, J., Xu, W., and Ma, M. (2012). The assembly of metals chelation by thiols and vacuolar compartmentalization conferred increased tolerance to and accumulation of cadmium and arsenic in transgenic *Arabidopsis thaliana*. *J. Hazard Mater.* 199–200, 309–313. doi: 10.1016/j.jhazmat.2011.11.008

Guo, W. J., Bundithya, W., and Goldsbrough, P. B. (2003). Characterization of the *Arabidopsis* metallothionein gene family: tissue-specific expression and induction during senescence and in response to copper. *New Phytol.* 159, 369–381. doi: 10.1046/j.1469-8137.2003.00813.x

Hall, J. L. (2002). Cellular mechanisms for heavy metal detoxification and tolerance. *J. Exp. Bot.* 53, 1–11. doi: 10.1093/jexbot/53.366.1

Hasanuzzaman, M., and Fujita, M. (2013). Exogenous sodium nitroprusside alleviate arsenic-induced oxidative stress in wheat seedlings by enhancing antioxidant defense and glyoxalase system. *Ecotoxicology* 22, 584–596. doi: 10.1007/s10646-013-1050-4

Hasanuzzaman, M., Gill, S. S., and Fujita, M. (2013). "Physiological role of nitric oxide in plants grown under adverse environmental conditions," in *Plant Acclimation to Environmental Stress*, eds N. Tuteja and S. S. Gill (New York, NY: Springer), 269–322.

Hasanuzzaman, M., Nahar, K., and Fujita, M. (2014). "Regulatory role of polyamines in abiotic stress tolerance in plants," in *Plant Adaptation to Environmental Change: Significance of Amino Acids and Their Derivatives*, eds N. A. Anjum, S. S. Gill, and R. Gill (Wallingford, CT: CAB International), 157–193.

Hassan, Z., and Aarts, M. G. M. (2011). Opportunities and feasibilities for biotechnological improvement of Zn, Cd or Ni tolerance and accumulation in plants. *Environ. Exp. Bot.* 72, 53–63. doi: 10.1016/j.envexpbot.2010.04.003

Hassinen, V. H., Tervahauta, A. I., Schat, H., and Kärenlampi, S. O. (2011). Plant metallothioneins–metal chelators with ROS scavenging activity? *Plant Biol.* 13, 225–232. doi: 10.1111/j.1438-8677.2010.00398.x

Hawrylak-Nowak, B., Dresler, S., and Wójcik, M. (2014). Selenium affects physiological parameters and phytochelatins accumulation in cucumber (*Cucumis sativus* L.) plants grown under cadmium exposure. *Sci. Hortic.* 172, 10–18. doi: 10.1016/j.scienta.2014.03.040

Haydon, M. J., Kawachi, M., Wirtz, M., Hillmer, S., Hell, R., and Krämer, U. (2012). Vacuolar nicotianamine has critical and distinct roles under iron deficiency and for zinc sequestration in *Arabidopsis*. *Plant Cell* 24, 724–737. doi: 10.1105/tpc.111.095042

Hoekenga, O. A., Maron, L. G., Piñeros, M. A., Cancado, G. M., and Shaff, J., et al. (2006). *AtALMT1*, which encodes a malate transporter, is identified as one of several genes critical for aluminum tolerance in *Arabidopsis*. *Proc. Natl. Acad. Sci. U.S.A.* 103, 9738–9743. doi: 10.1073/pnas.0602868103

Hossain, Z., and Komatsu, S. (2013). Contribution of proteomic studies towards understanding plant heavy metal stress response. *Front. Plant Sci.* 3:310. doi: 10.3389/fpls.2012.00310

Hu, S., Lau, K. W. K., and Wu, M. (2001). Cadmium sequestration in *Chlamydomonas reinhardtii*. *Plant Sci.* 161, 987–996. doi: 10.1016/S0168-9452(01)00501-5

Huang, C. F., Yamaji, N., Mitani, N., Yano, M., Nagamura, Y., and Ma, J. F. (2009b). A bacterial-type ABC transporter is involved in aluminum tolerance in rice. *Plant Cell* 21, 655–667. doi: 10.1105/tpc.108.064543

Huang, Z. Y., Li, L. P., Huang, G. L., Yan, Q. P., Shi, B., and Xu, X. Q. (2009a). Growth-inhibitory and metal binding proteins in *Chlorella vulgaris* exposed to cadmium or zinc. *Aquat. Toxicol.* 91, 54–61. doi: 10.1016/j.aquatox.2008.10.003

Ingle, R. A., Mugford, S. T., Rees, J. D., Campbell, M. M., and Smith, J. A. C. (2005). Constitutively high expression of the histidine biosynthetic pathway contributes to nickel tolerance in hyperaccumulator plants. *Plant Cell*, 17, 2089–2106. doi: 10.1105/tpc.104.030577

Inouhe, M. (2005). Phytochelatins. *Braz. J. Plant Physiol.* 17, 65–78. doi: 10.1590/S1677-04202005000100006

Irtelli, B., Petrucci, W. A., and Navari-Izzo, F. (2009). Nicotianamine and histidine/proline are, respectively, the most important copper chelators in xylem sap of *Brassica carinata* under conditions of copper deficiency and excess. *J. Exp. Bot.* 60, 269–277. doi: 10.1093/jxb/ern286

Jakkeral, S. A., and Kajjidoni, S. T. (2011). Root exudation of organic acids in selected genotypes under phosphorus deficient condition in blackgram (*Vigna mungo* L. Hepper). *Karnataka J. Agric. Sci.* 24, 316–319.

Jozefczak, M., Remans, T., Vangronsveld, J., and Cuypers, A. (2012). Glutathione is a key player in metal-induced oxidative stress defenses. *Int. J. Mol. Sci.* 13, 3145–3175. doi: 10.3390/ijms13033145

Kalinowska, R., and Pawlik-Skowrónska, B. (2010). Response of two terrestrial green microalgae (Chlorophyta, Trebouxiophyceae) isolated from Cu-rich and unpolluted soils to copper stress. *Environ. Pollut.* 158, 2778–2785. doi: 10.1016/j.envpol.2010.03.003

Kanneganti, V., and Gupta, A. K. (2008). Wall associated kinases from plants – an overview. *Physiol. Mol. Biol. Plant.* 14, 109–118. doi: 10.1007/s12298-008-0010-6

Kawachi, M., Kobae, Y., Mori, H., Tomioka, R., Lee, Y., and Maeshima, M. (2009). A mutant strain *Arabidopsis thaliana* that lacks vacuolar membrane zinc transporter MTP1 revealed the latent tolerance to excessive zinc. *Plant Cell Physiol.* 50, 1156–1170. doi: 10.1093/pcp/pcp067

Kerkeb, L., and Krämer, U. (2003). The role of free histidine in xylem loading of nickel in *Alyssum lesbiacum* and *Brassica juncea*. *Plant Physiol.* 131, 716–724. doi: 10.1104/pp102.010686

Kidd, P. S., Llugany, M., Poschenrieder, C., Gunse, B., and Barcelo, J. (2001). The role of root exudates in aluminium resistance and silicon-induced amelioration of aluminium toxicity in three varieties of maize (*Zea mays* L.). *J. Exp. Bot.* 52, 1339–1352. doi: 10.1093/jexbot/52.359.1339

Kim, S., Takahashi, M., Higuchi, K., Tsunoda, K., Nakanishi, H., Yoshimura, E., et al. (2005). Increased nicotianamine biosynthesis confers enhanced tolerance of high levels of metals, in particular nickel, to plants. *Plant Cell Physiol.* 46, 1809–1818. doi: 10.1093/pcp/pci196

Kopriva, S., Wiedemann, G., and Reski, R. (2007). Sulfate assimilation in basal land plants–what does genomic sequencing tell us? *Plant Biol.* 9, 556–564. doi: 10.1055/s-2007-965430

Kumchai, J., Huang, J. Z., Lee, C. Y., Chen, F. C., and Chin, S. W. (2013). Proline partially overcomes excess molybdenum toxicity in cabbage seedlings grown *in vitro*. *Genet. Mol. Res.* 12, 5589–5601. doi: 10.4238/2013.November.18.8

Lakra, N., Mishra, S. N., Singh, D. B., and Tomar, P. C. (2006). Exogenous putrescine effect on cation concentration in leaf of *Brassica juncea* seedlings subjected to Cd and Pb along with salinity stress. *J. Environ. Biol.* 27, 263–269.

Lal, N. (2010). "Molecular mechanisms and genetic basis of heavy metal toxicity and tolerance in plants," in *Plant Adaptation and Phytoremediation*, eds M. Ashraf, M. Ozturk, and M. S. A. Ahmad (Dordrecht: Springer), 35–58.

Lee, H. S., Spraggon, G., Schultz, P. G., and Wang, F. (2009). Genetic incorporation of a metal-ion chelating amino acid into proteins as a biophysical probe. *J. Am. Chem. Soc.* 131, 2481–2483. doi: 10.1021/ja808340b

Lee, M., Lee, K., Lee, J., Noh, E. W., and Lee, Y. (2005). AtPDR12 contributes to lead resistance in *Arabidopsis*. *Plant Physiol.* 138, 827–836. doi: 10.1104/pp.104.058107

Lefevre, I., Gratia, E., and Lutts, S. (2001). Discrimination between the ionic and osmotic components of salt stress in relation to free polyamine level in rice (*Oryza sativa*). *Plant Sci.* 16, 943–952. doi: 10.1016/S0168-9452(01)00485-X

Li, Y., Dankher, O. P., Carreira, L., Smith, A. P., and Meagher, R. B. (2006). The shoot-specific expression of γ-glutamylcysteine synthetase directs the longdistance transport of thiol-peptides to roots conferring tolerance to mercury and arsenic. *Plant Physiol.* 141, 288–298. doi: 10.1104/pp.105.074815

Li, Y., Dhankher, O., Carreira, L., Balish, R., and Meagher, R. (2005). Engineered overexpression of γ-glutamylcysteine synthetase in plants confers high level arsenic and mercury tolerance. *Environ. Toxicol. Chem.* 24, 1376–1386. doi: 10.1897/04-340R.1

Ligaba, A., Katsuhara, M., Ryan, P. R., Shibasaka, M., and Matsumoto, H. (2006). The *BnALMT1* and *BnALMT2* genes from rape encode aluminum-activated malate transporters that enhance the aluminum resistance of plant cells. *Plant Physiol.* 142, 1294–1303. doi: 10.1104/pp.106.085233

Liu, J. H., Nada, K., Honda, C., Kitashiba, H., and Wen, X. P. (2006). Polyamine biosynthesis of apple callus under salt stress. Importance of the arginine decarboxylase pathway in stress responses. *J. Exp. Bot.* 57, 2589–2599. doi: 10.1093/jxb/erl018

Liu, T., Liu, S., Guan, H., Ma, L., Chen, Z., Gu, H., et al. (2009). Transcriptional profiling of *Arabidopsis* seedlings in response to heavy metal lead (Pb). *Environ. Exp. Bot.* 67, 377–386. doi: 10.1016/j.envexpbot.2009.03.016

Løvaas, E. (1997). Antioxidant and metal-chelating effects of polyamines. *Adv. Pharmacol.* 38, 119–149. doi: 10.1016/S1054-3589(08)60982-5

Lv, Y., Deng, X., Quan, L., Xia, Y., and Shen, Z. (2013). Metallothioneins *BcMT1* and *BcMT2* from *Brassica campestris* enhance tolerance to cadmium and copper and decrease production of reactive oxygen species in *Arabidopsis thaliana*. *Plant Soil* 367, 507–519. doi: 10.1007/s11104-012-1486-y

Ma, J. F., Ryan, P. R., and Delhaize, E. (2001). Aluminium tolerance in plants and the complexing role of organic acids. *Trends Plant Sci.* 6, 273–278. doi: 10.1016/S1360-1385(01)01961-6

Maestri, E., Marmiroli, M., Visioli, G., and Marmiroli, N. (2010). Metal tolerance and hyperaccumulation: costs and trade-offs between traits and environment. *Environ. Exp. Bot.* 68, 1–13. doi: 10.1016/j.envexpbot.2009.10.011

Manara, A. (2012). "Plant responses to heavy metal toxicity," in *Plants and Heavy Metals*, ed A. Furini (New York, NY: Springer), 27–53.

Margoshes, M., and Vallee, B. L. (1957). A cadmium protein from equine kidney cortex. *J. Am. Chem. Soc.* 79, 4813–4814. doi: 10.1021/ja01574a064

Mari, S., and Lebrun, M. (2006). "Metal immobilization: where and how?," in *Molecular Biology of Metal Homeostasis and Detoxification: From Microbes to Man*, eds M. J. Tamàs and E. Martinoia (Berlin: Springer), 273–298.

Marmiroli, M., Pigoni, V., Savo-Sardaro, M. L., and Marmiroli, N. (2014). The effect of silicon on the uptake and translocation of arsenic in tomato (*Solanum lycopersicum* L.). *Environ. Exp. Bot.* 99, 9–17. doi: 10.1016/j.envexpbot.2013.10.016

Maron, L. G., Piñeros, M. A., Guimarães, C. T., Magalhaes, J. V., Pleiman, J. K., Mao, C., et al. (2010). Two functionally distinct members of the MATE (multi-drug and toxic compound extrusion) family of transporters potentially underlie two major aluminum tolerance QTLs in maize. *Plant J.* 61, 728–740. doi: 10.1111/j.1365-313X.2009.04103.x

Massey, L. (2003). Dietary influences on urinary oxalate and risk of kidney stones. *Front. Biosci.* 8:s584-94. doi: 10.2741/1082

Mehes-Smith, M., Nkongolo, K., and Cholewa, E. (2013). "Coping mechanisms of plants to metal contaminated soil," in *Environmental Change and Sustainability*, ed S. Steven (InTech-Open). doi: 10.5772/55124

Mejáre, M., and Bülow, L. (2001). Metal-binding proteins and peptides in bioremediation and phytoremediation of heavy metals. *Trends Biotechnol.* 19, 67–73. doi: 10.1016/S0167-7799(00)01534-1

Mench, M., Schwitzguebel, J. P., Schroeder, P., Bert, V., Gawronski, S., and Gupta, S. (2009). Assessment of successful experiments and limitations of phytotechnologies: contaminant uptake, detoxification and sequestration, and consequences for food safety. *Environ. Sci. Pollut. Res.* 16, 876–900. doi: 10.1007/s11356-009-0252-z

Mendoza-Cózatl, D. G., Butko, E., Springer, F., Torpey, J. W., Komives, E. A., Kehr, J., et al. (2008). Identification of high levels of phytochelatins, glutathione and cadmium in the phloem sap of *Brassica napus*. A role for thiol-peptides

in the long-distance transport of cadmium and the effect of cadmium on iron translocation. *Plant J.* 54, 249–259. doi: 10.1111/j.1365-313X.2008.03410.x

Mera, R., Torres, E., and Abalde, J. (2014). Sulphate, more than a nutrient, protects the microalga *Chlamydomonas moewusii* from cadmium toxicity. *Aquat. Toxicol.* 148, 92–103. doi: 10.1016/j.aquatox.2013.12.034

Merrifield, M. E., Chaseley, J., Kille, P., and Stillman, M. J. (2006). Determination of the Cd/S cluster stoichiometry in *Fucus vesiculosus* metallothionein. *Chem. Res. Toxicol.* 19, 365–375. doi: 10.1021/tx050206j

Minocha, R., Thangavel, P., Dhankher, O. P., and Long, S. (2008). Separation and quantification of monothiols and phytochelatins from a wide variety of cell cultures and tissues of trees and other plants using high performance liquid chromatography. *J. Chromatogr. A* 1207, 72–83. doi: 10.1016/j.chroma.2008.08.023

Miyasaka, S. C., George Buta, J., Howell, R. K., and Foy, C. D. (1991). Mechanism of aluminum tolerance in snapbeans: root exudation of citric acid. *Plant Physiol.* 96, 737–743. doi: 10.1104/pp.96.3.737

Morelli, E., and Scarano, G. (2001). Synthesis and stability of phytochelatins induced by cadmium and lead in the marine diatom *Phaeodactylum tricornutum*. *Mar. Environ. Res.* 52, 383–395. doi: 10.1016/S0141-1136(01)00093-9

Mori, S., Higuchi, K., Suzuki, K., Nishizawa, N., and Nakanishi, H. (2007). *Nicitianamine Synthase and Gene Encoding the Same*. United States Patent No. 7,192,755B1.

Murphy, A., and Taiz, T. (1995). Comparison of metallothionein gene expression and nonprotein thiols in ten *Arabidopsis* ecotypes. *Plant Physiol.* 109, 945–954 doi: 10.1104/pp.109.3.945

Nahar, K., Hasanuzzaman, M., Alam, M. M., and Fujita, M. (2015). Exogenous glutathione confers high temperature stress tolerance in mung bean (*Vigna radiata* L.) by modulating antioxidant defense and methylglyoxal detoxification system. *Environ. Exp. Bot.* 112, 44–54. doi: 10.1016/j.envexpbot.2014.12.001

Nasibi, F., Heidari, T., Asrar, Z., and Mansoori, H. (2013). Effect of arginine pretreatment on nickel accumulation and alleviation of the oxidative stress in *Hyoscyamus niger*. *J. Soil Sci. Plant Nutr.* 13, 680–689. doi: 10.4067/S0718-95162013005000054

Nath, S., Panda, P., Mishra, S., Dey, M., Choudhury, S., Sahoo, L., et al. (2014). Arsenic stress in rice: redox consequences and regulation by iron. *Plant Physiol. Biochem.* 80, 203–210. doi: 10.1016/j.plaphy.2014.04.013

Nishikawa, K., Onodera, A., and Tominaga, N. (2006). Phytochelatins do not correlate with the level of Cd accumulation in *Chlamydomonas* spp. *Chemosphere* 63, 1553–1559. doi: 10.1016/j.chemosphere.2005.09.056

Ortega-Villasante, C., Rellán-Álvarez, R., del Campo, F. F., Carpena-Ruiz, R. O., and Hernández, L. E. (2005). Cellular damage induced by cadmium and mercury in *Medicago sativa*. *J. Exp. Bot.* 56, 2239–2251. doi: 10.1093/jxb/eri223

Ovečka, M., and Takáč, T. (2014). Managing heavy metal toxicity stress in plants: biological and biotechnological tools. *Biotechnol. Adv.* 32, 73–86. doi: 10.1016/j.biotechadv.2013.11.011

Oven, M., Grill, E., Golan-Goldhirsh, A., Kutchan, T. M., and Zenk, M. H. (2002). Increase of free cysteine and citric acid in plant cells exposed to cobalt ions. *Phytochemistry* 60, 467–474. doi: 10.1016/S0031-9422(02)00135-8

Padmavathiamma, P. K., and Li, L. Y. (2007). Phytoremediation technology: hyper-accumulation metals in plants. *Water Air Soil Pollut.* 184, 105–126. doi: 10.1007/s11270-007-9401-5

Paleg, L. G., Douglas, T. J., Van Daal, A., and Keech, D. B. (1981). Proline and betaine protect enzymes against heat inactivation. *Aust. J. Plant Physiol.* 9, 47–57.

Park, J., Song, W. Y., Ko, D., Eom, Y., Hansen, T. H., Schiller, M., et al. (2012). The phytochelatin transporters *AtABCC1* and *AtABCC2* mediate tolerance to cadmium and mercury. *Plant J.* 69, 278–288. doi: 10.1111/j.1365-313X.2011.04789.x

Pawlik-Skowrónska, B. (2002). Correlations between toxic Pb effects and production of Pb-induced thiol peptides in the microalga *Stichococcus bacillaris*. *Environ. Pollut.* 119, 119–127. doi: 10.1016/S0269-7491(01)00280-9

Pawlik-Skowrónska, B. (2003). When adapted to high Zn concentrations the periphytic greenalga *Stigeoclonium tenue* produces high amounts of novel phytochelatin-related peptides. *Aquat. Toxicol.* 62, 155–163. doi: 10.1016/S0166-445X(02)00080-2

Petraglia, A., De Benedictis, M., Degola, F., Pastore, G., Calcagno, M., Ruotolo, R., et al. (2014). The capability to synthesize phytochelatins and the presence of constitutive and functional phytochelatin synthases are ancestral (plesiomorphic) characters for basal land plants. *J. Exp. Bot.* 65, 1153–1163. doi: 10.1093/jxb/ert472

Pianelli, K., Mari, S., Marquès, L., Lebrun, M., and Czernic, P. (2005). Nicotianamine over-accumulation confers resistance to nickel in *Arabidopsis thaliana*. *Transgenic Res.* 14, 739–748. doi: 10.1007/s11248-005-7159-3

Piñeros, M. A., Magalhaes, J. V., Carvalho Alves, V. M., and Kochian, L. V. (2002). The physiology and biophysics of an aluminum tolerance mechanism based on root citrate exudation in maize. *Plant Physiol.* 129, 1194–1206. doi: 10.1104/pp.002295

Piñeros, M. A., Shaff, J. E., Manslank, H. S., Carvalho, A. V. M., and Kochian, L. (2005). Aluminum resistant in maize cannot be solely explained by root organic acid exudation. A comparative physiological study. *Plant Physiol.* 137, 231–241. doi: 10.1104/pp.104.047357

Pokora, W., Baścik-Remisiewicz, A., Tukaj, S., Kalinowska, R., Pawlik-Skowrońska, B., Dziadziuszko, M., et al. (2014). Adaptation strategies of two closely related *Desmodesmus armatus* (green alga) strains contained different amounts of cadmium: a study with light-induced synchronized cultures of algae. *J. Plant Physiol.* 171, 69–77. doi: 10.1016/j.jplph.2013.10.006

Popova, T. N., and Pinheiro de Carvalho, M. A. A. (1998). Citrate and isocitrate in plant abolism. *Biochim. Biophys. Acta* 1364, 307–325. doi: 10.1016/S0005-2728(98)00008-5

Rascio, N., and Navari-Izzo, F. (2011). Heavy metal hyperaccumulating plants: how and why do they do it? And what makes them so interesting? *Plant Sci.* 180, 169–181. doi: 10.1016/j.plantsci.2010.08.016

Rellán-Álvarez, R., Abadía, J., and Álvarez-Fernández, A. (2008). Formation of metal-nicotianamine complexes as affected by pH, ligand exchange with citrate and metal exchange. A study by electrospray ionization time-of-flight mass spectrometry. *Rapid Commun. Mass Spectrom.* 22, 1553–1562. doi: 10.1002/rcm.3523

Rellán-Álvarez, R., Ortega-Villasante, C., Aìlvarez-Hernaìndez, A., Del Campo, F. F., and Hernaìndez, L. E. (2006). Stress responses of *Zea mays* to cadmium and mercury. *Plant Soil* 279, 41–50. doi: 10.1007/s11104-005-3900-1

Richau, K. H., Kozhevnikova, A. D., Seregin, I. V., Vooijs, R., Koevoets, P. L. M., Smith, J. A. C., et al. (2009). Chelation by histidine inhibits the vacuolar sequestration of nickel in roots of the hyperaccumulator *Thlaspi caerulescens*. *New Phytol.* 183, 106–116. doi: 10.1111/j.1469-8137.2009.02826.x

Richau, K. H., and Schat, H. (2009). Intraspecific variation of nickeland zinc accumulation and tolerance in the hyperaccumulatoro *Thlaspi caerulescens*. *Plant Soil* 314, 253–262. doi: 10.1007/s11104-008-9724-z

Roosens, N. H., Bernard, C., Leplae, R., and Verbruggen, N. (2004). Evidence for copper homeostasis function of metallothionein (MT3) in the hyperaccumulator *Thlaspi caerulescens*. *FEBS Lett.* 577, 9–16. doi: 10.1016/j.febslet.2004.08.084

Roosens, N. H., Leplae, R., Bernard, C., and Verbruggen, N. (2005). Variations in plant metallothioneins: the heavy metal hyperaccumulator *Thlaspi caerulescens* as a study case. *Planta* 222, 716–729. doi: 10.1007/s00425-005-0006-1

Ruttkay-Nedecky, B., Nejdl, L., Gumulec, J., Zitka, O., Masarik, M., Eckschlager, T., et al. (2013). The role of metallothionein in oxidative stress. *Int. J. Mol. Sci.* 14, 6044–6066. doi: 10.3390/ijms14036044

Salt, D. E., Prince, R. C., Baker, A. J. M., Raskin, I., and Pickering, I. J. (1999). Zinc legands in the metal hyperaccumulator *Thalspi caerulescens* as determined using X-absorption spectroscopy. *Environ. Sci. Technol.* 33, 713–717. doi: 10.1021/es980825x

Sasaki, T., Yamamoto, Y., Ezaki, B., Katsuhara, M., Ahn, S. J., Ryan, P. R., et al. (2004). A wheat gene encoding an aluminum-activated malate transporter. *Plant J.* 37, 645–653. doi: 10.1111/j.1365-313X.2003.01991.x

Schützendübel, A., and Polle, A. (2002). Plant responses to abiotic stresses: heavy metal induced oxidative stress and protection by mycorrhization. *J. Exp. Bot.* 53, 1351–1365. doi: 10.1093/jexbot/53.372.1351

Sekhar, K., Priyanka, B., Reddy, V. D., and Rao, K. V. (2011). *Metallothionein 1 (CcMT1)* of pigeonpea (*Cajanus cajan* L.) confers enhanced tolerance to copper and cadmium in *Escherichia coli* and *Arabidopsis thaliana*. *Environ. Exp. Bot.* 72, 131–139. doi: 10.1016/j.envexpbot.2011.02.017

Seth, C., Remans, T., Keunen, E., Jozefczak, M., Gielen, H., Opdenakker, K., et al. (2012). Phytoextraction of toxic metals: a central role for glutathione. *Plant Cell Environ.* 35, 334–346. doi: 10.1111/j.1365-3040.2011.02338.x

Sharma, S. S., and Dietz, K. J. (2006). The significance of amino acids and amino acid-derived molecules in plant responses and adaptation to heavy metal stress. *J. Exp. Bot.* 57, 711–726. doi: 10.1093/jxb/erj073

Sharma, S. S., Schat, H., and Vooijs, R. (1998). *In vitro* alleviation of heavy metal-induced enzyme inhibition by proline. *Phytochemistry* 49, 1531–1535. doi: 10.1016/S0031-9422(98)00282-9

Shevyakova, N. I., Il'ina, E. N., Stetsenko, L. A., and Kuznetsov, V. V. (2011). Nickel accumulation in rape shoots (*Brassica napus* L.) increased by putrescine. *Int. J. Phytoremed.* 13, 345–356. doi: 10.1080/15226514.2010.495147

Shukla, D., Kesari, R., Mishra, S., Dwivedi, S., Tripathi, R. D., Nath, P., et al. (2012). Expression of phytochelatin synthase from aquatic macrophyte *Ceratophyllum demersum* L. enhances cadmium and arsenic accumulation in tobacco. *Plant Cell Rep.* 31, 1687–1699. doi: 10.1007/s00299-012-1283-3

Shukla, D., Kesari, R., Tiwari, M., Dwivedi, S., Tripathi, R. D., Nath, P., et al. (2013). Expression of *Ceratophyllum demersum* phytochelatin synthase, CdPCS1, in *Escherichia coli* and *Arabidopsis* enhances heavy metal(loid)s accumulation. *Protoplasma* 250, 1263–1272. doi: 10.1007/s00709-013-0508-9

Simões, C. C., Melo, J. O., Magalhaes, J. V., and Guimarães, C. T. (2012). Genetic and molecular mechanisms of aluminum tolerance in plants. *Genet. Mol. Res.* 11, 1949–1957. doi: 10.4238/2012.July.19.14

Singh, D., and Chauhan, S. K. (2011). Organic acids of crop plants in aluminium detoxification. *Curr. Sci.* 100, 1109–1515.

Singh, R. K., Anandhan, S., Singh, S., Patade, V. Y., Ahmed, Z., and Pande, V. (2011). Metallothionein-like gene from *Cicer microphyllum* is regulated by multiple abiotic stresses. *Protoplasma* 248, 839–847. doi: 10.1007/s00709-010-0249-y

Sobrino-Plata, J., Ortega-Villasante, C., Flores-Cáceres, M. L., Escobar, C., Del Campo, F. F., and Hernández, L. E. (2009). Differential alterations of antioxidant defenses as bioindicators of mercury and cadmium toxicity in alfalfa. *Chemosphere* 77, 946–954. doi: 10.1016/j.chemosphere.2009.08.007

Solanki, R., and Dhankhar, R. (2011). Biochemical changes and adaptive strategies of plants under heavy metal stress. *Biologia* 66, 195–204. doi: 10.2478/s11756-011-0005-6

Solt, J. P., Sneller, F. E. C., Bryngelsson, T., Lundborg, T., and Schat, H. (2003). Phytochelatin and cadmium accumulation in wheat. *Environ. Exp. Bot.* 49, 21–28. doi: 10.1016/S0098-8472(02)00045-X

Song, H. M., Wang, H. Z., and Xu, X. B. (2012). Overexpression of *AtHsp90.3* in *Arabidopsis thaliana* impairs plant tolerance to heavy metal stress. *Biol. Plant* 56, 197–199. doi: 10.1007/s10535-012-0042-1

Song, W. Y., Mendoza-Cózatl, D. G., Lee, Y., Schroeder, J. I., Ahn, S. N., Lee, H. S., et al. (2014). Phytochelatin-metal(loid) transport into vacuoles shows different substrate preferences in barley and *Arabidopsis*. *Plant Cell Environ.* 37, 1192–1201. doi: 10.1111/pce.12227

Spisso, A. A., Cerutti, S., Silva, F., Pacheco, P. H., and Martinez, L. D. (2014). Characterization of Hg-phytochelatins complexes in vines (*Vitis vinifera* cv. Malbec) as defense mechanism against metal stress. *Biometals* 27, 591–599. doi: 10.1007/s10534-014-9732-9

Srivalli, S., and Khanna-Chopra, R. (2008). Delayed wheat flag leaf senescence due to the removal of spikelets is associated with increased activities of leaf antioxidant enzymes, reduced glutathione/oxidized glutathione ratio and oxidative damage to mitochondrial proteins. *Plant Physiol. Biochem.* 47, 663–670. doi: 10.1016/j.plaphy.2009.03.015

Takahashi, M., Terada, Y., Nakai, I., Nakanishi, H., Yoshimura, E., Mori, S., et al. (2003). Role of nicotianamine in the intracellular delivery of metals and plant reproductive development. *Plant Cell* 15, 1263–1280. doi: 10.1105/tpc.010256

Tariq Javed, M., Lindberg, S., and Greger, M. (2014). Cellular proton dynamics in *Elodea canadensis* leaves induced by cadmium. *Plant Physiol. Biochem.* 77, 15–22. doi: 10.1016/j.plaphy.2014.01.009

Tennstedt, P., Peisker, D., Bottcher, C., Trampczynska, A., and Clemens, S. (2009). Phytochelatin synthesis is essential for the detoxification of excess zinc and contributes significantly to the accumulation of zinc. *Plant Physiol.* 149, 938–948. doi: 10.1104/pp.108.127472

Thangavel, P., Long, S., and Minocha, R. (2007). Changes in phytochelatins and their biosynthetic intermediates in red spruce (*Picea rubens* Sarg.) cell suspension cultures under cadmium and zinc stress. *Plant Cell Tissue Organ Cult.* 88, 201–216. doi: 10.1007/s11240-006-9192-1

71

Theriappan, P., Gupta, A. K., and Dhasarathan, P. (2011). Accumulation of pro-line under salinity and heavy metal stress in cauliflower seedlings. *J. Appl. Sci. Environ. Manag.* 15, 251–255. doi: 10.4314/jasem.v15i2.68497

Trejo-Tellez, L. I., Gomez-Merino, F. C., and Schmitt, J. M. (2012). "Citric acid: biosynthesis, properties and applications on higher plants," in *Citric Acid*, eds D. A. Vargas and J. V. Medina (New York, NY: Nova Science Publishers, Inc.), 43–70.

Ueno, D., Iwashita, T., Zhao, F. J., and Ma, J. F. (2008). Characterization of Cd translocation and identification of the Cd form in xylem sap of the Cd-hyperaccumulator *Arabidopsis halleri*. *Plant Cell Physiol.* 49, 540–548. doi: 10.1093/pcp/pcn026

Usha, B., Venkataraman, G., and Parida, A. (2009). Heavy metal and abiotic stress inducible metallothionein isoform from *Populus juliflora* (SW) D.C. show differences in binding to heavy metals *in vitro*. *Mol. Genet. Genomics* 281, 99–108. doi: 10.1007/s00438-008-0398-2

Vacchina, V., Mari, S., Czernic, P., Marquès, L., Pianelli, K., Schaumlöffel, D., et al. (2003). Speciation of nickel in a hyperaccumulating plant by high-performance liquid chromatography-inductively coupled plasma mass spectrometry and electrospray MS/MS assisted by cloning using yeast complementation. *Anal. Chem.* 75, 2740–2745. doi: 10.1021/ac020704m

Valero, D., Pérez-Vicente, A., Martínez-Romero, D., Castillo, S., Guillén, F., and Serrano, M. (2002). Plum storability improved after calcium and heat postharvest treatments: role of polyamines. *J. Food Sci.* 67, 2571–2575. doi: 10.1111/j.1365-2621.2002.tb08778.x

van de Mortel, J. E., Almar Villanueva, L., Schat, H., Kwekkeboom, J., Coughlan, S., Moerland, P. D., et al. (2006). Large expression differences in genes for iron and zinc homeostasis, stress response, and lignin biosynthesis distinguish roots of *Arabidopsis thaliana* and the related metal hyperaccumulator *Thlaspi caerulescens*. *Plant Physiol.* 142, 1127–1147. doi: 10.1104/pp.106.082073

Vangronsveld, J., Herzig, R., Weyens, N., Boulet, J., Adriaensen, K., Ruttens, A., et al. (2009). Phytoremediation of contaminated soils and groundwater: lessons from the field. *Environ. Sci. Pollut. Res.* 16, 765–794. doi: 10.1007/s11356-009-0213-6

Vatamaniuk, O. K., Bucher, E. A., Ward, J. T., and Rea, P. A. (2001). A new pathway for heavy metal detoxification in animals. Phytochelatin synthase is required for cadmium tolerance in *Caenorhabditis elegans*. *J. Biol. Chem.* 276, 20817–20820. doi: 10.1074/jbc.C100152200

Vatamaniuk, O. K., Mari, S., Lang, A., Chalasani, S., Demkiv, L. O., and Rea, P. A. (2004). Phytochelatin synthase, a dipeptidyltransferase that undergoes multisite acylation with γ-glutamylcysteine during catalysis. Stoichiometric and site-directed mutagenic analysis of *Arabidopsis thaliana* PCS1-catalyzed phytochelatin synthesis. *J. Biol. Chem.* 279, 22449–22460. doi: 10.1074/jbc.M313142200

Verbruggen, N., Hermans, C., and Schat, H. (2009). Molecular mechanisms of metal hyperaccumulation in plants. *New Phytol.* 181, 759–776. doi: 10.1111/j.1469-8137.2008.02748.x

Verma, D. P. S., and Zhang, C. S. (1999). "Regulation of proline and arginine biosynthesis inn plants," in *Plant Amno Acids: Biochemistry and Biotechnology*, ed B. K. Singh (New York, NY: Marcel Dekker), 249–266.

Volland, S., Bayer, E., Baumgartner, V., Andosch, A., Lütz, C., Sima, E., et al. (2014). Rescue of heavy metal effects on cell physiology of the algal model system Micrasterias by divalent ions. *J. Plant Physiol.* 171, 154–163. doi: 10.1016/j.jplph.2013.10.002

Wang, F., Wang, Z., and Zhu, C. (2012). Heteroexpression of the wheat phytochelatin synthase gene (*TaPCS1*) in rice enhances cadmium sensitivity. *Acta Biochim. Biophys. Sin.* 44, 886–893. doi: 10.1093/abbs/gms073

Wang, H. C., Wu, J. S., Chia, J. C., Yang, C. C., Wu, Y. J., and Juang, R. H. (2009). Phytochelatin synthase is regulated by protein phosphorylation at a threonine residue near its catalytic site. *J. Agric. Food Chem.* 57, 7348–7355. doi: 10.1021/jf9020152

Wang, X., Shi, G., Xu, Q., and Hu, J. (2007). Exogenous polyamines enhance copper tolerance of *Nymphoides peltatum*. *J. Plant Physiol.* 164, 1062–1070. doi: 10.1016/j.jplph.2006.06.003

Wen, X. P., Pang, X. M., Matsuda, N., Kita, M., Inoue, H., Hao, Y. J., et al. (2008). Over-expression of the apple spermidine synthase gene in pear confers mul-tiple abiotic stress tolerance by altering polyamine titers. *Transgenic Res.* 17, 251–263. doi: 10.1007/s11248-007-9098-7

Wycisk, K., Kim, E. J., Schroeder, J. I., and Krämer, U. (2004). Enhancing the first enzymatic step in the histidine biosynthesis pathway increases the free histidine pool and nickel tolerance in *Arabidopsis thaliana*. *FEBS Lett.* 578, 128–134. doi: 10.1016/j.febslet.2004.10.086

Yang, H., Huang, Z. Y., Li, J., and Hu, Y. (2014). MT-like proteins: potential bio-indicators of *Chlorella vulgaris* for zinc contamination in water environment. *Ecol. Ind.* 45, 103–109. doi: 10.1016/j.ecolind.2014.03.017

Yang, L. T., Qi, Y. P., Jiang, H. X., and Chen, L. S. (2013). Roles of organic acid anion secretation in aluminum tolerance of higher plants. *BioMed. Res. Int.* 2013:173682. doi: 10.1155/2013/173682

Yokosho, K., Yamaji, N., and Ma, J. F. (2010). Isolation and characterization of two *MATE* genes in rye. *Funct. Plant Biol.* 37, 296–303. doi: 10.1071/FP09265

Yokosho, K., Yamaji, N., and Ma, J. F. (2011). An Al-inducible *MATE* gene is involved in external detoxification of Al in rice. *Plant J.* 68, 1061–1069. doi: 10.1111/j.1365-313X.2011.04757.x

Zacchini, M., Pietrini, F., Mugnozza, G. S., Iori, V., Pietrosanti, L., and Massacci, A. (2009). Metal tolerance, accumulation and translocation in poplar and willow clones treated with cadmium in hydroponics. *Water Air Soil Pollut.* 197, 23–34. doi: 10.1007/s11270-008-9788-7

Zenk, M. H. (1996). Heavy metal detoxification in higher plants–a review. *Gene* 179, 21–30. doi: 10.1016/S0378-1119(96)00422-2

Zhang, H., Xu, W., Dai, W., He, Z., and Ma, M. (2006). Functional characterization of cadmium-responsive garlic gene *AsMT2b*: a new member of metallothionein family. *Chin. Sci. Bull.* 51, 409–416. doi: 10.1007/s11434-006-0409-9

Zhang, Z., Gao, X., and Qiu, B. (2008). Detection of phytochelatins in the hyper-accumulator *Sedum alfredii* exposed to cadmium and lead. *Phytochemistry* 69, 911–918. doi: 10.1016/j.phytochem.2007.10.012

Zhao, H., and Yang, H. (2008). Exogenous polyamines alleviate the lipid peroxidation induced by cadmium chloride stress in *Malus hupehensis* Rehd. *Sci. Hortic.* 116, 442–447. doi: 10.1016/j.scienta.2008.02.017

Zhao, J., Shi, G. X., and Yuan, Q. H. (2008). Polyamines content and physiological and biochemical responses to ladder concentration of nickel stress in *Hydrocharis dubia* (Bl.) Backer leaves. *Biometals* 21, 665–674. doi: 10.1007/s10534-008-9151-x

Zhou, B., Yao, W., Wang, S., Wang, Y., and Jiang, T. (2014). The metallothionein gene, *TaMT3*, from *Tamarix androssowii* confers Cd2+ tolerance in tobacco. *Int. J. Mol. Sci.* 15, 10398–10409. doi: 10.3390/ijms150610398

Zhou, J., and Goldsbrough, P. B. (1994). Functional homologs of fungal metallothionein genes from *Arabidopsis*. *Plant Cell* 6, 875–884. doi: 10.1105/tpc.6.6.875

Zhu, X. F., Zheng, C., Hu, Y. T., Jiang, T., Liu, Y., Dong, N. Y., et al. (2011). Cadmium-induced oxalate secretion from root apex is associated with cadmium exclusion and resistance in *Lycopersicon esulentum*. *Plant Cell Environ.* 34, 1055–1064. doi: 10.1111/j.1365-3040.2011.02304.x

Zimeri, A. M., Dhankher, O. P., McCaig, B., and Meagher, R. B. (2005). The plant *MT1 metallothioneins* are stabilized by binding cadmiums and are required for cadmium tolerance and accumulation. *Plant Mol. Biol.* 58, 839–855. doi: 10.1007/s11103-005-8268-3

3.5. Review II

Participation in the work of the author M.A. Merlos Rodrigo literature research 50% and manuscript preparation 50%.

MALDI-TOF is a powerful tool for surveying proteins and peptides comprising the realm for clinical analysis. MALDI-TOF has the potential to revolutionize cancer diagnostics by facilitating biomarker discovery, enabling tissue imaging and quantifying biomarker levels. MALDI-TOF profiling techniques as tools for the detection of cancer biomarkers in various cancers and latest available data were summarized in following review.

Review

MALDI-TOF MS as evolving cancer diagnostic tool: A review

Miguel Angel Merlos Rodrigo [a,b], Ondrej Zitka [a,b], Sona Krizkova [a,b], Amitava Moulick [a,b], Vojtech Adam [a,b], Rene Kizek [a,b,*]

[a] Department of Chemistry and Biochemistry, Faculty of Agronomy, Mendel University in Brno, Zemedelska 1, CZ-613 00 Brno, Czech Republic
[b] Central European Institute of Technology, Brno University of Technology, Technicka 3058/10, CZ-616 00 Brno, Czech Republic

ARTICLE INFO

ABSTRACT

Recent developments in mass spectrometry have introduced clinical proteomics to the forefront of diseases diagnosis, offering reliable, robust and efficient analytical method for biomarker discovery and monitoring. MALDI-TOF is a powerful tool for surveying proteins and peptides comprising the realm for clinical analysis. MALDI-TOF has the potential to revolutionize cancer diagnostics by facilitating biomarker discovery, enabling tissue imaging and quantifying biomarker levels. Healthy (control) and cancerous tissues can be analyzed on the basis of mass spectrometry (MALDI-TOF) imaging to identify cancer-specific changes that may prove to be clinically useful. We review MALDI-TOF profiling techniques as tools for detection of cancer biomarkers in various cancers. We mainly discuss recent advances including period from 2011 to 2013.

© 2014 Elsevier B.V. All rights reserved.

Contents

1. Cancer biomarkers analyzed by MALDI-TOF

MALDI-TOF mass spectrometry (MALDI-TOF MS) is renowned for its easy operation and requirement of inexpensive matrixes for preparation of a sample. However, the instrumentation is more important which is fully automated and thus it can provide the screening of a large set of samples in a short period of time of analysis due to advanced laser technology and hardware, as shown in Fig. 1. We review MALDI-TOF profiling techniques as tools for the detection of cancer biomarkers in various cancers. It is not surprising that this technique has been used in various studies to determine different markers and mechanisms involved in the development of cancer [1]. In the following section, contribution of MALDI-TOF MS in cancer research is summarized and discussed based mainly on the literature published in 2011–2013.
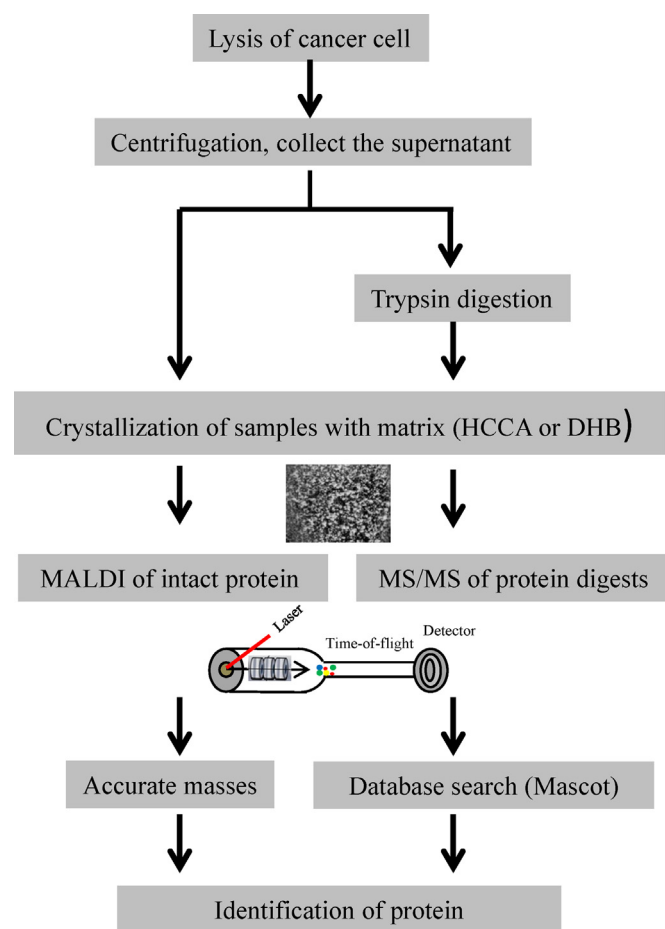

Fig. 1. Stepwise scheme for rapid identification of biomarker in cancer cells by MALDI-TOF/TOF-MS. (1) Lysis with appropriate buffer – optional by the protocol used. (2) Centrifugation at $25,000 \times g$, 4 °C for 20 min. (3) Mixture of same volumes of supernatant and trypsin (0.1 mg/mL at 50 mM ammonium bicarbonate). Digestion in thermoblock for 2 h at 45 °C, pH > 8. Digestion stopped at pH < 4 by addition of acetic acid. (4) 1–2 μl of sample/matrix mixture (1:1) deposited on MALDI plate and dried at room temperature (dried-droplet method). (5) Analysis by MALDI-TOF/TOF mass spectrometer in linear and reflector mode. (6 and 7) Masses of biomarker digests are used for database search – peptide mass fingerprinting (PMF). Biomarkers are identified using database search results.

1.1. Gastrointestinal cancer

Zhang et al. used degAla-FPA (fibrinipeptide-A with alanine truncation at the N-terminal) as a biomarker. The sensitivity was 85.4% for patients suffering from gastric cancer with lymph node metastases, and the specificity was 100% for patients without lymph node metastases [2]. The high sensitivity and specificity achieved with serum levels of degAla-FPA indicated that MALDI-TOF MS technology could facilitate the discovery of a novel and quantitative prognostic biomarker for gastric cancer with the development of lymph node metastasis. Moreover, the identification of glycosylation changes in proteins, circulating in serum of patients with precursor lesions of gastric cancer, is one of the highest interests and it represents a source of putative new biomarkers for early diagnosis and intervention. Gomes et al. [3] used MALDI-TOF/TOF mass spectrometry for the identification of circulating proteins, carrying altered glycans and provided the evidence of serum proteins displaying abnormal O-glycosylation in patients with precursor lesions of gastric carcinoma and also included a panel of putative targets for the non-invasive clinical diagnosis of individuals with gastritis. MALDI-TOF MS is also important for proteomic profiling and early diagnosis of colorectal cancer [4–8] and others (Fig. 2), such as bladder or gastric cancers [9–14]. Therefore, MALDI-TOF spectra of small tissue biopsies, generated with this straightforward method, can be used to detect rapidly numerous cancer-associated biochemical changes. These can be used to identify upper esophageal cancers. Normal esophageal and gastric tissue generated distinct MALDI-TOF spectra were characterized by higher levels of calgranulins in esophageal tissue. MALDI-TOF spectra of polypeptides and lipids can be used to differentiate between esophageal adenocarcinoma and Barrett's and normal esophagus, and between gastric cancer and normal stomach [15].

1.2. Cancer of the respiratory system

In recent studies, MALDI-TOF MS has been proven as the innovative tool for the determination and identification of biomolecules involved in different types and stages of lung cancer. Pastor et al. [16] showed a total of 15 oxidative stress regulatory proteins were differentially expressed in lung cancer and/or chronic obstructive
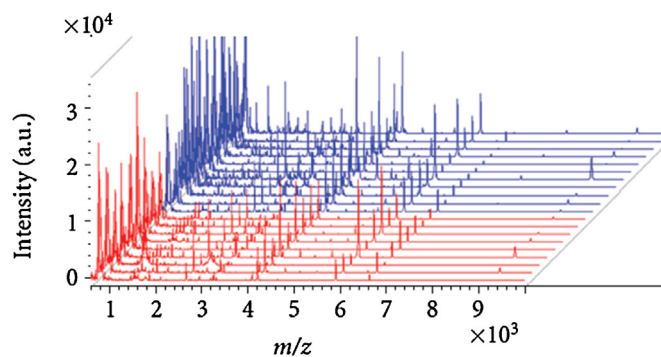
Fig. 2. View of the aligned mass spectra of the serum protein profile of model construction group obtained by MALDI-TOF MS after purification with magnetic beads in colorectal cancer patients (red: 10 healthy subjects, blue: 10 colorectal cancer patients). (For interpretation of the references to color in this figure legend, the reader is referred to the web version of this article.)
Reprinted with permission from [5].
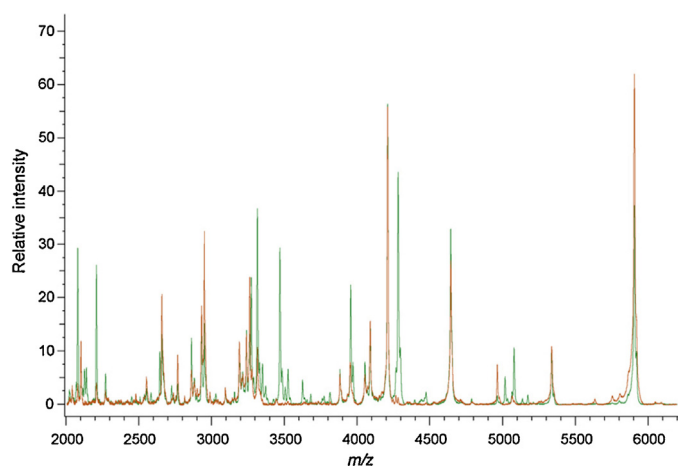
Fig. 3. Overall sum spectra in the mass range from 2000 to 6000 Da, obtained from all bladder cancer patients (orange) and all healthy controls (green). m/z = mass-to-charge ratio. (For interpretation of the references to color in this figure legend, the reader is referred to the web version of this article.)
Reprinted with permission from [23].

pulmonary disease patients as compared to the control group. These findings highlight the role of the oxidative stress response proteins in the pathogenic pathways of both the diseases, and provide new candidate biomarkers and predictive tools for diagnosis of lung cancer. Lung cancer and chronic obstructive pulmonary disease (COPD) commonly coexist in smokers. Pastor et al. identified distinct proteomic profiles able to discriminate these two pathological entities. The protein profiles identified contribute to elucidate the underlying pathogenic pathways of both the diseases, and provide new tools of potential use as biomarkers for the early diagnosis of lung cancer [16]. Chen et al. identified 10 membrane-associated proteins being significantly overexpressed in the high migration/invasion group of lung cancer by MALDI-TOF MS [17]. An important study was the comparison of plasma from healthy non-smokers, smokers, and patients with lung cancer where pattern-based differentiation profiling of low molecular weight proteins and peptides by magnetic bead technology with MALDI-TOF MS was performed. It was shown that the peaks (signals) of selected markers can serve as a distinguished tool for the lung cancer patients with the high sensitivity and specificity [18]. Further study searched for a pathway-based approach to investigate the association between the potentially functional genetic polymorphisms of the corresponding genes and the outcomes of platinum-based chemotherapy in advanced non-small-cell lung cancer (NSCLC). A MALDI-TOF MS mass spectrometer was used for genotyping of 10 polymorphisms of eight apoptosis-related genes, including BCL2, BAX, caspase 3 (CASP3), 8 (CASP8), and 1 (CASP1), tumor necrosis factor α (TNF α), and macrophage migration inhibitory factor (MIF) [19].

1.3. Renal and bladder cancer

It is possible to identify novel biomarkers for bladder cancer in urine [20,21]. Alterations in the serum peptidome in renal cell carcinoma (RCC) were used to distinguish benign and malignant tumors [22], however, there is a need for more effective biomarkers for both detecting bladder cancer and distinguishing muscle-invasive from non-invasive disease. The screening of serum protein patterns using MALDI-TOF MS shows high sensitivity and specificity in the identification of patients with bladder cancer, regardless the stage of tumor (Fig. 3). Due to high-throughput capability, the differential panel of the identified differential proteins may improve the diagnosis and thus prognosis of bladder cancer [23].

1.4. Prostate cancer

Yan et al. suggested that the LNCaP cell model resembles the clinical scenario of castration-resistant prostate cancer to investigate the effect of regulation of metabolism on androgen-independent growth of prostate cancer because the metabolism of cancer cells, responsive to androgen deprivation therapy, may be involved in the development and progression of prostate cancer and ultimate failure of androgen-deprivation therapy [24]. Numerous studies can be found in the database describing utilization of the MALDI-TOF MS for the determination of markers of prostate cancer or advances in this type of cancer [25–27].

1.5. Breast cancer

MALDI-TOF MS is known as a sensitive analytical tool for characterization of different types of biologically active compounds in breast cancer. Numerous recently published studies have used MALDI-TOF MS for the determination of biomarkers in breast cancer [28–33]. Mass spectrometry, based on the analysis of proteins in serum samples, is a promising approach for obtaining the profile of biomarkers for detection of early stages of cancer [34]. Methylation of vimentin predicts poor overall survival (prognosis) independent on race, subtype, stage, nodal status, or metastatic disease, and acts as a new prognostic biomarker for patients suffering from breast cancer [35]. Hyaluronan (HA) is a component of extracellular matrix that influences cell development and proliferation, migration, remodeling and regeneration of normal tissue, and interactions of tumor cells. A study by Srinivas et al. demonstrated the overexpression of HA-hexa binding protein in human tumors of breast and its involvement in cancerogenesis by MALDI-TOF MS [36]. The key regulatory molecules in breast cancer were detected using the Western Blot analysis, two-dimensional (2-D) electrophoresis and MALDI-TOF MS. Gao et al. performed a study of reduction of enolase-1 expression, that significantly decreases the response to hypoxia and enhances the sensitivity of the cells to radiation therapy; and therefore, enolase-1 may become a drug of interest for the treatment of breast cancer [37].

1.6. Ovarian cancer

Major part of the research related to profiling of proteome in ovaries is centered on different factors of disease such as polycystic ovary syndrome, ovarian cancer, etc. Ween et al. investigated the ovarian cancer-peritoneal interaction by means of in vitro culture experiments with ovarian cancer (OVCAR-5 and SKOV-3) and peritoneal (LP-9) cells, because metastasing of ovarian cancer is characterized by the shedding of malignant cells from the surface of the ovary with their subsequent implantation onto the peritoneal surface, which forms the abdominal cavity. The extracellular matrix protein, transforming growth factor-beta-induced protein (TGFBIp, also known as beta ig-H3) was identified as one of the proteins, differentially expressed in the culture secretome by MALDI-TOF/TOF mass spectrometry [38]. The acquisition of chemoresistance is the major therapeutic obstacle in the clinical treatment of ovarian cancer. Li et al. demonstrated that the protein, phosphorylated cofilin 1 (p-CFL1) correlates with resistance to taxol in human ovarian cancer cells. The total proteins of two sensitive (SKOV3 and A2780) and three taxol-resistant (SKOV3/TR2500, SKOV3/TR30 and A2780/TR) human ovarian cancer cell lines were isolated by 2-dimensional gel electrophoresis (2DGE). Twenty-two protein spots in all samples were revealed to be significantly different in the intensity of spots by statistical analysis, whereas 16 of them were identified by MALDI-TOF MS. Cofilin 1 (CFL1) was selected as a candidate, which may play an

important role in the resistance to taxol [39]. MALDI-TOF MS can serve also as a tool for helping us to investigate the effect of cytostatics and to verify the positive effect on a tumor development. Huang et al. confirmed that Orlistat, also known as tetrahydrolipstatin, is a potential inhibitor of ovarian cancer and can be used as a novel adjuvant antitumor agent. Orlistat is an anti-obesity oral drug that has shown significant antitumor activity in a variety of tumor cells. To identify the proteins, involved in antitumor activity, the authors employed a proteomic approach to reveal the changes in the protein expression in the human ovarian cancer cell line SKOV3 after treatment with that drug [40]. Moreover, the significantly up-regulated level of ceruloplasmin in the ascites fluid of intrinsic chemoresistant serous epithelial ovarian cancer patients suggests its potential as a prognostic biomarker for response to the chemotherapy [41].

1.7. Leukemia

Development of modern proteomic methods in recent years has also opened new perspectives in the identification of new biomarkers which ensure more effective diagnosis, treatment monitoring and prediction of therapeutic outcome in leukemia. Kazmierczak et al. evaluated usefulness of comparative proteomics by MALDI-TOF MS in two subtypes of acute myeloid leukemia [42]. Several papers have already been published about the use of MALDI-TOF MS to analyze leukemia [43–45]. Wang et al. showed changes in the expression of 15 proteins, which were obtained by digestion *in situ*, and then analyzed by MALDI-TOF MS in childhood acute lymphoblastic leukemia (c-ALL) cells. Eight different proteins are expected to become new diagnostic markers and drug targets for c-ALL [46].

2. Cancer biomarkers investigated by MALDI-TOF imaging mass spectrometry

Mass spectrometry is considered to be particularly well suited to serve as a diagnostic or biomarker discovery tool in studies of cancer. There is emerging evidence of the fact that the cancer cells and/or the surrounding microenvironment generate proteins and peptides of different types and in different concentrations than normal cells during the development of cancer. This abnormal distribution of proteins in tissue can be analyzed by imaging-based mass spectrometry (MALDI-TOF imaging mass spectrometry) and the patterns may help to identify cancer-specific changes (compared with controls) that may prove to be useful clinically. MALDI-TOF imaging mass spectrometry has been recognized as a powerful method for clinical proteomics, particularly in cancer research. The technology has particular potential for discovering new candidates of tissue biomarkers, classification of tumors, early diagnosis or prognosis, elucidating pathways of pathogenesis, and monitoring the therapy. Over recent years, MALDI imaging mass spectrometry has been used for molecular profiling and imaging directly in cancer tissues [47–50]. This technique represents a method that allows the combination of mass spectrometric analyses with simultaneous histological evaluation to analyze various analytes such as proteins, peptides, lipids, or small molecules in cancer tissues [51].

2.1. Gastrointestinal cancer

Cheng et al. showed that human neutrophil peptides HNPs 1–3, which are found to be increased in the gastric cancer tissues, could be used as potential biomarkers, detected by the MALDI-TOF imaging mass spectrometry, implying that elevated neutrophils may be used as a target for tumor treatment. Moreover, the binding capacity of HNPs-1 with gastric cancer cells implies that tracking

molecules conjugated with HNPs-1 could be applied as a specific probe to diagnose gastric cancer (Fig. 4) [52]. MALDI-TOF imaging mass spectrometry allows us to investigate proteomics-based histology to identify proteins, predicting disease outcome (progression, remission) in gastric cancer after surgical resection. The protein pattern, described by Balluff et al., serves as a new independent indicator of the survival of patients complementing the previously identified clinical parameters in the terms of prognostic relevance. The results showed an advantage of tissue-based proteomic approach that may provide clinically relevant information and might be beneficial in improving the risk stratification for gastric cancer patients [53]. In study by Meding et al. a tissue-based proteomic approach was used for identification of proteins in colon cancer cells associated with metastasing into regional lymph node because it negatively affects prognosis in these patients. The study revealed FXYD3, S100A11 and GSTM3 as novel markers for development of metastases in regional lymph node in colon cancer [54].

### 2.2. Cancer of the respiratory system

Végvári et al. reported a brief summary on the contemporary state of lung cancer and chronic obstructive pulmonary disease, the principles of monitoring multiple reaction and MALDI-TOF imaging mass spectrometry [55]. Another recently published study was aimed at the investigation where direct tissue MALDI-TOF imaging mass spectrometric analysis focused on lipid profile which may assist the histopathologic diagnosis of non-small cell lung cancers. The result showed that several phospholipids including phosphatidylcholines (PCs) were overexpressed in lung cancer cells [56]. In addition, the drug therapy at the molecular level includes aiming at the activity of epidermal growth factor receptor tyrosine kinase by using inhibitors. Marko-Varga et al. performed the first report on personalized characterization of drug with localizations, which allowed to map these compounds at attomolar concentrations within the microenvironment of lung tumor tissue (Fig. 5) [57]. Alexandrov et al. showed how the recently introduced method of spatial segmentation can be applied to analyze and interpret the sections of larynx carcinoma and to compare them with the spatial segmentation with the histological annotation of the same tissue section [58]. These results can be considered as a good base for personalized medicine.

2.3. Renal and bladder cancer

Herring et al. reported the methodologies of preparation of sample, acquisition and analysis of MS data, and identification of proteins used for profiling/imaging MS as well as application in the study of kidney disease and toxicity [59]. With the help of these findings, a novel grading system for papillary non-invasive bladder cancer was introduced as low grade (LG) and high grade (HG) in lieu of the former G1 (grade 1), G2 (grade 2), and G3 (grade 3). This change allowed increased reproducibility as well as to diminish inter-observer variability in the histopathological grading among individual pathologists. MALDI-TOF imaging mass spectrometry was thus presented as an automatic and objective tool to assist grading of urothelial neoplasms and to facilitate accuracy (Fig. 6) [60].

2.4. Prostate cancer

Bonnel et al. presented a prostate cancer study on formalin-fixed paraffin-embedded tissue [61]. Chuang et al. presented a three-step method to predict prostate cancer (PCa) regions in biopsy of tissue samples based on high confidence, and low resolution of prostate cancer regions marked by a pathologist.
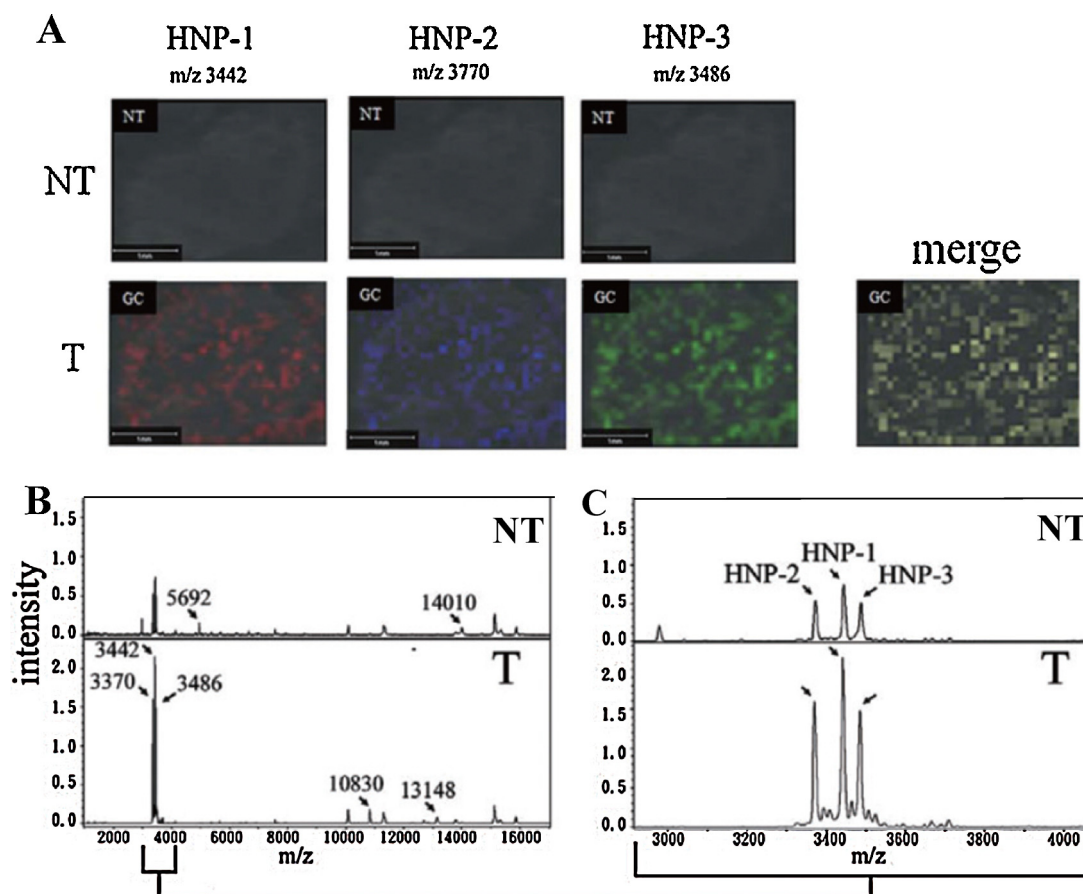
Fig. 4. Detection of human neutrophil peptide (HNPs-1, -2 and -3) using the MALDI-Imaging MS analytical technique. (A) HNPs-1 (red, m/z 3442), -2 (blue, m/z 3770), and -3 (green, m/z 3486) in the same cancerous tissue were determined by MALDI-TOF imaging mass spectrometry. (B) Differential peaks on the spectral protein profile between T and NT tissues. Two peaks (m/z 5692 and 14,010) were present in the normal region of gastric specimens and two defined peaks (m/z 10,830 and 13,148) specifically existed in the cancerous region. Furthermore, three peaks (m/z 3370, 3442, and 3486) showed significantly higher intensity in the cancerous region, compared to the normal region. Each peak was labeled with a black arrow. (C) The detailed spectra of the peaks at m/z 3370, 3442, and 3486 were determined to be HNPs-1, -2 and -3, respectively. (For interpretation of the references to color in this figure legend, the reader is referred to the web version of this article.)

Reprinted with permission from [52].

The authors suggested and designed the prediction model for the same purpose that take an advantage of MALDI-TOF imaging mass spectrometric data from the adjacent slice. Results of experiments showed that the texture analysis-based prediction is sensitive but less specific, whereas the prediction based on the data processing of MALDI spectra is not sensitive but supremely specific (100%) [62]. This technique provides the possibility in the rapid identification of specific markers from different histological samples and their direct localization in tissues.

2.5. Breast cancer

Recent developments in MALDI-TOF imaging mass spectrometry enable rapid and specific detection of lipids directly in thin tissue sections. Chughtai et al. performed multimodal imaging of acylcarnitines, phosphatidylcholines, lysophosphatidyl-choline, and sphingomyelin from different microenvironments of the xenograft models of breast tumor, which carried tomato fluorescent protein, a very bright red fluorescent protein, as a hypoxia-response element-driven reporter gene. The mass spectrometry imaging of molecular lipids revealed special heterogeneous lipid distribution within the tumor tissue [63]. Moreover, Kang et al. used MALDI-TOF imaging to compare the molecular profiles of tissues from the interface zone of breast cancer, tumor zone, and zone of normal tissue [64].

2.6. Ovarian cancer

Novel and more sensitive proteomic strategies such as MALDI mass spectrometry imaging studies are well suited more efficiently to identify markers for both diagnosis and prognosis in ovarian cancer. Longuespee et al. focused on such proteomic strategies in regards to signaling pathways in ovarian cancer, development of ovarian cancer and escape from the immune response [65]. The same authors also reported that proteasome activator complex (PA28 or Reg alpha) on the C-terminal fragment of the 11S is a novel ovary-specific biomarker of early and late stages of relapse of ovarian cancer in biopsies of patient after chemotherapy. Due to specific cellular localization of this fragment, this complex is a suitable candidate for early diagnosis of ovarian cancer, prognosis of tumor disease and follow-up during therapy and discriminating borderline of cancer (tumor) [66]. In 2012, Lagarrigue et al. published a review that considered some of the recent publications in the field, addressing a range of issues covering embryonic development, profiling of product of gene expression during gametogenesis, and seeking and identifying biomarkers of cancers of reproductive system [67].

3. SELDI-TOF MS for detection/identification biomarker for cancer

Although this review focuses on MALDI-TOF, surface-enhanced laser desorption/ionization mass spectrometry (SELDI) has a great
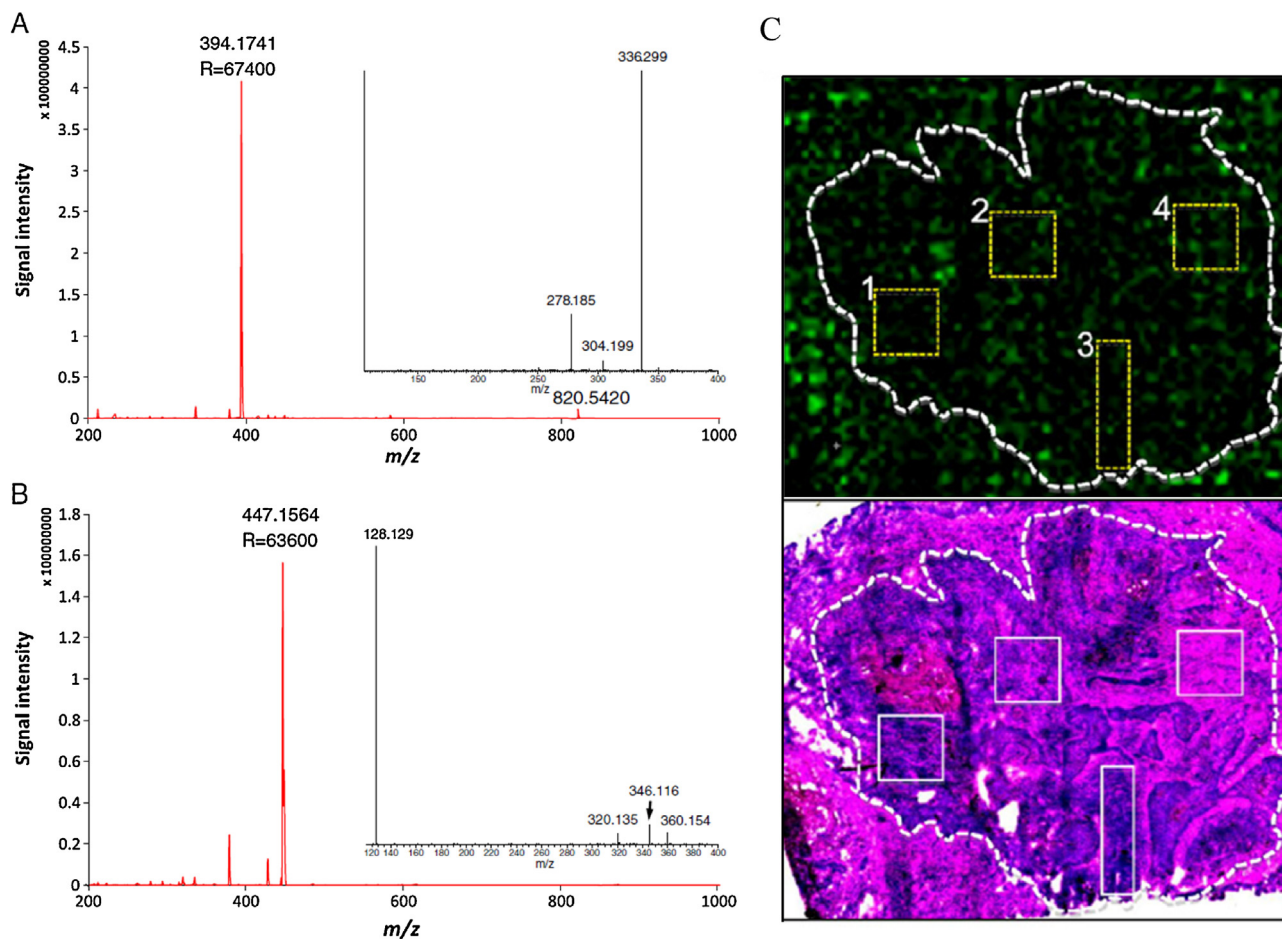
Fig. 5. Full mass and fragmentation spectra of (A) erlotinib and (B) gefitinib as obtained in dry droplet experiments on MTP using 10 μg/ml compound in 50% MeOH and 7.5 mg/mL CHCA as matrix. (C) Enlarged region of a planocellular lung cancer section with MALDI-l magin MS read out of the erlotinib fragment ion (m/z 336.19) and HE stained histological details, which shows the area of tumor cells in dark blue (compared to stroma cells in light purple). Regions with various rates of tumor cells are indicated with yellow dashed lines and numbers. (For interpretation of the references to color in this figure legend, the reader is referred to the web version of this article.) Reprinted with permission from [57].
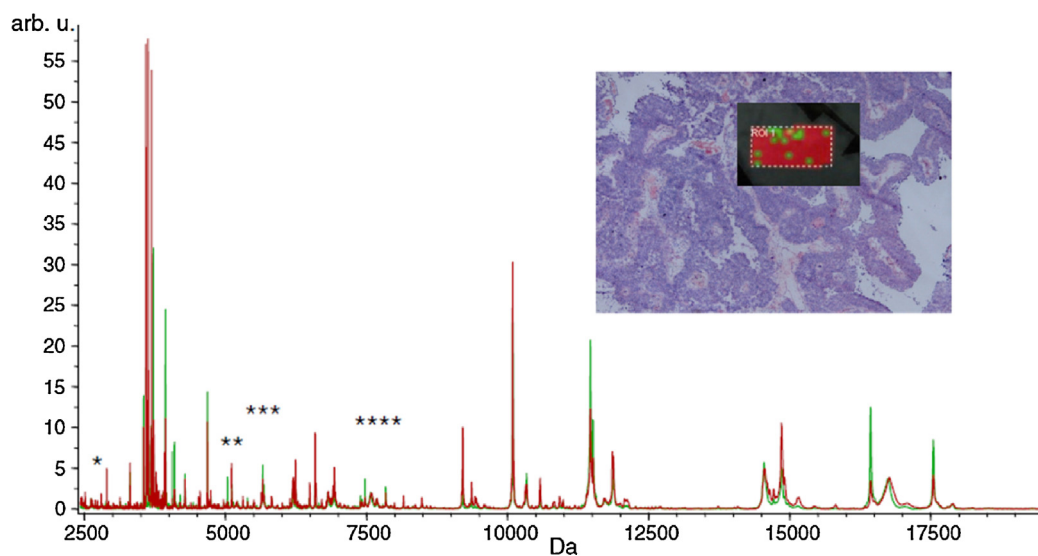
Fig. 6. Relative peak intensity *versus* mass to charge ratio (m/z) ranging from 2500 to 18,000 Da of an overall sum spectrum of pTaG1 (green) and pTaG3 (red) bladder cancer is shown. Four significant peaks implemented and indicated by one, two, three or four asterisks respectively. Merged overlay of a Hematoxilin–Eosin (H.E.) stained light microscope picture (20× magnification) and the corresponding region of interest (ROI) of a pTa G3 tumor are shown in the inset. FlexImaging (Bruker Daltonics) was used to illustrate the ratio of G3 areas (red), G1 areas (green) and not classified areas (yellow) within the region of interest. (For interpretation of the references to color in this figure legend, the reader is referred to the web version of this article.) Reprinted with permission from [60].

interest for the identification of biomarkers in cancer in recent years. SELDI-TOF MS was developed from MALDI-TOF MS and it was firstly used in 1993. The surface of target for SELDI-TOF MS is variously modified in order to achieve the affinity between targeted molecules and surface. Thanks to this modification the targeted molecules are separated from the sample directly on the target and so the analytes do not need to be separated before the application. This is probably the main advantage of this method before the MALDI-TOF. Matrix is usually applied after the deposition of sample. The target's surface can be modified by antibodies, ion exchange, hydrophobic sorbents, metal-binding sorbents and so forth [68]. SELDI-TOF has high sensitivity for small proteins/peptides with molecular weights lower than 15 kDa and due to the possibility of analysing samples without previous separation it can be used for analysing body fluids and tissue extracts [69]. Significant results obtained in lung, pancreatic, colon, ovarian, cervical, prostate, breast, hepatocellular and brain tumors have been described [68,70–75]. Bertucci et al. investigated the post-operative sera of 83 high-risk breast cancer patients using SELDI-TOF MS, by constructing a 40-protein signature that correctly predicted outcome in 83% of patients. These results should be interpreted cautiously, as the number of proteins used for classification is rather high in comparison with the limited study population, indicating possible over-fitting of the data [76]. Simsek et al. showed that protein peaks detected by SELDI-TOF analyses in lung cancer may be helpful in differentiating healthy individuals from lung cancer cases in a noninvasive method, and also SELDI-TOF MS analysis may be used for early diagnosis of lung cancer as well as its screening in the future, but further studies with larger sample sizes will be required [73]. SELDI-TOF has also been used extensively in studies of renal cell carcinomas (RCC) with initial publications reporting the analysis of tissues, cell lines and biological fluids [77]. Success in validation has already been achieved in some cases, yet the overall conclusion is that SELDI technology represents one component of a broader spectrum of versatile investigation technologies that may finally lead to setting up a more "clinical friendly" set of dedicated diagnostics tools [70]. Many factors, such as sample processing and operating procedures for the experiments, can affect the reproducibility of disease biomarkers in SELDI-TOF. Some challenges still remain, as for all other proteomic approaches, due in part to the complexity and the wide dynamic range of the samples. Sample fractionation and/or enrichment procedure, such as peptide ligand affinity beads, will certainly be the solution to visualize the deep proteome. In addition, improvements in mass spectrometry instrumental performances could be expected (higher resolution, reducing adduct formation, and ion suppression), contributing further to more reliable and faster biomarkers discovery [78–81]. Although SELDI-TOF MS can produce reliable classification results in serum samples of cancer patients, it will not be applicable in routine patient care [82].

4. Peptide mass fingerprinting as identification of proteins and a safe hint for the presence of cancer

MALDI-TOF peptide mass fingerprinting (PMF) is the fastest and cheapest method of protein identification. Recent advances in MALDI-TOF MS and proteomic instrumentations offer unique chance for rapid identification of these markers, and give information about diagnostic and prognostic for cancer related biological fluids, as we have outlined in the previous chapters in this review. PMF is one of the foundational technologies driving the growth of proteomics and detection of biomarker for cancer. We believe that PMF will continue to grow in importance for cancer identification. At present, Mascot and PeptIdent software's against NCBInr or Swiss-Prot databases are used in most of the studies

[65–70]. MALDI-TOF MS has been developed for use in clinical chemistry as a primary investigative tool to characterize a number of cancers, protein markers of disease or susceptibility to disease. Applications in cancer and in particular colorectal cancer have led the way in demonstrating clinical usefulness of MALDI-TOF MS with many other applications, now in research and development [83].

5. Novel approaches for quantification of mass of proteins

5.1. Limitations in successful biomarker detection by MALDI-TOF MS

In recent years, MALDI-TOF has gained greater attention from proteomic scientists as it produces high resolution data for proteome studies for looking biomarker of cancer. Its main advantages include speed of analysis, low sample volume used, high sensitivity, ease of use, inexpensive consumables, and wide mass range coverage, make this platform potentially applicable for the screening of large sample numbers. Other studies revealed various shortcomings related to the reproducibility and quantification capabilities of the platform. Although MALDI-TOF MS continuously improves in sensitivity and accuracy, it is characterized by its high dimensionality and complex patterns with substantial amount of noise. Firstly, the data quality of MALDI-TOF is very much dependent on the settings of the instrument. These settings include user-controlled parameters, i.e. deflection mass to remove suppressive ions and the types of calibration used for peak identification; and instrument-embedded settings, i.e. the time delayed extraction which is automatically optimized by the instrument from time-to-time based on the preset criteria in the instrument, peak identification protocols in the calibration and the software version used to generate and to visualize MS data [84]. Typical raw MS data contains a range of noise sources, as well as true signal elements. These noise sources include mechanical noise that caused by the instrument settings, electronic noise from the fluctuation in an electronic signal and travel distance of the signal, chemical noise that is influenced by sample preparation and sample contamination, temperature in the flight tube and software signal read errors. This makes identification/discovery of marker ions relevant to a sample state difficult. Therefore, data preprocessing is often required to reduce the noise and systematic biases in the raw data before any analysis takes place. Numerous data preprocessing techniques have been proposed. These include baseline correction, smoothing/denoising, data binning, peak alignment, peak detection and sample normalization. Biological variability and heterogeneity in samples further complicate the MALDI-TOF MS-based biomarker discovery. In addition, robust computational methods are needed to minimize the impact of biological variability caused by unknown intrinsic biological differences [85–87].

In nearly all types of ionization processes including MALDI-TOF and MADI-TOF imaging, a phenomenon often referred to as "ion suppression" can occur. Some desorbed species that preferentially capture protons in the ionization process can appear to be at higher abundance in the spectrum, and conversely others can appear at lower abundance relative to their true compositions in the sample. Thus, although the relative intensity measurements of the same protein in several samples can be compared with reasonable reproducibility, this comparison may not apply to the relative intensities of two separate proteins in a spectrum because their ionization efficiencies may be different [88].

MALDI profiling of human serum is confined to the detection and quantification of highly abundant proteins and, in particular, abundant peptide. The few established cancer serum proteins are

present in concentrations well below the detection limit in MALDI serum profiling [89]. Albalat et al. showed that a main problem of MALDI TOF for general biomarker discovery is sample composition and dilution severely affect peptide quantification in urine [90]. A disadvantage of mass spectrometry methods are the less precision of detection of the biomarkers in early stage cancer in body fluid. Despite the great advances in the application of MS in serum biomarker discovery, several challenges remain. The identification of differential serum protein profiles and specific molecules able to discriminate normal from diseased subjects requires a technology able to highlight small differences and to process large series of serum samples. Although MS is the most powerful approach for biomarker identification, there are some boundaries in the analysis of serum. These can be attributable to the complex nature of serum and its tremendous dynamic range, to diurnal variation in protein expression, instability of proteins due to *in vivo* or *ex vivo* protease activity, pre-analytical methods reproducibility as well as to the intrinsic MS sensitivity (>μg/ml) in detecting analytes which usually range between 50 pg/mL and 10 ng/ml [91]. Nossov et al. showed that elevated levels of cancer antigen 125 (CA-125), CA-125 is the most widely used biomarker for ovarian cancer, was detected in about 80% of patients with advanced-stage disease, but they were increased in only 50% of patients with early stage ovarian cancer [92]. Different studies showed that serum carcinoembryonic antigen (CEA) has been widely used for colorectal cancer (CRC), its lack of specificity and sensitivity preclude the use of CEA for the early detection of CRC. Though so far a number of CRC-associated tissue proteins have been discovered in multiple studies, with the greater majority being 2D gel-based discoveries coupled to MS/MS, only a limited number of them have been validated in serum for non-invasive testing for CRC [4,93].

MALDI-TOF imaging has the advantage that proteins can be measured *in situ* while the tissue morphology remains fully intact [94], but this method has the disadvantage that is not possible to measure proteins larger than 25 kDa [95]. Meding et al. showed that most of the identified proteins by MALDI-TOF imaging were not reported in the context of lymph node metastasis in colon cancer. This indicates the potential of screening approach to identify novel markers was low. Three of them were selected for validation on an independent cohort. It could be clearly shown that the expression levels of FXYD3, S100A11, and GSTM3 are associated with lymph node metastasis. Elucidating their role in tumor metastasis and testing their usefulness as clinical markers will have to be carried out in future studies [54]. Another aspect of MALDI-TOF imaging that is important to consider is the laser spot size on target and the tradeoff between image resolution and sensitivity. The limit of detection currently is estimated to be in the high attomole to low femtomole range, depending on the molecule being analyzed, but it is difficult to measure accurately in tissue [88].

Future technology for tissue by MALDI-TOF and MALDI-TOF imaging will be great and novel in future studies in detection and/or identification biomarker in cancer. MALDI-TOF imaging has made remarkable advances in the realm of imaging intact tissue samples. The aforementioned advantages of this technique can be combined with the growing field of 3D cell culture and tissue engineering to provide quick, inexpensive and detailed information on disease states, drug delivery and biomarker of cancer on either a global proteomic or individual protein scale. Additionally, the combination of MALDI-TOF imaging and cytochemical/histological techniques will increase the knowledge gained from each experiment [96]. Furthermore, coupled with laser capture microdissection (LCM), MALDI-TOF or/and SELDI-TOF can be an ideal approach for generation of separate protein profiles of the invasive tumor and normal epithelial components of tumors and tissues of cancer [71,97–99].

Further improvement in sensitivity is a never-ending challenge. Clearly there is the need to achieve higher sensitivity to measure proteins of low expression levels.

5.2. Reproducibility in cancer biomarker semi-quantification by MALDI-TOF MS

MALDI-TOF MS technologies have been evolving, and successfully used in genome, proteome, metabolome, and clinical diagnostic research. Emerging evidence has shown that they are not only useful in qualitative analyses, but also beneficial in quantitative analyses of proteins, as biomarkers in clinical analysis [100]. Many groups suggested that moderate reproducibility in relative peptide quantification is a major limitation of MALDI-TOF MS. Several research groups have applied MALDI-TOF MS for relative quantitative measurements of biomarkers. At the same time, the non-quantitative character of this method has been widely reported. Albalat et al. highlighted the unpredictable effect of sample dilution when using MALDI-TOF MS. They observed that potential biomarkers might be detectable at certain concentration ranges only and that valuable information is lost when too restricted dilution ranges are analyzed. The sample composition or the variation in analyte concentrations severely affects the correlation between ion-counts and concentration, which hinders the identification/assessment of biomarkers using this platform. This was observed when single sample dilutions were analyzed, which resulted in substantial discrepancies [90]. Szajli et al. conducted experiments to test the reliability of this technique of quantitation using the statistical method of the inverse confidence limit calculation. The relationship between relative intensities of known amounts of standard peptides and their concentration ratios was investigated. They found that the concentration ratios determined by the relative intensity measurements were highly inaccurate and strongly influenced by the molecular milieu of the sample analyzed. Thus, they emphasized the necessity of the use the sample itself for calibration and recommend to perform a similar statistical analysis to demonstrate reliability for every system where MALDI-TOF MS is used for quantitative measurements [83]. Mirgorodskaya et al. developed a method for quantification of proteins and peptides in very low, picomolar and sub-picomolar, concentrations using MALDI-TOF MS with internal ^{18}O-labeled standards. Mathematical algorithm that uses the isotopic patterns of the substance, the internal standard, and the substance/internal standard mixture for accurate quantitation of the substance was developed. A great advantage of the suggested method consists in the absence of limitation in molecular weight for the quantitation of proteins and the possibility of quantitation without previous fractionation of proteins and peptides [101]. Even though MALDI is a powerful technique for mass spectrometry of peptides and proteins, it is not quite useful for their quantification. This is one of the issues in the quantitative proteomics. The main difficulty lies in the poor reproducibility of MALDI spectra. Park et al. showed a novel method to quantify any analyte amenable to MALDI-TOF MS [56]. This method is based on the previous observations that the reaction quotient for the matrix-to-peptide proton transfer evaluated in temperature-selected MALDI was nearly constant regardless of the peptide concentration in the solid sample. This implied a direct proportionality between the relative abundance of an analyte ion in a temperature-selected MALDI spectrum and the concentration of the corresponding neutral in the solid sample. This relation was confirmed by calibration curves obtained for some peptides. Another characteristic of the relation is that it works even when other analytes are present. This was demonstrated for mixtures that contain peptides and proteins. Moreover, the method does not require the addition of internal standards and allows rapid

and inexpensive quantification of any analyte amenable to MALDI [102].

6. Conclusions and outlooks

Early and sensitive diagnostics are the key how to treat cancer successfully. Therefore, it is not surprising that modern bio-analytical chemistry and tools, which has been developed, serves more or less for finding good markers or some fingerprints [103]. Mass spectrometry is powerful tool for identification of new metabolites, peptides, proteins and nucleic acids associated with the cancer development. Based on the above mentioned facts, MALDI-TOF MS can be used not only for identification of one specific analyte, but also for mass fingerprinting. Both approaches have advantages and disadvantages, however, their combination could open a new window in the cancer diagnostics.

Therefore, proteomic profiling by MALDI-TOF MS shows various advantages (speed of analysis, ease of use, relatively low cost, sensitivity, and possibility of automation). Earlier studies provided by many groups suggested that moderate reproducibility in relative peptide quantification is a major limitation of MALDI-TOF MS.

Acknowledgements

References

[1] Y. Zhang, L.L. Li, P.Y. Yang, H.J. Lu, On-plate enrichment methods for MALDI-MS analysis in proteomics, Anal. Methods 4 (2012) 2622–2631.

[2] M.H. Zhang, X.H. Xu, Y. Wang, Q.X. Linq, Y.T. Bi, X.J. Miao, C.F. Ye, S.X. Gao, C.Y. Gong, H. Xiang, M.S. Dong, A prognostic biomarker for gastric cancer with lymph node metastases, Anat. Rec. 296 (2013) 590–594.

[3] C. Gomes, A. Almeida, J.A. Ferreira, L. Silva, H. Santos-Sousa, J. Pinto-De-Sousa, L.L. Santos, F. Amado, T. Schwientek, S.B. Levery, U. Mandel, H. Causen, L. David, C.A. Reis, H. Osorio, Glycoproteomic analysis of serum from patients with gastric precancerous lesions, J. Proteome Res. 12 (2013) 1454–1466.

[4] D.X. Zhu, J. Wang, L. Ren, Y. Li, B. Xu, Y. Wei, Y.S. Zhong, X.Z. Yu, S.Y. Zhai, J.M. Xu, X.Y. Qin, Serum proteomic profiling for the early diagnosis of colorectal cancer, J. Cell. Biochem. 114 (2013) 448–455.

[5] N.J. Fan, C.F. Gao, X.L. Wang, G. Zhao, Q.Y. Liu, Y.Y. Zhang, B.G. Cheng, Serum peptidome patterns of colorectal cancer based on magnetic bead separation and MALDI-TOF mass spectrometry analysis, J. Biomed. Biotechnol. 2012 (2012) 1–8.

[6] W.T. Liu, B.Y. Liu, Q. Cai, J.F. Li, X.H. Chen, Z.G. Zhu, Proteomic identification of serum biomarkers for gastric cancer using multi-dimensional liquid chromatography and 2D differential gel electrophoresis, Clin. Chim. Acta 413 (2012) 1098–1106.

[7] M. Pietrowska, J. Polanska, R. Suwinski, M. Widel, T. Rutkowski, M. Marczyk, I. Dominczyk, L. Ponge, L. Marczak, A. Polanski, P. Widlak, Comparison of peptide cancer signatures identified by mass spectrometry in serum of patients with head and neck, lung and colorectal cancers: association with tumor progression, Int. J. Oncol. 40 (2012) 148–156.

[8] B. Vafadar-Isfahani, S.A.S. Laversin, M. Ahmad, G. Ball, C. Coveney, C. Lemetre, A.K. Miles, G. van Schalkwyk, R. Rees, B. Matharoo-Ball, Serum biomarkers which correlate with failure to respond to immunotherapy and tumor progression in a murine colorectal cancer model, Proteom. Clin. Appl. 4 (2010) 682–696.

[9] P.F. Aquino, J.S.G. Fischer, A.G.C. Neves-Ferreira, J. Perales, G.B. Domont, G.D.T. Araujo, V.C. Barbosa, J. Viana, S.R.S. Chalub, A.Q.L. de Souza, M.G.C. Carvalho, A.D.L. de Souza, P.C. Carvalho, Are gastric cancer resection margin proteomic profiles more similar to those from controls or tumors? J. Proteome Res. 11 (2012) 5836–5842.

[10] D. Fujimoto, Y. Hirono, T. Goi, K. Katayama, S. Matsukawa, A. Yamaguchi, The activation of proteinase-activated receptor-1 (PAR1) promotes gastric cancer cell alteration of cellular morphology related to cell motility and invasion, Int. J. Oncol. 42 (2013) 565–573.

[11] Q. Hou, H.T. Tan, K.H. Lim, T.K. Lim, A. Khoo, I.B.H. Tan, K.G. Yeoh, M.C.M. Chung, Identification and functional validation of caldesmon as a potential gastric cancer metastasis-associated protein, J. Proteome Res. 12 (2013) 980–990.

[12] A.L. Li, P. Gao, Z.N. Wang, Y.X. Song, Y.Y. Xu, Y. Miao, J.L. Zhu, H.M. Xu, Positive association of the vascular endothelial growth factor-A +405 GG genotype and poor survival in stage I–II gastric cancer in the Northern Chinese population, Mol. Biol. Rep. 40 (2013) 2741–2748.

[13] Q. Meng, T. Lei, M. Zhang, J. Zhao, X.H. Zhao, Identification of proteins differentially expressed in adriamycin-resistant (pumc-91/ADM) and parental (pumc-91) human bladder cancer cell lines by proteome analysis, J. Cancer Res. Clin. Oncol. 139 (2013) 509–519.

[14] X.X. Yang, X.Q. He, F.X. Li, Y.S. Wu, Y. Gao, M. Li, Risk-association of DNA methyltransferases polymorphisms with gastric cancer in the Southern Chinese population, Int. J. Mol. Sci. 13 (2012) 8364–8378.

[15] R. Singhal, J.B. Carrigan, W.B. Wei, P. Taniere, R.K. Hejmadi, C. Forde, C. Ludwig, J. Bunch, R.L. Griffiths, P.J. Johnson, O. Tucker, D. Alderson, U.L. Gunther, D.G. Ward, MALDI profiles of proteins and lipids for the rapid characterisation of upper GI-tract cancers, J. Proteomics 80 (2013) 207–215.

[16] M.D. Pastor, A. Nogal, S. Molina-Pinelo, R. Melendez, B. Romero-Romero, M.D. Mediano, J.L. Lopez-Campos, R. Garcia-Carbonero, A. Sanchez-Gastaldo, A. Carnero, L. Paz-Ares, Identification of oxidative stress related proteins as biomarkers for lung cancer and chronic obstructive pulmonary disease in bronchoalveolar lavage, Int. J. Mol. Sci. 14 (2013) 3440–3455.

[17] W.L. Chen, K.T. Kuo, T.Y. Chou, C.L. Chen, C.H. Wang, Y.H. Wei, L.S. Wang, The role of cytochrome c oxidase subunit Va in non-small cell lung carcinoma cells: association with migration, invasion and prediction of distant metastasis, BMC Cancer 12 (2012) 1–13.

[18] S.G. Musharraf, N. Hashmi, M.I. Choudhary, N. Rizvi, A. Usman, R. Atta ur, Comparison of plasma from healthy nonsmokers, smokers, and lung cancer patients: pattern-based differentiation profiling of low molecular weight proteins and peptides by magnetic bead technology with MALDI-TOF MS, Biomarkers 17 (2012) 223–230.

[19] S.H. Gu, Q.H. Wu, X.Y. Zhao, W.T. Wu, Z.Q. Gao, X.M. Tan, J. Qian, H.Y. Chen, Y. Xie, L. Jin, B.H. Han, D.R. Lu, Association of CASP3 polymorphism with hematologic toxicity in patients with advanced non-small-cell lung carcinoma treated with platinum-based chemotherapy, Cancer Sci. 103 (2012) 1451–1459.

[20] F. Li, D.N. Chen, C.W. He, Y. Zhou, V.M. Olkkonen, N. He, W. Chen, P. Wan, S.S. Chen, Y.T. Zhu, K.J. Lan, W.L. Tan, Identification of urinary Gc-globulin as a novel biomarker for bladder cancer by two-dimensional fluorescent differential gel electrophoresis (2D-DIGE), J. Proteomics 77 (2012) 225–236.

[21] R.T. Bryan, W.B. Wei, N.J. Shimwell, S.I. Collins, S.A. Hussain, L.J. Billingham, P.G. Murray, N. Deshmukh, N.D. James, D.M.A. Wallace, P.J. Johnson, M.P. Zeegers, K.K. Cheng, A. Martin, D.G. Ward, Assessment of high-throughput high-resolution MALDI-TOF-MS of urinary peptides for the detection of muscle-invasive bladder cancer, Proteom. Clin. Appl. 5 (2011) 493–503.

[22] E. Gianazza, C. Chinello, V. Mainini, M. Cazzaniga, V. Squeo, G. Albo, S. Signorini, S.S. Di Pierro, S. Ferrero, S. Nicolardi, Y.E.M. van der Burgt, A.M. Deelder, F. Magni, Alterations of the serum peptidome in renal cell carcinoma discriminating benign and malignant kidney tumors, J. Proteomics 76 (2012) 125–140.

[23] K. Schwamborn, R.C. Krieg, J. Grosse, N. Reulen, R. Weiskirchen, R. Knuechel, G. Jakse, C. Henkel, Serum proteomic profiling in patients with bladder cancer, Eur. Urol. 56 (2009) 989–996.

[24] L. Yan, Z.Q. Xing, Z.X. Guo, Z.Q. Fang, W. Jiao, X.Y. Guo, Z.H. Xu, Z.H. Fang, A. Holmberg, S. Nilsson, Z.X. Liu, Somatostatin derivative (smsDX) targets cellular metabolism in prostate cancer cells after androgen deprivation therapy, PLoS ONE 8 (2013) 1–10.

[25] C.L. Nilsson, F. Berven, F. Selheim, H.L. Liu, J.R. Moskal, R.A. Kroes, E.P. Sulman, C.A. Conrad, F.F. Lang, P.E. Andren, A. Nilsson, E. Carlsohn, H. Lilja, J. Malm, D. Fenyo, D. Subramaniyam, X.D. Wang, M. Gonzales-Gonzales, N. Dasilva, P. Diez, M. Fuentes, A. Vegvari, K. Sjodin, C. Welinder, T. Laurell, T.E. Fehniger, H. Lindberg, M. Rezeli, G. Edula, S. Hober, G. Marko-Varga, Chromosome 19 annotations with disease speciation: a first report from the Global Research Consortium, J. Proteome Res. 12 (2013) 135–150.

[26] E.F. Shin, D.I. Vodolazhsky, A.Y. Golikov, T.N. Belova, N.V. Boyko, D.V. Zimakov, E.N. Cherkasova, M.I. Kogan, M.B. Chibichian, S.A. Moshkovskii, V.A. Tarasov, D.G. Matishov, Separation and study of the range of plasminogen isoforms in patients with prostate cancer, Biochem.-Moscow 77 (2012) 1065–1071.

[27] M.H. Teiten, S. Gaigneaux, S. Chateauvieux, A.M. Billing, S. Planchon, F. Fack, J. Renaut, F. Mack, C.P. Muller, M. Dicato, M. Diederich, Identification of differentially expressed proteins in curcumin-treated prostate cancer cell lines, Omics 16 (2012) 289–300.

[28] H. Montgomery, N. Rustogi, A. Hadjisavvas, K. Tanaka, K. Kyriacou, C.W. Sutton, Proteomic profiling of breast tissue collagens and site-specific characterization of hydroxyproline residues of collagen alpha-1-(I), J. Proteome Res. 11 (2012) 5890–5902.

[29] D. Bohm, K. Keller, J. Pieter, N. Boehm, D. Wolters, W. Siggelkow, A. Lebrecht, M. Schmidt, H. Kolbl, N. Pfeiffer, F.H. Grus, Comparison of tear protein levels in breast cancer patients and healthy controls using a de novo proteomic approach, Oncol. Rep. 28 (2012) 429–438.

[30] D. Bohm, K. Keller, N. Wehrwein, A. Lebrecht, M. Schmidt, H. Kolbl, F.H. Grus, Serum proteome profiling of primary breast cancer indicates a specific biomarker profile, Oncol. Rep. 26 (2011) 1051–1056.

[31] E. Lopez-Arias, A. Aguilar-Lemarroy, L.F. Jave-Suarez, G. Morgan-Villela, I. Mariscal-Ramirez, M. Martinez-Velazquez, A.H. Alvarez, A. Gutierrez-Ortega, R. Hernandez-Gutierrez, Alpha 1-antitrypsin: a novel tumor-associated antigen identified in patients with early-stage breast cancer, Electrophoresis 33 (2012) 2130–2137.

[32] X.J. Qin, B.X. Ling, Proteomic studies in breast cancer, Oncol. Lett. 3 (2012) 735–743.

[33] Y.R. Jeon, S.Y. Kim, E.J. Lee, Y.N. Kim, D.-Y. Noh, S.Y. Park, A. Moon, Identification of annexin II as a novel secretory biomarker for breast cancer, Proteomics 13 (2013) 3145–3156.

[34] B. Velstra, Y.E.M. van der Burgt, B.J. Mertens, W.E. Mesker, A.M. Deelder, R. Tollenaar, Improved classification of breast cancer peptide and protein profiles by combining two serum workup procedures, J. Cancer Res. Clin. Oncol. 138 (2012) 1983–1992.

[35] J. Ulirsch, C. Fan, G. Knafl, M.J. Wu, B. Coleman, C.M. Perou, T. Swift-Scanlan, Vimentin DNA methylation predicts survival in breast cancer, Breast Cancer Res. Treat. 137 (2013) 383–396.

[36] P. Srinivas, S.P. Kollapalli, A. Thomas, K.K. Mortha, S. Das Banerjee, Bioactive hyaluronan fragment (hexasaccharide) detects specific hexa-binding proteins in human breast and stomach cancer: possible role in tumorogenesis, Indian J. Biochem. Biophys. 49 (2012) 228–235.

[37] J. Gao, R.R. Zhao, Y. Xue, Z.X. Niu, K. Cui, F.C. Yu, B. Zhang, S. Li, Role of enolase-1 in response to hypoxia in breast cancer: exploring the mechanisms of action, Oncol. Rep. 29 (2013) 1322–1332.

[38] M.P. Ween, N.A. Lokman, P. Hoffmann, R.J. Rodgers, C. Ricciardelli, M.K. Oehler, Transforming growth factor-beta-induced protein secreted by peritoneal cells increases the metastatic potential of ovarian cancer cells, Int. J. Cancer 128 (2011) 1570–1584.

[39] M. Li, J. Yin, N. Mao, L.Y. Pan, Upregulation of phosphorylated cofilin 1 correlates with taxol resistance in human ovarian cancer in vitro and in vivo, Oncol. Rep. 29 (2013) 58–66.

[40] H.Q. Huang, J. Tang, S.T. Zhou, T. Yi, H.L. Peng, G.B. Shen, N. Xie, K. Huang, T. Yang, J.H. Wu, C.H. Huang, Y.Q. Wei, X. Zhao, Orlistat, a novel potent antitumor agent for ovarian cancer: proteomic analysis of ovarian cancer cells treated with Orlistat, Int. J. Oncol. 41 (2012) 523–532.

[41] H. Huang, Y.J. Li, J.H. Liu, M.H. Zheng, Y.L. Feng, K.H. Hu, Y.W. Huang, Q.D. Huang, Screening and identification of biomarkers in ascites related to intrinsic chemoresistance of serous epithelial ovarian cancers, PLoS ONE 7 (2012) 1–9.

[42] M. Kazmierczak, M. Luczak, K. Lewandowski, L. Handschuh, A. Czyz, M. Jarmuz, M. Gniot, M. Michalak, M. Figlerowicz, M. Komarnicki, Esterase D and gamma 1 actin level might predict results of induction therapy in patients with acute myeloid leukemia without and with maturation, Med. Oncol. 30 (2013) 1–9.

[43] P.C. He, Y.F. Liu, M. Zhang, X.N. Wang, H.Y. Wang, J.Y. Xi, K.H. Wei, H.L. Wang, J. Zhao, Establishment of two-dimensional gel electrophoresis profiles of the human acute promyelocytic leukemia cell line NB4, Mol. Med. Rep. 6 (2012) 570–574.

[44] I. Kapoor, P. Pal, S. Lochab, J.K. Kanaujiya, A.K. Trivedi, Proteomics approaches for myeloid leukemia drug discovery, Expert. Opin. Drug Discov. 7 (2012) 1165–1175.

[45] U.H. Sk, S.P. Kambhampati, M.K. Mishra, W.G. Lesniak, F. Zhang, R.M. Kannan, Enhancing the efficacy of Ara-C through conjugation with PAMAM dendrimer and linear PEG: a comparative study, Biomacromolecules 14 (2013) 801–810.

[46] D. Wang, Y.Q. Lv, Y.F. Liu, X.J. Du, B. Li, Differential protein analysis of lymphocytes between children with acute lymphoblastic leukemia and healthy children, Leuk. Lymphoma 54 (2013) 381–386.

[47] S. Chughtai, K. Chughtai, B. Cillero-Pastor, A. Kiss, P. Agrawal, L. MacAleese, R.M.A. Heeren, A multimodal mass spectrometry imaging approach for the study of musculoskeletal tissues, Int. J. Mass Spectrom. 325 (2012) 150–160.

[48] H. Dihazi, R. Bohrer, O. Jahn, C. Lenz, A. Majcherczyk, B. Schmidt, H. Urlaub, O. Valerius, A.R. Asif, Mass spectrometry imaging: linking molecule profiles to tissue spatial distribution, Expert Rev. Proteomics 10 (2013) 17–20.

[49] L.A. McDonnell, R.M.A. Heeren, P.E. Andren, M. Stoeckli, G.L. Corthals, Going forward: increasing the accessibility of imaging mass spectrometry, J. Proteomics 75 (2012) 5113–5121.

[50] H. Bateson, S. Saleem, P.M. Loadman, C.W. Sutton, Use of matrix-assisted laser desorption/ionisation mass spectrometry in cancer research, J. Pharmacol. Toxicol. Methods 64 (2011) 197–206.

[51] C. Schone, H. Hofler, A. Walch, MALDI imaging mass spectrometry in cancer research: combining proteomic profiling and histological evaluation, Clin. Biochem. 46 (2013) 539–545.

[52] C.C. Cheng, J.S. Chang, L.Y. Cheng, A.S. Ho, K.J. Huang, S.C. Lee, F.D. Mai, C.C. Chang, Human neutrophil peptides 1–3 as gastric cancer tissue markers measured by MALDI-imaging mass spectrometry: Implications for infiltrated neutrophils as a tumor target, Dis. Markers 32 (2012) 21–31.

[53] B. Balluff, S. Rauser, M.P. Ebert, J.T. Siveke, H. Hofler, A. Walch, Direct molecular tissue analysis by MALDI imaging mass spectrometry in the field of gastrointestinal disease, Gastroenterology 143 (2012) U514–U544.

[54] S. Meding, B. Balluff, M. Elsner, C. Schone, S. Rauser, U. Nitsche, M. Maak, A. Schafer, S.M. Hauck, M. Ueffing, R. Langer, H. Hofler, H. Friess, R. Rosenberg, A. Walch, Tissue-based proteomics reveals FXYD3, S100A11 and GSTM3 as novel markers for regional lymph node metastasis in colon cancer, J. Pathol. 228 (2012) 459–470.

[55] A. Végvári, B. Döme, State-of-the-art MS technology applications in lung disease, Bioanalysis 3 (2011) 2665–2677.

[56] G.K. Lee, H.S. Lee, Y.S. Park, J.H. Lee, S.C. Lee, S.J. Lee, S.R. Shanta, H.M. Park, H.R. Kim, I.H. Kim, Y.H. Kim, J.I. Zo, K.P. Kim, H.K. Kim, Lipid MALDI profile classifies non-small cell lung cancers according to the histologic type, Lung Cancer 76 (2012) 197–203.

[57] G. Marko-Varga, T.E. Fehniger, M. Rezeli, B. Döme, T. Laurell, A. Végvári, Drug localization in different lung cancer phenotypes by MALDI mass spectrometry imaging, J. Proteomics 74 (2011) 982–992.

[58] T. Alexandrov, M. Becker, O. Guntinas-Lichius, G. Ernst, F. von Eggeling, MALDI-imaging segmentation is a powerful tool for spatial functional

proteomic analysis of human larynx carcinoma, J. Cancer Res. Clin. Oncol. 139 (2013) 85–95.

[59] K.D. Herring, S.R. Oppenheimer, R.M. Caprioli, Direct tissue analysis by matrix-assisted laser desorption ionization mass spectrometry: application to kidney biology, Semin. Nephrol. 27 (2007) 597–608.

[60] R.F. Oezdemir, N.T. Gaisa, K. Lindemann-Docter, S. Gostek, R. Weiskirchen, M. Ahrens, K. Schwamborn, C. Stephan, D. Pfister, A. Heidenreich, R. Knuechel, C. Henkel, Proteomic tissue profiling for the improvement of grading of noninvasive papillary urothelial neoplasia, Clin. Biochem. 45 (2012) 7–11.

[61] D. Bonnel, R. Longuespee, J. Franck, M. Roudbaraki, P. Gosset, R. Day, M. Salzet, I. Fournier, Multivariate analyses for biomarkers hunting and validation through on-tissue bottom-up or in-source decay in MALDI-MSI: application to prostate cancer, Anal. Bioanal. Chem. 401 (2011) 149–165.

[62] S.H. Chuang, J. Li, X.Y. Sun, A. Vadlamudi, B. Sun, L. Cazares, J. Nyalwidhe, D. Troyer, J. Semmes, F.D. McKenzie, Prostate cancer region prediction by fusing results from MALDI spectra-processing and texture analysis, Simul.-Trans. Soc. Model. Simul. Int. 88 (2012) 1247–1259.

[63] K. Chughtai, L. Jiang, T.R. Greenwood, K. Glunde, R.M.A. Heeren, Mass spectrometry images acylcarnitines, phosphatidylcholines, and sphingomyelin in MDA-MB-231 breast tumor models, J. Lipid Res. 54 (2013) 333–344.

[64] S.K. Kang, H. Maeng, B.G. Kim, G.M. Qing, Y.P. Choi, H.Y. Kim, P.S. Kim, Y. Kim, Y.H. Kim, Y.D. Choi, N.L. Cho, In situ identification and localization of IGHA2 in the breast tumor microenvironment by mass spectrometry, J. Proteome Res. 11 (2012) 4567–4574.

[65] R. Longuespee, C. Boyon, A. Desmons, D. Vinatier, E. Leblanc, I. Farre, M. Wisztorski, K. Ly, F. D'Anjou, R. Day, I. Fournier, M. Salzet, Ovarian cancer molecular pathology, Cancer Metastasis Rev. 31 (2012) 713–732.

[66] R. Longuespee, C. Boyon, C. Castellier, A. Jacquet, A. Desmons, O. Kerdraon, D. Vinatier, I. Fournier, R. Day, M. Salzet, The C-terminal fragment of the immunoproteasome PA28S (Reg alpha) as an early diagnosis and tumor-relapse biomarker: evidence from mass spectrometry profiling, Histochem. Cell Biol. 138 (2012) 141–154.

[67] M. Lagarrigue, R. Lavigne, B. Guevel, E. Com, P. Chaurand, C. Pineau, Matrix-assisted laser desorption/ionization imaging mass spectrometry: a promising technique for reproductive research, Biol. Reprod. 86 (2012) 1–7.

[68] C.B. Liu, The application of SELDI-TOF-MS in clinical diagnosis of cancers, J. Biomed. Biotechnol. 2011 (2011) 1–6.

[69] C.H. Clarke, D.L.B. McCarthy, in: C.H. Clarke, D.L.B. McCarthy (Eds.), SELDI-TOF Mass Spectrometry: Methods and Protocols, 2012, pp. 1–239.

[70] I.D. Popescu, R. Albulescu, E. Raducan, A. Dinischiotu, C. Tanase, Applications of SELDI-TOF technology in cancer biomarkers discovery, Rom. Biotech. Lett. 15 (2010) 5654–5667.

[71] I. Cadron, T. Van Gorp, F. Amant, I. Vergote, P. Moerman, E. Waelkens, A. Daemen, R. Van De Plas, B. De Moor, R. Zeillinger, The use of laser microdissection and SELDI-TOF MS in ovarian cancer tissue to identify protein profiles, Anticancer Res. 29 (2009) 1039–1045.

[72] K.L. Tang, T.H. Li, W.W. Xiong, K. Chen, Ovarian cancer classification based on dimensionality reduction for SELDI-TOF data, BMC Bioinformatics 11 (2010) 1–8.

[73] C. Simsek, O. Sonmez, A.I. Keyf, A.S. Yurdakul, C. Ozturk, O. Gulbahar, F. Ozmen, N. Zengin, D. Kubilay, S.C. Karatayli, M. Bozdayi, Importance of serum SELDI-TOF-MS analysis in the diagnosis of early lung cancer, Asian Pac. J. Cancer Prev. 14 (2013) 2037–2042.

[74] L.B. Mordhorst, B. Sorbe, C. Ahlin, A study of serum biomarkers associated with relapse of cervical cancer, Anticancer Res. 32 (2012) 4913–4922.

[75] V.M. Garrisi, A. Tufaro, P. Trerotoli, I. Bongarzone, M. Quaranta, V. Ventrella, S. Tommasi, G. Giannelli, A. Paradiso, Body mass index and serum proteomic profile in breast cancer and healthy women: a prospective study, PLoS ONE 7 (2012) 1–6.

[76] F. Bertucci, A. Goncalves, Clinical proteomics and breast cancer: strategies for diagnostic and therapeutic biomarker discovery, Future Oncol. 4 (2008) 271–287.

[77] R.A. Craven, N.S. Vasudev, R.E. Banks, Proteomics and the search for biomarkers for renal cancer, Clin. Biochem. 46 (2013) 456–465.

[78] M. De Bock, D. de Seny, M.A. Meuwis, J.P. Chapelle, E. Louis, M. Malaise, M.P. Merville, M. Fillet, Challenges for biomarker discovery in body fluids using SELDI-TOF-MS, J. Biomed. Biotechnol. 2010 (2010) 1–15.

[79] J.F. Zou, G.N. Hong, X.W. Guo, L. Zhang, C. Yao, J. Wang, Z. Guo, Reproducible cancer biomarker discovery in SELDI-TOF MS using different pre-processing algorithms, PLoS ONE 6 (2011) 1–9.

[80] T.C.W. Poon, Opportunities and limitations of SELDI-TOF-MS in biomedical research: practical advices, Expert Rev. Proteomics 4 (2007) 51–65.

[81] R.E. Caffrey, in: A.J. Rai (Ed.), Urinary Proteome: Methods and Protocols, Humana Press Inc., Totowa, 2010, pp. 167–183.

[82] W. Wegdam, P.D. Moerland, D. Meijer, S.M. de Jong, H.C.J. Hoefsloot, G.G. Kenter, M.R. Buist, J. Aerts, A critical assessment of SELDI-TOF-MS for biomarker discovery in serum and tissue of patients with an ovarian mass, Proteome Sci. 10 (2012).

[83] E. Szajli, T. Feher, K.F. Medzihradszky, Investigating the quantitative nature of MALDI-TOF MS, Mol. Cell. Proteomics 7 (2008) 2410–2418.

[84] M. Kirchner, B.T. Xu, H. Steen, J.A.J. Steen, A C++ implementation for fast box intersection and application to sparse mass spectrometry data, Bioinformatics 27 (2011) 1166–1167.

[85] C. Yang, Z.Y. He, W.C. Yu, Comparison of public peak detection algorithms for MALDI mass spectrometry data analysis, BMC Bioinformatics 10 (2009) 1–13.

[86] D. Mantini, F. Petrucci, D. Pieragostino, P. Del Boccio, P. Sacchetta, G. Candiano, G.M. Ghiggeri, A. Lugaresi, G. Federici, C. Di Ilio, A. Urbani, A computational platform for MALDI-TOF mass spectrometry data: application to serum and plasma samples, J. Proteomics 73 (2010) 562–570.

[87] L.C. Wu, H.H. Chen, J.T. Horng, C. Lin, N.E. Huang, Y.C. Cheng, K.F. Cheng, A novel preprocessing method using Hilbert Huang transform for MALDI-TOF and SELDI-TOF mass spectrometry data, PLoS ONE 5 (2010) 1–15.

[88] E.H. Seeley, R.M. Caprioli, Molecular imaging of proteins in tissues by mass spectrometry, Proc. Natl. Acad. Sci. U.S.A. 105 (2008) 18126–18131.

[89] M.A. Karpova, S.A. Moshkovskii, I.Y. Toropygin, A.I. Archakov, Cancer-specific MALDI-TOF profiles of blood serum and plasma: biological meaning and perspectives, J. Proteomics 73 (2010) 537–551.

[90] A. Albalat, A. Stalmach, V. Bitsika, J. Siwy, J.P. Schanstra, A.D. Petropoulos, A. Vlahou, J. Jankowski, F. Persson, P. Rossing, T.W. Jaskolla, H. Mischak, H. Husi, Improving peptide relative quantification in MALDI-TOF MS for biomarker assessment, Proteomics 13 (2013) 2967–2975.

[91] E. Kuhn, T. Addona, H. Keshishian, M. Burgess, D.R. Mani, R.T. Lee, M.S. Sabatine, R.E. Gerszten, S.A. Carr, Developing multiplexed assays for troponin I and interleukin-33 in plasma by peptide immunoaffinity enrichment and targeted mass spectrometry, Clin. Chem. 55 (2009) 1108–1117.

[92] V. Nossov, M. Amneus, F. Su, J. Lang, J.M.T. Janco, S.T. Reddy, R. Farias-Eisner, The early detection of ovarian cancer: from traditional methods to proteomics. Can we really do better than serum CA-125? Am. J. Obstet. Gynecol. 199 (2008) 215–223.

[93] C.R. Jimenez, J.C. Knol, G.A. Meijer, R.J.A. Fijneman, Proteomics of colorectal cancer: overview of discovery studies and identification of commonly identified cancer-associated proteins and candidate CRC serum markers, J. Proteomics 73 (2010) 1873–1895.

[94] B. Balluff, M. Elsner, A. Kowarsch, S. Rauser, S. Meding, C. Schuhmacher, M. Feith, K. Herrmann, C. Rocken, R.M. Schmid, H. Hofler, A. Walch, M.P. Ebert, Classification of HER2/neu status in gastric cancer using a breast-cancer derived proteome classifier, J. Proteome Res. 9 (2010) 6317–6322.

[95] B. Balluff, C. Schone, H. Hofler, A. Walch, MALDI imaging mass spectrometry for direct tissue analysis: technological advancements and recent applications, Histochem. Cell Biol. 136 (2011) 227–244.

[96] E.M. Weaver, A.B. Hummon, Imaging mass spectrometry: from tissue sections to cell cultures, Adv. Drug Deliv. Rev. 65 (2013) 1039–1055.

[97] M.E. Sanders, E.C. Dias, B.J. Xu, J.A. Mobley, D. Billheimer, H. Roder, J. Grigorieva, M. Dowsett, C.L. Arteaga, R.M. Caprioli, Differentiating proteomic biomarkers in breast cancer by laser capture microdissection and MALDI MS, J. Proteome Res. 7 (2008) 1500–1507.

[98] R.B.H. Braakman, T.M. Luider, J.W.M. Martens, J.A. Foekens, A. Umar, in: G.I. Murray (Ed.), Laser Capture Microdissection: Methods and Protocols, 2nd ed., Humana Press Inc., Totowa, 2011, pp. 143–154.

[99] B.J.G. Xu, J. Li, R.D. Beauchamp, Y. Shyr, M. Li, M.K. Washington, T.J. Yeatman, R.H. Whitehead, R.J. Coffey, R.M. Caprioli, Identification of early intestinal neoplasia protein biomarkers using laser capture microdissection and MALDI MS, Mol. Cell. Proteomics 8 (2009) 936–945.

[100] E.W.Y. Ng, M.Y.M. Wong, T.C.W. Poon, Advances in MALDI mass spectrometry in clinical diagnostic applications, Top. Curr. Chem. 336 (2014) 139–175.

[101] O.A. Mirgorodskaya, Y.P. Kozmin, M.I. Titov, R. Korner, C.P. Sonksen, P. Roepstorff, Quantitation of peptides and proteins by matrix-assisted laser desorption/ionization mass spectrometry using O-18-labeled internal standards, Rapid Commun. Mass Spectrom. 14 (2000) 1226–1232.

[102] K.M. Park, Y.J. Bae, S.H. Ahn, M.S. Kim, A simple method for quantification of peptides and proteins by matrix-assisted laser desorption ionization mass spectrometry, Anal. Chem. 84 (2012) 10332–10337.

[103] V. Adam, R. Kizek, Fingerprinting in cancer diagnostics, Expert Rev. Proteomics 10 (2013) 211–213.

3.6. Review III

HEGER Z., **RODRIGO M.A**., KRIZKOVA S., RUTTKAY-NEDECKY B., ZALEWSKA M., DEL POZO E.M., PELFRENE A., POURRUT B., STIBOROVA M., ECKSCHLAGER T., EMRI G., KIZEK R., ADAM V. Metallothionein as a Scavenger of Free Radicals - New Cardioprotective Therapeutic Agent or Initiator of Tumor Chemoresistance? (2015). *Curr Drug Targets.*

Participation in the work of the author M.A. Merlos Rodrigo literature research 40% and manuscript preparation 30%.

The most serious adverse effect of anthracyclines is, thus, cardiomyopathy leading to congestive heart failure, which is caused by the same mechanisms. In this review, we briefly summarize the basic types of free radicals formed by anthracyclines and the main processes how to scavenge them. From these, the main attention is paid to MTs. The main function of MTs is their activity are as scavengers of free radicals, antioxidant action, metal detoxication and homeostasis but they are also involved as new cardioprotective therapeutic agent or initiator of tumor chemoresistance.

Metallothionein as a Scavenger of Free Radicals – New Cardioprotective Therapeutic Agent or Initiator of Tumor Chemoresistance?

Zbynek Heger[1,2], Miguel Angel Merlos Rodrigo[1,2], Sona Krizkova[1,2], Branislav Ruttkay-Nedecky[1,2], Marta Zalewska[3], Elena Maria Planells del Pozo[4], Aurelie Pelfrene[5], Bertrand Pourrut[5], Marie Stiborova[6], Tomas Eckschlager[7], Gabriella Emri[8], Rene Kizek[1,2] and Vojtech Adam[1,2*]

[1]*Central European Institute of Technology, Brno University of Technology, Technicka 3058/10, CZ-616 00 Brno, Czech Republic, European Union*
[2]*Department of Chemistry and Biochemistry, Mendel University in Brno, Zemedelska 1, CZ-613 00 Brno, Czech Republic, European Union*
[3]*Department of Biomedical and Environmental Analysis, Faculty of Pharmacy, Wroclaw Medical University, Borowska 211, 50-556 Wroclaw, Poland, European Union*
[4]*Department of Physiology, School of Pharmacy, Institute of Nutrition and Food Technology "José Mataix", Biomedical Research Center, University of Granada, Spain, European Union*
[5]*Groupe ISA, Laboratoire Génie Civil et géo-Environnement (LGCgE), 48 boulevard Vauban, 59046 Lille cedex, France*
[6]*Department of Biochemistry, Faculty of Science, Charles University, Albertov 2030, CZ-128 40 Prague 2, Czech Republic, European Union*
[7]*Department of Paediatric Haematology and Oncology, 2nd Faculty of Medicine, Charles University, and University Hospital Motol, V Uvalu 84, CZ-150 06 Prague 5, Czech Republic, European Union*
[8]*Department of Dermatology, Faculty of Medicine, University of Debrecen, Debrecen, Hungary, European Union*

*Corresponding author

Vojtech Adam, Department of Chemistry and Biochemistry, Mendel University in Brno, Zemedelska 1, CZ-613 00 Brno, Czech Republic; E-mail: vojtech.adam@mendelu.cz; phone: +420-5-4513-3350; fax: +420-5-4521-2044

Abstract

Cardiotoxicity is a serious complication of anticancer therapy by anthracycline antibiotics. Except for intercalation into DNA/RNA structure, inhibition of DNA-topoisomerase and histone eviction from chromatin, the main mechanism of their action is iron-mediated formation of various forms of free radicals, which leads to irreversible damage to cancer cells. The most serious adverse effect of anthracyclines is, thus, cardiomyopathy leading to congestive heart failure, which is caused by the same mechanisms. Here, we briefly summarize the basic types of free radicals formed by anthracyclines and the main processes how to scavenge them. From these, the main attention is paid to metallothioneins. These low-molecular cysteine-rich proteins are introduced and their functions and properties are reviewed. Further, their role in detoxification of metals and drugs is discussed. Based on these beneficial roles, their use as a new therapeutic agent against oxidative stress and for cardioprotection is critically evaluated with respect to their ability to increase chemoresistance against some types of commonly used cytostatics.

Running title: Metallothionein - a key molecule in chemotherapy.

Content

1. *Introduction. The main purpose of the review*

Cardiotoxicity is a serious complication of anticancer therapy by anthracycline cytostatics (Fig. 1) [1]. The main mechanisms of anthracyclines action are intercalation into DNA structure, inhibition of topoisomerase II and reactive oxygen species (ROS) generation [2]. Heart tissue is, due to its minimal regeneration capacity, constant activity and intensive aerobic metabolism, highly susceptible to oxidative stress injury [3].

While at tumors the mechanisms of chemoresistance were investigated, in the case of healthy cells, the possibilities of drugs side effects minimization on healthy cells and organs are still searched. The same mechanisms that contribute to resistance of cancer cells can be used to suppress the cytostatic side effects [4]. Mechanisms involved in resistance of cancer cells to cytostatic drugs include: i) reduced drug uptake; ii) increased drug efflux; iii) increased DNA repair; iv) increased tolerance to DNA damage; v) changes in target structure; vi) defects in apoptotic pathways; vii) increased levels of intracellular thiols such as glutathione and metallothionein (MT) [5]. MT role in chemoresistance has been intensively studied not only at heavy metal-based cytostatics, but also at "non-metal cytostatic drugs", especially doxorubicin (DOX) [6]. It is supposed, that main MT functions in detoxification of cytostatics are their antioxidant capability [7], heavy metals chelation and homeostasis [8].

In the presented review, we briefly summarize the basic types of free radicals formed by anthracyclines and the main processes how to scavenge them with special focus on metallothioneins. Available literature covering the given topic was searched in following databases as Scopus (Elsevier, Amsterdam, Netherland), Web of Science (Thomson Reuters, New York, NY, USA), Cochrane Library (Cochrane Collaboration, Baltimore, MD, USA) and PubMed (United States National Library of Medicine, Bethesda, MD, USA)..

2. *Free radicals and their role in the organism*

ROS, the cellular products of myriad physiological processes have been understood to damage cells if produced in excess [9]. They are characterized as having a single unpaired electron in outer shell and are thus highly reactive [10]. ROS refer to a group of small reactive molecules that include superoxide anion ($^\cdot O_2^-$), hydrogen peroxide (H_2O_2), hydroxyl ($^\cdot OH^-$), and hypochlorite (OCl^-) which may cause adverse effects due to irreversible modification of macromolecules such as proteins, DNA and membranes [11]. Under physiological conditions, the intracellular levels of ROS are steadily maintained to prevent cells from damage. Subsequent detoxification is facilitated by non-enzymatic molecules (glutathione [12], flavonoids [13], vitamins C and E [14, 15]) and by antioxidant enzymes (superoxide

dismutases, glutathione peroxidase, and catalase) [16]. ROS affect ROS-sensitive signaling pathways (MAPK/Erk1/2, PI3K/Akt, IKK/NF-κB), linked to many types of cancer. Affecting those pathways regulates growth, development and differentiation of cells [17]. In particular, H_2O_2 acts as a second messenger, regulating protein activity through reversible oxidation of its targets - tyrosine phosphatases, tyrosine kinases and important transcription factors [18-20]. This phenomenon results in a broad spectrum of health complications as tumorigenesis [21], and it is also linked with pathogenesis of many other diseases e.g. cardiovascular, diabetes etc. [22-24]. ROS, which are responsible for the side effects of anthracyclines [1], are generated as a product of an electron transfer between a quinone moiety of anthracyclines and oxygen and other donor molecules [2, 25]. Interestingly, it was also shown that short-term oxidative stress may be important as the aging prevention, due to a process known as mitohormesis [26]. Although the exact mechanisms were not elucidated yet, the most probable effectors include metal trafficking (metallothioneins and ferritins [27]) and enhanced innate immunity [28, 29] - both described in long lived mutants. The information mentioned above raise question: Is selective introduction of expression of maintenance processes (metallothioneins) sufficient to protect myocard against anthracycline-associated heart damage?

2.1. Mechanisms of anti-ROS protection

The formation of free radicals and superoxides belongs to the current accepted hypothesis for the mechanism, by which anthracyclines cause cardiotoxicity [30-33]. "DOX is the most probably able to damage the mitochondria of cardiomyocytes, whereas several mitochondrial enzymes such as NADH dehydrogenase, cytochrome P-450 reductase and xanthine oxidase are involved in generating ROS [30-32, 34]". "The free radical theory says that it starts with a one-electron reduction of doxorubicin to form a DOX semiquinone radical by a reduced flavoenzyme such as NADPH-cytochrome P450 reductase (Fig. 2). The semiquinone radical forms a complex with iron, which leads to an anthracycline-iron (Fe^{2+}) free radical complex. Resulting complex reduces oxygen to produce superoxide and to regenerate DOX. The superoxide is dismutated into hydrogen peroxide and oxygen [35]". "DOX also increases superoxide formation by increasing endothelial nitric oxide synthase [36], which promotes intracellular hydrogen peroxide formation [37]." The consequent formation of peroxynitrite could play a role in the cardiotoxicity, too [38]. Lipid peroxidation may also occur by the combination of superoxide, hydrogen peroxide and free iron.

In anti-ROS protection a number of antioxidants and iron-chelating agents have been tested. The first tested antioxidant was vitamin E, which was found to be efficient only against the acute cardiotoxic effects of DOX, but it was ineffective against development of chronic cardiomyopathy [30, 39-41]. Vitamin E in combination with selenium was shown to have no significant protective action against DOX-induced mortality and cardiotoxicity [42, 43]. A lot of other antioxidants as melatonin, vitamin A and vitamin C [44] thiol-containing reducing agents (glutathione, N-acetylcysteine, S-allylcysteine, amifostine) and reduced glutathione [45] have been also tested however, the results found have not been so encouraging...

Moreover, probucol is a lipid-lowering drug exerting an antioxidant effect and promoting the activities of endogenous antioxidants, can also prevent DOX cardiomyopathy and heart failure, which was confirmed in animal experiments without impairing the antitumor effect of the drug [30, 46-48]. "There was also found an increase in myocardial glutathione peroxidase and superoxide dismutase activities with concomitant decrease in lipid peroxidation during treatment with probucol [47]." "In addition, carvedilol, which acts as both a β-adrenergic receptor blocker and an antioxidant [49, 50], also appears to reduce DOX cardiotoxicity [51-53]." Carvedilol significantly prevented lipid peroxidation and increase in both myocardial and plasma cholesterol concentration caused by DOX [49]. Carvedilol in addition to its antioxidant action also has been shown to prevent apoptotic cell death of cardiac myocytes [50].

The iron-chelating agent dexrazoxane (ICRF-187) [54, 55] significantly reduced the development of DOX cardiomyopathy in a dog model [56]. This agent has been introduced into clinical practice [57]. Metallothioneins have also been shown to have protective role against acute [58-60] and chronic myocardial toxicity of DOX due to zinc chelation, antioxidant properties and ROS scavenging abilities, for details see *chapter 3.1*. MT elevation also effectively prevented chronic cardiotoxicity and decreased the oxidative stress caused by DOX [61], for details see *chapter 5.3*. MTs cardioprotective effect is based mainly on their antioxidant function [62, 63] in connection with other antioxidant enzymes and molecules [64], other possibilities are metals release and chelation by MT in dependence on its oxidative state [65, 66].

3. *Metallothioneins – isoforms, structure and function*

MTs are low-molecular (7 kDa) cysteine-rich, heat-stable and metal binding proteins [67, 68]. In mammals, distinct MT isoforms designated MT-1 through MT-4 have been found [69, 70]. "Human MTs are encoded by 17 genes located on chromosome 16q13; MT-2, MT-3, and

MT-4 are encoded by a single gene, while the MT-1 has many subtypes (MT-1A,-B,-E,-F,-G,-H,-M,-X) [71, 72]." "Expression of MTs can be started by binding of metal regulatory-transcription factor-1 (MTF-1) to the regulative region of *MT* genes called metal-responsive element (MRE) [73]. The most widely expressed isoforms in the body are MT-1 and MT-2 [74, 75]." "The MT-3 protein was first isolated as a growth inhibiting factor (GIF) from brain neurons, but its message is expressed also in tongue, stomach, heart, kidney and reproductive tissues [76, 77]." Finally, the MT-4 protein was found in stratified epithelium [78]. The main function of MTs are scavenging of free radicals, antioxidant action, metal detoxification and homeostasis but they are also involved in regulation of fundamental cell processes [70, 72, 79-81].

3.1. *Metallothioneins as ROS scavengers*

MT has, due to the presence of thiol moieties from cysteine residues, antioxidant properties. Moreover, together with reduced glutathione (GSH) it is able to decrease the level of ROS [82, 83]. MT plays a role in many intracellular physiological processes, where the increased occurrence of molecules causing oxidative stress can be expected and/or where preservation of structures susceptible to free radicals (nucleic acids, phospholipids membranes, proteins etc.) [84] is needed such as proliferation or embryo development [85, 86].

"The most critical advance in MT research is the demonstration of the redox regulation of Zn-S interaction and the coupling of zinc and redox metabolism [87, 88]. The cluster structure of Zn-MT provides a chemical basis by which the cysteine ligand can induce oxidoreductive properties [89] that constitutes MT redox cycle." "Studies using cultured cells and intact animal models have provided further evidence supporting the antioxidant function of MT [88, 90-94]."

3.2. *Metallothioneins as heavy metal chelators*

"MTs have, as described above, unique structural characteristics that offer effective metal-binding. MTs are involved in the transport, storage, and regulation of essential metal ions (Zn, Cu, Se) and detoxification of heavy metals (such as Cd, Hg, Ag and As) [95]." In the physiological state, MTs are associated mostly with the Zn^{2+} ions, but may be dissociated and replaced by other metals that have a higher affinity for MT, for example Cd^{2+}, Hg^{2+} and Cu^{1+} [95]. The absence of MT-1/2 increases inorganic Cd-induced lethality and hepatotoxicity, whereas overexpression is associated with protection [96]. MT carries Cd ions to the kidney and provides intracellular protection against Cd toxicity. The uptake of MT complexes with

heavy metals in the kidneys distorts numerous functions within proximal tubules [97]. After Cd-MT complex endocytosis, Cd^{2+} is released and is transported outside the endosomes/lysosomes, where free Cd^{2+} triggers apoptosis [72, 98]. "Transport and storage of essential metal ions, detoxification of toxic metals, free radical scavenging and immune response belong to the key functions of MT [99]." Besides intracellular environment, recent studies show that these proteins can be found in extracellular environment, too. "Outside of cells, they may act as an antioxidant, transporter of essential metals, it may be responsible for the redistribution of heavy metals between tissues, and can influence cell proliferation, being released during normal immune challenge to moderate the vigor of the humoral response and following restraint stress and upon exposure to toxic metals [100]."

"Expression of MT is highly inducible. MT synthesis is primarily induced by essential metals (Zn, Cu), toxic metals (Cd, Hg) and free radicals. Moreover, other compounds and factors, including glucocorticoids, cytokines, growth factors, cytotoxic agents and tumor promoters, as well as various stress-related conditions, up-regulate MT production by generating oxidative stress and free radicals in the affected cells [88, 99, 101, 102]."

3.3. *Metallothioneins as regulators*

MTs are involved in numerous key processes, and the most important include metal homeostasis and protection against oxidative stress. Regulation of Zn accessibility by MT contributes to the regulation of gene expression and affects apoptosis, proliferation, or cell differentiation [72, 82]. Apo-MT can retrieve Zn ions from transcription factors or Zn-containing enzymes, deactivating them or on the other hand Zn-MT can supply Zn^{2+} to protein targets thus activating them. The active p53 can induce a response of cells, which includes DNA repair, inhibition of angiogenesis, differentiation and aging, cell cycle arrest, and apoptosis [103]. Zn-MT is also associated with resistance to apoptosis by regulation the Zn-dependent antiapoptotic transcription factor - nuclear factor κB (NF-κB) [104].

MT is involved in the controlled release of iron from ferritin (Ft) to prevent Fe oxidative damage. "Physiologically, Fe is released from Ft to activate other Fe proteins. Under conditions, which are associated with oxidative damage, the protective pathway fails and iron reacts to form ROS. The complexes of Zn-MT may be electron donors for the reduction of Fe^{3+} and facilitate the release of iron from Ft. At the same time, MT thiolates are oxidized to disulfides, releasing Zn^{2+} [105]."

3.4. *Metallothionein role in chemoresistance*

Chemoresistance is a complex system with multiple and heterogeneous mechanisms [106]. The mechanisms underlying drug resistance are as follows: (i) downregulation, overexpression or modification of target molecules; (ii) increased drug efflux; (iii) the induction of antiapoptotic mechanisms or the activation of pro-apoptotic mechanisms; (iv) changes in drug activating detoxifying enzymes; and (v) pharmacological and physiological factors, such as changes in drug metabolism and excretion, and inadequate access of the drug to the tumor. In view of rich biochemical properties of MTs, it is not surprising that they are believed to participate in emergence of chemo- and/or radioresistance in tumor cells. It has been proposed that increased expression of MT provides protection against apoptosis and promote cell proliferation, leading to tumorigenesis [107]. The most important role of MT in cancer cell chemoresistance is their ability to bind platinum in therapy by platinum cytostatics [108]. Moreover resistance to "nonplatinum cytostatics" has been postulated to be mainly the result of protection against ROS damage, anti-apoptotic properties and by the direct sequestering of alkylating agents by MT cysteines [8, 109]. Recent evidence supports also the interactions with other important thiol compounds, involved in chemoresistance, i.e. glutathione [110, 111]; however, direct mechanism of interaction is still not properly elucidated. As it was shown by Yap and coworkers, si-RNA-based silencing of *MT-2A* gene in MCF-7 cells, exposed to DOX, led to a significant reduction in cell viability and the corresponding elevation of apoptosis [6]. Similarly, in bladder tumors expressing higher levels of MT, survival is significantly poorer, due to mediation of resistance towards alkylating agents [112]. MT was also shown to be an initiator of DOX resistance in non-small cell lung carcinomas (NSCLC) [113], in which significant relationship between MT expression and resistance was found. Moreover, significant correlation was also revealed between MT and glutathione-S-transferase-pi expression. However, the role of MTs in the development of chemoresistance in the clinical conditions is still controversial and their importance may vary in different tumors.

4. *Anthracycline cytostatics*

Anthracyclines are one of the most effective anticancer drugs. Their main adverse effect is cardiotoxicity, which limits their usefulness [114]. Daunorubicin that was isolated from *Streptomyces peucetius* [115] and showed activity against acute lymphoblastic (ALL) and acute myeloid leukemia (AML). Doxorubicin, isolated afterwards, [116] is active against a wider range of tumors (e.g. soft tissue and bone sarcomas, nephroblastoma, neuroblastoma,

hepatoblastoma, non-Hodgkin´s (NHL) and Hodgkin´s lymphomas (HL), multiple myeloma, lung, ovarian, gastric, thyreoid and breast carcinoma) [114]. "There have also been developed newer anthracyclines as epirubicin, a less cardiotoxic doxorubicin analogue active in sarcomas, breast and gastric cancer, idarubicin a daunorubicin analogue having an increased efficacy in AML, or valrubicin, which is used for the intravesical treatment of bladder cancer [114]."

"All anthracyclines share a quinone containing rigid planar aromatic ring structure bound by a glycosidic bond to an amino sugar daunosamine", which is shown in Figs. 1 A, B, E, and F. "Doxorubicin and daunorubicin share aglyconic and sugar moieties. The only difference between DOX and daunorubicin is that the side chain of DOX terminates with a primary alcohol, whereas that of daunorubicin terminates with a methyl group. This difference has fundamental consequences on their activity [117]." Epirubicin is a DOX derivative obtained by an axial-to-equatorial epimerization of the hydroxyl group at C-4´ in daunosamine. This positional change influences mainly pharmacokinetics and metabolism [118, 119] and epirubicin may be used at cumulative doses almost double those of DOX, resulting in equal activity but not in increased cardiotoxicity [120]. Idarubicin, active in AML, multiple myeloma, non-Hodgkin's lymphoma, and breast cancer, was obtained from daunorubicin by removal of the 4-methoxy group in ring D [121]. "Its broader spectrum of activity compared with daunorubicin is attributed to an increased lipophilicity and its higher cellular uptake [122]." In addition, it may be administered orally [123]. *In vitro* studies have indicated that it is more effective than daunorubicin in cells with overexpression of P-glycoprotein [124, 125].

Only a few more anthracyclines is approved: pirarubicin, aclacinomycin A (aclarubicin), and mitoxantrone (substituted aglyconic anthraquinone) (see Figs. 1 C, D, and G). Aclarubicin and pirarubicin show only modest improvements over DOX and daunorubicin in terms of multidrug resistance [126]. Pirarubicin (4-tetrahydropyranyl doxorubicin) has been reported to be less cardiotoxic than DOX in animals [127], but it was not proved in humans [128, 129]. Aclarubicin, a trisaccharide anthracycline, was shown to be active and well tolerated in AML patients [130, 131], but it induced late cardiac events [132]. Mitoxantrone is active in breast cancer, AML, and prostate cancer. Early reports indicated that mitoxantrone was less cardiotoxic than other anthracyclines [133], but it was refuted in later studies [134].

Anthracyclines enter cells by diffusion, their intracellular level are greater than extracellular and the efficiency of their uptake depends on their lipophilicity [118]. "All anthracyclines are substrates for the P-glycoprotein. Idarubicin is a less avid P-glycoprotein substrate that may explain its efficacy in chemoresistant tumors. In addition, the resistance to anthracyclines may

be caused by mutations or down-regulation of topoisomerase II." Moreover, chemoresistance is usually caused by a combination of several mechanisms [135, 136].

Anthracyclines clearance is mediated mainly by biliary excretion after hepatic metabolism. Daunorubicin and Adriamycin are metabolized by aldoketoreductases, which forms daunorubicinol and adriamycinol by reduction of the C-13 carbonyl. Those active products are in microsomes inactivated to aglycones [137].

4.1. *Side effects of anthracyclines*

"Anthracyclines, in addition to side effects common to all cytostatics like myelosuppression, nausea and vomiting, mouth ulcers, local aggressivity and alopecia, are cardiotoxic. Cardiotoxicity limits administration exceeding an accumulated dose of approximately 350 mg doxorubicin/m^2 [138, 139]." Although the mechanisms of their cardiotoxicity are not fully understood, interactions of anthracyclines with iron are supposed to be the main mechanism. "The redox state of iron can be converted between Fe^{2+} and Fe^{3+} states by interaction with anthracyclines, generating toxic ROS which cause DNA damage (Fig. 2) [140]. Cardiomyocytes are vulnerable to free radical damage because of their low activity of antioxidant enzyme systems [139, 141]."

Reversible acute cardiotoxicity develops within days of anthracycline administration. Clinical signs are tachycardia, hypotension, and arrhythmias. The irreversible chronic cardiotoxicity, namely, a congestive heart failure, is more frequent and develops mainly 1- 3 months but may occur even years after chemotherapy [142]. Risk of cardiotoxicity is increased in persons with previous history of heart disease, hypertension, mediastinum irradiation, and age below 4 years [114]. There is no specific treatment of anthracycline induced cardiotoxicity, standard therapy for chronic heart failure is used [142].

4.2. *Mechanisms of anthracycline (cyto)toxicity*

The mechanism of anthracyclines cytotoxicity involves different pathways, but the precise mechanisms remain still to be explained. "The following mechanisms were considered: 1) interference with DNA unwinding or DNA strand separation; 2) intercalation into DNA that inhibits synthesis of DNA, RNA and proteins; 3) generation of free radicals, leading to DNA damage and lipid peroxidation; 4) DNA binding and alkylation; 5) DNA cross-linking; 6) direct membrane effects; 7) helicase activity inhibition; 8) antiangiogenic effect; and 9) inhibition of topoisomerase II [139, 143, 144]." Intercalation into DNA is considered to be the main mechanism, the anthraquinone ring intercalates between DNA base pairs [145].

"Concentrations of anthracyclines used in clinical practice inhibit topoisomerase II. DNA lesions, which are caused by formation of free radical, reactivity on the DNA backbone and lipid peroxidation occurred only in the cells treated with concentrations higher than therapeutic ones [139, 146, 147]."

Doxorubicin forms unstable covalent bonds with DNA when redox-activated with NAD(P)H oxidoreductases and transition metals. Iron-mediated free radical reactions enable DOX to produce formaldehyde from spermine and lipids [148]. "DOX and formaldehyde form a conjugate that may produce an active monomeric metabolite, in which the carbon of formaldehyde is recovered in the form of a Schiff's base at the amino group of daunosamine. Similar reactions occur only with anthracyclines containing 3′-amino group (epirubicin, daunorubicin) [149]. The anthracycline-formaldehyde conjugates intercalate into DNA [150]." "Overexpression of formaldehyde-dehydrogenase is supposed to be the mechanism of resistance to the formation of anthracycline-formaldehyde conjugates. The expression levels of formaldehyde-dehydrogenase in DOX-resistant small-cell lung carcinoma cells were lower than in sensitive ones [151]." "Genomic dsDNA isolated from neuroblastoma cells was studied by adsorptive transfer technique in connection with square wave voltammetry. Decrease in CA signal was found in DNA isolated from neuroblastoma cells sensitive to anthracyclines cultivated in the presence of DOX but not from resistant ones cultivated in the same conditions. The concentration of 0.5 mM which is approximately 100 times higher than clinical doses decreased CA signal for more than 30% [152]." This phenomenon displays that in chemoresistant cells the covalent binding of anthracyclines to DNA is decreased [139]. On the other hand, there have been defined groups of plant secondary metabolites serving as potential protectors against these adverse effects [153].

5. *Reversal of anthracycline toxicity*

Standard prevention of anthracycline cardiotoxicity is in compliance with cumulative dose (900-1000 mg/m^2 of epirubicin, 550 mg/m^2 of daunorubicin and 300- 450 mg/m^2 of doxorubicin). Slowing of anthracycline infusion reduces risk of acute cardiotoxicity [114]. Clinical studies showed that dexrazoxane, statins, angiotensin antagonists and beta-blockers are beneficial in prevention of anthracycline-induced cardiotoxicity [154, 155]. "These findings are in good agreement with the protective role of these agents in cell cultures and animal models treated with anthracyclines, which was accompaniedby reducing oxidative stress, cellular inflammation, myocyte apoptosis and cytokine release (for detailed description see *chapter 5.2*). Angiotensin-converting-enzyme inhibitors (drugs used for the treatment of

hypertension and congestive heart failure) inhibit the action of the mitogenic factor, through its interaction with the angiotensin 2 type-1 receptor, and suppressing epidermal growth factor mediated signal transduction in the cardiovascular myocytes. Some beta blockers (carvidilol and nebivolol) have also antioxidant effects [155]." Anthracyclines also increase mitochondrial iron levels and their decrease by dexrazoxane may decrease risk of anthracycline induced cardiomyopathy – for detail see *5.2*.

Liposomal encapsulation, which changes their tissue distribution and pharmacokinetics belongs to the most successful strategy to decrease the cardiotoxicity of anthracyclines [156]. "The cardiac safeties of liposomal daunorubicin, liposomal DOX, and pegylated liposomal DOX have been studied in a number of clinical trials which indicate that the risk of cardiotoxicity is significantly lower with liposomal anthracyclines [139, 157]." The liposomal components of pegylated liposome encapsulated DOX change pharmacology and pharmacokinetics of DOX. These changes concentrate cytostatics in tumors with decreased exposure of normal cells. Liposomal anthracyclines can be used instead of conventional ones to reduce the risk of cardiotoxicity without reduced efficacy [158]. There are approved three liposomal anthracyclines Doxil/Caelyx (PEGylated HCl doxorubicin), DaunoXome (Daunorubicin) and Myocet (non-PEGylated doxorubicin) [159].

5.1. *Heavy metals supplementation*

"In human body, there is a sophisticated system how to manage and regulate the amount of key trace metals circulating in blood and stored in cells [160]. When this system fails to function properly, abnormal levels and ratios of trace metals can occur. The elevated copper and depressed zinc belong to the most common trace-metal imbalances [161, 162]." The ratio of copper to zinc is clinically more important than the concentration of either of these trace metals [163].

"Zinc is involved in numerous aspects of cellular metabolism, whereas it is needed for the catalytic activity of more than 300 enzymes playing key role in immune function, wound healing, protein synthesis, DNA synthesis and cell division [164]. Zinc possesses antioxidant properties, which may protect against accelerated aging and helps speed up the healing process after an injury [165]."

"Copper plays an important role in our metabolism, largely because it allows many critical enzymes to function properly [161], whereas it plays a role in the production of hemoglobin, myelin, melanin and it also keeps thyroid gland functioning normally. Copper can act as both an antioxidant and a pro-oxidant. As an antioxidant, Cu ions scavenge or neutralize free

radicals and may reduce or help prevent some of the damage they cause [166]. When copper acts as a pro-oxidant at times, it promotes free radical damage [167]. More than the concentration of Zn or Cu in blood serum, the balance between them is important. If the balance is changed several organic systems can be affected [8, 163]."

"Because MT primarily binds Zn under physiological conditions, Zn has been shown to be an effective inducer of MT synthesis in the heart that can provide effective protection against oxidative damage [168]. In addition, that MT upregulation in response to Zn supplementation prevents various pathogeneses has been documented in humans."

Wang *et al.* [169] investigated the role of MT in cardiac protection by zinc supplementation in cultured cardiac cells that were directly exposed to a treatment that mimics diabetic conditions, suggesting that the prevention of diabetic cardiomyopathy by zinc supplementation is predominantly mediated by an increase in cardiac MT.

"Oxidative stress induced by maternal diabetes plays an important role in the development of cardiac malformations [170], whereas zinc supplementation of animals and humans has been shown to be able to ameliorate oxidative stress induced by diabetic cardiomyopathy. Kumar *et al.* [171] showed that supplementation with Zn significantly decreased apoptosis and reduced the levels of oxidative stress induced by maternal diabetes that could play a role in the development and progression of cardiac embryopathy, thus Zn supplementation could be a potential therapeutic agent for diabetic cardiac embryopathy."

5.2. *Decreasing of ROS formation*

Cardiac toxicity of anthracyclines has been at least in part attributed to the generation of ROS and lipid peroxidation [172-176], which can be the consequence of low antioxidant capacity [174]. Selective overexpression of catalase [174] or MT [176, 177] in the heart of mice has been demonstrated to effectively diminish the cardiotoxicity of DOX. Moreover, agents (e.g. plantainoside D, hydrogen sulfide, N-acetyl-L-cysteine, rosmarinic acid, salidroside, sesamol) that can lower the level of ROS thereby suppressing the activation of mitogen-activated protein kinase (MAPK) (p38 kinase, extracellular signal-regulated kinase, c-Jun NH(2)-terminal protein kinase)/nuclear factor-κB pathways and modulating the changes in the expression and activity of antioxidant enzymes (glutathione peroxidase, manganese superoxide dismutase) in cardiomyocytes upon anthracycline exposure, protect against inflammation and/or cytotoxicity induced by these drugs [178-182]. Cardioprotective role of free radical scavengers (e.g. davallialactone, probucol, polyoxalate containing vanillyl alcohol

nanoparticles) against anthracycline induced toxicity has been shown also *in vivo* in animal models [183-185].

Production of ROS is mediated by iron; therefore iron chelation seems to be a realistic approach to reduce the cardiac toxicity of anthracyclines [186]. Aroylhydrazone lipophilic iron chelators (e.g. salicylaldehyde isonicotinoyl hydrazone) have been found to lower the cardiotoxicity of anthracyclines without compromising the antitumor effect of these chemotherapeutics [186, 187]. Interestingly, the cardioprotection does not correlate with the reduction of free radical production. Flavonoids are iron chelating and antioxidant compounds that are also able to protect against cardiac toxicity induced by anthracyclines without influencing the antiproliferative effect of the drugs, and clinical use of a semi-synthetic flavonoid 7-monohydroxyethylrutoside has already been tested [188, 189]. Dexrazoxane (ICRF-187), an established cardioprotectant is a highly effective bisdioxopiperazine agent to reduce the cardiac toxicity of anthracyclines [142]. Dexrazoxane is the prodrug of iron chelating agent ADR-925, but more complex modes of cardioprotective action are assumed [142, 190]. "Several randomized trials in both children and adults have concluded that dexrazoxane is an effective cardioprotectant against anthracycline-induced toxicity [191]." However, one study showed increased risk of second malignant neoplasms and AML/MDS i group of patients suffering from Hodgkin lymphoma treated by regiments containing adriamycin if they received dexrazoxane [192].

Strong reduction of cardiac toxicity by a mitochondria-targeted antioxidant, a nitroxide conjugated to a triphenylphosphonium cation (Mito-Tempol (4)) emphasizes the importance of anthracycline induced mitochondrial dysfunction in the development of cardiomyopathy [190].

5.3. *MT induction*

Cardioprotective role of MT seems to be complex [177]. On one hand, MT can function as a free radical scavenger due to its high sulfhydryl content [193]. Formation of MT disulfide bonds occurs *in vivo* under physiological circumstances and increases under oxidative stress conditions e.g. as a response to DOX exposure, and it is related to zinc release from MT [194]. The reduced cytotoxic effect of DOX in MT overexpressing cardiomyocytes correlates with the inhibition of lipid peroxidation induced by the drug [176]. On the other hand, analysis of the transcriptomes of cardiac cells derived from MT deficient and wild type mice exposed to DOX demonstrated the implication of several signaling pathways in the protection against anthracycline induced cardiotoxicity that is related to MT [195]. Zinc release and

transfers from MT, which is a redox regulated process, can impact on several cellular stress responses such as apoptosis and energy metabolism changes [177]. It has been shown that MT inhibits anthracycline-induced apoptosis interfering with the p38-MAPK signaling pathway as well as mitochondrial cytochrome c-release [177]. The mitochondrial respiration and energy metabolism can be modulated through the posttranslational regulation of proteins by zinc-MT [177]. Cardiac toxicity of anthracyclines at least in part seems to be mediated by the inhibition of peroxisome proliferator-activated receptor γ coactivator-1 α (PGC-1α) leading to impaired mitochondrial biogenesis, downregulation of manganese superoxide dismutase and increased mitochondrial superoxide production [196]. Comparing MT deficient and wild type mice Guo *et al.* have found that cardioprotective role of MT against DOX induced cytotoxicity can partially be attributed to the preservation of the function of PGC-1α by MT [196].

Cardiac toxicity induced by DOX is significantly lower in MT overexpressing transgenic mice compared to the wild type animals suggesting that elevation of the level of MT prior to chemotherapy can protect the cardiomyocytes effectively against anthracycline induced oxidative stress [197]. Likewise, although treatment with DOX induces superoxide and peroxynitrite production and cardiac damage in both MT deficient and wild type mice, it could however be prevented by the preadministration of zinc in MT wild type animals [198]. Administration of daunorubicin to Sprague-Dawley rats has been found to induce MT-1 in the heart and liver of animals; however, to a much lower degree than a treatment with zinc dose 20 mg/kg [172]. They proposed to consider the administration of zinc prior to anthracycline chemotherapy to reduce the cardiac and liver toxicities. However, MTs can be induced by several endogenous (cytokines, hormones) and exogenous (heavy metals) stimuli [193]. Nevertheless, possibility of the induction of MT in cancer cells has to be critically evaluated to avoid fatal consequences such as the initiation of aggressive tumor growth [199]. Noteworthy, a novel human MT isoform (hMT-1p) has been isolated and cloned from a tumor cell line (AML-2), which is resistant to the superoxide generator paraquat [200]. Transfection of another cancer cell line (SNU-601) with hMT-Ip resulted in the inhibition of oxidation damage and anthracycline induced toxicity. Cardiac specific expression of hMT-1p might be utilized in the prevention of chemotherapy associated cardiotoxicity [200]. Furthermore, the findings of Satoh *et al.* suggest that tissue specific induction of MT is feasible [175]. They have demonstrated that the level of MT is increased either in bone marrow, in the heart or in the tumor tissue of colon cancer bearing mice given zinc, but it is elevated solely in the tumor upon administration of copper, while selectively in the heart and bone marrow of the mice given bismuth [175]. Maintained antitumor activity of adriamycin could be observed with

reduced cardiac and bone marrow toxicity in mice that were treated with bismuth prior to chemotherapy [175]. Importantly, though there were less toxic adverse events, the antitumor activity of adriamycin was reduced in the mice given zinc [175].

Noteworthy, another research group has demonstrated that combination of zinc with chemotherapeutic agents such as cisplatin and adriamycin can even re-establish the chemosensitivity of cancer cells by reactivating p53 and enhance immunogenic type cell death [201, 202].

6. *Metallothioneins as cardioprotectors*

"Oxidative stress has been associated with diverse pathophysiological events, including cancer, and neurodegeneration. ROS also play a role in the development of vasculopathies and cardiac hypertrophy [203, 204]." "ROS stimulate myocardial growth, matrix remodeling, and cellular dysfunction. ROS activate a broad variety of hypertrophy signaling kinases and transcription factors [205]." MT has been shown to inhibit cardiac oxidative stress and protect against the cardiotoxicity induced by chemotherapeutic agents [206], prevent cardiac pathological changes in diabetes [207], and protects the cardiac endoplasmic reticulum against stress and apoptosis [208, 209].

6.1. *MT roles in cardioprotection*

MT was found to diminish apoptosis and myocardial infarction through inhibition of oxidative stress [208]. MT 1 and 2 are the key molecules in cardiac signal transducer and activator of transcription 3 (STAT3)-mediated attenuation of ischemia/reperfusion (I/R) injury. "Cardiac specific activation of STAT3 transduces antioxidative signals through MT and confers resistance against ROS stress in the heart [210]."

MT's cardioprotection against DOX is mediated by preservation of mitochondrial biogenesis throughout peroxisome proliferators–activated receptor γ coactivator-1 α (PGC-1α) pathway [196]. PGC-1α is a key regulator for mitochondrial biogenesis, which is important source of cellular ROS as well as targets of ROS. MT protects against DOX-induced inhibition on PGC-1α for details see *5.3*. Zhou *et al.* have shown that chronic exposures of mice to intermittent hypoxia (IH) could induce cardiac ER stress and associated apoptotic cell death along with cardiac inflammation [208]. *In vitro* study with H9c2 cardiac and primary neonatal cardiomyocytes showed that MT protection from ER stress-induced apoptosis is mediated by up-regulating Akt phosphorylation [208]. Inhibition of the Akt phosphorylation level with a PI3K inhibitor abolished the preservation of the normal Akt phosphorylation level. It was

noted that exposure to IH caused significantly early and severer decrease in the Akt phosphorylation level in mice with global MT gene deletion (MT-KO) but did not have such effect in mice with overexpression of *MT* gene (MT-TG). These studies indicate that activation of Akt can rescue cardiac ER stress, cell death, and cardiac dysfunction induced remodeling induced by tunicamycin or thapsigargin *in vitro* and *in vivo* [208].

ER stress-induced changes in the myocardial function, autophagy was reduced by MT. MT significantly attenuated tunicamycin-induced cardiac contractile dysfunction, intracellular Ca^{2+} homeostasis, ER stress, oxidative stress, and the induction of autophagy [209].

Cardiac MT expression is up-regulated in response to short-term IH insults but decreases after long-term chronic IH (CIH) exposures. IH induces the accumulation of hypoxia-inducible transcription factor-1α (HIF-1α) which is essential for induction of MT expression by hypoxia. Hypoxia-induced MT in turn stabilizes HIF-1α protein, suggesting that early response of MT expression to IH exposures could be regulated by HIF-1α. The decrease in MT at the late stage of IH exposures could be regulated by inhibitory molecules induced by long-term IH insults or arise from cardiac cell death which results in a loss of cellular capability to up-regulate MT expression [211].

Administration of MT or induction of MT expression may be used as a strategy in prevention and therapy of cardiovascular diseases.

6.2. *Strategies for targeted increase of MT expression*

Similarly as in cancer there are some strategies of targeted MT silencing to prevent chemoresistance [212], in cardioprotection the increasing of MTs expression would help to overcome the adverse action of anthracyclines (Fig. 3). MT synthesis in heart can be increased by zinc administration, mild oxidative stress conditions and corticoids, as described above. Unlike MT silencing [213], no strategies have been developed for targeted increasing of MT synthesis except stable or transient transfection by *MT* genes.

Heart-specific MT overexpression as a cardioprotective factor was initially published in 1997, where the mice overexpressing MT-2a in heart exhibited a decreased acute heart injury after treatment with DOX [59, 60]. It has also been found that MT elevation is a highly effective approach to prevent DOX's chronic cardiotoxicity [61]. In the opposite, the increased apoptosis and myocardial injuries were observed at MT-null mice exposed to DOX [214-216]. Tissue-specific increase in MT synthesis can be achieved by stable or transient transfection, as shown at paraquat-resistant AL-2 cell lines stable transfected with human MT-1, which led to the cells resistance to DOX and pirarubicin [217].

MT expression can be increased also by other proteins as STAT3, already mentioned in section *6.1*. STAT3 mediated cardioprotection against I/R injury through MT induction in the heart of transgenic mice [210]. Injection of TNF caused tissue-specific induction of MT-1 synthesis in the liver, lung and heart, but not in the kidney and thymus [218].

Except heavy metals and pro-oxidant compounds, which are discussed above, corticoids in doses physiologically relevant stress conditions led to up-regulation of *MT* genes in primary cultured cardiomyocytes exposed to DOX. Compared to cells exposed to DOX only, the antiapoptotic, antioxidant and detoxication genes were up-regulated, such as glutathione-peroxidases, glutathione-S transferases and bcl-xL. However, expression of bcl-2 and pro-apoptotic factors bax, bak and bad at protein level was inhibited [219].

7. *Conclusions*

Since anthracyclines exhibit high efficiency in treatment of various malignant tumors, the unwanted cardiotoxicity significantly decreases their therapeutic index. Currently few synthetic approaches are employed to decrease this undesired effect, such as encapsulation of drug into PEG or non-PEG liposome, leading to prolongation of persistence of the drug in circulation. Nevertheless, although the therapeutic index was increased, cardiotoxicity still forms a problem. Thus, biological approaches such as induction of cardioprotectors may be highly interesting for cancer patients, particularly when treated with doxorubicin. Metallothioneins are able to do that, however their induction has to be site-specific, due to their scavenging attributes, leading to development of drug resistance. Heart-specific overexpression of MTs by transient transfection, induction of other proteins or metals would thus help to overcome the adverse action of anthracyclines without elevation of tumor resistance. Development of such approach in combination with liposomal forms of doxorubicin can results in significant increase of DOX application doses, which can fundamentally enhance the treatment success of broad spectrum of tumor diseases.

Conflict of Interest

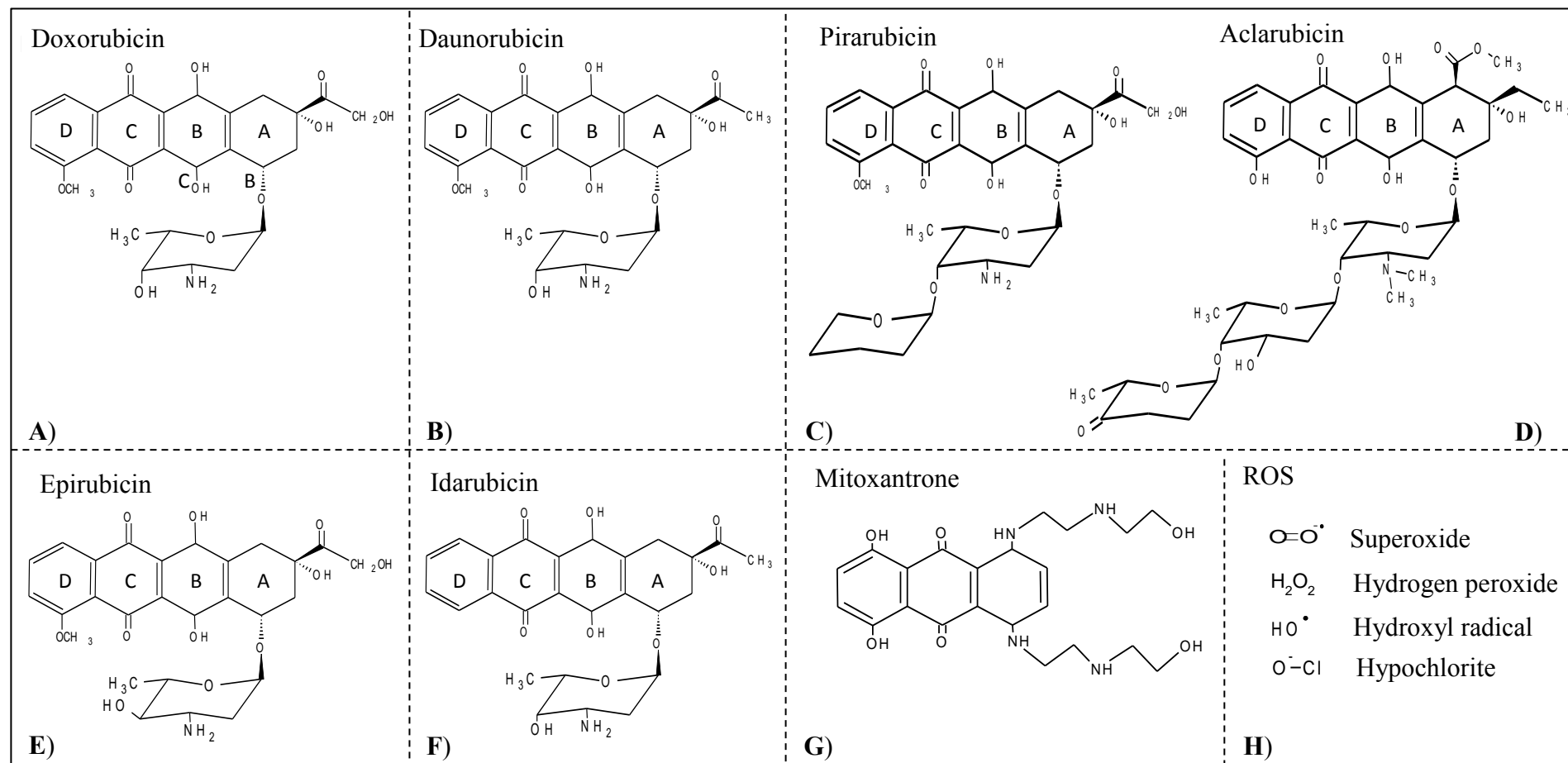The authors declare no conflict of interests

Acknowledgements

Figure 1. Structures of the most frequent anthracycline cytostatics: doxorubicin (**A**), daunorubicin (**B**), pirarubicin (**C**), aclarubicin (**D**), epirubicin (**E**), idarubicin (**F**), mitoxantrone (**G**) and structures of the most common ROS (**H**).
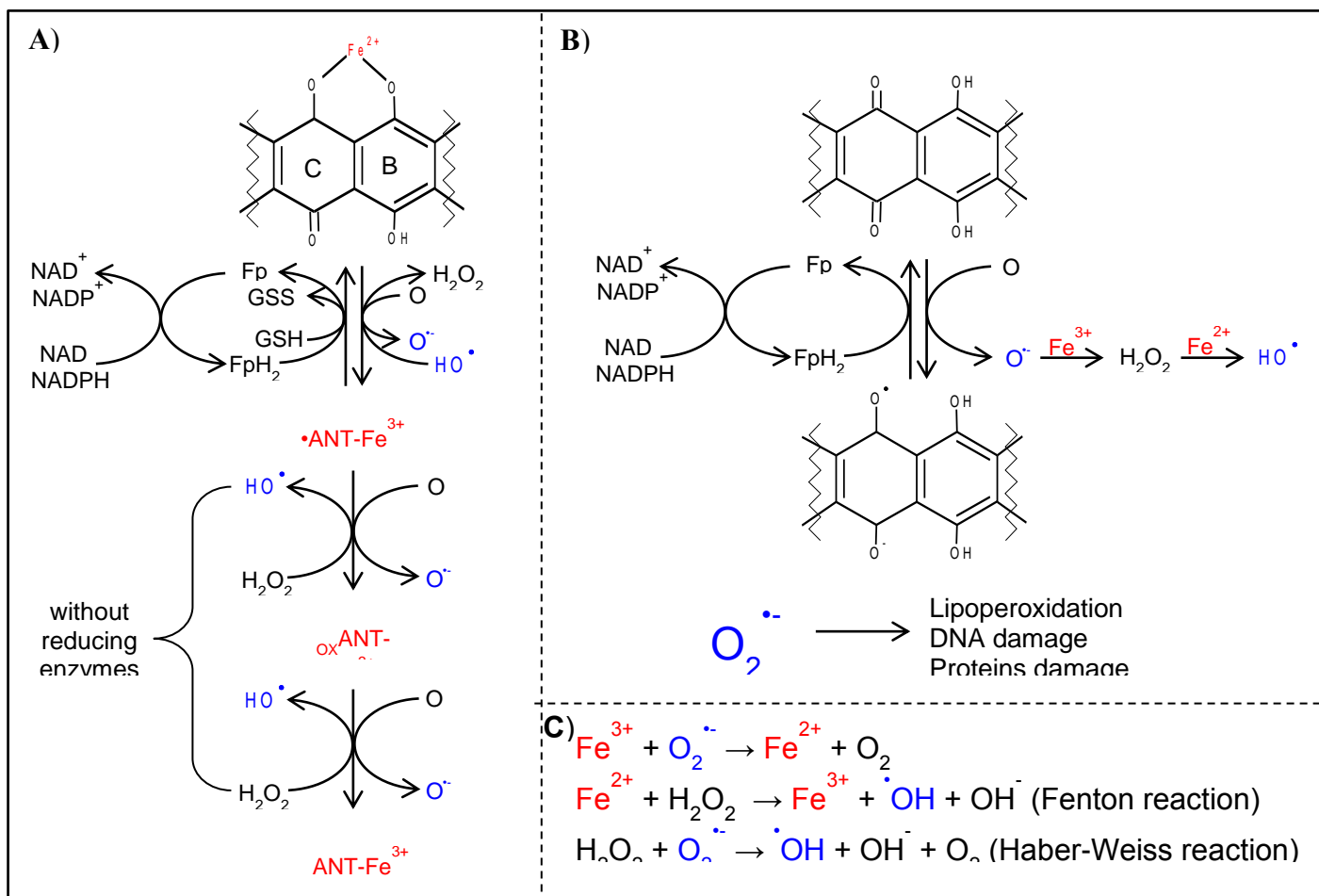
Figure 2. Mechanism of anthracycline cardiotoxicity formation. (**A**) Schematic representation of production of free radicals after chelation of doxorubicin and iron in presence of NADPH and without reducing enzymes, which both lead to generation of hydroxyl and superoxide free radicals. (**B**) Role of iron in superoxide and hydroxyl radicals formation and further actions of superoxide radicals. (**C**) Representation of possible free radicals evolution through Fenton reaction, where iron and hydrogen peroxide are capable oxidizing a wide range of substrates, which leads to biological damage; and Haber-Weiss reaction, which generates hydroxyl radicals from hydrogen peroxide and superoxide. The first step of reaction involves reduction of ferric ions to ferrous. GSH – reduced glutathione, GSSG – oxidized glutathione, Fp – flavoprotein, FpH_2 – reduced flavoprotein, ANT – anthracycline.
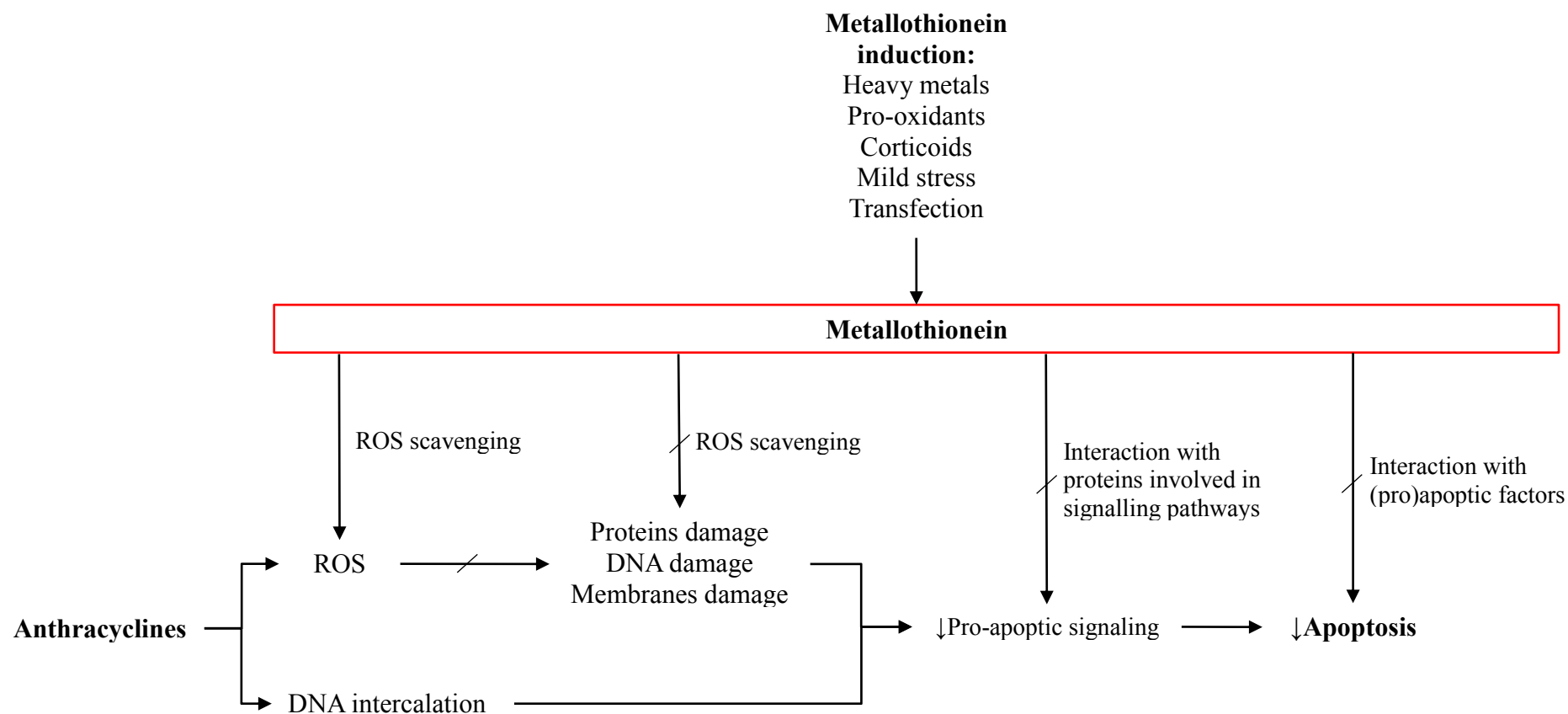
Figure 3. Involvement of MT in a decrease in cardiotoxicity of antracyclines. Due to its ability to scavenge free radicals, interaction with regulatory proteins involved in (pro)apoptotic and signaling pathways, MT contributes to resistance against anthracyclines both in tumor and heart tissues. While in tumour tissue its action is suppressed, targeted increasing of MT expression in heart can decrease the cardiotoxic effects of anthracyclines.

Abbreviations:

Akt – protein kinase B

ALL – acute lymphoblastic leukaemia

AML – acute myeloid leukaemia

bcl-xL – B-cell lymphoma-extra large

CIH – chronic intermittent hypoxia

c-Jun - Transcription factor AP-1

DNA – deoxyribonucleic acid

DOX – doxorubicin

ER – endoplasmic reticulum

Erk1/2 – Extracellular signal-Regulated Kinase 1/2

Ft – ferritin

GIF – growth inhibiting factor

GSH – glutathione

HIF-1α – hypoxia-inducible transcription factor-1α

HL – Hodgkin's lymphoma

IH – intermittent hypoxia

IKK/NF-κB – IκB kinase/NF-κB signaling pathway

kDa - kilodalton

MAPK – mitogen-activated protein kinase

MDS – myelodysplastic syndrome

MRE – metal-responsive element

MT – metallothionein

MTF-1 – metal regulatory-transcription factor-1

MTs – metallothioneins

NAD(P)H – nicotine adenine dinucleotide (phosphate)

NF-κB – nuclear factor κB

NHL – non-Hodgkin's lymphoma

NSCLS – non-small cell lung carcinoma

p38 – member of the second MAPK-related pathway

p53 – tumor suppressor p53

PEG – polyethylene glycol

PGC-1α – peroxisome proliferator-activated receptor γ coactivator-1 α

PI3K – phosphoinositide 3-kinase

PI3K/Akt – signaling pathway

RNA – ribonucleic acid

ROS – reactive oxygen species

siRNA – small interfering RNA

SOD – superoxide dismutase

STAT3 – signal transducer and activator of transcription 3

TNF – tumor necrosis factor

References

[1]   Heger Z, Cernei N, Kudr J, Gumulec J, Blazkova I, Zitka O, et al. A Novel Insight into the Cardiotoxicity of Antineoplastic Drug Doxorubicin. Int J Mol Sci. 2013 Nov;14(11):21629-46.

[2]   Vejpongsa P, Yeh ETH. Prevention of Anthracycline-Induced Cardiotoxicity. J Am Coll Cardiol. 2014 Sep;64(9):938-45.

[3]   Arafa MH, Mohammad NS, Atteia HH, Abd-Elaziz HR. Protective effect of resveratrol against doxorubicin-induced cardiac toxicity and fibrosis in male experimental rats. J Physiol Biochem. 2014 Sep;70(3):701-11.

[4]   Prochazka P, Libra A, Zemanova Z, Hrebackova J, Poljakova J, Hrabeta J, et al. Mechanisms of ellipticine-mediated resistance in UKF-NB-4 neuroblastoma cells. Cancer Sci. 2012 Feb;103(2):334-41.

[5]   Maccarinelli F, Gammella E, Asperti M, Regoni M, Biasiotto G, Turco E, et al. Mice lacking mitochondrial ferritin are more sensitive to doxorubicin-mediated cardiotoxicity. J Mol Med. 2014 Aug;92(8):859-69.

[6]   Yap XL, Tan HY, Huang JX, Lai YY, Yip GWC, Tan PH, et al. Over-expression of metallothionein predicts chemoresistance in breast cancer. J Pathol. 2009 Mar;217(4):563-70.

[7]   Choi CH, Kim HS, Kweon OS, Lee TB, You HJ, Rha HS, et al. Reactive oxygen species-specific mechanisms of drug resistance in paraquat-resistant acute myelogenous leukemia sublines. Mol Cells. 2000 Feb;10(1):38-46.

[8]   Habel N, Hamidouche Z, Girault I, Patino-Garcia A, Lecanda F, Marie PJ, et al. Zinc chelation: a metallothionein 2A's mechanism of action involved in osteosarcoma cell death and chemotherapy resistance. Cell Death Dis. 2013 Oct;4:1-10.

[9]   Harrison IP, Selemidis S. Understanding the biology of reactive oxygen species and their link to cancer: NADPH oxidases as novel pharmacological targets. Clin Exp Pharmacol Physiol. 2014 Aug;41(8):533-42.

[10]   Liou GY, Storz P. Reactive oxygen species in cancer. Free Radical Res. 2010 May;44(5):479-96.

[11]   Yang Y, Karakhanova S, Werner J, Bazhin AV. Reactive Oxygen Species in Cancer Biology and Anticancer Therapy. Curr Med Chem. 2013 Oct;20(30):3677-92.

[12]   Sullivan LB, Martinez-Garcia E, Nguyen H, Mullen AR, Dufour E, Sudarshan S, et al. The Proto-oncometabolite Fumarate Binds Glutathione to Amplify ROS-Dependent Signaling. Mol Cell. 2013 Jul;51(2):236-48.

[13]   Mishra B, Sangwan RS, Mishra S, Jadaun JS, Sabir F, Sangwan NS. Effect of cadmium stress on inductive enzymatic and nonenzymatic responses of ROS and sugar metabolism in multiple shoot cultures of Ashwagandha (Withania somnifera Dunal). Protoplasma. 2014 Sep;251(5):1031-45.

[14]   Molina N, Morandi AC, Bolin AP, Otton R. Comparative effect of fucoxanthin and vitamin C on oxidative and functional parameters of human lymphocytes. Int Immunopharmacol. 2014 Sep;22(1):41-50.

[15]   Venditti P, Napolitano G, Barone D, Di Meo S. Vitamin E supplementation modifies adaptive responses to training in rat skeletal muscle. Free Radical Res. 2014 Oct;48(10):1179-89.

[16]   Seto NOL, Hayashi S, Tener GM. Overexpression of Cu-Zn superoxide-dismutase in Drosophila does not affect life-span. Proc Natl Acad Sci U S A. 1990 Jun;87(11):4270-4.

[17]   Groitl B, Jakob U. Thiol-based redox switches. BBA-Proteins Proteomics. 2014 Aug;1844(8):1335-43.

[18]   Storz P. Reactive oxygen species in tumor progression. Front Biosci. 2005 May;10:1881-96.

[19]   Chiarugi P, Fiaschi T. Redox signalling in anchorage-dependent cell growth. Cell Signal. 2007 Apr;19(4):672-82.

[20]   Rhee SG, Bae YS, Lee SR, Kwon J. Hydrogen peroxide: a key messenger that modulates protein phosphorylation through cysteine oxidation. Sci STKE. 2000 2000 Oct;2000(53):1-2.

[21]   Harris IS, Blaser H, Moreno J, Treloar AE, Gorrini C, Sasaki M, et al. PTPN12 promotes resistance to oxidative stress and supports tumorigenesis by regulating FOXO signaling. Oncogene. 2014 Feb;33(8):1047-54.

[22]   Satoh K, Godo S, Saito H, Enkhjargal B, Shimokawa H. Dual roles of vascular-derived reactive oxygen species-With a special reference to hydrogen peroxide and cyclophilin A. J Mol Cell Cardiol. 2014 Aug;73:50-6.

[23]   Kohler AC, Sag CM, Maier LS. Reactive oxygen species and excitation-contraction coupling in the context of cardiac pathology. J Mol Cell Cardiol. 2014 Aug;73:92-102.

[24]   Luczak ED, Anderson ME. CaMKII oxidative activation and the pathogenesis of cardiac disease. J Mol Cell Cardiol. 2014 Aug;73:112-6.

[25]   Doroshow JH. Effect of anthracycline antibiotics on oxygen radical formation in rat-heart. Cancer Res. 1983;43(2):460-72.

[26]   Gems D, Partridge L. Stress-response hormesis and aging: "That which Does Not Kill Us Makes Us Stronger". Cell Metab. 2008 Mar;7(3):200-3.

[27]   Schmeisser S, Schmeisser K, Weimer S, Groth M, Priebe S, Fazius E, et al. Mitochondrial hormesis links low-dose arsenite exposure to lifespan extension. Aging Cell. 2013 Jun;12(3):508-17.

[28]   Pearce OMT, Laubli H, Verhagen A, Secrest P, Zhang JQ, Varki NM, et al. Inverse hormesis of cancer growth mediated by narrow ranges of tumor-directed antibodies. Proc Natl Acad Sci U S A. 2014 Apr;111(16):5998-6003.

[29]   Shore DE, Ruvkun G. A cytoprotective perspective on longevity regulation. Trends Cell Biol. 2013 Sep;23(9):409-20.

[30]   Takemura G, Fujiwara H. Doxorubicin-induced cardiomyopathy from the cardiotoxic mechanisms to management. Prog Cardiovasc Dis. 2007 Mar-Apr;49(5):330-52.

[31]   Davies KJA, Doroshow JH. Redox cycling of anthracyclines by cardiac mitochondria.1. anthracycline radical formation by NADH dehydrogenase. J Biol Chem. 1986 Mar;261(7):3060-7.

[32]   Berlin V, Haseltine WA. Reduction of adriamycin to a semiquinone-free radical by NADPH cytochrome-P-450 reductase produces DNA cleavage in a reaction mediated by molecular-oxygen J Biol Chem. 1981;256(10):4747-56.

[33]   VasquezVivar J, Martasek P, Hogg N, Masters BSS, Pritchard KA, Kalyanaraman B. Endothelial nitric oxide synthase-dependent superoxide generation from adriamycin. Biochemistry. 1997 Sep;36(38):11293-7.

[34]   Bachur NR, Gordon SL, Gee MV, Kon H. NADPH cytochrome-P-450 reductase activation of quinone anti-cancer agents to free-radicals. Proc Natl Acad Sci U S A. 1979;76(2):954-7.

[35]   Schimmel KJM, Richel DJ, van den Brink RBA, Guchelaar HJ. Cancer Treat. Rev. Cancer Treat Rev. 2004 Apr;30(2):181-91.

[36]   Sabuncuoglu S. Antiapoptotic effect of aminoguanidine on doxorubicin-induced apoptosis. Mol Cell Biochem. 2014 Sep;394(1-2):129-35.

[37]   Beyer AM, Durand MJ, Hockenberry J, Gamblin TC, Phillips SA, Gutterman DD. An acute rise in intraluminal pressure shifts the mediator of flow-mediated dilation from nitric oxide to hydrogen peroxide in human arterioles. Am J Physiol-Heart Circul Physiol. 2014 Dec;307(11):H1587-H93.

[38]   Pall ML. The NO/ONOO-Cycle as the Central Cause of Heart Failure. Int J Mol Sci. 2013 Nov;14(11):22274-330.

[39]   Myers CE, McGuire WP, Liss RH, Ifrim I, Grotzinger K, Young RC. Adriamycin - role of lipid peroxidation in cardiac toxicity and tumor response Science. 1977;197(4299):165-7.

[40]   Mimnaugh EG, Siddik ZH, Drew R, Sikic BI, Gram TE. Effects of alpha-tocopherol on the toxicity, disposition, and metabolism of adriamycin in mice Toxicol Appl Pharmacol. 1979;49(1):119-26.

[41]   Chatterjee K, Zhang JQ, Honbo N, Karliner JS. Doxorubicin Cardiomyopathy. Cardiology. 2010;115(2):155-62.

[42]   Hermansen K, Wassermann K. The effect of vitamin-E and selenium on doxorubicin (adriamycin) induced delayed toxicity in mice. Acta Pharmacol Toxicol. 1986 Jan;58(1):31-7.

[43]   Vanvleet JF, Ferrans VJ, Weirich WE. Cardiac disease induced by chronic adriamycin administration in dogs and an evaluation of vitamin-E and selenium as cardioprotectants Am J Pathol. 1980;99(1):13-41.

[44]   Shimpo K, Nagatsu T, Yamada K, Sato T, Niimi H, Shamoto M, et al. Ascorbic-acid and adriamycin toxicity. Am J Clin Nutr. 1991 Dec;54(6):S1298-S301.

[45]   Yoda Y, Nakazawa M, Abe T, Kawakami Z. Prevention of doxorubicin myocardial toxicity in mice by reduced glutathione. Cancer Res. 1986 May;46(5):2551-6.

[46]   Siveskiiliskovic N, Hill M, Chow DA, Singal PK. Probucol protects against adriamycin cardiomyopathy without interfering with its antitumor effect Circulation. 1995 Jan;91(1):10-5.

[47]   Siveskiiliskovic N, Kaul N, Singal PK. Probucol promotes endogenous antioxidants and provides protection against adriamycin-induced cardiomyopathy in rats Circulation. 1994 Jun;89(6):2829-35.

[48]   El-Demerdash E, Ali AA, Sayed-Ahmed MM, Osman AMM. New aspects in probucol cardioprotection against doxorubicin-induced cardiotoxicity. Cancer Chemother Pharmacol. 2003 Nov;52(5):411-6.

[49]   Matsui H, Morishima I, Numaguchi Y, Toki Y, Okumura K, Hayakawa T. Protective effects of carvedilol against doxorubicin-induced cardiomyopathy in rats. Life Sci. 1999 Aug;65(12):1265-74.

[50]   Feuerstein G, Yue TL, Ma XL, Ruffolo RR. Novel mechanisms in the treatment of heart failure: Inhibition of oxygen radicals and apoptosis by carvedilol. Prog Cardiovasc Dis. 1998 Jul-Aug;41(1):17-24.

[51]   Oliveira PJ, Bjork JA, Santos MS, Leino RL, Froberg MK, Moreno AJ, et al. Carvedilol-mediated antioxidant protection against doxorubicin-induced cardiac mitochondrial toxicity. Toxicol Appl Pharmacol. 2004 Oct;200(2):159-68.

[52]   Fazio S, Palmieri EA, Ferravante B, Bone F, Biondi B, Sacca L. Doxorubicin-induced cardiomyopathy treated with carvedilol. Clin Cardiol. 1998 Oct;21(10):777-9.

[53]   Santos DL, Moreno AJM, Leino RL, Froberg MK, Wallace KB. Carvedilol protects against doxorubicin-induced mitochondrial cardiomyopathy. Toxicol Appl Pharmacol. 2002 Dec;185(3):218-27.

[54]   Seifert CF, Nesser ME, Thompson DF. Dexrazoxane in the prevention of doxorubicin-induced cardiotoxicity. Ann Pharmacother. 1994 Sep;28(9):1063-72.

[55]   Vile GF, Winterbourn CC. DL-N,N'-dicarboxamidomethyl-N,N'-dicarboxymethyl-1,2-diaminopropane (ICRF-198) and D-1,2-bis(3,5-dioxopiperazine-1-yl)propane (ICRF-187) inhibition of Fe^{3+} reduction, lipid-peroxidation, and caatpase inactivation in heart microsomes exposed to adriamycin. Cancer Res. 1990 Apr;50(8):2307-10.

[56]   Herman EH, Ferrans VJ. Reduction of chronic doxorubicin cardiotoxicity in dogs by pretreatment with (+/-)-1,2-bis(3,5-dioxopiperazinyl-1-yl)propane(ICRF-187). Cancer Res. 1981;41(9):3436-40.

[57]   Vonhoff DD, Howser D, Lewis BJ, Holcenberg J, Weiss RB, Young RC. Phase-1 study of ICRF-187 using a daily for 3 days schedule. CancTreat Rep. 1981;65(3-4):249-52.

[58]   Kimura T, Fujita I, Itoh N, Muto N, Nakanishi T, Takahashi K, et al. Metallothionein acts as a cytoprotectant against doxorubicin toxicity. J Pharmacol Exp Ther. 2000 Jan;292(1):299-302.

[59]   Kang YJ, Chen Y, Yu AD, VossMcCowan M, Epstein PN. Overexpression of metallothionein in the heart of transgenic mice suppresses doxorubicin cardiotoxicity. J Clin Invest. 1997 Sep;100(6):1501-6.

[60]   Wu HY, Kang YJ. Inhibition of buthionine sulfoximine-enhanced doxorubicin toxicity in metallothionein overexpressing transgenic mouse heart. J Pharmacol Exp Ther. 1998 Nov;287(2):515-20.

[61]   Sun XH, Zhou ZX, Kang YJ. Attenuation of doxorubicin chronic toxicity in metallothionein-overexpressing transgenic mouse heart. Cancer Res. 2001 Apr;61(8):3382-7.

[62]   Kang YJ. The antioxidant function of metallothionein in the heart. Proc Soc Exp Biol Med. 1999 Dec;222(3):263-73.

[63]   Kang YJ. Antioxidant defense against anthracycline cardiotoxicity by metallothionein. Cardiovasc Toxicol. 2007;7(2):95-100.

[64]   Yin XH, Wu HY, Chen Y, Kang YJ. Induction of antioxidants by Adriamycin in mouse heart. Biochem Pharmacol. 1998 Jul;56(1):87-93.

[65]   Minotti G, Cairo G, Monti E. Role of iron in anthracycline cardiotoxicity: new tunes for an old song? Faseb J. 1999 Feb;13(2):199-212.

[66]   Merten KE, Jiang YC, Kang YJ. Zinc inhibits doxorubicin-activated calcineurin signal transduction pathway in H9c2 embryonic rat cardiac cells. Exp Biol Med. 2007 May;232(5):682-9.

[67]   Sutherland DEK, Stillman MJ. The "magic numbers" of metallothionein. Metallomics. 2011 2011;3(5):444-63.

[68]   Margoshes M, Vallee BL. A cadmium protein from equine kidney cortex. J Am Chem Soc. 1957 1957;79(17):4813-4.

[69]   Vasak M, Meloni G. Chemistry and biology of mammalian metallothioneins. J Biol Inorg Chem. 2011 Oct;16(7):1067-78.

[70]   Thirumoorthy N, Sunder AS, Kumar KTM, Kumar MS, Ganesh GNK, Chatterjee M. A Review of Metallothionein Isoforms and their Role in Pathophysiology. World J Surg Oncol. 2011 May;9:1-7.

[71]   Vasak M. Advances in metallothionein structure and functions. J Trace Elem Med Bio. 2005 2005;19(1):13-7.

[72]   Zalewska M, Trefon J, Milnerowicz H. The role of metallothionein interactions with other proteins. Proteomics. 2014 Jun;14(11):1343-56.

[73]   Andrews GK. Regulation of metallothionein gene expression by oxidative stress and metal ions. Biochem Pharmacol. 2000 Jan;59(1):95-104.

[74]   Takahashi S. Molecular functions of metallothionein and its role in hematological malignancies. J Hematol Oncol. 2012 Jul;5:1-8.

[75]   Park Y, Yu E. Expression of metallothionein-1 and metallothionein-2 as a prognostic marker in hepatocellular carcinoma. J Gastroen Hepatol. 2013 Sep;28(9):1565-72.

[76]   Masters BA, Quaife CJ, Erickson JC, Kelly EJ, Froelick GJ, Zambrowicz BP, et al. Metallothionein-III is expressed in neurons that sequester zinc in synaptic vesicles J Neurosci. 1994 Oct;14(10):5844-57.

[77]   Hoey JG, Garrett SH, Sens MA, Todd JH, Sens DA. Expression of MT-3 mRNA in human kidney, proximal tubule cell cultures, and renal cell carcinoma. Toxicol Lett. 1997 Jul 21;92(2):149-60.

[78]   Meloni G, Zovo K, Kazantseva J, Palumaa P, Vasak M. Organization and assembly of metal-thiolate clusters in epithelium-specific metallothionein-4. J Biol Chem. 2006 May;281(21):14588-95.

[79]   Carpene E, Andream G, Isam G. Metallothionein functions and structural characteristics. J Trace Elem Med Bio. 2007 2007;21:35-9.

[80]   Raudenska M, Gumulec J, Podlaha O, Sztalmachova M, Babula P, Eckschlager T, et al. Metallothionein polymorphisms in pathological processes. Metallomics. 2014;6(1):55-68.

[81]   Skutkova H, Babula P, Stiborova M, Eckschlager T, Trnkova L, Provaznik I, et al. Structure, polymorphisms and electrochemistry of mammalian metallothioneins – A review. Int J Electrochem Sci. 2012;7(12):12415-31.

[82]   Coyle P, Philcox JC, Carey LC, Rofe AM. Metallothionein: The multipurpose protein. Cell Mol Life Sci. 2002 Apr;59(4):627-47.

[83]   Krizkova S, Masarik M, Eckschlager T, Adam V, Kizek R. Effects of redox conditions and zinc(II) ions on metallothionein aggregation revealed by chip capillary electrophoresis. J Chromatogr A. 2010;1217(51):7966-71.

[84]   Chubatsu LS, Meneghini R. Metallothionein protects DNA from oxidative damage. Biochem J. 1993 Apr;291:193-8.

[85]   Moffatt P, Seguin C. Expression of the gene encoding metallothionein-3 in organs of the reproductive system. DNA Cell Biol. 1998 Jun;17(6):501-10.

[86]   Cherian MG, Kang YJ. Metallothionein and liver cell regeneration. Exp Biol Med. 2006 Feb;231(2):138-44.

[87]   Maret W. Zinc and sulfur: A critical biological partnership. Biochemistry. 2004 Mar;43(12):3301-9.

[88]   Ruttkay-Nedecky B, Nejdl L, Gumulec J, Zitka O, Masarik M, Eckschlager T, et al. The role of metallothionein in oxidative stress. Int J Mol Sci. 2013;14(3):6044-66.

[89]   Pinter TBJ, Stillman MJ. The Zinc Balance: Competitive Zinc Metalation of Carbonic Anhydrase and Metallothionein 1A. Biochemistry. 2014 Oct;53(39):6276-85.

[90]   Iszard MB, Liu J, Klassen CD. Effect of several metallothionein inducers on oxidative stress defense mechanisms in rats. Toxicology. 1995 Dec;104(1-3):25-33.

[91]   Schwarz MA, Lazo JS, Yalowich JC, Allen WP, Whitmore M, Bergonia HA, et al. Metallothionein protects against the cytotoxic and DNA-damaging effects of nitric-oxide Proc Natl Acad Sci U S A. 1995 May;92(10):4452-6.

[92]   Satoh M, Kondo Y, Mita M, Nakagawa I, Naganuma A, Imura N. Prevention of carcinogenity of anticancer drugs by metallothionein induction Cancer Res. 1993 Oct;53(20):4767-8.

[93]   Quesada AR, Byrnes RW, Krezoski SO, Petering DH. Direct reaction of H2O2 with sulfhydryl groups in HL-60 cells: Zinc-metallothionein and other sites. Arch Biochem Biophys. 1996 Oct;334(2):241-50.

[94]   Cai L, Cherian MG. Zinc-metallothionein protects from DNA damage induced by radiation better than glutathione and copper- or cadmium-metallothioneins. Toxicol Lett. 2003 Jan;136(3):193-8.

[95]   Sabolic I, Breljak D, Skarica M, Herak-Kramberger CM. Role of metallothionein in cadmium traffic and toxicity in kidneys and other mammalian organs. Biometals. 2010 Oct;23(5):897-926.

[96]   Klaassen CD, Liu J. Metallothionein transgenic and knock-out mouse models in the study of cadmium toxicity. J Toxicol Sci. 1998;23(Supplement II):97-102.

[97]   Kowalska K, Zalewska ABM, Milnerowicz H. The influence of biological and environmental factors on metallothionein concentration in the blood. J Trace Elem Med Bio. 2015;29:99-103.

[98]   Nordberg G, Jin TY, Wu XW, Lu J, Chen L, Liang YH, et al. Kidney dysfunction and cadmium exposure - Factors influencing dose-response relationships. J Trace Elem Med Bio. 2012;26(2-3):197-200.

[99]   Nordberg M, Nordberg GF. Metallothioneins: Historical development and overview. In: Sigel A, Sigel H, Sigel RKO, eds. *Metallothioneins and Related Chelators : Metal Ions in Life Sciences*. Cambridge: Royal Society of Chemistry 2009:544.

[100] Lynes MA, Zaffuto K, Unfricht DW, Marusov G, Samson JS, Yin XY. The physiological roles of extracellular metallothionein. Exp Biol Med. 2006 Oct;231(9):1548-54.

[101] Cernei N, Heger Z, Gumulec J, Zitka O, Masarik M, Babula P, et al. Sarcosine as a potential prostate cancer biomarker – A review. Int J Mol Sci. 2013;14(7):13893-908.

[102] Cherian MG, Jayasurya A, Bay BH. Metallothioneins in human tumors and potential roles in carcinogenesis. Mutat Res-Fundam Mol Mech Mutagen. 2003 Dec;533(1-2):201-9.

[103] Ryan KM, Phillips AC, Vousden KH. Regulation and function of the p53 tumor suppressor protein. Curr Opin Cell Biol. 2001 Jun;13(3):332-7.

[104] Butcher HL, Kennette WA, Collins O, Zalups RK, Koropatnick J. Metallothionein mediates the level and activity of nuclear factor kappa B in murine fibroblasts. J Pharmacol Exp Ther. 2004 Aug;310(2):589-98.

[105] Orihuela R, Fernandez B, Palacios O, Valero E, Atrian S, Watt RK, et al. Ferritin and metallothionein: dangerous liaisons. Chem Commun. 2011;47(44):12155-7.

[106] Hanahan D, Weinberg RA. Hallmarks of Cancer: The Next Generation. Cell. 2011 Mar;144(5):646-74.

[107] Cherian MG, Howell SB, Imura N, Klaassen CD, Koropatnick J, Lazo JS, et al. Contemporary-issues in toxicology-role of metallothionein in carcinogenesis. Toxicol Appl Pharmacol. 1994 May;126(1):1-5.

[108] Eckschlager T, Adam V, Hrabeta J, Figova K, Kizek R. Metallothioneins and Cancer. Curr Protein Pept Sci. 2009 Aug;10(4):360-75.

[109] Lai YY, Yip GWC, Bay BH. Targeting Metallothionein for Prognosis and Treatment of Breast Cancer. Recent Pat Anti-Canc. 2011 May;6(2):178-85.

[110] Naito S, Yokomizo A, Koga H. Mechanisms of drug resistance in chemotherapy for urogenital carcinoma. Int J Urol. 1999 Sep;6(9):427-39.

[111] Tanner B, Pilch H, Schmidt M, Hengstler JG. Expression of metallothionein and glutathione in ovarian carcinomas. Geburtsh Frauenheilk. 2002 Feb;62(2):145-54.

[112] Wulfing C, van Ahlen H, Eltze E, Piechota H, Hertle L, Schmid KW. Metallothionein in bladder cancer: correlation of overexpression with poor outcome after chemotherapy. World J Urol. 2007 Apr;25(2):199-205.

[113] Mattern J, Volm M. Increased resistance to doxorubicin in human non-small cell lung carcinomas with metallothionein expression. Int J Oncol. 1992 Nov;1(6):687-9.

[114] DeVita VK, Lawrence TS, Rosenberg SA, DePinho MD, Weinberg RA. Cancer: Principles & Practice of Oncology. 9 ed. Philadelphia: Lippincot Williams & Wilkins 2011.

[115] Grein A, Spalla C, Canevazz.G, Dimarco A. Descrizione e classificazione di un attiomicete (Streptomyces peucetius sp. nova) produttore di una sostanza ad attivita antitumorale - la daunomicina. Gior Microbiol. 1963;11(2):109-18.

[116] Bonadonna G, Monfardini S, De Lena M, Fossati-Bellani F. Clinical evaluation of adriamycin, a new antitumour antibiotic. Br Med J. 1969 1969/08//;3(5669):503-6.

[117] Minotti G, Menna P, Salvatorelli E, Cairo G, Gianni L. Anthracyclines: Molecular advances and pharmacologic developments in antitumor activity and cardiotoxicity. Pharmacol Rev. 2004 Jun;56(2):185-229.

[118]   Robert J, Gianni L. Pharmacokinetics and metabolism of anthracyclines. Canc Surv. 1993;17:219-52.

[119]   Danesi R, Fogli S, Gennari A, Conte P, Del Tacca M. Pharmacokinetic-pharmacodynamic relationships of the anthracycline anticancer drugs. Clin Pharmacokinet. 2002;41(6):431-44.

[120]   Robert J. Epirubicin. Drugs. 1993 1993/05/01;45(2):20-30.

[121]   Borchmann P, Hübel K, Schnell R, Engert A. Idarubicin: a brief overview on pharmacology and clinical use. Int J Clin Pharmacol Ther. 1997 1997/02//;35(2):80-3.

[122]   Binaschi M, Bigioni M, Cipollone A, Rossi C, Goso C, Maggi CA, et al. Anthracyclines: Selected New Developments. Curr Med Chem. 2001;1(2):113-30.

[123]   Toffoli G, Sorio R, Aita P, Crivellari D, Corona G, Bearz A, et al. Dose-finding and pharmacologic study of chronic oral idarubicin therapy in metastatic breast cancer patients. Clin Cancer Res. 2000 Jun;6(6):2279-87.

[124]   Toffoli G, Simone F, Gigante M, Boiocchi M. Comparison of mechanisms responsible for resistance to idarubicin and daunorubicin in multidrug-resistant lovo cell-lines. Biochem Pharmacol. 1994 Nov;48(10):1871-81.

[125]   Jonsson-Videsater K, Andersson G, Bergh J, Paul C. Doxorubicin-resistant, MRP1-expressing U-1285 cells are sensitive to idarubicin. Ther Drug Monit. 2003 Jun;25(3):331-9.

[126]   Lothstein L, Israel M, Sweatman TW. Anthracycline drug targeting: cytoplasmic versus nuclear - A fork in the road. Drug Resist Update. 2001 Jun;4(3):169-77.

[127]   Koh E, Ueda Y, Nakamura T, Kobayashi A, Katsuta S, Takahashi H. Apoptosis in young rats with adriamycin-induced cardiomyopathy - Comparison with pirarubicin, a new anthracycline derivative. Pediatr Res. 2002 Feb;51(2):256-9.

[128]   Dhingra K, Frye D, Newman RA, Walters R, Theriault R, Fraschini G, et al. Phase II clinical and pharmacological study of pirarubicin in combination with 5-fluorouracil and cyclophosphamide in metastatic breast cancer. Clin Cancer Res. 1995 Jul;1(7):691-7.

[129]   Niitsu N, Yamazaki J-I, Nakayama M, Umeda M. Pirarubicin-induced Myocardial Damage in Elderly Patients with Non-Hodgkin's Lymphoma. Nip Ron Igakkai Zas. 1998;35(5):358-62.

[130]   Case DC, Ervin TJ, Boyd MA, Bove LG, Sonneborn HL, Paul SD. Phase-II study of aclarubicin in acute myeloblastic-leukemia. Am J Clin Oncol-Canc. 1987 Dec;10(6):523-6.

[131]   Wojnar J, Mandecki M, Wnuk-Wojnar AM, Hołowiecki J. Clinical studies on aclacinomycin A cardiotoxicity in adult patients with acute non lymphoblastic leukaemia. Folia Haematol. 1989 1989;116(2):297-303.

[132]   Dabich L, Bull FE, Beltran G, Athens JW, Coltman CA, Weick JK, et al. Phase-II evaluation of aclarubicin in refractory adult acute-leukemia - A southwest-oncology-group study. CancTreat Rep. 1986 Aug;70(8):967-9.

[133]   Estorch M, Carrio I, Martinezduncker D, Berna L, Torres G, Alonso C, et al. Myocyte cell-damage after administration of doxorubicin or mitoxantrone in breast-cancer patients assessed by in-111 antimyosin monoclonal-antibody studies. J Clin Oncol. 1993 Jul;11(7):1264-8.

[134]   Thomas X, Le QH, Fiere D. Anthracycline-related toxicity requiring cardiac transplantation in long-term disease-free survivors with acute promyelocytic leukemia. Ann Hematol. 2002 Sep;81(9):504-7.

[135]   Bedrnicek J, Vicha A, Jarosova M, Holzerova M, Cinatl J, Michaelis M, et al. Characterization of drug-resistant neuroblastoma cell lines by comparative genomic hybridization. Neoplasma. 2005;52(5):415-9.

[136]   Huska D, Adam V, Babula P, Hrabeta J, Stiborova M, Eckschlager T, et al. Square wave voltammetry as a tool for investigation of doxorubicin interactions with DNA isolated from neuroblastoma cells. Electroanalysis. 2009;21(3-5):487-94.

[137]   Schwartz HS, Parker NB. Initial biotransformations of daunorubicin to aglycones by rat-liver microsomes. Cancer Res. 1981;41(6):2343-8.

[138]   Singal PK, Iliskovic N, Li TM, Kumar D. Adriamycin cardiomyopathy: pathophysiology and prevention. Febs J. 1997 Oct;11(12):931-6.

[139]   Kizek R, Adam V, Hrabeta J, Eckschlager T, Smutny S, Burda JV, et al. Anthracyclines and ellipticines as DNA-damaging anticancer drugs: Recent advances. Pharmacol Ther. 2012;133(1):26-39.

[140]   Myers C. The role of iron in doxorubicin-induced cardiomyopathy. Semin Onco. 1998 Aug;25(4):10-4.

[141]   Xu XX, Persson HL, Richardson DR. Molecular pharmacology of the interaction of anthracyclines with iron. Mol Pharmacol. 2005 Aug;68(2):261-71.

[142]   Sterba M, Popelova O, Vavrova A, Jirkovsky E, Kovarikova P, Gersl V, et al. Oxidative stress, redox signaling, and metal chelation in anthracycline cardiotoxicity and pharmacological cardioprotection. Antioxid Redox Sign. 2013 Mar 10;18(8):899-929.

[143]   Menna P, Paz OG, Chello M, Covino E, Salvatorelli E, Minotti G. Anthracycline cardiotoxicity. Expert Opin Drug Saf. 2012 May;11:S21-S36.

[144]   Sieswerda E, Kremer LCM, Caron HN, van Dalen EC. The use of liposomal anthracycline analogues for childhood malignancies: A systematic review. Eur J Cancer. 2011 Sep;47(13):2000-8.

[145]   Perez-Arnaiz C, Busto N, Leal JM, Garcia B. New Insights into the Mechanism of the DNA/Doxorubicin Interaction. J Phys Chem B. 2014 Feb;118(5):1288-95.

[146]   Nikitovic D, Juranek I, Wilks MF, Tzardi M, Tsatsakis A, Tzanakakis GN. Anthracycline-Dependent Cardiotoxicity and Extracellular Matrix Remodeling. Chest. 2014 Oct;146(4):1123-30.

[147]   Zhou QB, Turnbull KD. Phosphodiester alkylation with a quinone methide. J Org Chem. 1999 Apr;64(8):2847-51.

[148]   Taatjes DJ, Gaudiano G, Koch TH. Production of formaldehyde and DNA-adriamycin or DNA-daunomycin adducts, initiated through redox chemistry of dithiothreitol/iron, xanthine oxidase/NADH/iron, or glutathione/iron. Chem Res Toxicol. 1997 Sep;10(9):953-61.

[149]   Podell ER, Harrington DJ, Taatjes DJ, Koch TH. Crystal structure of epidoxorubicin-formaldehyde virtual crosslink of DNA and evidence for its formation in human breast-cancer cells. Acta Crystallogr Sect D-Biol Crystallogr. 1999 Sep;55:1516-23.

[150]   Koch TH, Barthel BL, Kalet BT, Rudnicki DL, Post GC, Burkhart DJ. Anthracycline-formaldehyde conjugates and their targeted prodrugs. In: Krohn K, ed. *Anthracycline Chemistry and Biology II: Mode of Action, Clinical Aspects and New Drugs*. Berlin: Springer-Verlag Berlin 2008:141-70.

[151]   Brazzolotto X, Andriollo M, Guiraud P, Favier A, Moulis JM. Interactions between doxorubicin and the human iron regulatory system. Biochim Biophys Acta-Mol Cell Res. 2003 Feb;1593(2-3):209-18.

[152]   Huska D, Adam V, Burda J, Hrabeta J, Eckschlager T, Babula P, et al. Electrochemical and computational study of doxorubicin interactions with DNA. Febs J. 2009 Jul;276:109-.

[153]   Subramanian R, Asmawi MZ, Sadikun A. A bitter plant with a sweet future? A comprehensive review of an oriental medicinal plant: Andrographis paniculata. Phytochem Rev. 2012 Mar;11(1):39-75.

[154]   Deng SW, Yan TD, Jendrny C, Nemecek A, Vincetic M, Godtel-Armbrust U, et al. Dexrazoxane may prevent doxorubicin-induced DNA damage via depleting both Topoisomerase II isoforms. BMC Cancer. 2014 Nov;14:1-11.

[155] Kalam K, Marwick TH. Role of cardioprotective therapy for prevention of cardiotoxicity with chemotherapy: A systematic review and meta-analysis. Eur J Cancer. 2013 Sep;49(13):2900-9.

[156] Suzuki T, Ichihara M, Hyodo K, Yamamoto E, Ishida T, Kiwada H, et al. Influence of dose and animal species on accelerated blood clearance of PEGylated liposomal doxorubicin. Int J Pharm. 2014 Dec;476(1-2):205-12.

[157] Safra T. Cardiac safety of liposomal anthracyclines. Oncologist. 2003;8:17-24.

[158] Rahman AM, Yusuf SW, Ewer MS. Anthracycline-induced cardiotoxicity and the cardiac-sparing effect of liposomal formulation. Int J Nanomed. 2007;2(4):567-83.

[159] Nazir S, Hussain T, Ayub A, Rashid U, MacRobert AJ. Nanomaterials in combating cancer: Therapeutic applications and developments. Nanomed-Nanotechnol. 2014 Jan;10(1):19-34.

[160] Caruso JA, O'Connor N. Metallomics: integrating research related to biometals-a journal for an emerging community. Metallomics. 2009 Jan;1(1):14-24.

[161] Gaetke LM, Chow-Johnson HS, Chow CK. Copper: toxicological relevance and mechanisms. Arch Toxicol. 2014 Nov;88(11):1929-38.

[162] Liuzzi JP, Guo L, Yoo C, Stewart TS. Zinc and autophagy. Biometals. 2014 Dec;27(6):1087-96.

[163] Osredkar J, Sustar N. Copper and Zinc, Biological Role and Significance of Copper/Zinc Imbalance. J Clin Toxicol. 2011;S3:1-18.

[164] Leoni G, Rosato A, Perozzi G, Murgia C. Zinc proteome interaction network as a model to identify nutrient-affected pathways in human pathologies. Genes Nutr. 2014 Nov;9(6):1-9.

[165] Efeovbokhan N, Bhattacharya SK, Ahokas RA, Sun Y, Guntaka RV, Gerling IC, et al. Zinc and the Prooxidant Heart Failure Phenotype. J Cardiovasc Pharmacol. 2014 Oct;64(4):393-400.

[166] Apak R, Gucclu K, Ozyurek M, Bektasoglu B, Bener M. Cupric Ion Reducing Antioxidant Capacity Assay for Antioxidants in Human Serum and for Hydroxyl Radical Scavengers. In: Armstrong D, ed. *Advanced Protocols in Oxidative Stress II*. Totowa: Humana Press Inc 2010:215-39.

[167] Zhao WJ, An CH, Long DD, Zhang ZQ, Han JR. Effect of copper-induced oxidative stress on sclerotial differentiation and antioxidants contents of Penicillium thomii Q1. J Basic Microbiol. 2014 Dec;54(12):1395-402.

[168] Kimura T, Okumura F, Oguro I, Nakanishi T, Sone T, Isobe M, et al. Metal Response Element-binding Transcription Factor-1 Is Activated by Degradation of Metallothionein. J Health Sci. 2009 Feb;55(1):72-6.

[169] Wang JX, Song Y, Elsherif L, Song ZY, Zhou GH, Prabhu SD, et al. Cardiac metallothionein induction plays the major role in the prevention of diabetic cardiomyopathy by zinc supplementation. Circulation. 2006 Jan;113(4):544-54.

[170] Bohuslavova R, Skvorova L, Sedmera D, Semenza GL, Pavlinkova G. Increased susceptibility of HIF-1 alpha heterozygous-null mice to cardiovascular malformations associated with maternal diabetes. J Mol Cell Cardiol. 2013 Jul;60:129-41.

[171] Kumar SD, Vijaya M, Samy RP, Dheen ST, Ren MQ, Watt F, et al. Zinc supplementation prevents cardiomyocyte apoptosis and congenital heart defects in embryos of diabetic mice. Free Radical Bio Med. 2012 Oct;53(8):1595-606.

[172] Ali MM, Frei E, Straub J, Breuer A, Wiessler M. Induction of metallothionein by zinc protects from daunorubicin toxicity in rats. Toxicology. 2002 Sep 30;179(1-2):85-93.

[173] Kang YJ. The antioxidant function of metallothionein in the heart. Proc Soc Exp Biol Med. 1999 Dec;222(3):263-73.

[174] Kang YJ, Chen Y, Epstein PN. Suppression of doxorubicin cardiotoxicity by overexpression of catalase in the heart of transgenic mice. J Biol Chem. 1996 May 24;271(21):12610-6.

[175] Satoh M, Naganuma A, Imura N. Modulation of adriamycin toxicity by tissue-specific induction of metallothionein synthesis in mice. Life Sci. 2000 Jun 30;67(6):627-34.

[176] Wang GW, Kang YJ. Inhibition of doxorubicin toxicity in cultured neonatal mouse cardiomyocytes with elevated metallothionein levels. J Pharmacol Exp Ther. 1999 Mar;288(3):938-44.

[177] Kang YJ. Antioxidant defense against anthracycline cardiotoxicity by metallothionein. Cardiovasc Toxicol. 2007;7(2):95-100.

[178] Guo R, Wu K, Chen J, Mo L, Hua X, Zheng D, et al. Exogenous hydrogen sulfide protects against doxorubicin-induced inflammation and cytotoxicity by inhibiting p38MAPK/NFkappaB pathway in H9c2 cardiac cells. Cell Physiol Biochem. 2013;32(6):1668-80.

[179] Kim DS, Kim HR, Woo ER, Hong ST, Chae HJ, Chae SW. Inhibitory effects of rosmarinic acid on adriamycin-induced apoptosis in H9c2 cardiac muscle cells by inhibiting reactive oxygen species and the activations of c-Jun N-terminal kinase and extracellular signal-regulated kinase. Biochem Pharmacol. 2005 Oct 1;70(7):1066-78.

[180] Kim DS, Woo ER, Chae SW, Ha KC, Lee GH, Hong ST, et al. Plantainoside D protects adriamycin-induced apoptosis in H9c2 cardiac muscle cells via the inhibition of ROS generation and NF-kappaB activation. Life Sci. 2007 Jan 2;80(4):314-23.

[181] Nayak PG, Paul P, Bansal P, Kutty NG, Pai KS. Sesamol prevents doxorubicin-induced oxidative damage and toxicity on H9c2 cardiomyoblasts. J Pharm Pharmacol. 2013 Jul;65(7):1083-93.

[182] Wang XL, Wang X, Xiong LL, Zhu Y, Chen HL, Chen JX, et al. Salidroside improves doxorubicin-induced cardiac dysfunction by suppression of excessive oxidative stress and cardiomyocyte apoptosis. J Cardiovasc Pharmacol. 2013 Dec;62(6):512-23.

[183] Arunachalam S, Kim SY, Lee SH, Lee YH, Kim MS, Yun BS, et al. Davallialactone protects against adriamycin-induced cardiotoxicity in vitro and in vivo. J Nat Med. 2012 Jan;66(1):149-57.

[184] Li T, Danelisen I, Bello-Klein A, Singal PK. Effects of probucol on changes of antioxidant enzymes in adriamycin-induced cardiomyopathy in rats. Cardiovasc Res. 2000 Jun;46(3):523-30.

[185] Park S, Yoon J, Bae S, Park M, Kang C, Ke Q, et al. Therapeutic use of H2O2-responsive anti-oxidant polymer nanoparticles for doxorubicin-induced cardiomyopathy. Biomaterials. 2014 Jul;35(22):5944-53.

[186] Kaiserova H, Simunek T, Sterba M, den Hartog GJ, Schroterova L, Popelova O, et al. New iron chelators in anthracycline-induced cardiotoxicity. Cardiovasc Toxicol. 2007;7(2):145-50.

[187] Simunek T, Sterba M, Popelova O, Kaiserova H, Adamcova M, Hroch M, et al. Anthracycline toxicity to cardiomyocytes or cancer cells is differently affected by iron chelation with salicylaldehyde isonicotinoyl hydrazone. Br J Pharmacol. 2008 Sep;155(1):138-48.

[188] Bast A, Haenen GR, Bruynzeel AM, Van der Vijgh WJ. Protection by flavonoids against anthracycline cardiotoxicity: from chemistry to clinical trials. Cardiovasc Toxicol. 2007;7(2):154-9.

[189] Bast A, Kaiserova H, den Hartog GJ, Haenen GR, van der Vijgh WJ. Protectors against doxorubicin-induced cardiotoxicity: flavonoids. Cell Biol Toxicol. 2007 Jan;23(1):39-47.

[190]   Dickey JS, Gonzalez Y, Aryal B, Mog S, Nakamura AJ, Redon CE, et al. Mito-tempol and dexrazoxane exhibit cardioprotective and chemotherapeutic effects through specific protein oxidation and autophagy in a syngeneic breast tumor preclinical model. PLoS One. 2013;8(8):1-14.

[191]   Harake D, Franco VI, Henkel JM, Miller TL, Lipshultz SE. Cardiotoxicity in childhood cancer survivors: strategies for prevention and management. Fut Cardiol. 2012 2012/07/01;8(4):647-70.

[192]   Tebbi CK, London WB, Friedman D, Villaluna D, De Alarcon PA, Constine LS, et al. Dexrazoxane-Associated risk for acute myeloid leukemia/myelodysplastic syndrome and other secondary malignancies in pediatric Hodgkin's disease. J Clin Oncol. 2007 Feb;25(5):493-500.

[193]   Viarengo A, Burlando B, Ceratto N, Panfoli I. Antioxidant role of metallothioneins: a comparative overview. Cell Mol Biol. 2000 Mar;46(2):407-17.

[194]   Feng W, Benz FW, Cai J, Pierce WM, Kang YJ. Metallothionein disulfides are present in metallothionein-overexpressing transgenic mouse heart and increase under conditions of oxidative stress. J Biol Chem. 2006 Jan 13;281(2):681-7.

[195]   Shuai Y, Guo J, Dong Y, Zhong W, Xiao P, Zhou T, et al. Global gene expression profiles of MT knockout and wild-type mice in the condition of doxorubicin-induced cardiomyopathy. Toxicol Lett. 2011 Jan 15;200(1-2):77-87.

[196]   Guo J, Guo Q, Fang H, Lei L, Zhang T, Zhao J, et al. Cardioprotection against doxorubicin by metallothionein Is associated with preservation of mitochondrial biogenesis involving PGC-1alpha pathway. Eur J Pharmacol. 2014 Aug 15;737:117-24.

[197]   Sun X, Kang YJ. Prior increase in metallothionein levels is required to prevent doxorubicin cardiotoxicity. Exp Biol Med. 2002 Sep;227(8):652-7.

[198]   Shuai Y, Guo JB, Peng SQ, Zhang LS, Guo J, Han G, et al. Metallothionein protects against doxorubicin-induced cardiomyopathy through inhibition of superoxide generation and related nitrosative impairment. Toxicol Lett. 2007 Apr 5;170(1):66-74.

[199]   Krizkova S, Ryvolova M, Hrabeta J, Adam V, Stiborova M, Eckschlager T, et al. Metallothioneins and zinc in cancer diagnosis and therapy. Drug Metab Rev. 2012 Dec;44(4):287-301.

[200]   Choi CH. Cloning and functional study of a novel human metallothionein-I isoform induced by paraquat. Biochem Biophys Res Commun. 2003 May 2;304(2):236-40.

[201]   Margalit O, Simon AJ, Yakubov E, Puca R, Yosepovich A, Avivi C, et al. Zinc supplementation augments in vivo antitumor effect of chemotherapy by restoring p53 function. Int J Cancer. 2012 Aug;131(4):E562-E8.

[202]   Cirone M, Garufi A, Di Renzo L, Granato M, Faggioni A, D'Orazi G. Zinc supplementation is required for the cytotoxic and immunogenic effects of chemotherapy in chemoresistant p53-functionally deficient cells. Oncoimmunology. 2013 Sep;2(9):1-9.

[203]   Zablocki D, Sadoshima J. Angiotensin II and Oxidative Stress in the Failing Heart. Antioxid Redox Sign. 2013 Oct;19(10):1095-109.

[204]   Griendling KK, FitzGerald GA. Oxidative stress and cardiovascular injury - Part I: Basic mechanisms and in vivo monitoring of ROS. Circulation. 2003 Oct 21;108(16):1912-6.

[205]   Tsutsui H, Kinugawa S, Matsushima S. Oxidative stress and heart failure. Am J Physiol-Heart C. 2011 Dec;301(6):H2181-H90.

[206]   Guo J, Guo Q, Fang H, Lei L, Zhang T, Zhao J, et al. Cardioprotection against doxorubicin by metallothionein Is associated with preservation of mitochondrial biogenesis involving PGC-1 alpha pathway. European Journal of Pharmacology. 2014 Aug 15;737:117-24.

[207]   Cong WT, Zhao T, Zhu ZX, Huang BB, Ma WD, Wang YH, et al. Metallothionein prevents cardiac pathological changes in diabetes by modulating nitration and inactivation of cardiac ATP synthase. J Nutr Biochem. 2014 Apr;25(4):463-74.

[208]   Zhou SS, Yin X, Zheng Y, Miao X, Feng WK, Cai J, et al. Metallothionein prevents intermittent hypoxia-induced cardiac endoplasmic reticulum stress and cell death likely via activation of Akt signaling pathway in mice. Toxicol Lett. 2014 Jun;227(2):113-23.

[209]   Yang LF, Hu N, Jiang SS, Zou YZ, Yang J, Xiong LZ, et al. Heavy metal scavenger metallothionein attenuates ER stress-induced myocardial contractile anomalies: Role of autophagy. Toxicol Lett. 2014 Mar;225(3):333-41.

[210]   Oshima Y, Fujio Y, Nakanishi T, Itoh N, Yamamoto Y, Negoro S, et al. STAT3 mediates cardioprotection against ischemia/reperfusion injury through metallothionein induction in the heart. Cardiovasc Res. 2005 Feb;65(2):428-35.

[211]   Yin X, Zhou SS, Zheng Y, Tan Y, Kong MY, Wang B, et al. Metallothionein as a compensatory component prevents intermittent hypoxia-induced cardiomyopathy in mice. Toxicol Appl Pharmacol. 2014 May;277(1):58-66.

[212]   Krizkova S, Ryvolova M, Hrabeta J, Adam V, Stiborova M, Eckschlager T, et al. Metallothioneins and zinc in cancer diagnosis and therapy. Drug Metab Rev. 2012 Dec;44(4):287-301.

[213]   Tarapore P, Shu Y, Guo PX, Ho SM. Application of Phi29 Motor pRNA for Targeted Therapeutic Delivery of siRNA Silencing Metallothionein-IIA and Survivin in Ovarian Cancers. Mol Ther. 2011 Feb;19(2):386-94.

[214]   Fu Z, Guo JB, Jing L, Li RS, Zhang TF, Peng SQ. Enhanced toxicity and ROS generation by doxorubicin in primary cultures of cardiomyocytes from neonatal metallothionein-I/II null mice. Toxicol Vitro. 2010 Sep;24(6):1584-91.

[215]   Guo JB, Peng SQ. Enhanced apoptosis and myocardial injuries in metallothionein-null mice by doxorubicin treatment. Acta Pharmacol Sin. 2006 Jul;27:142-.

[216]   Yang HY, Wang YM, Peng SQ. Metallothionein-I/II null cardiomyocytes are sensitive to Fusarium mycotoxin butenolide-induced cytotoxicity and oxidative DNA damage. Toxicon. 2010 Jun;55(7):1291-6.

[217]   Choi CH. Cloning and functional study of a novel human metallothionein-I isoform induced by paraquat. Biochem Biophys Res Commun. 2003 May;304(2):236-40.

[218]   Sato M, Sasaki M, Hojo H. Tissue specific induction of metallothionein synthesis by tumor-necrosis-factor-alpha. Res Commun Chem Pathol Pharm. 1992 Feb;75(2):159-72.

[219]   Chen QM, Alexander D, Sun HP, Xie LF, Lin Y, Terrand J, et al. Corticosteroids inhibit cell death induced by doxorubicin in cardiomyocytes: Induction of antiapoptosis, antioxidant, and detoxification genes. Mol Pharmacol. 2005 Jun;67(6):1861-73.

4. MATERIAL AND METHODS

4.1 Isolation, cloning and expression mammalian MT in bacteria

4.1.1. Isolation metallothionein by PCR and cloning

The human MT3 protein (hMT3) was cloned in the pRSET-B vector (Invitrogen, Waltham, MA, USA). The construction of human MT3-pRSET-B plasmid (**Figure 9**) was obtained at Faculty of Science, Masaryk University, Brno, Czech Republic. Strains were stored as a frozen stock suspension in 20% (*v/v*) glycerol at −20 °C until their used. High levels of expression of DNA sequences cloned into the pRSET vectors were made possible by the presence of the T7 promoter. The chemical transformation protocol was performed following the instructions of New England Biolabs (Ipswich, MA, USA), using as host BL21 (DE3) pLysS Chemically Competent *E. coli* strain. Bacteria transformed with *hMT3-pRSET-B* plasmid were selected by ampicillin resistance. For human *MT2A* gene isolation, the MagNA Pure Compact Nucleic Acid Isolation Kit I (Roche, IN, USA) was used to isolation of DNA from human blood samples, using the MagNA Pure Compact Instrument (Roche, IN, USA). This procedure and results are explained in section **Results and discussion**. The rabbit MT2 protein (rMT2) was isolated from rabbit liver using FPLC.
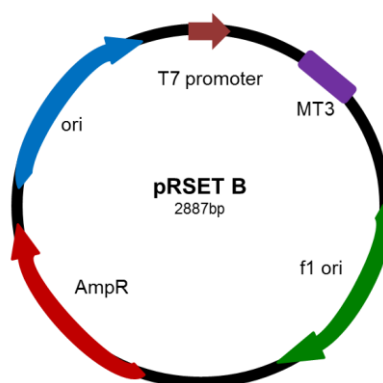
Figure 9. The map below shows the features of hMT3-pRSET-B. Vector pRSET is control vector expressing β-galactosidase. Note that β-galactosidase is fused to an N-terminal peptide containing the Xpress peptide, 6x-His tag and an enterokinase recognition site. High levels of expression of DNA sequences cloned into the pRSET vectors were made possible by the presence of the T7 promoter.

Transformation protocol was as follows: addition of 1-5 μl containing 1 pg-100 ng of plasmid DNA to the cell mixture. Carefully flick the tube 4-5 times to mix cells and DNA. Do not vortex. Place the mixture on ice for 30 minutes. Do not mix. Heat shock at exactly 42 °C for exactly 30 seconds. Do not mix. Place on ice for 5 minutes. Do not mix. Pipette 950 μl of room temperature SOC (super optimal broth with catabolite repression) medium into the mixture. Place at 37 °C for 60 minutes. Shake vigorously (250 rpm) or rotate. Warm selection plates to 37 °C. Mix the cells thoroughly by flicking the tube and inverting, then perform several 10-fold serial dilutions in SOC. Spread 50-100 μl of each dilution onto a selection plate (LB medium with Ampicilin) and incubate overnight at 37 °C.

4.1.2. Isolation of MT from rabbit liver

The rabbit MT-2 protein (rMT2) was isolated from rabbit liver. Amount of 2 g of defrosted rabbit liver was homogenized on ice using Ultra-turrax T8 (Scholler instruments, Germany) in 8 ml of 10 mM Tris–HCl buffer (pH 8.6). The obtained sample was subsequently vortexed (Vortex Genuie, Germany) and centrifuged (Universal 320, Hettich Zentrifugen, Germany) at 5,000 rpm (30 min, 4 °C). Taken supernatant was centrifuged again (Eppendorf centrifuge 5417R) in 1.5 ml micro test tube at 4 °C (25,000 rpm, 30 min). The supernatant was subsequently heated in thermomixer (Eppendorf thermomixer comfort, Germany) at 99 °C (10 min) and centrifuged (Eppendorf centrifuge 5417R, Germany) in 1.5 ml micro test tube at 4 °C (25,000 rpm, 30 min). Sample prepared like this was used for isolation of MT. The purification of MTs was performed by FPLC.

4.1.3. Expression of MT in *Escherichia coli*

The positive transformants of all MTs (hMT2A and hMT3) were grown in LB (Luria-Bertani) broth with 50 μg.ml^{-1} ampicillin shaking at 37 °C overnight. The next day, the culture was grown to 0.1 of OD 600 nm. When the culture reached the exponential phase (0.4-0.6), isopropyl β-D-1-thiogalactopyranoside (IPTG) was added to a final concentration of 1 mM and continued to grow the cells during 4 hours.

The pellet was frozen at -20 °C and then was resuspended with 20 mM phosphate buffer at neutral pH. The method of cell lysis was carried out by freeze-thaw cycles. The lysate was frozen in liquid nitrogen and was thawed at 42 °C (this freeze-

thaw cycle was repeated two to three additional times). The isolation protocol was performed following the instructions of pRSET A, B, and C for high-level expression of recombinant proteins in *E. coli* (Invitrogen, USA). The protein fraction was harvested by centrifugation during 10 minutes at 4000 rpm at 4 °C. The purification of MTs was performed by FPLC.

4.2. Isolation and purification of MT by FPLC

FPLC was purchased from Biologic DuoFlow system (Biorad, USA), which consisted of two chromatographic pumps for the application of elution buffers, a gel-filtration column (HiLoad 26/60, 75 PG, GE Healthcare, Sweden), an injection valve with 2 ml sample loop, an UV–Vis detector and an automated fraction collector. Solution of 150 mM NaCl in 10 mM Tris–HCl buffer (pH 8.6) was used as a mobile phase. Flow of the mobile phase was set to 4 ml/min. Isocratic elution was used for MT separation. Column was washed for 60 min by mobile phase prior to every separation. Process of MT-2 isolation from rabbit liver after Cd(II) application was performed according to [193]. Fraction containing MT was collected in elution volume of 240 ml. Signal of MT was well evident due to binding of Cd(II) ions into protein structure, which caused change in the absorbance measured at 254 nm. Dialysis and lyophilisation of corresponding fraction were also carried out in deionised water.

4.3. SDS-PAGE

The electrophoresis was performed using a Mini Protean Tetra apparatus with gel dimension of 8.3 × 7.3 cm (Bio-Rad, USA). Firstly, 12.5% (m/V) running, then 5% (m/V) stacking gel was poured. The gels were prepared from 30% (m/V) acrylamide stock solution with 1% (m/V) bisacrylamide. The polymerization of the running or stacking gels was carried out at room temperature for 45 min prior to analysis the samples were mixed with non-reduction sample buffer in a 2:1 ratio. The samples were incubated at 93 °C for 3 min, and the sample was loaded into a gel. For determination of the molecular mass, the protein ladder from Biorad was used. The electrophoresis was run at 120V for 1 h 15 min at 4 °C (Power Basic, Biorad USA) in tris-glycine buffer (0.025 M Trizma-base, 0.19 M glycine and 3.5 mM SDS, pH = 8.3). Then the gels were stained Coomassie blue and consequently with silver, if proteins concentration in the samples was below detection limit of Coomassie blue staining.

The procedure of rapid Coomassie blue staining was adopted from Wong *et al.* [194], silver staining was performed according to Krizkova *et al.* [159] with omitting the fixation (1.1% (*v/v*) acetic acid, 6.4% (*v/v*) methanol and 0.37% (*v/v*) formaldehyde) and first two washing steps with 50% (*v/v*) methanol).

4.4. The Matrix-Assisted Laser Desorption/Ionization time-of-flight Mass Spectrometry (MALDI-TOF MS)

The matrix used in the MALDI-TOF MS for characterisation of PC was α-cyano-4-hydroxycinnamic acid (HCCA) (Bruker). The matrix was prepared in 70% methanol. Mixture was thoroughly vortexed and ultrasonicated using Bandelin 152 Sonorex Digital 10P ultrasonic bath (Bandelin electronic GmbH, Germany) to 2 minutes 50% of intensity at ambient temperature. Working standard solutions were prepared daily by dilution of the stock solutions. The sample solutions were TA30 (30% acetonitrile, 0.1% trifluoroacetic acid solution). The solutions for analysis were mixed in volume ratio 1:1 (matrix/substance). After obtaining a homogeneous solution, 1µl was applied on the MTP ground target plate (Bruker Daltonik GmbH) and dried under atmospheric pressure and 25 °C.

Samples preparation crystallization method for MALDI-TOF MS was done in three different ways: Dried Droplet (DD), Thin Layer (TL) and Double Layer (DL). For DD, a saturated matrix solution is prepared. This matrix solution was mixed in equal volumes with the sample solution (1:1). The sample solution was TA30. The mixture was pipeted on the target (1 µl) and dried at 25 °C. The preparation yielded relatively large crystals on the target surface as well as regions without matrix or analyte. For TL, the matrix was prepared on the target to form a thin layer of very small and homogenous crystals. After spotting of this solution spreaded on the target it was evaporated very fast. The thin matrix layer remained on the surface of the target. The sample was applied on top of this thin layer. After the sample was dried, the analyte molecules remained on top of the matrix, and one way to combine DD and TL preparation is the DL method. Here, a thin layer of matrix was prepared as described above and on top of that thin layer a normal dried droplet was applied.

For Cd-PC2 complexes formation were used final concentrations of PC2 (250 ng/µl) and $CdCl_2$ (500 ng·µl^{-1}) in water (ACS) incubated 1 h at 20 °C.

MTs were analyzed by MALDI-TOF MS (ultrafleXtreme instrument, Bruker Daltonik, Germany) equipped with a laser operating at a wavelength of 355 nm with an accelerating voltage of 25 kV, cooled with nitrogen and a maximum energy of 43.2 μJ with repetition rate 2000 Hz, and with software for data acquisition and processing of mass spectra flexControl version 3.4 and flexAnalysis version 2.2. As matrices were used HCCA and 2,5-dihydroxybenzoic acid (DHB) (Bruker) prepared in TA30 for optimization of the conditions for determination of MTs. Mixture was thoroughly vortexed. Working standard solutions were prepared daily by dilution of the stock solutions. The sample solutions were TA30. The solutions for analysis were mixed in ratio of 1:1 (matrix/substance). After obtaining a homogeneous solution, 1μl was applied on the target and dried under atmospheric pressure and ambient temperature.

For find the optimal condition of characterization MTs rabbit liver by MALDI-TOF MS, the samples preparation crystallization method was done in two different ways: Dried Droplet (DD) and Thin Layer (TL) for HCCA matrix. For DD, a saturated matrix solution is prepared. This matrix solution is mixed in equal volumes with the sample solution (1:1). The sample solution was TA30. The mixture is pipeted on the target (1 μl) and dried at ambient temperature. The preparation will yield relatively large crystals on the target surface a well as regions without matrix or analyte. For TL, the matrix is prepared on the target to form a thin layer of very small and homogenous crystals. After spotting this solution spreads on the target and evaporates very fast. The thin matrix layer remains on the surface of the target. The sample was applied on top of this thin layer. After the sample was dried, the analyte molecules remain on top of the matrix. Before measuring samples, a mixture of peptide calibration standards (Bruker) was used to externally calibrate the instrument. The MS spectra were typically acquired by averaging 20 sub spectra from a total of 500 shots of the laser (Smartbeam 2. Version: 1_0_38.5).

4.5. Ion Exchange Chromatography

For determination of PC2 an IEC (Model AAA-400, Ingos, Prague, Czech Republic) with post column derivatisation with ninhydrin and Vis detector was used. A glass column with inner diameter of 3.7 mm and 350 mm in length was filled manually with a strong cation exchange resin in sodium cycle LG ANB (Ingos) with approximately 12 μm particles and 8% porosity. The column was tempered within the range from 40 to

115 °C. A double channel Vis detector with 5 µl cells was set to detection wavelengths 440 nm and 570 nm. A solution of ninhydrin (Ingos) was prepared with 75% (v/v) methylcelosolve (Ingos) and with 2% (v/v) 4 M acetic buffer (pH 5.5). Tin chloride ($SnCl_2$) was used as a reducing agent. The prepared solution of ninhydrin was stored under an inert atmosphere (N_2) in dark at 4 °C. The flow rate of mobile phase was 0.25 ml·min^{-1} and flow rate of ninhydrin was tested within the range from 0.1 to 0.35 ml·min^{-1}. The reactor temperature was optimised within the range from 90 to 130 °C.

4.6. Synthesis and functionalization of magnetic particles (MPs)

$Fe(NO_3)_3 \cdot 9H_2O$ (1.5 g) was dissolved in water (80 ml). Under stirring was added 0.2 g of $NaBH_4$, which was dissolved in 10 ml of 3.5% NH_3 and heated (2 h, 100 °C). After cooling, the mixture was left overnight and magnetic nanoparticles were separated by external magnetic field, washed several times with water and used as a core for surface modifications.

MAN-53

Maghemite was suspended in water solution (20 ml) of 7.5% polyvinylpyrrolidone (PVP), mixed with 25 ml of 1 mM $HAuCl_4$ and finally 0.75 ml of trisodium citrate (26 mg·ml^{-1}) was added in order to produce a shell structure. Resulting mixture was stirred overnight, separated using an external magnetic force field and dried at 40 ºC. Procedure of this material fabrication was published previously [33].

MAN-131

Maghemite was mixed with a water solution (20 ml) of polyethylenimine (0.5 g) and stirred for 1 h. 25 ml of $HAuCl_4$ (1 mM) was added, stirred 1 h and sodium citrate (0.75 ml, 26 mg·ml^{-1}) was poured into the solution. The mixture was stirred overnight. C-dots covered with PVP (C-dots-PVP) were prepared similarly to works [34,35] from 10.0 ml of ethylene glycol, 1.0 ml of PVP solution (average Mw ~ 10 kDa) and 1.0 g of citric acid. The solution was heated at 180 ºC for 4 h under N_2. The solution was purified by dialyzing than centrifuged at 10 000 rpm and 5 ml of the supernatant was used for modification of maghemite. The mixture was stirred for 4 h, separated by magnet, washed 3 times with water and dried at 40 ºC.

MAN-132

Maghemite was suspended in water solution (20 ml) of polyethylene glycol (PEG 4000), mixed with 25 mL of 1 mM $HAuCl_4$ and finally 0.75 ml of trisodium citrate (26 mg·ml^{-1}) was added. Resulting mixture was stirred overnight, separated using an external magnetic force field and dried at 40 ºC.

MAN-133

The preparation way was similar to preparation of MAN-132 only PEG of molecular weight 1500 (0.5 g) was used.

MAN-134

Maghemite suspension was added to a solution of poly(4-styrenesulfonic acid) (0.5 g) and mixed for 1 h. 25 ml of 1 mM $HAuCl_4$ was added, mixed for 1 h and finally 0.75 ml of trisodium citrate (26 mg·ml^{-1}) was added. The mixture was stirred overnight, separated by magnet and dried at 40 ºC.

MAN-135

Maghemite suspension was added to a solution of polyacrylamide (0.5 g) and mixed for 1 h. 25 ml of 1 mM $HAuCl_4$ was added, mixed for 1 h and finally 0.75 ml of trisodium citrate (26 mg·ml^{-1}) was added. The mixture was stirred overnight, separated by magnet and dried at 40 ºC.

4.7. Characterization of synthesized MPs

The morphologies of MPs were studied using scanning electron microscope MIRA3 LMU (Tescan, a.s., Brno, Czech Republic). An accelerating voltage of 15 kV and beam current about 1 nA was applied with satisfactory results regarding to maximum throughput. MPs size and their δ-potential were observed by Particle Size Analyzer (Zetasizer Nano ZS90, Malvern instruments, Malvern, UK). MPs were dispersed in phosphate buffered saline (PBS, 137 mM NaCl, 2.7 mM KCl, 1.4 mM NaH_2PO_4, and 4.3 mM Na_2HPO_4, pH 7.4) and incubated at 25 °C for 15 min before the measurement.

4.8. Manual isolation of MTs using MPs

Prior to isolation process, MPs (40 mg·ml^{-1}) were washed using PBS (6 × 250 µl, pH =7) to remove impurities. For isolation, MT isolated from rabbit liver (50 µg·ml^{-1}) was incubated with MPs (0.5 mg·ml^{-1}) under conditions as follows: 37 ^{o}C, 30 min, 1190 rpm in thermomixer (Eppendorf Thermomixer comfort, Hamburg, Germany). MPs with bound MT were forced using external magnetic field and six times washed with PBS or combination of PBS (3 x 250 µl, pH 7) and 200 mM borate buffer (3 × 250 µl, pH 6). In order to detect MTs, MPs with bound MT were dissolved in hydrochloric acid (250 µl, 3 M HCl). Obtained solution was evaporated using nitrogen evaporator Ultravap RC (Porvair Sciences, Leatherhead, UK). Finally, the evaporated sample was resuspended with ACS H$_2$O (250 µl) and final product was detected by DPV.

4.9. Fully automated pipetting system

Fully automated MTs isolation procedure had the same specific parameters as in the way of manual isolation procedure. Here the whole procedure carried out on automated pipetting system epMotion 5075 (Eppendorf, Hamburg, Germany). The pipetting provides a robotic arm with dispensing tools (TS50, TS300, TS1000), which are in the positions T1 – T4. The samples are placed in the positions B2 and C2 in Eppendorf Rack for 96 Test Tubes. Eppendorf Reservoir Holder with 7 × 30 ml reservoirs (maximum filling volume: 30 ml, working volume: 25 ml, detection limit of optical sensor: 3 µl) was located in the position B1. The device was controlled by the PC software (Eppendorf). The tips were located in the A3 (epTIPS Motion, 50 µl) and A2 (epTIPS Motion, 300 µl) positions. The experimental program is described in **Results and discussion section**.

4.10. Electrochemical methods

4.10.1. Flow injection analysis coupled with electrochemical detection Coulochem III

The instrument for flow injection analysis with electrochemical detection (FIA-ED) consisted of solvent delivery pump operating in range of 0.001-9.999 ml·min^{-1} (Model 582 ESA Inc., Chelmsford, MA, USA), a guard cell (Model 5020 ESA, USA), a reaction coil (1 m) and/or a chromatographic column Zorbax eclipse AAA C18

(150 × 4.6; 3,5 μm particles, Agilent Technologies, USA), UV-Vis (Model 528, ESA Inc., Chelmsford, MA, USA) and an electrochemical detector. The electrochemical detector included one low volume flow-through analytical cell (Model 5040, ESA, USA), which consisted of glassy carbon working electrode, hydrogen-palladium electrode as reference electrode and auxiliary electrode, and Coulochem III as a control module. The sample (20 μl) was injected using autosampler (Model 542, ESA Inc., Chelmsford, MA, USA). The data obtained were evaluated by Clarity software (Version 3.0.04.444, Data Apex, Czech Republic). The experiments were carried out at room temperature. Guard cell potential was set as 0 V. A glassy carbon electrode was polished mechanically by 0.1 μm of alumina (ESA Inc., Chelmsford, MA, USA) and sonicated at room temperature for 5 min using a Sonorex Digital 10 P Sonicator (Bandelin, Berlin, Germany) at 40 W. Flow rate of mobile phase was 1 ml·min^{-1}. Hydrodynamic voltammograms has been analyzed in range 100–1000 mV with 100 mV step.

4.10.2. Flow injection analysis coupled with electrochemical detection Coularray

FIA-ED system consisted of two solvent delivery pumps operating in the range of 0.001-9.999 ml·min^{-1} (Model 582 ESA Inc., Chelmsford, MA), a reaction coil (1 m) and a CoulArray electrochemical detector (Model 5600A, ESA Inc., Chelmsford, MA, USA). The electrochemical detector included three flow cells (Model 6210, ESA Inc., Chelmsford, MA, USA). Each cell consisted of four working carbon porous electrodes, each one with auxiliary and dry H/Pd reference electrodes. Both the detector and the reaction coil/column were thermostated. The sample (20 μl) was injected using autosampler (Model 542 HPLC, ESA Inc., Chelmsford, MA, USA). Flow rate of mobile phase was 1 ml·min^{-1}. Hydrodynamic voltammograms has been analyzed in range 100 – 1000 mV with 100 mV step.

4.10.3. Differential Pulse Voltammetry on a hanging mercury drop electrode by Brdicka reaction

Products of isolation procedure were detected by differential pulse voltammetry on a hanging mercury drop electrode (HMDE) with a drop area of 0.4 mm^2 as the working

electrode. An Ag/AgCl/3M KCl electrode was the reference and platinum electrode was auxiliary. An electrochemical cell was cooled to 5 °C (Julabo F25, JulaboDE, Labortechnik, Wasserburg, Germany). The analyzed samples were deoxygenated prior to measurements by purging with argon (99.999 %) saturated with water for 10 s. Brdicka supporting electrolyte containing 1 mM $[Co(NH_3)_6]Cl_3$ and 1 M ammonia buffer ($NH_3(aq)$ and NH_4Cl, pH = 9.6) was used and changed after each analysis. The parameters of the measurement were as follows: initial potential of -0.7 V, end potential of -1.75 V, pulse period 0.80 s, sample period 10 ms, pulse width 30 ms, step potential 2 mV, modulation amplitude -25 mV, sweep rate 2.5 mV·s^{-1}, E_{ads} = 0 V, t_{ads} = 120 s, stirring 1000 min^{-1}, volume of injected sample: 5 μl, volume of measurement cell 2 ml (5 μl of sample and 1995 μl Brdicka solution). Manual determination was performed on the 693 VA Stand (Metrohm, Herisau, Switzerland). Automated electrochemical detection was performed with 747 VA Stand instrument connected to 693 VA Processor and 695 Autosampler (Metrohm, Herisau, Switzerland). For data processing VA Database 2.2 by Metrohm was employed.

5. RESULTS AND DISCUSSION

Results and Discussion part of this Ph.D. thesis is presented as three publications in scientific journals and Experimetal chapter (future publication) and supplemented by the comments of the author. For each work also author contribution on the creation of publication is marked.

5.1 Optimization of MALDI-TOF for PC2 and Cd-PC complex determination

The next step of the study was demonstrated that MALDI-TOF MS is the ideal and promising techniques for screening and characterization in Cd-PC2 complexes.

5.1.1. Reseach article I

MIGUEL ANGEL MERLOS RODRIGO, ONDREJ ZITKA, MARKETA KOMINKOVA, VOJTECH ADAM, MIROSLAVA BEKLOVA AND RENE KIZEK. Analysis of Cadmium-Phytochelatins 2 Complexes Using Flow Injection Analysis Coupled with Electrochemical Detection Mass Spectrometry. *Int. J. Electrochem. Sci.*, 8 (2013) 4409 – 4421.

Participation in the work of the author M.A. Merlos Rodrigo: experimental part 40% and manuscript preparation 50%.

Cd is a heavy metal that is of great threat in the environment. Concentrations of Cd can be accumulated by plants with toxic effect to them. Notably, higher plants, algae, certain yeasts and animals are equipped with a repertoire of mechanisms to counteract metal toxicity. The key elements of these are chelation of metals by forming PCs and related cysteine-rich polypeptides. PCs are produced from glutamine, cysteine and glycine and the process is catalysed by PC synthases known as γ-glutamylcysteine (γ-Glu-Cys) dipeptidyl transpeptidases. The role of PCs in metal detoxification likely results from immobilization of metals, preventing non-specific binding to important biomolecules, followed by the transport of the Metal-PC complexes into the vacuole, or

its excretion. It is therefore of interest to attempt to directly characterized of Cd-PC complexes.

The aim of this work was characterization PC2 and Cd-PC2 complexes using MALDI-TOF MS and flow injection analysis/high performance liquid chromatography with CoulArray or Coulochem electrochemical detector.

Cd-PC2 complexes and optimal method of the formation of complex by the MALDI-TOF MS was confirmed. We proved the creation Cd-PC2 complex using MALDI-TOF MS and these results indicated that the optimum conditions for the determination of PC2 by utilizing α-Cyano-4-hydroxycinnamic acid as matrix was a laser intensity of 43.3 μJ and the concentration of the matrix more convenient was 15 mg·ml^{-1} in methanol 70%.

Base on the results obtained the highest response for PC2 was with applied pH 2 and with increasing pH the signal has been decreasing using electrochemical detector Coulochem III in flow injection system. Higher temperature around used 40°C is positively influencing the interaction between Cd and thiol groups of PC-2 by Coulochem III. The time was not affecting the forming of complex. The higher intensity of creation complex is due to applied concentration of 100 μg·ml^{-1} and no distinct change in HDV trend is observed by higher applied concentrations by CoulArray.

In this study, the obtained data show that MALDI-TOF MS in combination with the flow injection analysis coupled with electrochemical detection Coulochem III or/and Coularray is a reliable and fast method for the determination of these complexes.

Article

Analysis of Cadmium-Phytochelatins 2 Complexes Using Flow Injection Analysis Coupled with Electrochemical Detection Mass Spectrometry

Miguel Angel Merlos Rodrigo [1,2,3], *Ondrej Zitka* [1,2,3,4], *Marketa Kominkova* [1], *Vojtech Adam* [2,3], *Miroslava Beklova* [4] *and Rene Kizek* [1,2,3*]

[1]Department of Chemistry and Biochemistry, and [2]Lead and Cadmium Initiatives, United Nation Environment Program, Faculty of Agronomy, Mendel University in Brno, Zemedelska 1, CZ-613 00 Brno, Czech Republic
[3]Central European Institute of Technology, Brno University of Technology, Technicka 3058/10, CZ-616 00 Brno, Czech Republic
[4]Department of Veterinary Ecology and Environmental Protection, Faculty of Veterinary Hygiene and Ecology, University of Veterinary and Pharmaceutical Sciences, Palackeho 1-3, CZ-612 42 Brno, Czech Republic
[*]E-mail: kizek@sci.muni.cz

In this study, *in vitro* synthesized Cd-phytochelatin (PC2) complexes were characterized using flow injection analysis/high performance liquid chromatography with CoulArray or Coulochem electrochemical detector of PC2 and Cd-PC2 complexes. Method of the formation of complex by the matrix-assisted laser desorption/ionization time-of-flight mass spectrometer (MALDI-TOF-MS) was confirmed. Higher pH had lowered effect for Cd(II) detection but PC2 detection suffers much in task of sensitivity and for further analysis we thus used the Britton-Robinson buffer at pH 2 as electrolyte. Higher temperature than 40 °C positively influenced the interaction between Cd and thiol groups of PC2 by Coulochem III. The time did not affect the forming of complex. The concentration had bigger effect on the formation of complex than time of incubation. The biggest change was, with regards to concentration, observed under applied concentration 400 μg/ml and where the slope was the most decreasing which means the decreasing the amount of PC2 and increasing of amount of complex. In the case of the influence of time, 400 μg/ml reported the most decreasing trend after 8 hour of incubation. Subsequently we proved the formation Cd-PC2 complex using MALDI-TOF-MS and these results indicated that the optimum conditions for the determination of PC2 utilizing HCCA as matrix was a laser intensity of 43.3 μJ and the concentration of the matrix was 15 mg/ml in 70% methanol (*v/v*). The obtained data show that the flow injection analysis coupled with electrochemical detection Coulochem III or/and Coularray in combination with MALDI-TOF is a reliable and fast method for the determination of these complexes.

1. INTRODUCTION

Heavy metals, such as cadmium (Cd), are potentially toxic to all organisms. It is not surprising that organisms have protective mechanisms to resist, at least partially, the adverse effect of metals. Cd is a non-essential heavy metal ubiquitously dispersed in the environment by natural and anthropogenic activities [1-3]. Biological systems respond to potentially toxic levels of metal ions mainly by chelation and sequestration of the excess of the element. Plants respond to Cd toxicity of different ways such as immobilization, exclusion, chelation and compartmentalization of the metal ions, and the expression of more general stress response mechanisms as stress peptides [4-6].

Phytochelatins (PC) are enzymatically synthesized peptides produced in a wide variety of plant species including monocots, dicots, gymnosperms, and algae as heavy metal binding ligands, such as cadmium. PCs form a family of structures with increasing repetitions of the -Glu-Cys dipeptide units followed by a terminal Gly, (γ-Glu-Cys)n-Gly or (γ–EC)n-Gly, where n ranges from 2–11 [4,7-9]. PCs are synthesized from reduced glutathione (GSH) by the constitutive enzyme PC synthase, activated by a variety of metal ions, among which Cd is the most effective [10-16].

PC are usually analysed by using a method developed by Grill et al. [17]. In addition to this method, Doring et al. used pre-column derivatization, high-performance liquid chromatography and fluorescence-detection for analysis of PC in plant [18]. In order to determine the Cd-PC complexes, different methodologies have been used in recent years. Techniques, such as high performance liquid chromatography inductively coupled plasma mass spectrometry (HPLC-ICP-MS) and high performance liquid chromatography electrospray mass spectrometry (HPLC-ESI-MS) are analytical instruments to study metal speciation in plants. They were applied in phytoremediation research as well as in the understanding of metal accumulation mechanism. Chen et al. characterized in vitro synthesized Cd-PC complexes and in vivo Cd-PC complexes in Cd-stressed plants, using size exclusion chromatography (SEC) ICP-MS and ESI-MS/MS [19]. Nano-electrospray ionization tandem mass spectrometry and capillary liquid chromatography/electrospray ionization tandem mass spectrometry method was used for the analysis of Cd-PC complexes in plant tissue culture [20]. Liquid chromatography coupled with on line chemical vapour generation and atomic fluorescence spectrometric detection [21], and inductively coupled plasma-mass spectrometry (ICP-MS) [22,23], were methods used for the determination of Cd-PC complexes.

The innovation of flow injection analysis (FIA) for the analysis of peptides or proteins with a sensitivity of low concentrations has greatly enhanced our capability to analyse metallic complexes, including the interaction between a peptide and a metal ion [24]. So far, few studies of the use of flow injection analysis in the analysis of PCs have been reported [24], but the direct analysis of PC-Cd complexes has not been explored. Therefore, the main aim of this study was to optimize flow injection analysis/high performance liquid chromatography coupled with CoulArray or Coulochem electrochemical detector for analysis of PC2 and Cd-PC2 complexes synthesized in vitro. The results were further evaluated by MALDI-TOF.

2. EXPERIMENTAL PART

2.1 Chemicals

Phytochelatin2 (PC2) (γ-Glu-Cys)2-Gly was synthesized in Clonestar Biotech (Brno, Czech Republic) with a purity above 90 %. HPLC-grade methanol (>99.9%; v/v) from Sigma-Aldrich (St. Louis, USA) was used. Other chemicals (H_3PO_4, CH_3COOH, H_3BO_3, NaOH and $CdCl_2$) were purchased from Sigma-Aldrich in ACS purity unless noted otherwise. Stock standard solutions of the PC2 (1 mg/ml) were prepared with ACS water and stored in dark at -20 °C. Working standard solutions were prepared daily by dilution of the stock solutions. All solutions were filtered through 0.45 μm Nylon filter discs (Millipore, Billerica, Mass., USA) prior to FIA-ED analysis. The pH value was measured using InoLab pH 730 WTW (Weilheim, Germany).

2.2 Flow injection analysis coupled with electrochemical detector Coulochem III

The instrument for flow injection analysis with electrochemical detection (FIA-ED) consisted of solvent delivery pump operating within the range from 0.001 to 9.999 ml/min (Model 582 ESA Inc., Chelmsford, MA, USA), a guard cell (Model 5020 ESA, USA), a reaction coil (1 m) and/or a chromatographic column Zorbax eclipse AAA C18 (150 × 4.6; 3.5 μm particles, Agilent Technologies, USA), UV-VIS (Model 528, ESA Inc., Chelmsford, MA, USA) and an electrochemical detector. The electrochemical detector includes one low volume flow-through analytical cell (Model 5040, ESA, USA), which is consisted of glassy carbon working electrode, hydrogen-palladium electrode as reference electrode and auxiliary electrode, and Coulochem III as a control module. The sample (20 μl) was injected using autosampler (Model 542, ESA Inc., Chelmsford, MA, USA). The data obtained were treated with Clarity software (Version 3.0.04.444, Data Apex, Czech Republic). The experiments were carried out at room temperature. Guard cell potential was set as 0 V. A glassy carbon electrode was polished mechanically by 0.1 μm of alumina (ESA Inc., Chelmsford, MA, USA) and sonicated at room temperature for 5 min using a Sonorex Digital 10 P Sonicator (Bandelin, Berlin, Germany) at 40 W. Flow rate of mobile phase was 1 ml/min. Hydrodynamic voltammograms were analyzed in range 100 – 1000 mV with 100 mV steps.

2.3 Flow injection analysis coupled with electrochemical detector Coularray

FIA-ED system consisted of two solvent delivery pumps operating within the range from 0.001 to 9.999 ml/min (Model 582 ESA Inc., Chelmsford, MA), a reaction coil (1 m) and a CoulArray electrochemical detector (Model 5600A, ESA Inc., Chelmsford, MA, USA). The electrochemical detector includes three flow cells (Model 6210, ESA Inc., Chelmsford, MA, USA). Each cell consists of four working carbon porous electrodes, each one with auxiliary and dry H/Pd reference electrodes. Both the detector and the reaction coil/column were thermostated. The sample (20 μl) was injected using autosampler (Model 542 HPLC, ESA Inc., Chelmsford, MA, USA). Flow rate of mobile phase was 1 ml/min. Hydrodynamic voltammograms were analyzed in range 100 – 1000 mV with 100 mV steps.

2.4 Matrix-Assisted Laser Desorption/Ionization Time-of-Flight Mass Spectrometry

The mass spectrometry experiments were performed on a MALDI-TOF mass spectrometer Bruker Ultraflextreme (Bruker Daltonik GmbH, Germany) equipped with a laser operating at wavelength of 355 nm with an accelerating voltage of 25 kV, cooled with nitrogen and a maximum energy of 43.2 μJ with repetition rate 2000 Hz in linear and positive mode, and with software for data acquisition and processing of mass spectra flexControl version 3.4 and flexAnalysis version 2.2. The matrix used in the MALDI method was α-cyano-4-hydroxycinnamic acid (HCCA) (Bruker). The matrix was prepared in 70% methanol. Mixture was thoroughly vortexed and ultrasonicated using Bandelin 152 Sonorex Digital 10P ultrasonic bath (Bandelin electronic GmbH, Germany) to 2 minutes 50% of intensity at room temperature. Working standard solutions were prepared daily by dilution of the stock solutions. The sample solutions were TA30 (30% acetonitrile, 0.1% trifluoroacetic acid solution). The solutions for analysis were mixed in ratio of 1:1 (matrix/substance). After obtaining a homogeneous solution, 1 μl was applied on the MTP ground target plate (Bruker) and dried under atmospheric pressure and room temperature. A mixture of peptide calibrations standard (Bruker) was used to externally calibrate the instrument.

Samples preparation crystallization method for MALDI-TOF was done in three different ways: Dried Droplet (DD), Thin Layer (TL) and Double Layer (DL). For DD, a saturated matrix solution was prepared. This matrix solution was mixed in equal volumes with the sample solution (1:1). The sample solution was TA30. The mixture was pipetted on the target (1 μl) and dried at room temperature. The preparation yielded relatively large crystals on the target surface a well as regions without matrix or analyte. For TL, the matrix was prepared on the target to form a thin layer of very small and homogenous crystals. After spotting this solution spread on the target and evaporated very fast. The thin matrix layer remained on the surface of the target. The sample was applied on top of this thin layer. After the sample was dried, the analyte molecules remained on top of the matrix. One way to combine of DD and TL preparation is the DL method. Here, a thin layer of matrix was prepared as described above and on top of that thin layer a normal dried droplet was used.

PC2 (250 ng/μl) and CdCl2 (500 ng/μl) in ACS water incubated for 1 h at 20 °C were used for Cd-PC2 complexes formation. The MS spectra were typically acquired by averaging 20 sub spectra from a total of 500 shots of the laser (Smartbeam 2. Version: 1_0_38.5) with an energy of 43.2 μJ (50%).

3. RESULTS AND DISCUSSION

3.1 Optimization of FIA-ED for PC2 and Cd-PC complex determination

Our experiments were focused on studying of change of electrochemical profile based on hydrodynamic voltammogram (HDV) generated by HPLC-ED using two different electrochemical detectors. Primarily, we optimized a detection using electrochemical detector Coulochem III in flow injection system. During electrochemical analysis the pH is the most influencing factor with regards to the observed oxidizing or reducing maxima or even of the sensitivity of detection. Therefore we tested pH in wide range using Britton-Robinson buffer as the mobile phase, which covers pH 2, 3, 4, 5, 6, 7

and 8. The results obtained from the analysis of individual samples of free PC2 and free Cd(II) are shown in Fig. 1A and B. We presented the maxima of the HDV of PC2 as 900 mV (inset in Fig. 1A) and Cd(II) as 600 mV (inset in Fig. 1B). For better understanding the development of the HDV based on change of pH the border and middle values are displayed as well. It clearly follows from the results obtained that the highest response for PC2 was obtained at pH 2. The pH has been further increasing the signal has been decreasing. In the case of Cd(II), the influence of increasing pH was marginal. The pH 2 provides only about 30% lower signal than the highest tested pH 8. Change of pH across the tested spectrum from 2 to 8 much more negatively affected the PC2 detection (up to 95% decrease) in comparison to Cd(II) (only 30% increase). Therefore it is obvious that higher pH has lower effect for Cd(II) detection but PC2 detection suffers much in task of sensitivity and for further analysis we thus used the Britton-Robinson buffer at pH 2 as an electrolyte.
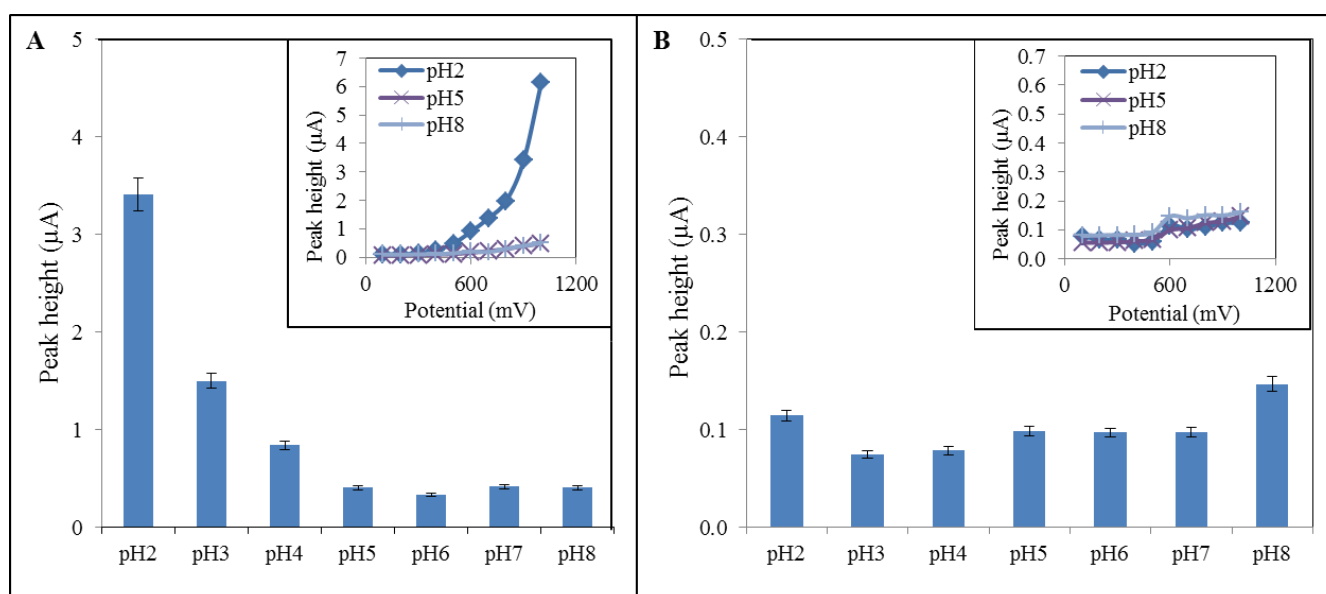
Figure 1. The obtained signal represented by peak height from FIA-ED determination using coulochem III electrochemical detector for (**A**) PC-2 and Cd(II) (**B**). In insets: the hydrodynamic voltammograms (HDV) obtained for pH 2, 5 and 8 for analysis of (**A**) PC-2 and (**B**) Cd(II).

3.2 Electrochemical studying complexes by Coulochem III

Further, we analysed the mixtures of PC2 and Cd(II) under applied concentration 100 μg/ml each. Therefore, we studied the influence of the incubation temperature (10, 20, 30 and 40 °C) and time of incubation (0, 2, 4, 6 and 8 h) on the forming of the complex during mixing in vortex under 600 rpm. Then, all variants were analyzed by Coulochem III for obtaining the HDVs (Fig. 2). Due to the optimal signal at 600 mV for Cd(II), we monitored the HDVs in this applied potential (Figs. 2A, B, C and D). There is also shown the change of profile of each HDV in greater details (Figs. 2Aa, Bb, Cc and Dd) for 0, 4, 6 and 8 hour at each temperature. It clearly follows from the results obtained that incubation time did not affect the interaction. With regards to applied temperature there is shown that 10-30°C caused signals lower than 1 μA. However, under the 40°C the intensity of signal was app. 1.5

µA, i.e. for 50 % higher. It clearly follows that higher temperature positively influenced the interaction between Cd and thiol groups of PC-2.
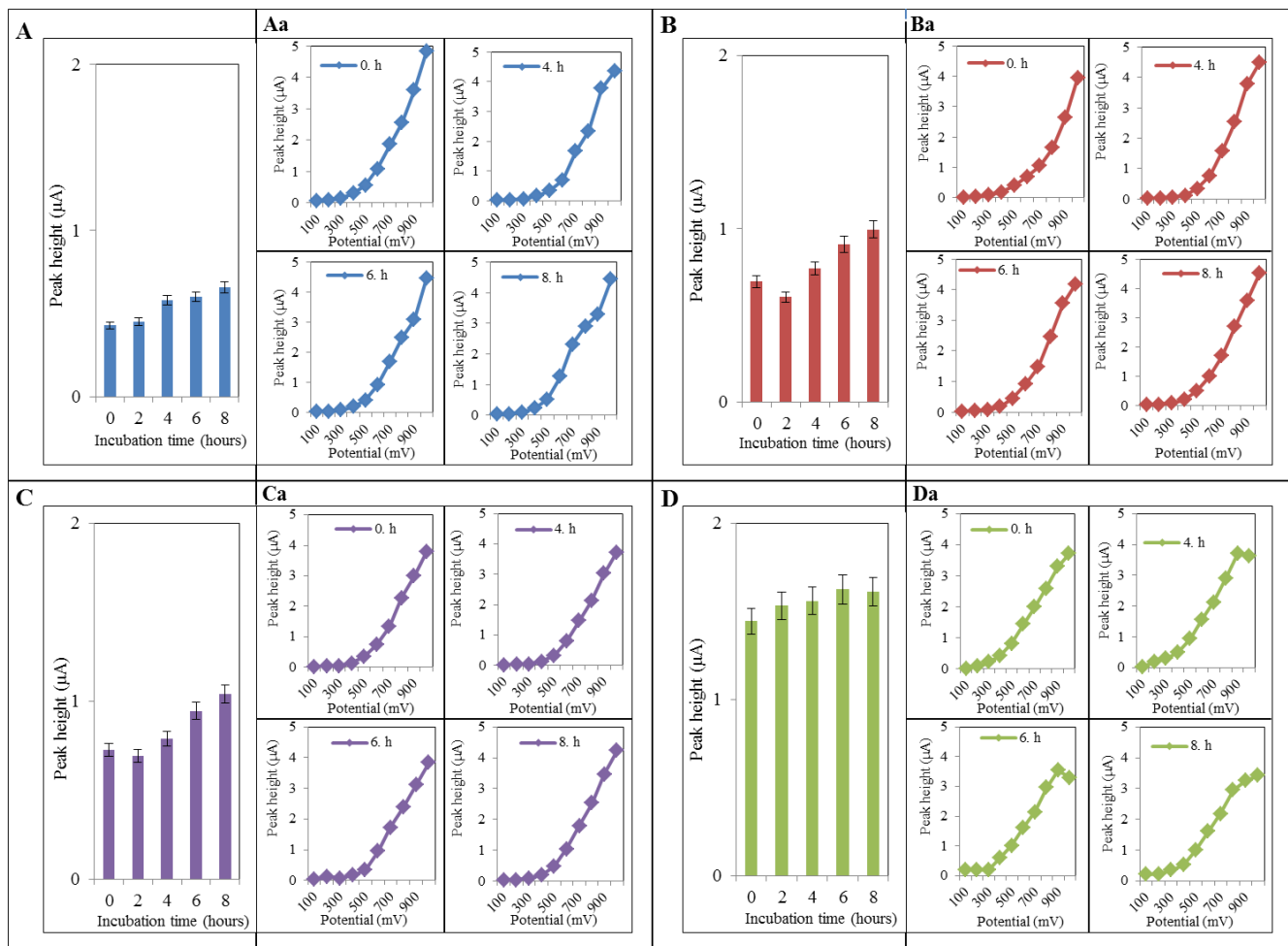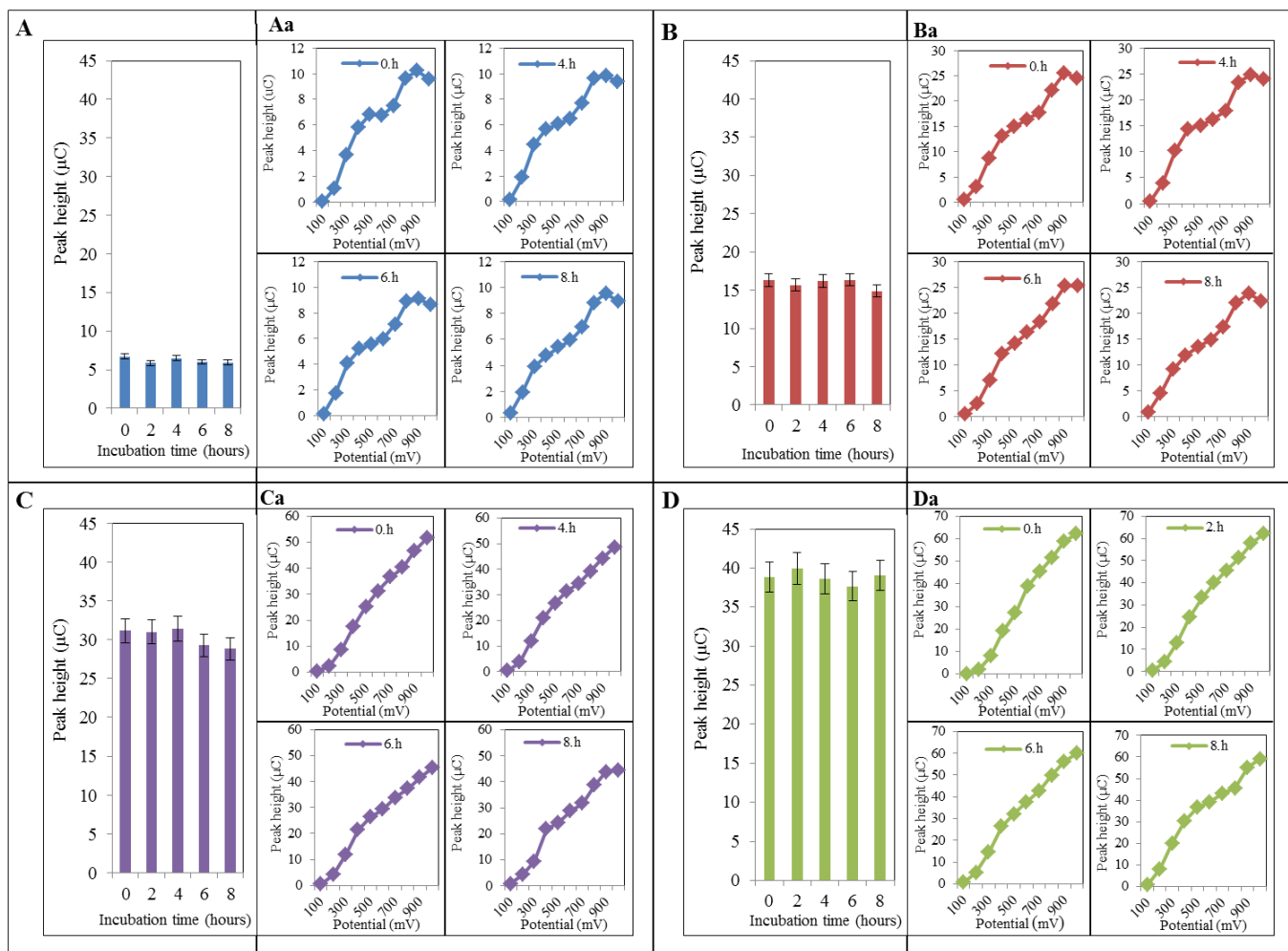

Figure 2. Signal intensities taken from hydrodynamic voltammograms of mixtures of PC2 (100 µg/ml) and CdCl$_2$ (100 µg/ml) under applied potential 600 mV in time of incubation 0, 2, 4, 6 and 8 hours under different temperatures as (**A**) 10 °C, (**B**) 20 °C, (**C**) 30 °C and (**D**) 40 °C. Real HDVs from the analysis for 0, 4, 6 a 8 hours for each tested temperature as (**Aa**) 10 °C, (**Ba**) 20 °C, (**Ca**) 30 °C and (**Da**) 40 °C.

3.3 Electrochemical studying of complexes by CoulArray

As we found the effect of temperature using Coulochem detector we attempted to use different detector for obtaining the HDV confirming the presence of complexes with different applied concentration. Coulometric detection enables to redox change more than 90% passing analyte in comparison with coulochem detection where less than 5% of passing analyte is detected [25]. Therefore Coularray as coulometric detector was used for this purpose. The various applied concentrations of PC2 were 100, 200, 300 and 400 µg/ml mixed with Cd(II) 100 µg/ml. Analysis was carried out under temperature 20° C and for 0, 2, 4, 6 and/or 8 h. Same as in the previous case all variants were analysed for obtaining the HDVs and at 600mV we monitored the change of the intensity of electrochemical signal (Figs. 3A, B, C and D). There is also shown the change of profile of each

HDV in greater details in Figs. 3Aa, Bb, Cc and Dd for 100, 200, 300 and 400 µg/ml. It clearly follows from the results obtained that time did not affect the forming of complex as much as applied concentration. The higher intensity of creation complex is due to applied concentration of 100 µg/ml and no distinct change in HDV trend was observed under higher applied concentrations.


Figure 3. Signal intensities taken from hydrodynamic voltammograms of mixtures of PC2 and $CdCl_2$ (100 µg/ml) under applied potential 600 mV in time of incubation 0, 2, 4, 6 and 8 hours in various concentration of PC2 as (**A**) 100 µg/ml, (**B**) 200 µg/ml, (**C**) 300 µg/ml and (**D**) 400 µg/ml. Real HDVs from the analysis of interactions lasted for 0, 4, 6 and 8 hours for each applied concentrations of PC2 as (**Aa**) 100 µg/ml, (**Ba**) 200 µg/ml, (**Ca**) 300 µg/ml and (**Da**) 400 µg/ml

3.4 Influence of concentration and temperature

We decided to make a graphical expression of the real influence of the time of incubation and applied concentration, which is shown in Fig. 4. For more accurate counting we took an inflection points from the first peak visible in HDV which was appearing near to 500 mV. This approach is in accordance with the method of counting the HDV maxima [25]. Due to counting of inflection points we found that the biggest change is made as creation of disproportion between the peaks in 500 and 900 mV in HDV. In the 900 mV there is maximal response of PC2, which was reported before [26]

and the increasing of signal in lower potentials app. 500 mV was reported to be pointing to the metal-thiol complex formation [24]. Here, this can be considered as the formation of Cd-thiol complex. After making the difference between these two maxima we obtained the figures for temperature influence (Fig. 4A) and for influence of concentration (Fig. 4B). These figures coincidently reported that due to affecting by selected factor (time, concentration) there is observed the change of the ratio which we expressed as the change of slope and we reported it in Fig. 4C, where it is obvious that concentration has bigger effect on the formation of complex than time of incubation. The biggest change is under applied concentration 400 µg/ml and (Fig. 4A) where the slope is the most decreasing which means the decreasing the amount of PC2 and increasing of amount of complex. Other concentrations has slowly decreasing trend in order to applied concentrations from 100 to 300 µg/ml. In the case of the influence of time the difference between 100-300 µg/ml was negligible but 400 µg/ml reported the most decreasing trend after 8 hour of incubation.
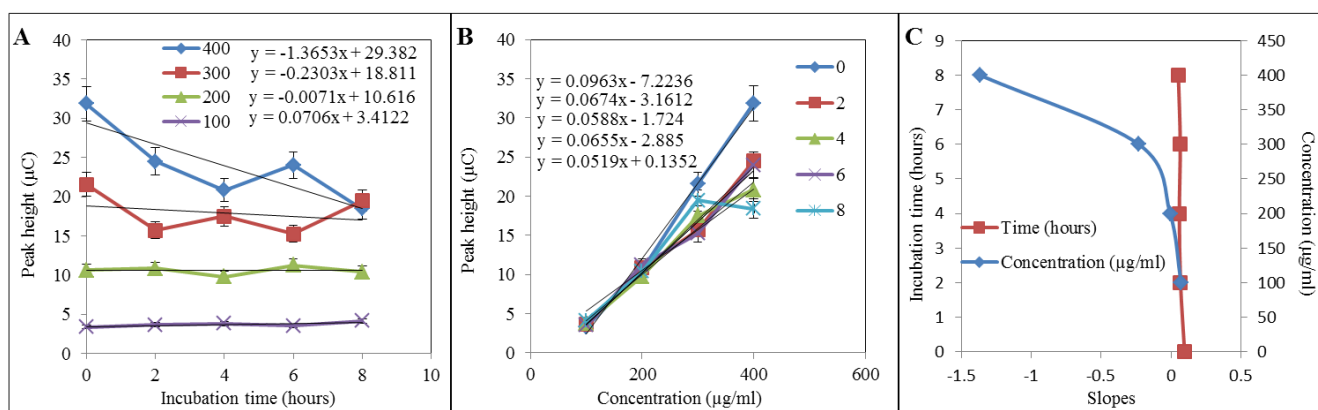
Figure 4. The peak height difference between 500 mV and 900 mV taken from HDV of mixture Cd(II) 100 µg/ml and PC2 in concentration of: 400, 300, 200 a 100 µg/ml with time of interaction 0, 2, 4, 6 a 8 hodin (**A**) Dependence of difference of the peak height on time. (**B**) Slopes from dependence of peak height for each variant of time of incubation. (**C**) Values of the slopes of the peak heights in dependence of the applied concentrations of PC2 and time of interactions

3.5 Study of the optimal conditions for the determination of PC2 and Cd-PC2 complexes in vitro in MALDI-TOF/TOF

We attempted to analyse the same sample mixture, as we used for electrochemical analysis, by mass spectrometer. During optimization we found number of factors as used matrix, on spot sample preparation approach and intensity of laser to be rather influencing of the subsequent MALDI analysis. Our results showed an increase in signal intensity (a.u) as a function of the intensity of the laser (%) in 5, 10 and 15 mg/ml of HCCA (Figs. 5A, B and C). The highest signal intensity (a.u) was obtained by using of concentration of 15 mg/ml HCCA. For the realization of this study, quantification the number of crystals by computer analysis of the matrix pictures was performed and showed that 1 µl of matrix and sample (1:1) had a mean of 3430 ± 80 (SE) crystals. The number of crystals was the highest and more homogeneous under application of 15 mg/ml HCCA than by application of lower concentrations.

Increasing the concentration of PC2 from 3 to 30 pg per crystal, the intensity of signal was increased linearly (y= 179.04 x-247.11; R2=0.9349) when the laser intensity was 28.8 µJ (30%), while the signal increased exponentially (y= 678.77 e0.122x; R2=0.9861) when the laser intensity was 43.3 µJ (50%), under the same concentrations of PC2 (Figs. 5D and E). These results indicated that the optimum conditions for the determination of PC2 by utilizing HCCA as matrix was a laser intensity of 50% (43.3µJ) and the concentration of the matrix more convenient for obtaining an appropriate signal was 15 mg/ml in methanol (70%, *v/v*).
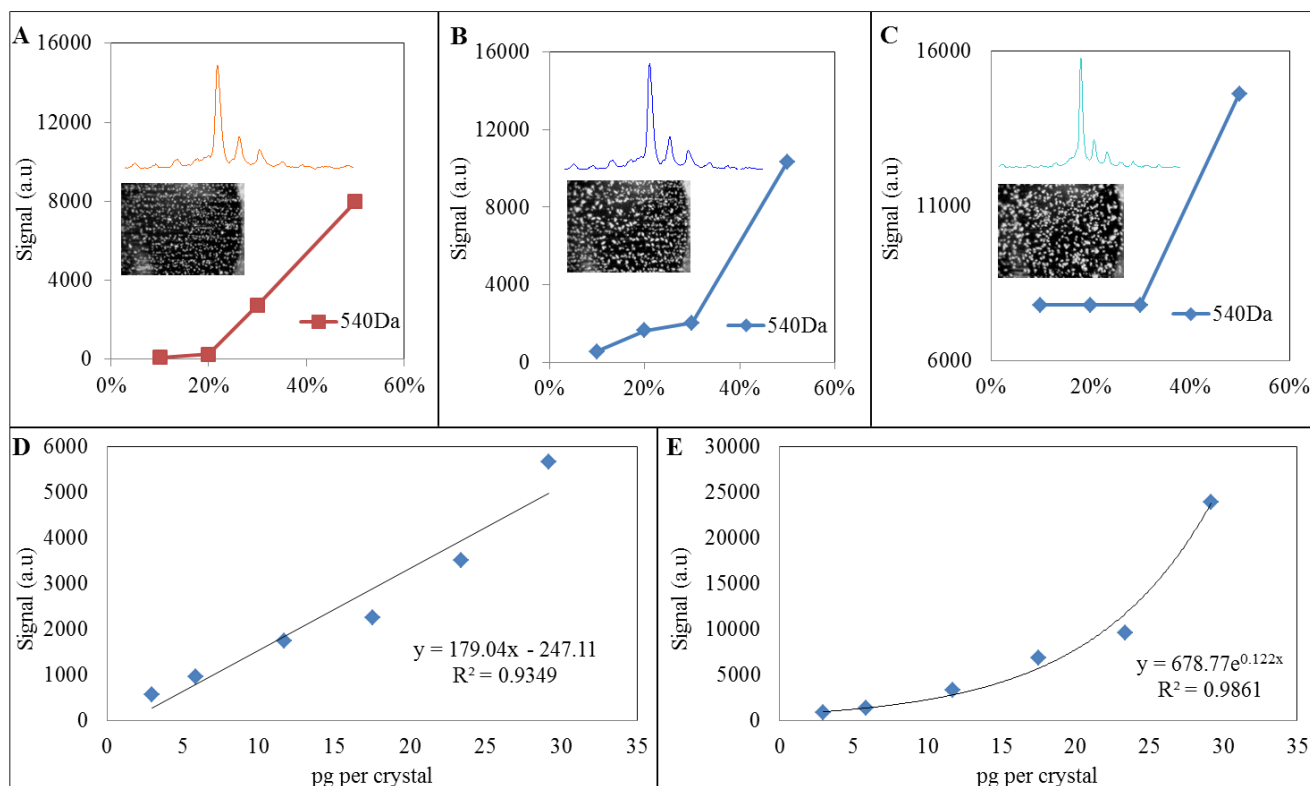
Figure 5. The signal intensity PC2 measured in the presence of different concentrations in cyano-4-hydroxycinnamic acid (HCCA) solution matrix as (**A**) 5, (**B**) 10 and (**C**) 15 mg/ml and different laser powers (%); in inset: spectra of PC2 (540 Da) measured at 50% laser power and the photos of spots in different concentration of HCCA with PC2 (100 ng/µl in TA30). Dependences of signal intensity for PC2 in different concentrations 10, 20, 30, 60, 80 and 100 ng/µl in TA30 measured under (**D**) 30 % and/or (**E**) 50% laser power.

Figure 6 shows the effect of methanol on PC2 when it used as samples solutions. Using of water and 20% methanol resulted in the spectra showed in Figs. 6A and B. The 70% methanol showed the loss of the signal (Fig. 6C), which interferes in the detection of PC2 signal and inhibits the formation of crystals. This result confirms that methanol at high concentrations (70%) cannot be used as the sample solution, but it is possible to use it in lower concentrations (up to 20%), because the intensity was similar to when the sample was water (Figs. 6A and B). However, the methanol 70% can be used in the HCCA because it facilitated the dilution of the matrix and homogeneous crystal formation and accurate for the determination of PC2 in MALDI-TOF. The spotting methods used for MALDI-TOF were dried droplet (DD), thin layer (TL) and double layer (DL). The quantification of

number of crystals in DD, TL and DL showed an average of 3430 ± 80, 4600 ± 200 and 4270 ± 70, respectively. The results showed that the three methods are reproducible for determination of PC2 as in Figs. 7A, B and C. However, DD was showed the highest intensity at the different concentrations of PC2 in both intensities of the laser as 28.8 and 43.3 µJ showed in Figs. 7D and E, respectively. DD spotting method was 64.5% higher than LT and 85 % than DL in 30 pg PC2 per crystal in 43.3 µJ. This method is surprisingly simple and provides good results for many different types of samples. Dried droplets were very stable and can be kept before running a MALDI-TOF experiment.
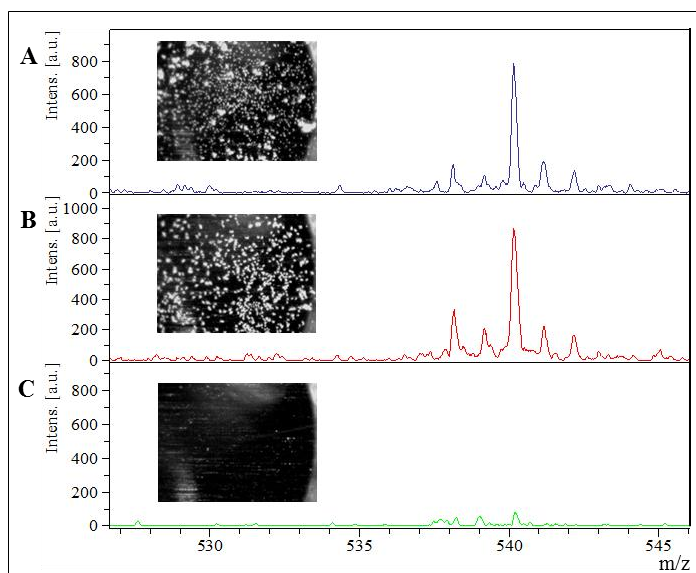
Figure 6. Spectra of 100 ng/µl PC2 in (**A**) water, (**B**) methanol (20%, *v/v*) in TA30 and (**C**) methanol (70%, *v/v*).
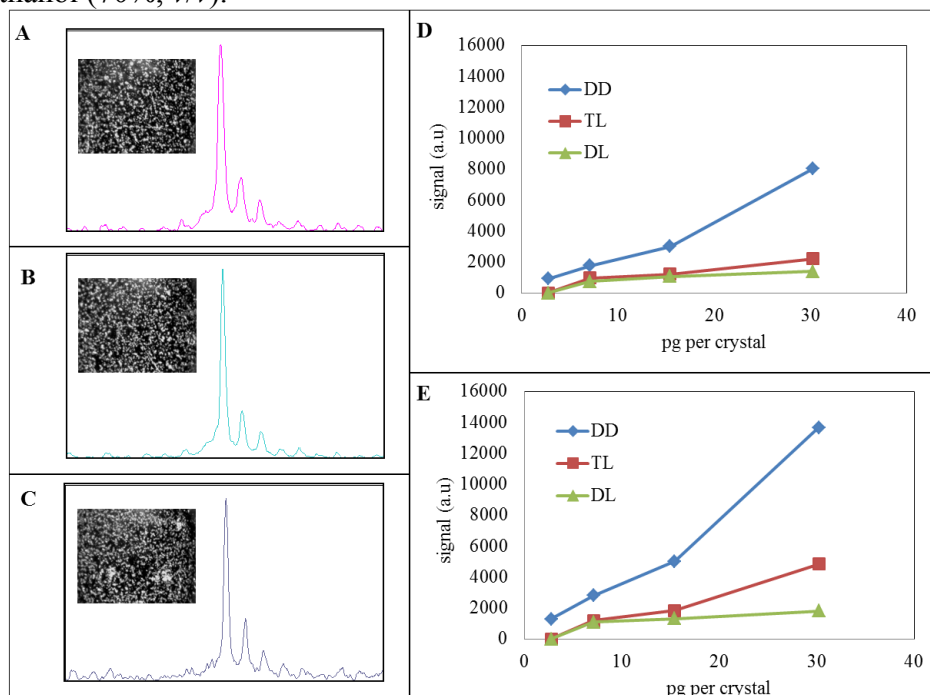

Figure 7. Spectra and crystal photos of different methods preparations (**A**) DD: Drop Dry, (**B**) TL: Thin Layer and (**C**) DL: Double Layer. Dependences of signal intensity of PC2 in different concentrations of PC2 in DD, TL and DL methods under (**D**) 30% and (**E**) 50% laser powers.

3.6 Determination of Cd-PC2 complexes in vitro in MALDI-TOF/TOF

These ideal conditions were used for determination of Cd-PC2 complex and to verify that Cd-PC2 complexes were formed. The main observed signals shown in Figure 8 were assigned as follows: [PC2+ H]+ (m/z 540.2), [M3+H]+ (m/z 568.2) (correspond to matrix cluster trimer) for determination of PC2 (Fig. 8A), while PC2 incubation with Cd(II) (Fig. 8B) showed a new signal corresponding to complexes: [Cd-PC2+ H]+ (m/z 650.1). It is evident that a suggested intramolecular complex, Cd-PC2, was found. The presence of the observed mass of 650.1 Da confirms the abundance of intramolecular complexes.
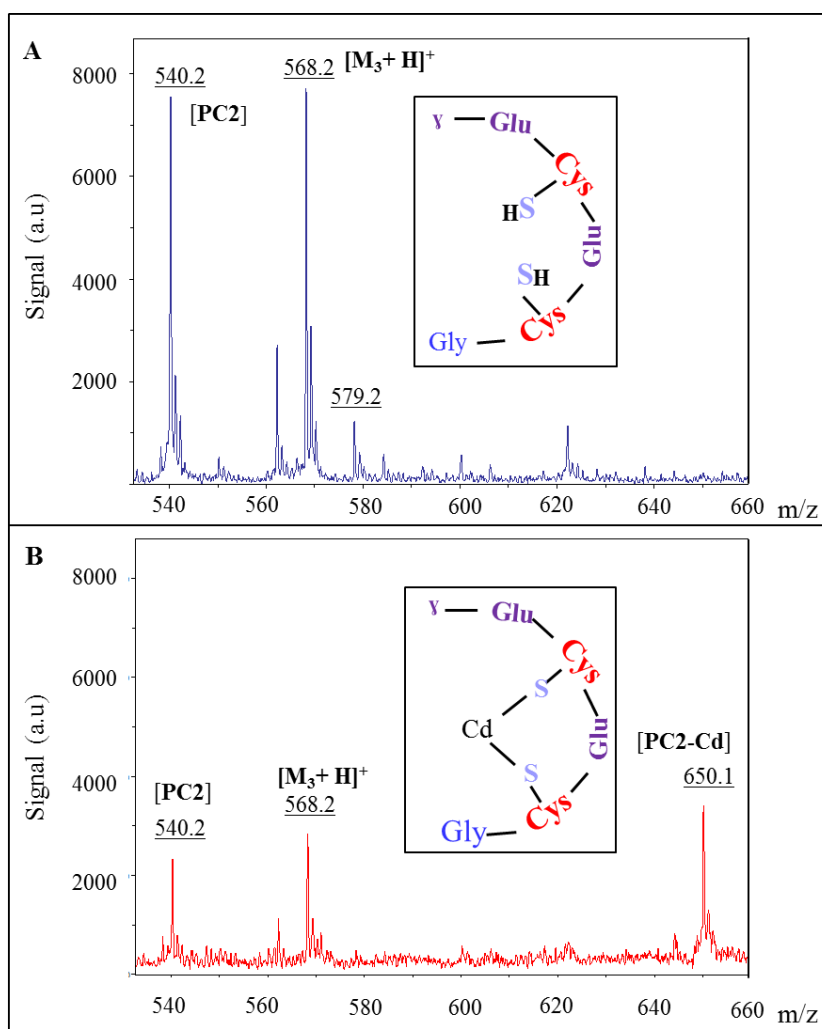
Figure 8. Mass spectra of (**A**) PC2 and (**B**) Cd-PC2 complexes in HCCA matrix by MALDI-TOF.

4. CONCLUSIONS

Studying of complexes among proteins and metals are of great interest for numerous branches. In this study, the obtained data show that the flow injection analysis coupled with electrochemical

detection Coulochem III or/and Coularray in combination with MALDI-TOF is a reliable and fast method for the determination of these complexes.

References

1. T. W. Lane and F. M. M. Morel, *Proc. Natl. Acad. Sci. U. S. A.*, 97 (2000) 4627.
2. J. L. Pan, J. A. Plant, N. Voulvoulis, C. J. Oates and C. Ihlenfeld, *Environ. Geochem. Health*, 32 (2010) 1.
3. G. J. Wagner, *Adv. Agron.*, 51 (1993) 173.
4. C. S. Cobbett, *Plant Physiol.*, 123 (2000) 825.
5. B. Semane, A. Cuypers, K. Smeets, F. Van Belleghem, N. Horemans, H. Schat and J. Vangronsveld, *Physiol. Plant.*, 129 (2007) 519.
6. B. M. Shanmugaraj, H. M. Chandra, B. Srinivasan and S. Ramalingam, *Int. J. Phytoremediat.*, 15 (2013) 206.
7. E. Grill, S. Loffler, E. L. Winnacker and M. H. Zenk, *Proc. Natl. Acad. Sci. U. S. A.*, 86 (1989) 6838.
8. R. Pal and J. P. N. Rai, *Appl. Biochem. Biotechnol.*, 160 (2010) 945.
9. W. E. Rauser, *Plant Physiol.*, 109 (1995) 1141.
10. M. H. Zenk, *Gene*, 179 (1996) 21.
11. D. Potesil, J. Petrlova, V. Adam, J. Vacek, B. Klejdus, J. Zehnalek, L. Trnkova, L. Havel and R. Kizek, *J. Chromatogr. A*, 1084 (2005) 134.
12. P. Babula, V. Adam, R. Opatrilova, J. Zehnalek, L. Havel and R. Kizek, *Environ. Chem. Lett.*, 6 (2008) 189.
13. V. Adam, I. Fabrik, V. Kohoutkova, P. Babula, J. Hubalek, R. Vrba, L. Trnkova and R. Kizek, *Int. J. Electrochem. Sci.*, 5 (2010) 429.
14. V. Supalkova, D. Huska, V. Diopan, P. Hanustiak, O. Zitka, K. Stejskal, J. Baloun, J. Pikula, L. Havel, J. Zehnalek, V. Adam, L. Trnkova, M. Beklova and R. Kizek, *Sensors*, 7 (2007) 932.
15. D. Huska, O. Zitka, O. Krystofova, V. Adam, P. Babula, J. Zehnalek, K. Bartusek, M. Beklova, L. Havel and R. Kizek, *Int. J. Electrochem. Sci.*, 5 (2010) 1535.
16. A. Kleckerova, P. Sobrova, O. Krystofova, J. Sochor, O. Zitka, P. Babula, V. Adam, H. Docekalova and R. Kizek, *Int. J. Electrochem. Sci.*, 6 (2011) 6011.
17. E. Grill, E. L. Winnacker and M. H. Zenk, *Method Enzymol.*, 205 (1991) 333.
18. S. Doring, S. Korhammer, M. Oetken and B. Markert, *Fresenius J. Anal. Chem.*, 366 (2000) 316.
19. L. Q. Chen, Y. F. Guo, L. M. Yang and Q. Q. Wang, *J. Anal. At. Spectrom.*, 22 (2007) 1403.
20. T. Y. Yen, J. A. Villa and J. G. DeWitt, *J. Mass Spectrom.*, 34 (1999) 930.
21. E. Bramanti, D. Toncelli, E. Morelli, L. Lampugnani, R. Zamboni, K. E. Miller, J. Zemetra and A. D'Ulivo, *J. Chromatogr. A*, 1133 (2006) 195.
22. I. Leopold, D. Gunther, J. Schmidt and D. Neumann, *Phytochemistry*, 50 (1999) 1323.
23. B. B. M. Sadi, A. P. Vonderheide, J. M. Gong, J. I. Schroeder, J. R. Shann and J. A. Caruso, *J. Chromatogr. B*, 861 (2008) 123.
24. O. Zitka, M. A. Merlos, V. Adam, N. Ferrol, M. Pohanka, J. Hubalek, J. Zehnalek, L. Trnkova and R. Kizek, *J. Hazard. Mater.*, 203 (2012) 257.
25. J. Sochor, J. Dobes, O. Krystofova, B. R. Nedecky, P. Babula, M. Pohanka, T. Jurikova, O. Zitka, V. Adam, B. Klejdus and R. Kizek, *Int. J. Electrochem. Sci.*, 7 (2013) 5429.

26. O. Zitka, H. Skutkova, O. Krystofova, P. Sobrova, V. Adam, J. Zehnalek, L. Havel, M. Beklova, J. Hubalek, I. Provaznik and R. Kizek, *Int. J. Electrochem. Sci.*, 6 (2011) 1367.

5.1.2. Reseach article II

MIGUEL ANGEL MERLOS RODRIGO, NATALIA CERNEI, MARKETA KOMINKOVA, ONDREJ ZITKA, MIROSLAVA BEKLOVA, JOSEF ZEHNALEK, RENE KIZEK AND VOJTECH ADAM. Ion Exchange Chromatography and Mass Spectrometric Methods for Analysis of Cadmium-Phytochelatin (II) Complexes. *Int. J. Environ. Res. Public Health* 2013, 10, 1304-1311; doi:10.3390/ijerph10041304.

Participation in the work of the author Miguel Angel Merlos Rodrigo: experimental part 60% and manuscript preparation 70%.

Cd is an extremely toxic metal commonly found in industrial workplaces. Plants respond to Cd toxicity in a variety of different ways. Such responses include immobilization, exclusion, chelation and compartmentalization of the metal ions, and the expression of more general stress response mechanisms such as ethylene and stress proteins. Higher plants, algae, certain yeasts and animals respond to heavy metals by synthesizing phytochelatins (PCs) and related cysteine-rich polypeptides. Phytochelatin synthases are γ-glutamylcysteine (γ-Glu-Cys) dipeptidyl transpeptidases that catalyze the synthesis of heavy metal-binding PCs. IEC is fast and effective method for PC and PC Metal-complexes determinations. MALDI-TOF MS technique has advanced from various years in investigations. Moreover, MALDI-TOF MS has become a popular and versatile method to analyze peptides, protein, nucleotide acid and glycans.

In the present work, Cd-PC2 complexes synthesized *in vitro* were studied using MALDI-TOF MS and IEC. Sample composition and the best conditions of analysis methods conditions to analyze of Cd complexes were optimized.

The optimum conditions for the detection of *in vitro* prepared intermolecular Cd-PC2 complex were reached for IEC as well as for MALDI. These two methods have been demonstrated to be ideal and promising techniques for screening and characterizing in vitro synthesized Cd-PC2 complexes. It has been demonstrated that both techniques have an ability to identify the formation of Cd-PC2 complex.

Article

Ion Exchange Chromatography and Mass Spectrometric Methods for Analysis of Cadmium-Phytochelatin (II) Complexes

Miguel Angel Merlos Rodrigo [1,2], Natalia Cernei [2], Marketa Kominkova [3], Ondrej Zitka [1,2,3], Miroslava Beklova [2,3], Josef Zehnalek [1,2], Rene Kizek [1,2,4] and Vojtech Adam [1,2,]*

[1] Department of Chemistry and Biochemistry, Faculty of Agronomy, Mendel University in Brno, Zemedelska 1, CZ-613 00 Brno, Czech Republic;
E-Mails: miguelangel.merlos@eez.csic.es (M.A.M.R.); zitkao@seznam.cz (O.Z.);
zehnalek@mendelu.cz (J.Z.); kizek@sci.muni.cz (R.K.)

[2] Central European Institute of Technology, Brno University of Technology, Technicka 3058/10, CZ-616 00 Brno, Czech Republic; E-Mails: cernei.natalia3@gmail.com (N.C.);
beklovam@vfu.cz (M.B.)

[3] Department of Veterinary Ecology and Environmental Protection, Faculty of Veterinary Hygiene and Ecology, University of Veterinary and Pharmaceutical Sciences, Palackeho 1-3, CZ-612 42 Brno, Czech Republic; E-Mail: kominkova.marketa@gmail.com

[4] Lead and Cadmium Initiatives, United Nations Environment Program, Faculty of Agronomy, Mendel University in Brno, Zemedelska 1, CZ-613 00 Brno, Czech Republic

* Author to whom correspondence should be addressed; E-Mail: vojtech.adam@mendelu.cz;
Tel.: +420-5-4513-3350; Fax: +420-5-4521-2044.

Abstract: In this study, *in vitro* formed Cd-phytochelatin (PC2) complexes were characterized using ion exchange chromatography (IEC) and matrix-assisted laser desorption/ionization time-of-flight (MALDI-TOF) mass spectrometry. The ratio of both studied compounds as well as experimental conditions were optimized. The highest yield of the complex was observed under an applied concentration of 100 $\mu g \cdot mL^{-1}$ PC2 and 100 $\mu g \cdot mL^{-1}$ of $CdCl_2$. The data obtained show that IEC in combination with MALDI-TOF is a reliable and fast method for the determination of these complexes.

1. Introduction

Cadmium still presents a threat to the environment. This metal can be accumulated by plants, resulting in damage to important cellular biochemical pathways. Therefore, plants, algae and fungi use intracellular metal-binding peptides, known as phytochelatins (PCs), for maintaining metal homeostasis and for detoxification of the accumulated cadmium(II) ions [1]. PCs are enzymatically synthesized peptides produced rich in the -SH group and having the structure of (γ-Glu-Cys)n-Gly, where n varies from two to five [1–3]. The role of PCs in metal detoxification results from immobilization of metals and, thus, preventing non-specific binding to important biomolecules, followed by the transport of the metal-PC complexes into the vacuole, or its excretion [4–10]. It is therefore of interest to attempt to characterize Cd-PC complexes.

Several analytical methods have been used to analyze PC and complexes of metal [11–16]. In *Nicotiana tabacum* grown under different doses of cadmium(II) ions, PC2 content was determined by using high performance liquid chromatography (HPLC) with electrochemical detection [17]. Other authors used a mass spectrometer coupled with HPLC to study GSH complexes [18] or stationary electrochemistry voltammetric analysis with subsequently ESI-MS for confirmation of PC2 with Cu^{2+}, Cd^{2+} and Pb^{2+} complexes [19]. An approach based on size-exclusion chromatography with off-line detection of phytochelatins, by reverse phase HPLC, and metal ions, by atomic absorption spectrometry, was used for studying the formation of Cd and PC complexes [20]. Size exclusion chromatography of the tissue extracts from seedlings exposed to 100 µM Cd revealed the presence of Cd-PC complexes in flax cultivars [21]. Raab *et al.* developed a method for separation (PCs)-metal(loid) complexes by HPLC system using parallel metal(loid)-specific (inductively coupled plasma-mass spectrometry) and organic-specific (electrospray ionization-mass spectrometry) detection approaches and used it to identify the nature of arsenic (As)-PC complexes in plant extracts [22]. Ion-exchange chromatography (IEC) coupled with colorimetric detection using post-column derivatization with ninhydrin is usually used for determination of free amino acids and other amino acids like compounds in biological samples [23]. IEC is a fast and effective method for PC and PC metal-complexes determination [24].

In this study, Cd-PC2 complexes synthesized *in vitro* were analyzed using IEC and mass spectrometry using a matrix-assisted laser desorption/ionization time-of-flight (MALDI-TOF) mass spectrometer. The ratio of both studied compounds as well as the experimental conditions were optimized.

2. Experimental Section

2.1. Chemicals

Phytochelatin2 (γ-Glu-Cys)$_2$ (PC2) was synthesized in Clonestar (Brno, Czech Republic) with a purity higher than 90 %. $CdCl_2$ and other chemicals used in this study were ACS grade and purchased

from Sigma Aldrich (St. Louis, MA, USA) unless noted otherwise. Standard solutions of PC2 and CdCl$_2$ were prepared daily by dilution of the stock solutions with ACS water. All buffers were prepared in ultrapure water (Mili-Q) obtained using reverse osmosis equipment Aqual 25 (Aqua Osmotic, Tišnov, Czech Republic) with further purification by using apparatus MiliQ Direct QUV equipped with the UV lamp (Millipore Corp., Billerica, USA). The resistance was 18 MΩ. The pH was measured using a WTW inoLab (Weilheim, Germany) pH meter. For preparation of the complex of PC2 with CdCl$_2$ we used the following chemicals: PC2 (300 μg·mL^{-1}), CdCl$_2$ (300 μg·mL^{-1}) and serine (300 μg·mL^{-1}) (internal standard was added before analysis only for determination using IEC). Concentration of the working solution of CdCl$_2$ was used within the range from 3 to 100 μg·mL^{-1}. Complexes were mixed using vortex BioVortex V1 (Biosan, Riga, Latvia) for 1 min, further, the complexes were interacted for 1 h at room temperature.

2.2. Ion Exchange Chromatography

For determination of PC2 an ion-exchange liquid chromatograph (Model AAA-400, Ingos, Prague, Czech Republic) with post column derivatisation with ninhydrin and VIS detector was used. A glass column with inner diameter of 3.7 mm and 350 mm in length was filled manually with a strong cation exchange resin in sodium cycle LG ANB (Ingos) with approximately 12 μm particles and 8% porosity. The column was tempered within the range 40–70 °C. A double channel VIS detector with 5 μL cell was set to detection wavelengths 440 nm and 570 nm. A solution of ninhydrin (Ingos) was prepared with 75 % (*v/v*) methylcelosolve (Ingos) and with 2% (*v/v*) 4 M acetic buffer (pH 5.5). Tin chloride (SnCl$_2$) was used as a reducing agent. The prepared solution of ninhydrin was stored under an inert atmosphere (N$_2$) in dark at 4 °C. The eluting mobile phase was containing 11.11 g of citric acid, 4.04 g of sodium citrate, 9.25 g of NaCl, 0.1 g of sodium azide, 2.5 ml of thiodiglycol per liter of solution and pH was 2.7. The flow rate of mobile phase was 0.25 mL·min^{-1} and flow rate of ninhydrin was tested within the range from 0.1 to 0.35 mL·min^{-1}. The reactor temperature was optimized within the range from 90 to 130 °C. The volume of injection of the sample was 100 μL.

2.3. Matrix-Assisted Laser Desorption/Ionization Time-of-Flight Mass Spectrometry

The mass spectrometry experiments were performed on a MALDI-TOF/TOF mass spectrometer Bruker Ultraflextreme (Bruker GmbH, Bremen, Germany) equipped with a laser (Bruker GmbH, Bremen, Germany) operating at wavelength of 355 nm with an accelerating voltage of 25 kV, cooled with nitrogen and a maximum energy of 43.2 μJ with repetition rate 2,000 Hz in linear and positive mode, and with software for data acquisition and processing of mass spectra flexControl version 3.4 and flexAnalysis version 2.2. The matrix used in the MALDI method was α-cyano-4-hydroxycinnamic acid (CCA) supplied by Bruker. The matrix was prepared in 70% methanol. Mixture was thoroughly vortexed and ultrasonicated using Bandelin 152 Sonorex Digital 10P ultrasonic bath (Bandelin, Berlin Germany) for 2 min at room temperature. The samples of the complexes were prepared with TA30 (30% acetonitrile, 0.1% trifluoroacetic acid solution). The solutions for analysis were mixed in ratio of 1:1 (matrix/substance). After obtaining a homogeneous solution, 1 μL was applied on the target and dried under atmospheric pressure and room temperature. A mixture of peptide calibrations standard

(Bruker) was used for calibration the instrument. The MS spectra were typically acquired by averaging 20 sub spectra from a total of 500 shots of the laser (Smartbeam 2, Version: 1_0_38.5).

3. Results and Discussion

3.1. Optimization of IEC for Cd-PC Complex Determination

Post-column derivatization used in IEC systems is based on the reaction of ninhydrin (2,2-dihydroxy-1,3-indandione) with nitrogen from an amino acid. Nitrogen from the amino moiety is oxidized under slightly acidic conditions maintained by acetate buffer (pH 4.3), under reduction conditions (maintained by $SnCl_2$), and higher temperatures maintained by flow reactor (90–130 °C) resulting in the stable product called as Ruhemann's red, which is well detectable in visible spectra under 570 nm. It principally works for all amines (peptides, biogenic amines even for ammonium ions). Therefore we used this method for detection of PC2 peptide in our IEC study. In our previously published paper [25], we found that the reactor temperature, column temperature and ninhydrin flow ratio belong to the most analysis influencing factors. In comparison to our previous paper we found the different effects of these factors on the sensitivity of detection, which are caused by various analytes. In the case of reactor temperature, which was tested within the range from 90 to 130 °C, we found that maximum peak area was increasing due to applied temperature almost linearly up to the limit of reactor as 130 °C (Figure 1(a)). This trend was different from this one we found in the study with taurine, where the maximum was found to be 110 °C [25], and then yield of derivatisation reaction was almost stable up to the 130 °C. This difference might by caused by higher efficiency of disintegration of peptide bonds, which are not so willing to react with ninhydrin as free amino groups under lower temperatures. Temperature of column, which was tested ranging from 40 to 70 °C, influences the detection based on the temperature initiation before post column mixing. It is obvious that it positively affected the detection with linear increasing trend (Figure 1(b)).

Figure 1. (**a**) Influence of reactor temperature, (**b**) column temperature and (**c**) ninhydrin flow rate on height of PC2 (50 µg ·mL^{-1}) peak. The peptide was measured by IEC.
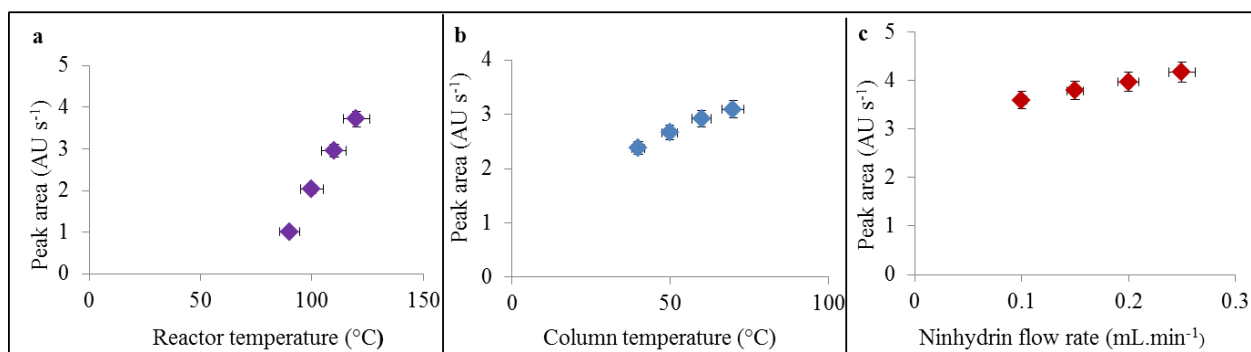

Ninhydrin flow as the last tested parameter exhibits the slightly linear increasing trend in detection efficacy within the tested range from 0.1 to 0.3 mL·min^{-1} with the upper mentioned value as the maximum (Figure 1(c)). The optimal conditions (reactor temperature 130 °C, column temperature 70 °C, ninhydrin flow rate 0.3 mL·min^{-1}) were used for analysis of Cd-PC complexes. Primarily, we

determined calibration curve of the PC2 under the optimal conditions. Calibration curve was determined as the dependence of the peak area on the concentration of PC2 (inset in Figure 2) and exhibited good linearity (R^2 = 0.9946) and R.S.D 1.8% (n = 6). Retention time of determined PC2 was 6.22 ± 0.30 min (Figure 2).

Figure 2. Calibration curve of PC2 in IEC: (a) 100, (b) 50, (c) 25, (d) 12.25, (e) 6 and (f) 3 μg·mL^{-1} PC2 in H2O. The experimental conditions were as follows: reactor temperature 130 °C, column temperature 70 °C, ninhydrin flow rate 0.3 mL·min^{-1}.
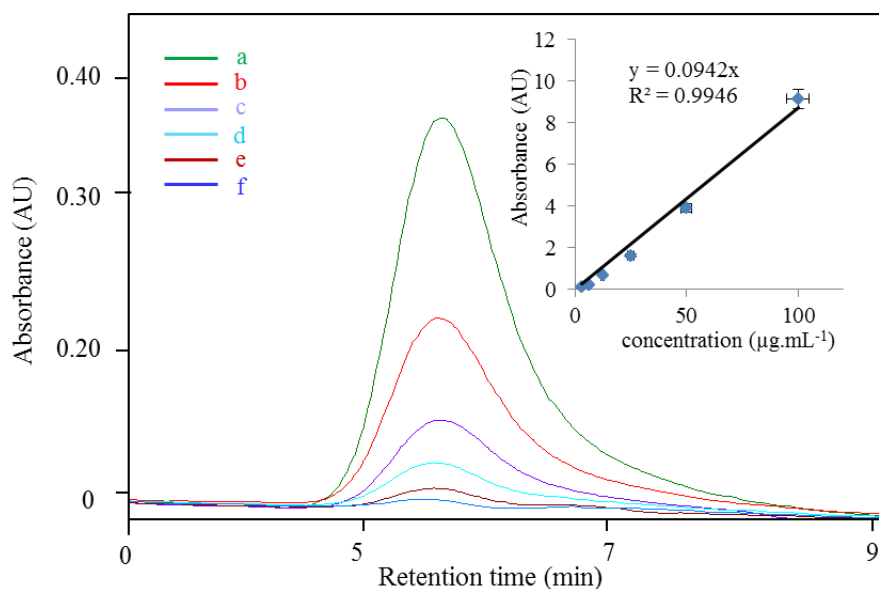
### 3.2. Study of Cd-PC2 Complexes by IEC and MALDI-TOF

To understand the nature of the possible Cd-PC complexes in Cd-stressed biological samples it is important to determine the formation of these complexes *in vitro*. Our hypothesis of the formation of Cd-PC2 is the binding of Cd to sulfhydryl groups of the two cysteine molecules that are a part of the PC2 with the loss of two hydrogen protons. Thus, we suggested that an intermolecular complex can be formed only as it is shown in Figure 3. Therefore we prepared and analyzed different complex mixtures with constant concentration of PC2 100 μg·mL^{-1} with addition of Cd^{2+} (in the form of CdCl$_2$) in concentration of 0, 5, 10, 25, 50 and 100 μg·mL^{-1} using of optimized IEC method. We observed none effect on the retention tine of the peak of PC2. Surprisingly we observed the nonlinear decreasing of the peak area. The decrease of the signal of PC2 in the presence of CdCl$_2$ was probably due to complexes formation accompanied with the increasing yield of suggested complex as it is shown in Figure 4(a). This was probably caused by inhibition of derivatisation reaction of peptide, which has been complexed with Cd(II) ions. No decreasing effect was observed on peak of internal standard of serine. The signal of PC2 decreased with the increasing concentration of CdCl$_2$ in the solution, showing the highest decrease in 100 μg·mL^{-1} CdCl$_2$ (28%). It is evident that CdCl$_2$ induced Cd-PC2 complexes formation. The increase of yield of Cd-PC2 complexes were suggested as a function of the CdCl$_2$ content of the solution, being highest in concentration 100 μg·mL^{-1} (97%).

Figure 3. Model of complex between cadmium Cd(II) ion and one molecules of PC2. Cys (cysteine), Glu (glutamic acid), Gly (glycine) and S (sulfur).
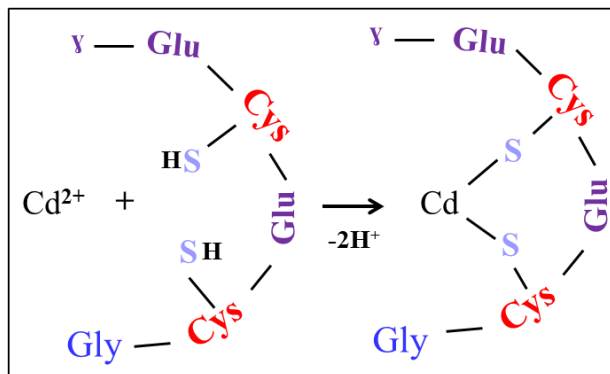
To verify that Cd-PC2 complexes were formed, we analyzed it by MALDI-TOF. The main observed signals shown in Figure 4(b) were assigned as follows: $[PC2 + H]^+$ (*m/z* 540.2), $[M_3 + H]^+$ (*m/z* 568.2) (correspond to matrix cluster trimer) and $[Cd-PC2 + H]^+$ (*m/z* 650.1). It is evident that a suggested intramolecular complex, Cd-PC2, was found, as it shown in Figure 4(b) (red line). The presence of observed mass of 650.1 Da confirms the abundance of intramolecular complexes according to scheme shown in Figure 3.

Figure 4. (**a**) Diagram of change in the signal of PC2 (%) and yield of Cd-PC2 complex (%) as function of CdCl₂ concentrations determined by IEC. (**b**) Mass spectra of PC2 (blue line) and Cd-PC2 complexes (red line) in CCA matrix measured by MALDI-TOF.
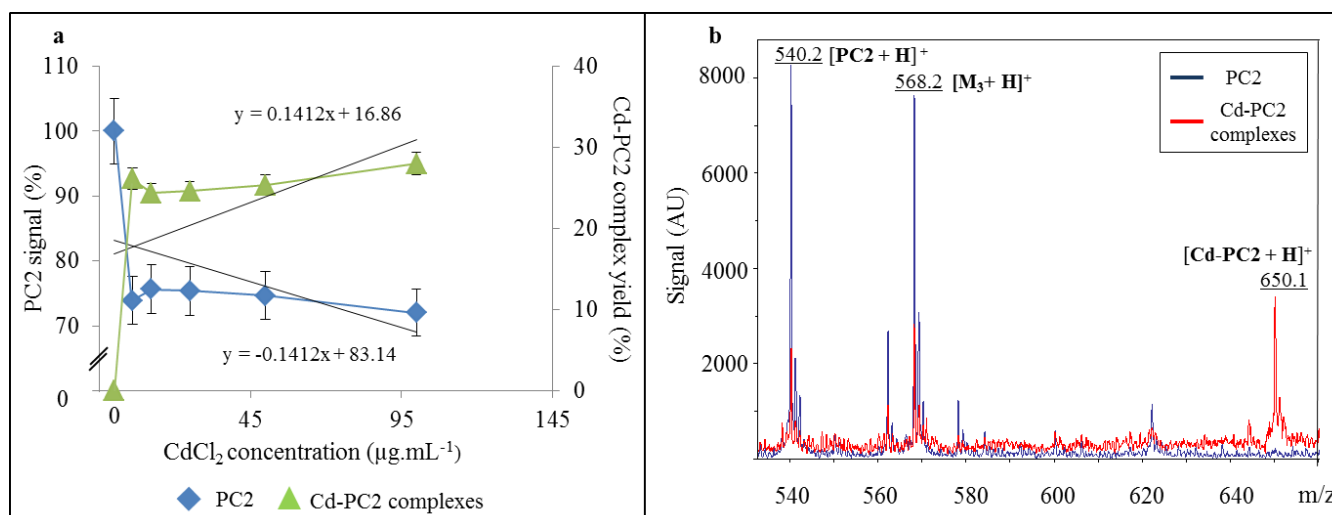
4. Conclusions

The optimum conditions for detection of intermolecular Cd-PC2 complexes prepared *in vitro* were determined for ion exchange chromatography as well as for matrix-assisted laser desorption/ ionization-time of flight mass spectroscopy These two methods have been demonstrated to be ideal and promising techniques for screening and characterizing *in vitro* peptide-metal complexes. It was demonstrated that both techniques had the ability to identify the formation of Cd-PC2 complex.

Acknowledgements

References

1. Rauser, W.E. Phytochelatins and related peptides—Structure, biosynthesis, and function. *Plant Physiol.* **1995**, *109*, 1141–1149.
2. Cobbett, C.S. Phytochelatins and their roles in heavy metal detoxification. *Plant Physiol.* **2000**, *123*, 825–832.
3. Hall, J.L. Cellular mechanisms for heavy metal detoxification and tolerance. *J. Exp. Bot.* **2002**, *53*, 1–11.
4. Cruz, B.H.; Diaz-Cruz, J.M.; Sestakova, I.; Velek, J.; Arino, C.; Esteban, M. Differential pulse voltammetric study of the complexation of Cd(II) by the phytochelatin (gamma-Glu-Cys)(2)Gly assisted by multivariate curve resolution. *J. Electroanal. Chem.* **2002**, *520*, 111–118.
5. Gekeler, W.; Grill, E.; Winnacker, E.L.; Zenk, M.H. Algae sequester heavy-metals via synthesis of phytochelatin complexes. *Arch. Microbiol.* **1988**, *150*, 197–202.
6. Grill, E.; Loffler, S.; Winnacker, E.L.; Zenk, M.H. Phytochelatins, the heavy-metal-binding peptides of plants, are synthesized from glutathione by a specific gamma-glutamylcysteine dipeptidyl transpeptidase (phytochelatin synthase). *Proc. Natl. Acad. Sci. USA* **1989**, *86*, 6838–6842.
7. Leopold, I.; Gunter, D.; Neumann, D. Application of high performance liquid chromatography—Inductively coupled plasma mass spectrometry to the investigation of phytochelatin complexes and their role in heavy metal detoxification in plants. *Analusis* **1998**, *26*, M28–M32.
8. Krystofova, O.; Adam, V.; Babula, P.; Zehnalek, J.; Beklova, M.; Havel, L.; Kizek, R. Effects of various doses of selenite on stinging nettle *(Urtica dioica* L.). *Int. J. Environ. Res. Public Health* **2010**, *7*, 3804–3815.
9. Skladanka, J.; Adam, V.; Zitka, O.; Krystofova, O.; Beklova, M.; Kizek, R.; Havlicek, Z.; Slama, P.; Nawrath, A. Investigation into the effect of molds in grasses on their content of low molecular mass thiols. *Int. J. Environ. Res. Public Health* **2012**, *9*, 3789–3805.
10. Miller, G.; Begonia, G.; Begonia, M.F.T. Selected morphological characteristics, lead uptake and phytochelatin synthesis by coffeeweed (*Sesbania exaltata* Raf.) grown in elevated levels of lead-contaminated soil. *Int. J. Environ. Res. Public Health* **2011**, *8*, 2401–2417.
11. Potesil, D.; Petrlova, J.; Adam, V.; Vacek, J.; Klejdus, B.; Zehnalek, J.; Trnkova, L.; Havel, L.; Kizek, R. Simultaneous femtomole determination of cysteine, reduced and oxidized glutathione, and phytochelatin in maize (*Zea mays* L.) kernels using high-performance liquid chromatography with electrochemical detection. *J. Chromatogr. A* **2005**, *1084*, 134–144.
12. Petrlova, J.; Mikelova, R.; Stejskal, K.; Kleckerova, A.; Zitka, O.; Petrek, J.; Havel, L.; Zehnalek, J.; Adam, V.; Trnkova, L.; *et al.* Simultaneous determination of eight biologically active thiol compounds using gradient elution-Liquid Chromatography with Coul-Array detection. *J. Sep. Sci.* **2006**, *29*, 1166–1173.

13. Diopan, V.; Stejskal, K.; Galiova, M.; Adam, V.; Kaiser, J.; Horna, A.; Novotny, K.; Liska, M.; Havel, L.; Zehnalek, J.; *et al.* Determination of plant thiols by liquid chromatography coupled with coulometric and amperometric detection in lettuce treated by lead(II) ions. *Electroanalysis* **2010**, *22*, 1248–1259.

14. Zitka, O.; Krystofova, O.; Sobrova, P.; Adam, V.; Zehnalek, J.; Beklova, M.; Kizek, R. Phytochelatin synthase activity as a marker of metal pollution. *J. Hazard. Mater.* **2011**, *192*, 794–800.

15. Zitka, O.; Merlos, M.A.; Adam, V.; Ferrol, N.; Pohanka, M.; Hubalek, J.; Zehnalek, J.; Trnkova, L.; Kizek, R. Electrochemistry of copper(II) induced complexes in mycorrhizal maize plant tissues. *J. Hazard. Mater.* **2012**, *203*, 257–263.

16. Supalkova, V.; Huska, D.; Diopan, V.; Hanustiak, P.; Zitka, O.; Stejskal, K.; Baloun, J.; Pikula, J.; Havel, L.; Zehnalek, J.; *et al.* Electroanalysis of plant thiols. *Sensors* **2007**, *7*, 932–959.

17. Zitka, O.; Skutkova, H.; Krystofova, O.; Sobrova, P.; Adam, V.; Zehnalek, J.; Havel, L.; Beklova, M.; Hubalek, J.; Provaznik, I.; *et al.* Rapid and ultrasensitive method for determination of phytochelatin(2) using high performance liquid chromatography with electrochemical detection. *Int. J. Electrochem. Sci.* **2011**, *6*, 1367–1381.

18. Jaeckel, P.; Krauss, G.; Menge, S.; Schierhorn, A.; Rucknagel, P.; Krauss, G.J. Cadmium induces a novel metallothionein and phytochelatin 2 in an aquatic fungus. *Biochem. Biophys. Res. Commun.* **2005**, *333*, 150–155.

19. Cavanillas, S.; Gusmao, R.; Arino, C.; Diaz-Cruz, J.M.; Esteban, M. Voltammetric analysis of phytochelatin complexation in ternary metal mixtures supported by multivariate analysis and ESI-MS. *Electroanalysis* **2012**, *24*, 309–315.

20. Chen, L.Q.; Guo, Y.F.; Yang, L.M.; Wang, Q.Q. SEC-ICP-MS and ESI-MS/MS for analyzing *in vitro* and *in vivo* Cd-phytochelatin complexes in a Cd-hyperaccumulator *Brassica chinensis*. *J. Anal. At. Spectrom.* **2007**, *22*, 1403–1408.

21. Najmanova, J.; Neumannova, E.; Leonhardt, T.; Zitka, O.; Kizek, R.; Macek, T.; Mackova, M.; Kotrba, P. Cadmium-induced production of phytochelatins and speciation of intracellular cadmium in organs of *Linum usitatissimum* seedlings. *Ind. Crop. Prod.* **2012**, *36*, 536–542.

22. Raab, A.; Feldmann, J.; Meharg, A.A. The nature of arsenic-phytochelatin complexes in *Holcus lanatus* and *Pteris cretica*. *Plant Physiol.* **2004**, *134*, 1113–1122.

23. Rigas, P.G. Review: Liquid chromatography-post-column derivatization for amino acid analysis: Strategies, instrumentation, and applications. *Instrum. Sci. Technol.* **2012**, *40*, 161–193.

24. Li-Chan, E.C.Y.; Sultanbawa, F.; Losso, J.N.; Oomah, B.D.; Mazza, G. Characterization of phytochelatin-like complexes from flax (*Linum usitatissimum*) seed. *J. Food Biochem.* **2002**, *26*, 271–293.

25. Nejdl, L.; Sochor, J.; Zitka, O.; Cernei, N.; Ruttkay-Nedecky, B.; Kopel, P.; Babula, P.; Adam, V.; Hubalek, J.; Kizek, R. Spectrometric and chromatographic study of reactive oxidants hypochlorous and hypobromous acids and their interactions with taurine. *Chromatographia* **2013**, in press.

5.2 Optimization of MALDI-TOF for MTs analyses

MALDI-TOF is a powerful tool for surveying proteins and peptides comprising the realm for clinical analysis. We show in this study the determination the optimal condiction for mammalian MT by MALDI-TOF.

5.2.1. Reseach article III

MIGUEL ANGEL MERLOS RODRIGO, LUDMILA KREJCOVA, JIRI KUDR, NATALIA CERNEI, PAVEL KOPEL, LUKAS RICHTERA, AMITAVA MOULICK, DAVID HYNEK, VOJTECH ADAM, MARIE STIBOROVA, TOMAS ECKSCHLAGER, ZBYNEK HEGER AND ONDREJ ZITKA. Fully automated assay for detection of methallothionein based on functionalised γ-Fe2O3 beads. *Journal of Chromatography B* (2016) (Submitted).

Participation in the work of the author M.A. Merlos Rodrigo: experimental part 40% and manuscript preparation 30%.

MTs are intracellular, low molecular, low molecular weight, cysteine-rich proteins. Ubiquitous in eukaryotes, MTs have unique structural characteristics to give potent metal-binding and redox capabilities. MTs are widely distributed in invertebrates and vertebrates, plant, prokaryote, even the fungi kingdoms. Owing to their rich thiol content, MTs bind a number of trace metals including zinc, cadmium, mercury, platinum and silver, and also protect cells and tissues against heavy metal toxicity. The other tasks as follows: storage of zinc homeostasis, radical scavenging and stress response. MTs are overexpressed in several tumors and this overexpression is accompanied by increased proliferation and protection against apoptosis. Therefore, MTs are a sign of worse prognosis in some malignancies. Several reports have disclosed MTs expression as a prognostic factor for tumor progression and drug resistance in a variety of malignancies particularly breast, prostatic, ovarial, head and neck, non-small cell lung cancer, melanoma, and soft tissue sarcoma. Due to their involvement in cell proliferation and survival, increased MTs levels in human neoplasms have been associated with poor prognosis . The transcriptional control of MTs and its nuclear/cytoplasmic localization changes during cell proliferation and

differentiation. In non-pathological tissues MTs are mainly cytoplasmic proteins, while in dividing cells MTs localization varies with cell cycle progression and is expressed in the nucleus during the S and G_2 phase, suggesting that altered levels of MT could be expected to contribute to abnormal cell growth, as seen in cancer, as well as in the acquisition of therapy resistance. Determination of MTs is usually coupled with several analytical methods as follows: capillary electrophoresis, liquid chromatography mass spectrometry, inductive coupled plasma mass spectrometry, immunoassays and electrochemistry. MALDI-TOF MS is an extremely sensitive technique that permits the detection of chemical and biological compound. MALDI-TOF MS is a powerful tool for surveying proteins and peptides comprising the realm for clinical analysis. We show in this study the determination the optimal condiction for rabbit MT by MALDI-TOF MS. Just the ability of the MT to bind heavy metals is the reason why MTs could be used for modification of electrodes in development of electrochemical biosensors. Numerous methods and approaches have been developed to shorten the time of isolation and to obtain biologically important molecules with sufficient purity to be analyzed by ultra-sensitive analytical tools . Magnetic particles/beads (MPs) represent promising tool for this purpose. In view of these facts, immobilization of MTs on MPs may provide many possibilities, such as simplification of biosensing of low levels of MTs, through its pre-concentration. Therefore, We also show in this study the novel method for detection of MTs based on functionalised γ-Fe_2O_3 beads.

Fully automated two-step assay for detection of metallothionein through magnetic isolation using functionalized γ-Fe$_2$O$_3$ particles

Miguel Angel Merlos Rodrigo[1,2], Ludmila Krejcova[1,2], Jiri Kudr[1,2], Natalia Cernei[1,2], Pavel Kopel[1,2], Lukas Richtera[1,2], Amitava Moulick[1,2], David Hynek[1,2], Vojtech Adam[1,2], Marie Stiborova[3], Tomas Eckschlager[4], Zbynek Heger[1,2] and Ondrej Zitka[1,2, *]

[1]Department of Chemistry and Biochemistry, Laboratory of Metallomics and Nanotechnology, Mendel University in Brno, Zemedelska 1, CZ-613 00 Brno, Czech Republic, European Union

[2]Central European Institute of Technology, Brno University of Technology, Purkynova 123, CZ-612 00 Brno, Czech Republic, European Union

[3]Department of Biochemistry, Faculty of Science, Charles University, Albertov 2030, CZ-128 40 Prague 2, Czech Republic, European Union

[4]Department of Paediatric Haematology and Oncology, 2nd Faculty of Medicine, Charles University, and University Hospital Motol, V Uvalu 84, CZ-150 06 Prague 5, Czech Republic, European Union

*Corresponding author

Ondrej Zitka, Department of Chemistry and Biochemistry, Mendel University in Brno, Zemedelska 1, CZ-613 00 Brno, Czech Republic; E-mail: zitkao@seznam.cz; phone: +420-5-4513-3350; fax: +420-5-4521-2044

Highlights

► Automated and high-throughput assay for metallothionein levels estimation is proposed

► The 2,5-dihydroxybenzoic acid matrix was used for MALDI-TOF MS

► Automated detection using pipetting robot provided higher recoveries of metallothionein

► The automated detection provided higher recoveries in all real samples

Abstract

Metallothioneins (MTs) are involved in heavy metal detoxification in a wide range of living organisms. Currently, it is well known that MTs play substantial role in many pathophysiological processes, including carcinogenesis and they can serve as diagnostic biomarkers. In order to increase the applicability of MT in cancer diagnostics, an easy-to-use and rapid method for its detection is required. Hence, the aim of this study was to develop a fully automated and high-throughput assay for the estimation of MT levels. Here, we report the optimal conditions for the isolation of MTs from rabbit liver and their characterization using MALDI-TOF MS. In addition, we described a two-step assay, which started with an isolation of the protein using functionalized paramagnetic particles and finished with their electrochemical analysis. The designed easy-to-use, cost-effective, error-free and fully automated procedure for the isolation of MT coupled with a simple analytical detection method can provide a prototype for the construction of a diagnostic instrument, which would be appropriate for the monitoring of carcinogenesis or MT-related chemoresistance of tumors.

Keywords

1. Introduction

Metallothioneins (MTs) make up a superfamily of low molecular-weight and cysteine-rich proteins that can specifically bind to closed-shell metal ions like zinc (II), cadmium (II), and copper (II) using the sulfur atoms of cysteine rich residues [1-3]. MTs are widely distributed in invertebrates and vertebrates, plants, prokaryotes and even in fungi kingdoms [4-7]. Despite the diversity of the amino acid sequences, the MTs are generally analogous in structure with respect to a high content of cysteine residues (up to 30%), and lack of aromatic amino acids [4]. MTs are involved in the metabolism of heavy metal ions, including their metal detoxification, homeostasis [8,9], storage of zinc [7], radical scavenging [2,10] and stress response [11]. MTs are overexpressed in several tumors and this overexpression is accompanied by an increased proliferation and protection against apoptosis. Therefore, MTs can be considered as a sign of worse prognosis in some malignancies [12-15]. Some previous studies showed that the MT level correlates inversely with tumor grade [16], which led us to consider the MTs as a potential cancer marker [6,7,17]. The biosynthesis of MT was shown to be elevated to protect the cells against heavy metal toxicity, cytotoxicity [18], and radiation and/or DNA damage [19]. Hence, the quantification of MTs should point out some

160

pathological states in living organisms. The determination of MTs is usually coupled with several analytical methods as follows: capillary electrophoresis, mass spectrometry, immunoassays, inductive coupled plasma mass spectrometry, liquid chromatography, matrix-assisted laser desorption/ionization time-of-flight mass spectrometry (MALDI-TOF MS) and electrochemistry [20-23]. In the present study, we have particularly aimed on the utilization of the three last mentioned methods (liquid chromatography, MALDI-TOF MS and electrochemistry). Many studies demonstrated the method of liquid chromatography is highly specific, sensitive, and reliable to improve the resolution of MTs separations [24-31]. MALDI-TOF MS has the potential to revolutionize the cancer diagnostics by facilitating biomarker discovery [32], enabling tissue imaging [32], and quantifying biomarker levels at abundances below sub-femtomole ($< 10^{-15}$ mol) [33]. Herein, we present the use of MALDI-TOF MS to characterize the MTs isolated from rabbit liver under the optimized conditions. MTs can be used to modify electrodes to develop electrochemical biosensors on the basis of their ability to bind heavy metals [20,21]. Such biosensors can be applied in the field of point-of-care testing for the patients. In a view of these facts, the immobilization of MTs on paramagnetic particles (PMPs) may provide many possibilities, such as simplification of biosensor systems for the low levels of MTs due to its pre-concentration. This study focuses on the design and optimization of the method based on the isolation of MTs by using PMPs (functionalized nano-maghemite γ-Fe_2O_3 core) with consequent electrochemical detection. The recovery of MTs was determined by differential pulse voltammetry (DPV). We tested six types of particles, which differ from each other in their composition and functionalization procedure. A comparative study was carried out between automated and manual procedure for the accuracy, efficiency and the consumption of the time of the assay. The optimization and automation of the assay increased its sensitivity and made it simple and fast. For the detection of the isolated products an electrochemical analysis by Brdicka reaction was carried out. The trends in electroanalytical detection of MTs by Brdicka reaction were described previously by Adam *et al.* [20].

2. Experimental

2.1 Chemicals

$Fe(NO_3)_3 \cdot 9H_2O$, $NaBH_4$, $HAuCl_4$ and other chemicals were purchased from Sigma-Aldrich (St. Louis, MO, USA) in ACS purity unless noted otherwise. For the isolation procedure, phosphate buffered saline (PBS, pH = 7.4) and borate buffer (pH = 6.0) were used. The buffers and solutions were prepared with ACS H_2O (Sigma-Aldrich, St. Louis, MO, USA).

High purity deionized water (Milli-Q Millipore 18.2 MΩ·cm^{-1}, Bedford, MA, USA) was used for washing and rinsing.

2.2 Preparation of samples for MT isolation

MT was isolated from rabbit liver and purified by using fast-protein liquid chromatography (FPLC) according to our previous study [31]. The males of New Zealand rabbits were kept in separate cages on regular pelleted laboratory chow (MaK-Bergman, Kocanda, Prague, Czech Republic) and allowed free access to drinking water. Intraperitoneal injection of 10 mg CdCl$_2$·kg^{-1} were given to the rabbits in three equal doses (day 1, day 3 and day 5). In the aforementioned day intervals,The animals were anaesthetised with Ketamine (30 mg·kg^{-1}) and Xylazine (3 mg·kg^{-1}) (Vétoquinol Biovet, France) and sibsequently the livers were collected. 2 g of liver was homogenised on ice using Ultra-turrax T8 (Scholler instruments, Germany) in 8 mL of 10 mM Tris–HCl buffer (pH 8.6). The obtained sample was subsequently vortexed (Vortex Genuie, Germany) and centrifuged (Universal 320, Hettich Zentrifugen, Germany) at 5,000 rpm for 30 min at 4 °C. The supernatant was again centrifuged (Eppendorf centrifuge 5417R) at 25,000 rpm, 4 °C for 30 min and new supernatant than was subsequently heated in a thermomixer (Eppendorf thermomixer comfort, Germany) at 99 °C for 10 min and centrifuged again with same condition.

2.3 Fast protein liquid chromatography (FPLC)

The FPLC (Biologic DuoFlow system, Biorad, USA) was composed of two chromatographic pumps for the transportation of the elution buffers, a gel filtration column (HiLoad26/60, GE Healthcare, Uppsala, Sweden), a UV-Vis detector and an automatic fraction collector. The separation was carried out using the isocratic elution of a mobile phase (150 mM NaCl in 10 mM Tris-HCl buffer (pH = 8.6)). The flow of mobile phase was 4 mL·min^{-1}. Before the separation, the column was washed with the mobile phase for 60 min. For validation, a standard of bovine serum albumin (BSA)(1.5 mg·mL^{-1}) was used. 254nm UV was used to detect MT. The fractions (15 mL per fraction) were collected from min 46 of the separation. After the isolation, the fractions of MT samples were pipetted into the microtiter plate (Sigma-Aldrich, St. Louis, MO, USA), and concentrated using a nitrogen evaporator Ultravap Mistral (Porvair Sciences, Norfolk, UK). Thereafter, each well of a microtiter plate has been washed with ACS to the final sample volume of 1.5 mL. Then, the samples were lyophilized and analyzed by sodium dodecyl sulphate-polyacrylamide gel electrophoresis (SDS-PAGE) and MALDI-TOF MS was carried out to confirm the purity.

2.4 MALDI-TOF MS for verification of MT

The isolated MT was validated for its mass and purity. The mass spectrometry experiments were performed using a MALDI-TOF MS Bruker Ultraflextreme (Bruker Daltonik GmbH, Germany) equipped with a laser operating system at a wavelength of 355 nm with an accelerating voltage of 25 kV (cooled with nitrogen) and a maximum energy of 43.2 μJ with repetition rate 2000 Hz in a linear and positive mode. The data acquisition and processing were performed using the softwares flexControl version 3.4 and flexAnalysis version 2.2 respectively. The matrices used in the MALDI method were 2,5-dihydroxybenzoic acid (DHB), α-cyano-4-hydroxycinnamic acid (HCCA) and sinapinic acid (SA) (Bruker). All the matrices were prepared in TA30 (30% acetonitrile, 0.1% trifluoroacetic acid solution). The Mixture was thoroughly vortexed and ultrasonicated using Bandelin 152 Sonorex Digital 10P ultrasonic bath (Bandelin Electronic GmbH, Germany) for 2 min, 50% of intensity at ambient temperature. The working matrix standard solutions were prepared freshly by diluting the stock solutions.

The used concentrations of MTs samples were 1.5, 3, 6 and 12 μg·mL^{-1}. The sample solutions were prepared with TA30. The solutions for the analysis were mixed in a ratio of 1:1 (matrix/substance). After obtaining a homogeneous solution, 1 μL was applied on the MTP ground target plate (Bruker Daltonik GmbH) and dried under atmospheric pressure and ambient temperature. A mixture of protein calibration standards I (Bruker) was used to externally calibrate the instrument. The protein mixture allowed the calibrations and testing of MALDI-TOF MS in a mass range between ~4000 and 20000 Da.

The samples preparation method for MALDI-TOF was carried out in two different ways: Dried Droplet (DD) and Thin Layer (TL) for HCCA matrix. For DD, a saturated matrix solution was prepared by mixing the matrix solution with the sample solution in a ration of 1:1. The sample solution was prepared with TA30. The mixture was pipetted on the target (1 μL) and dried at ambient temperature. The preparation should yield relatively large crystals on the target surface without the matrix or analyte. For TL, the matrix was prepared on the target to form a thin layer of very small and homogenous crystals. After spotting, the solution was spreaded on the target and evaporated. The thin matrix layer remained on the surface of the target. The MTs sample (in TA30 solution) was applied on the top of this thin layer. After drying of the sample, the analyte molecules remained on top of the matrix. Before measuring the samples, a mixture of protein calibrations standard I (Bruker Daltonik GmbH, Bremen, Germany) was used to calibrate the instrument. Then, air-dried MALDI target was loaded into

the mass spectrometer and the samples were analyzed. The MS spectra were typically acquired by averaging 20 sub spectra from a total of 500 shots of the laser (Smartbeam 2. Version: 1_0_38.5).

2.5 SDS-PAGE

The electrophoresis was performed using a Mini Protean Tetra apparatus (Bio-Rad, Hercules, CA, USA). The gels were prepared from 30% (*m/v*) acrylamide stock solution with 1% (*m/v*) bisacrylamide. The electrophoresis was run at 120V for 1 h 15 min at 4 °C (Power Basic, Bio-Rad USA) in tris-glycine buffer (0.025 M Trizma-base, 0.19 M glycine and 3.5 mM SDS, pH = 8.3). Then the gels were stained using Coomassie blue [27] and consequently with silver stain [34].

2.6 Synthesis and functionalization of PMPs

1.5g of $Fe(NO_3)_3 \cdot 9H_2O$ was dissolved in water (80 mL). Under stirring 0.2 g of $NaBH_4$ was added, which was dissolved in 10 mL of 3.5% NH_3 and heated (2 h, 100 °C). After cooling, the mixture was left overnight and the magnetic nanoparticles were separated by an external magnetic field, and subsequently washed several times with water and used as a core for the surface modifications.

MAN-53

The maghemite was suspended in a water solution (20 mL) of 7.5% polyvinylpyrrolidone (PVP), and mixed with 25 mL of 1 mM $HAuCl_4$ and finally 0.75 mL of trisodium citrate (26 mg·mL^{-1}) was added in order to produce a shell structure. The resulting mixture was stirred overnight, separated using an external magnetic force field and dried at 40 ºC. The procedure of this material fabrication was published previously **[35]**.

MAN-131

The maghemite was mixed with a water solution (20 mL) of polyethylenimine (0.5 g) and stirred for 1 h. 25 mL of $HAuCl_4$ (1 mM) was added, stirred 1 h and sodium citrate (0.75 mL) (26 mg·mL^{-1}) was poured into the solution. The mixture was stirred overnight, separated by magnet, washed 3 times with water and dried at 40 ºC.

MAN-132

The maghemite was suspended in a water solution (20 mL) of polyethylene glycol (PEG 4000), mixed with 25 mL of 1 mM $HAuCl_4$ and finally 0.75 mL of trisodium citrate (26 mg·mL^{-1}) was added. The resulting mixture was stirred overnight, separated using an external magnetic force field and dried at 40 ºC.

<u>MAN-133</u>

The preparation way was similar to the preparation of MAN-132, only PEG of molecular weight 1500 (0.5 g) was used instead of 4000.

<u>MAN-134</u>

A maghemite suspension was added to a solution of poly(4-styrenesulfonic acid) (0.5 g) and mixed for 1 h. 25 mL of 1 mM $HAuCl_4$ was added, mixed for 1 h and finally 0.75 mL of trisodium citrate (26 mg·mL^{-1}) was added to it. The mixture was stirred overnight, separated by magnet and dried at 40 ºC.

<u>MAN-135</u>

A maghemite suspension was added to a solution of polyacrylamide (0.5 g) and mixed for 1 h. 25 mL of 1 mM $HAuCl_4$ was added, mixed for 1 h and finally 0.75 mL of trisodium citrate (26 mg·mL^{-1}) was added to it. The mixture was stirred overnight, separated by magnet and dried at 40 ºC.

2.7 Characterization of synthesized PMPs

The morphologies of PMPs were studied using scanning electron microscope (SEM) MIRA3 LMU (Tescan, a.s., Brno, Czech Republic). An accelerating voltage of 15 kV and beam current about 1 nA was applied. The size of the PMPs and their ζ-potential were observed by dynamic light scattering (DLS) coupled with Particle Size Analyzer (Zetasizer Nano ZS90, Malvern instruments, Malvern, United Kingdom). The PMPs were dispersed in PBS (137 mM NaCl, 2.7 mM KCl, 1.4 mM NaH_2PO_4, and 4.3 mM Na_2HPO_4, pH = 7.4) and incubated at 25 °C for 15 min before the measurement.

2.8 Manual isolation of MTs using PMPs

Prior to the isolation process, the PMPs (40 mg·mL^{-1}) were washed using PBS (6 × 250 μL, pH = 7.0) to remove impurities. For the isolation, the MT from rabbit liver (50 μg·mL^{-1}) was incubated with the PMPs (0.5 mg·mL^{-1}) at 37 ºC, 1190 rpm in a thermomixer (Eppendorf Thermomixer comfort, Hamburg, Germany) for 30 min. The PMPs with the bound MT were separated using an external magnetic field and washed six times with PBS or combination of PBS (3 × 250 μL, pH = 7.0) and 200 mM borate buffer (3 × 250 μL, pH = 6.0). In order to detect MTs, the PMPs with the bound MT were dissolved in hydrochloric acid (250 μL, 3 M). The obtained solution was evaporated using a nitrogen evaporator Ultravap RC (Porvair Sciences, Leatherhead, United Kingdom). Finally, the evaporated sample was resuspended in H_2O (250 μL) and the final product was detected by DPV.

2.9 Fully automated pipetting system

The fully automated MTs isolation procedure used the same specific parameters of the manual procedure. Here, the whole procedure was carried out using an automated pipetting system epMotion 5075 (Eppendorf, Hamburg, Germany). The device was controlled by a PC software (Eppendorf). The experimental program is described in the section 3.

2.10 The testing of optimized protocol on real samples

As real samples, we used the sera of four Wistar rats, euthanized (1% Narkamon + 2% Rometar, 0.5 mL/100 g of weight) for other experimental purposes. We followed the European Community Guidelines as accepted principles for the use of experimental animals. The experiments were performed with the approval of the Ethics Commission at the Faculty of Agronomy, Mendel University in Brno, Czech Republic.

2.11 Electrochemical detection of isolated MT

The products of the isolation procedure were detected by DPV coupled with a hanging mercury drop electrode (HMDE) (a drop area of $0.4\,\text{mm}^2$) as a working electrode. An Ag/AgCl/3M KCl and a platinum electrode were used as a reference and an auxiliary electrode respectively. The analyzed samples were deoxygenated prior to the measurements by purging with argon (99.999%) saturated with water for 10 s. Brdicka supporting electrolyte, containing 1 mM $[Co(NH_3)_6]Cl_3$ and 1 M ammonia buffer (NH_3(aq) and NH_4Cl, pH = 9.6) was used and changed after each analysis. The parameters of the measurement were as follows: initial potential of -0.7 V, end potential of -1.75 V, pulse period 0.80 s, sample period 10 ms, pulse width 30 ms, step potential 2 mV, modulation amplitude -25 mV, sweep rate $2.5\,\text{mV·s}^{-1}$, $E_{ads} = 0$ V, $t_{ads} = 120$ s, stirring $1000\,\text{min}^{-1}$, volume of injected sample: 5 µL, volume of measurement cell 2 mL (5 µL of sample and 1995 µL Brdicka solution). A manual determination was performed on 693 VA Stand (Metrohm, Herissau, Switzerland). The automated electrochemical detection was performed using 747 VA Stand instrument connected to a 693 VA processor and a 695 autosampler (Metrohm, Herissau, Switzerland). For the data processing, VA Database 2.2 (Metrohm, Switzerland) was employed.

2.12 Mathematical treatment of data and estimation of detection limits

The mathematical analysis of the data and their graphical interpretation were realized by software EXCEL®. The results are expressed as mean ± standard deviation (S.D.) unless

noted otherwise. The detection limits (3 signal/noise, S/N) were calculated, whereas N was expressed as standard deviation of noise determined in the signal domain unless stated otherwise.

3. RESULTS AND DISCUSSION

All the experiments were carried out using the MT, isolated from rabbit liver by FPLC. The total time of the isolation procedure was 120 min. Fig 1A illustrates a chromatogram of the sample isolated from rabbit liver using FPLC and the different fractions (1; 2; 3; 4; 5; 6; 7 and 8), which were collected during the isolation. Subsequently, we analyzed the samples using SDS-PAGE and MALDI-TOF MS to confirm their purity. The SDS-PAGE of the collected fractions is shown in Fig 1B. The prominent bands of the fraction 3-7 are indicating the presence of MT monomers, dimers and trimers.
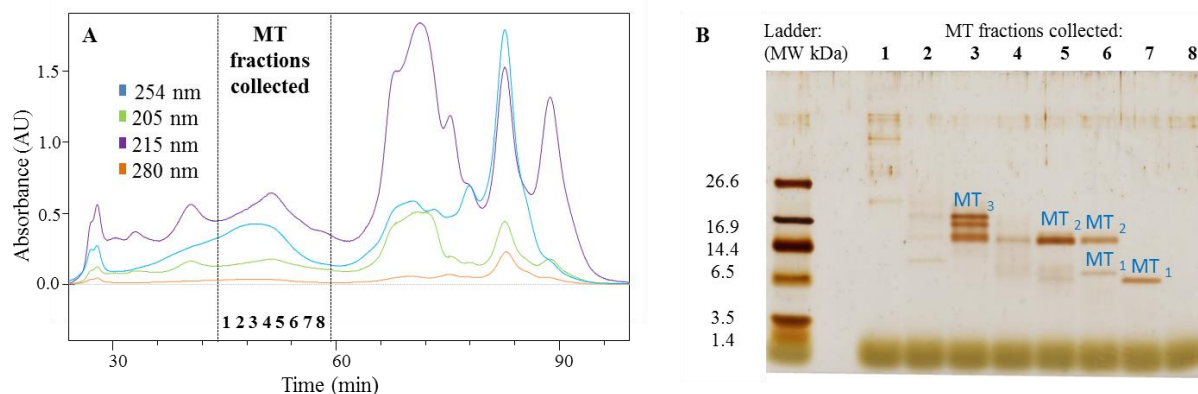

Figure 1. **A**) Chromatogram of the isolated MT from rabbit liver. Separation was carried out at flow rate of 4 mL·min^{-1} using 150 mM NaCl in 10 mM Tris-HCl (pH = 8.6). Wavelength for the detection of MT was set to 254 nm. MT was eluted from the column in 48 − 55 min (marked between bars). **B**) SDS-PAGE gel of collected fractions. The fractions were mixed with non-reducing buffer in a ratio of 2:1 and incubated at 93 °C for 3 min. For the analysis 15 % running and 5% stacking gel were used. The gels were prepared from 30 % acrylamide stock solution with 1 % bisacrylamide. In fractions 3-7 there are visible bands of MT monomer, dimer and trimer.

3.1 Study of the optimal conditions for the determination of MTs by MALDI-TOF MS

To study the optimal conditions for the determination of MT, three different matrices were used: DHB, HCCA and SA. Only the fraction 7 from FPLC was taken in this case. The MALDI-TOF MS spectra, obtained from the matrices are shown in Fig. 2. The results showed the presence of the MT monomer (fraction 7) (major peak ~ 6 kDa) in case of all the matrices. The main observed signal for MT was assigned as follows: $[M+H]^+$ (m/z 6126 Da).

Moreover, it was estimated that the isolated MT was highly-pure because each of the spectra showed only one peak of high intensity for the relevant protein.
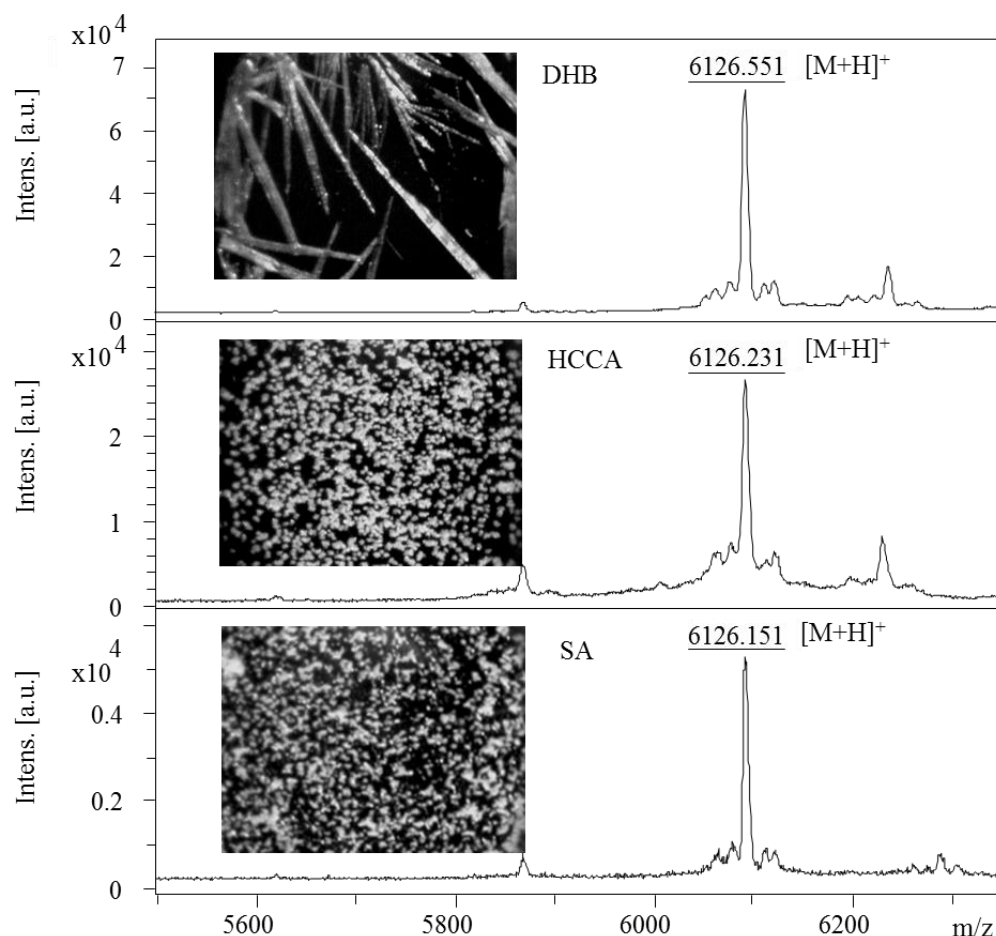

Figure 2. Crystal photo and MALDI-TOF spectra of MT from fraction 7 after the FPLC purification. In the linear positive mode analyses, DHB, HCCA and SA were used as matrixes. The spectra were analyzed with the Flex Analysis software (Version 3.4). Each spectrum was averaged from 2000 subspectra. M and H indicate the protonated quasi-molecular ion formed by MT and hydrogen.

Our results showed an increase in signal intensity as a function of the matrixes. HCCA and DHB showed 100-times more intensity of the MT signal (a.u.) as compared to SA (Fig. 2). For the optimization of this method, a comparative study was carried out between the two samples preparation procedures: DD and TL. In case of HCCA matrix, TL showed a higher intensity of the signal for both intensities of the laser (28.8 and 43.2 μJ) and for all the used concentrations of MTs (1.5; 3; 6 and 12 μg·mL^{-1}) (Fig. 3A and 3B) as compared to DD. The matrix DHB, heterogeneous and strong crystals, showed an increase in the intensity of the signal (a.u.) for both the intensities of the laser when the concentration of MTs was increased

(Fig. 3C). Our results also showed that the signal intensity (a.u.) for DHB (using the low-intensity laser, 28.8 µJ) was higher than that of HCCA matrix when the concentration of MTs was increased (Fig. 3D). In case of 12 µg·mL^{-1} MTs, the signal intensity (a.u.) was found to be two times higher in DHB (using the low-intensity laser) as compared to HCCA. From these results, we assumed that the DD method with DHB matrix is a faster and easier approach for the post-isolation characterization of MTs by MALDI-TOF MS analysis.
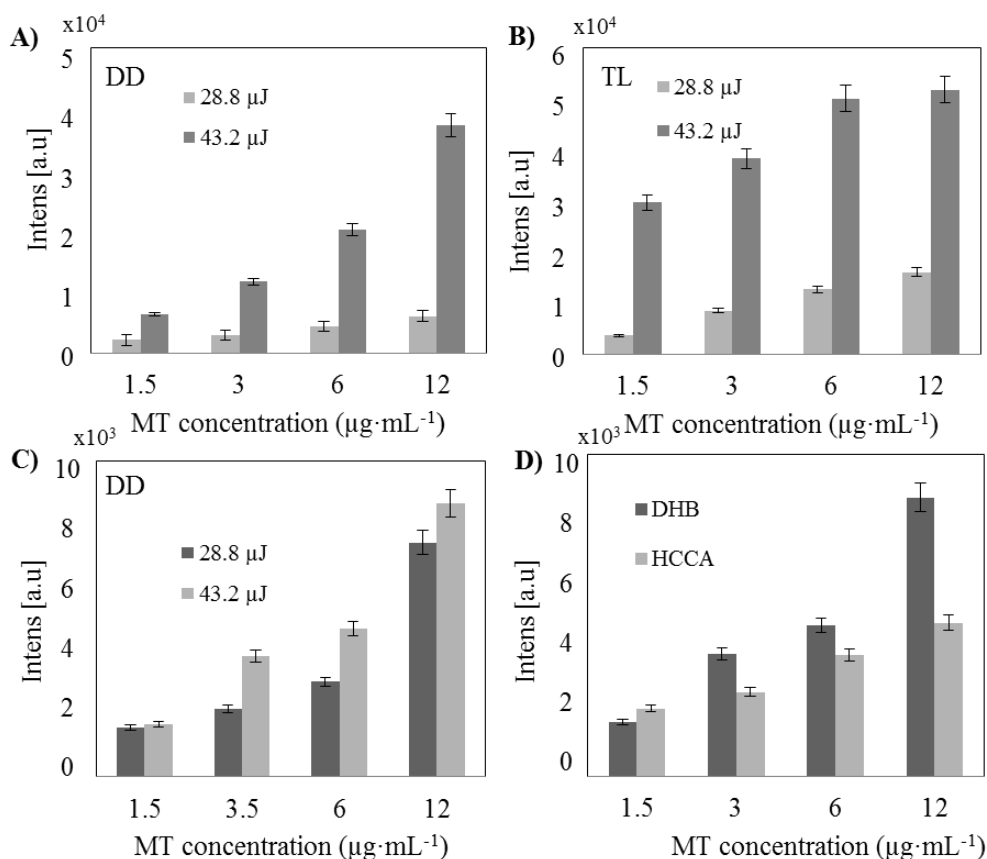

Figure 3. Signal intensities of rabbit MTs in different concentrations (µg·mL^{-1}) for 28.8 and 43.2 µJ power laser with HCCA matrix in different methods. Sample preparations: (**A**) DD: Drop Dry and (**B**) TL: Thin Layer. (**C**) Signal intensities of rabbit MTs in different concentrations (µg) in 28.8 and 43.2 µJ power laser with DHB using DD method. (**D**) Signal intensities (a.u.) of rabbit MTs in different concentrations (µg) for 28.8 µJ power laser between HCCA and DHB matrix using DD method.

3.2 Characterization of synthesized PMPs

The isolation procedure of MT was based on the non-specific immobilization of the protein on the surface of PMPs. These materials nanomaghemite cores which were functionalized with various modifications as follows: PVP, polyethyleneimine, PEG, poly(4-styrenesulfonic acid) and polyacrylamide. The morphology of the prepared materials was studied using SEM.

The DLS measurements were used for the determination of particle sizes in water dispersion and the ζ-potential measurement was carried out to determine the dispersion stability at current pH values. All of these results are summarized in Fig. 4. The morphology of individual materials was investigated by SEM where the presence of the aggregates of the particles is clearly visible for all materials. This effect was probably caused by the normal drying process during the sample preparation for the microscopy. The smallest particles were visible in the case of MAN-53. It was modified with PVP and the average particle size in water suspension was found to be 30 nm approximately (Fig. 4A). These particles had the highest ζ-potential (about −30 mV at pH = 7.0) which suggested their good stability in water dispersion. This was probably caused by the presence of H-bonds between water and the carbonyl group of the lactam circle in PVP [36,37]. MAN-131 PMPs were functionalized with polyethylenimine. This material showed the particle size about 2.7 µm and the ζ-potential 14.5 mV at pH = 8.7 (Fig. 4B). This material was slightly dispersed in the water suspension probably due to the prevalence of secondary amines instead of primary amines in the structure of branched polyethylenimine. MAN-132 and MAN-133 were modified with PEG. This is another usually applied polymer, soluble in water which is used for improving the biocompatibility of inorganic materials [38]. From the micrographs, the covering of the basic maghemite structure with PEG 4000 can be seen much better (Fig. 4C) as compared to that of PEG 1500 (Fig. 4D). MAN-132 and MAN-133 exhibited the ζ-potential in water suspension equaled to zero (at pH = 7.4). This fact was probably related to the basic structure of the polymer where no specific functional groups in PEG chains that are able to create specific charge of the material surface were presented. A major particle size was determined to be about 100 nm for both the MPs. The minor part of the particles had sizes about 820 and 615 nm for PEG 4000 and 1500 respectively. The fifth prepared material was modified with poly(4-styrenesulfonic acid). In this case, the prepared material had a ζ-potential equaled to zero at pH = 6.7 and therefore this material did not create stable particles in water solution (Fig. 4E). Nevertheless, the size of the particles/aggregates in water suspension was about 500 nm. The last material used for the modification of maghemite surface was polyacrylamide (Fig. 4F). This modification showed a formation of semi-stable particles in water dispersion because of their ζ-potential, −13.6 mV at pH = 7.0. The size of these particles was mostly around 100 nm.
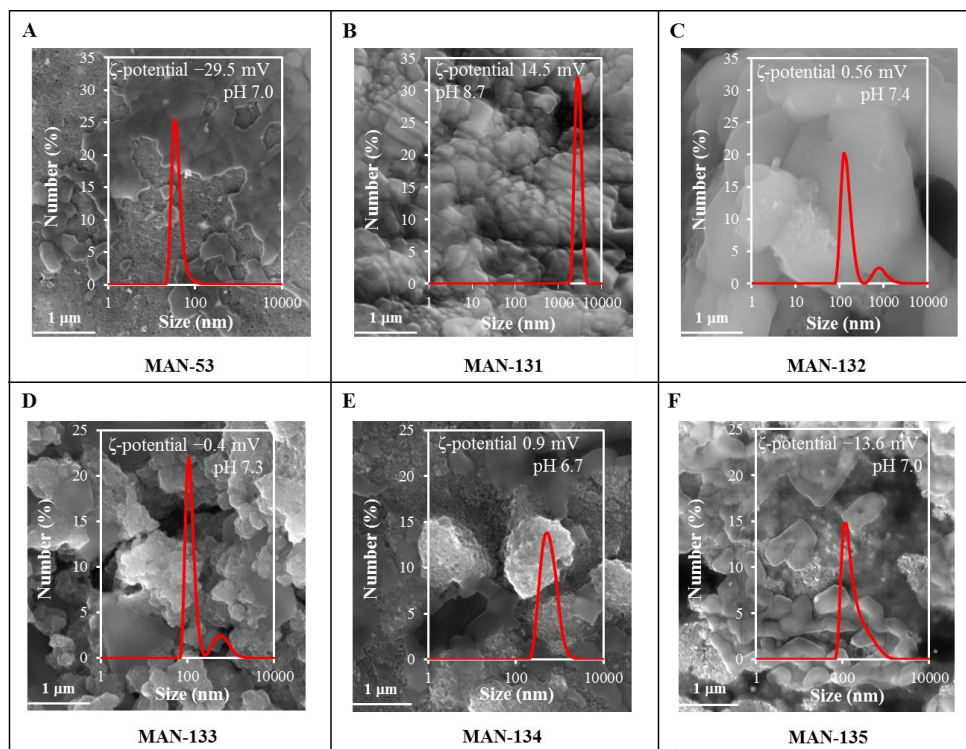
Figure 4. Characterization of six various PMPs: **A** to **F** as MAN-53, MAN-131, MAN-132, MAN-133, MAN-134 to MAN-135, respectively. Micrographs of the surface of PMPs were obtained using SEM (placed on background of pictures). The size and ζ-potential of the PMPs were observed by DLS. The size of the PMPs was expressed as a dependence of the number of particles (%) on size of the particles (nm). The ζ-potential at the relevant pH is enrolled at the heading of the pictures. Other experimental details are explained in the Experimental part.

3.3 MT Isolation procedure

Prior to the isolation procedure of MT, the PMPs were prepared and functionalized as mentioned above (section 2.4). The whole experiment was divided into two parts: manual and automatic processing, including isolation and detection steps (schematization is shown and described in section 3.4.). Our pilot experimental data have revealed that the PMPs can be simply used for the analysis of the real samples, such as polyadenine and/or other oligonucleotides [39,40]. The data obtained from the manual as well as automated electrochemical analysis were analyzed and processed in the same manner. The scheme of the sample processing together with the design of the isolation process is depicted in Fig. 5. First, the storage solution was discarded out of the PMPs (Fig. 5/1), followed by a washing of the PMPs which was involved to remove the undesired impurities formed during the synthesis process (Fig. 5/2), incubation of the PMPs with a sample (Fig. 5/3), washing away of unbound MTs (Fig. 5/4), dissolving of the PMPs with the bound MTs using 3 M HCl, followed by its evaporation, and the product was dissolved by addition of water to make a clear solution (Fig. 5/5).
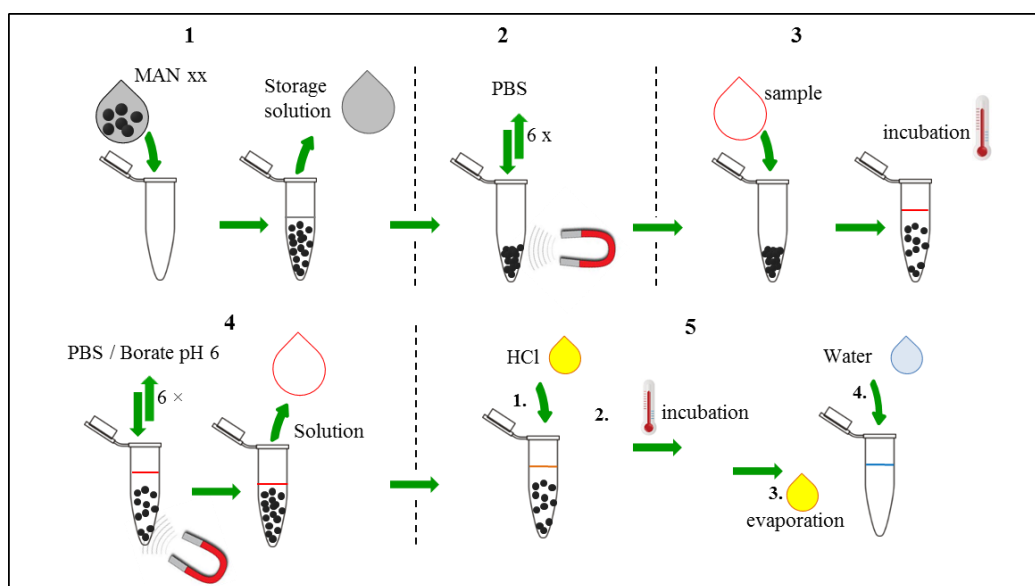
Figure 5. Detailed description of isolation procedure in a manual mode: (**1**) discarding of storage solution out of PMPs, (**2**) washing of PMPs using PBS (6× 250 µL, pH = 7.0) to remove impurities, (**3**) incubation of MT isolated from rabbit liver (50 µg·mL^{-1}) w with PMPs (0.5 mg·mL^{-1}) under conditions as follows: 37 °C, 30 min, 1190 rpm in thermomixer, (**4**). PMPs with bound MT were further forced using external magnetic field and six times washed with PBS or combination of PBS (3 × 250 µL, pH = 7.0) and 200 mM borate buffer (3× 250 µL, pH = 6.0) (**5**) PMPs with bound MT were dissolved in hydrochloric acid (250 µL, 3 M HCl). The obtained solution was evaporated using a nitrogen evaporator Ultravap RC (Porvair Sciences, Leatherhead, United Kingdom). Finally, the evaporated sample was resuspended in H$_2$O (250 µL) and the final product was detected by DPV.

3.4 Automated isolation and measuring system

The automated isolation procedure was carried out using an automatic pipetting station epMotion 5075. The epMotion is designed to help to automate routine pipetting tasks for time saving. It is not only one of the most accurate pipetting stations on the market, but also helps to eliminate manual pipetting errors by virtue of its automation and thereby may reduce the need for repeated work and save time. We have already described the epMotion 5075 original labware, employed in automatic isolation of MT in section 2.6 and Fig. 6A. The protocol for the isolation was processed using the ep*Motion*® software (Eppendorf) and was designed to copy a manual mode of isolation (Fig. 6B). For the detection of the isolated product (automated as well as manual procedure), an electrochemical analysis (DPV) was selected. While the manual detection exhibited a high accuracy, the automatic mode (higher LOD and LOQ) showed a faster and less time consuming procedure with a sufficiently accuracy, summarized in Table. 1. The Brdicka catalytic reaction principle is the specific reaction between the thiol groups of proteins and Brdicka´s solution. The Brdicka solution consists of

an ammonium buffer and hexamminecobalt chloride complex ($[Co(NH_3)_6]Cl_3$), which interact with -SH groups of the protein [41].
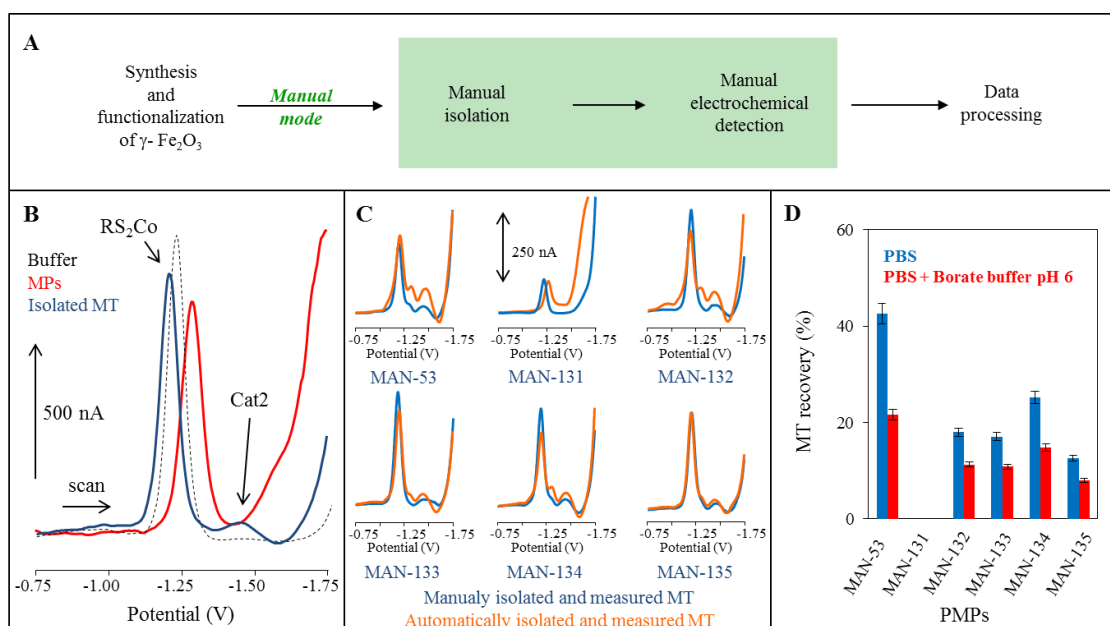

Figure 6. (**A**) Scheme of epMotion 5075 original labware, employed in automatic isolation of MT. (**B**) Workflow for automated isolation of MT: dosage of magnetic material (**B1**), washing of magnetic material (**B2**), dosage of sample containing MT to PMPs and incubation at 37 °C for 30 min (**B3**), washing with PBS of unbounded MT (**B4**) and dissolution of MT by HCl (**B5**).

Method	Regresion equation	R^2	LOD (nM)	LOQ (nM)	RSD %
MT manual	y = 10987x +3.0743	0.997	12	39	7.7
MT automated	y = 11623x + 3.8254	0.997	9	29	10.0

Table 1. Analytical data about regression equation, correlation (R^2), limit of detection (LOD), limit of quantification (LOQ) and relative standard deviation (RSD).

The scheme of the manual isolation and detection of MT using functionalized PMPs is shown in Fig. 7A. The DPV analysis of MT resulted in three characteristic signals as follows: RS_2Co (-1.25 ± 0.05 V), Cat1 (-1.4 ± 0.03 V) and Cat2 (-1.5 ± 0.02 V). A typical voltammogram of the isolated MT sample in Brdicka solution (with RS_2Co and Cat2 signals) (only RS_2Co signals) is shown in Fig. 7B. Both Cat1 and Cat2 signals were related to the reduction of the hydrogen developed from the electrolyte catalyzed by -SH groups on the mercury electrode [41]. Only the Cat2 signal (highlighted in Fig. 7B) showed a linear increase in a signal related

to the MT amount [42-45]. The ability of all the PMPs to bind to MT was verified by the electrochemical analysis using DPV in Brdicka solution. As it was mentioned above, the only Cat2 signal (potential -1.5 ± 0.02 V) showed a relation to the reduction of hydrogen catalyzed by -SH group and exhibited linearity corresponded to the MT amount. In this point, we have focused on tracking the Cat2 signal height and position. As expected, no peak corresponding to the Cat2 signal was found in the case of bare PMPs, but in the voltammogram of isolated MT samples the Cat2 signal was observed. Based on this difference, the binding of MT to the surface of the modified PMPs was confirmed. Moreover, the real voltammograms, obtained after manual and automated mode of isolation and detection of MT sample, were compared in Fig. 7C. Only MAN-131 was found to be unsuccessful in the suggested assay, whereas MAN-53 appeared to be the most successful. This phenomenon was likely caused by the functionalization of the surface of nanomaghemite core using reduced gold, which attracted MT thiol moieties, well described in literature [46].
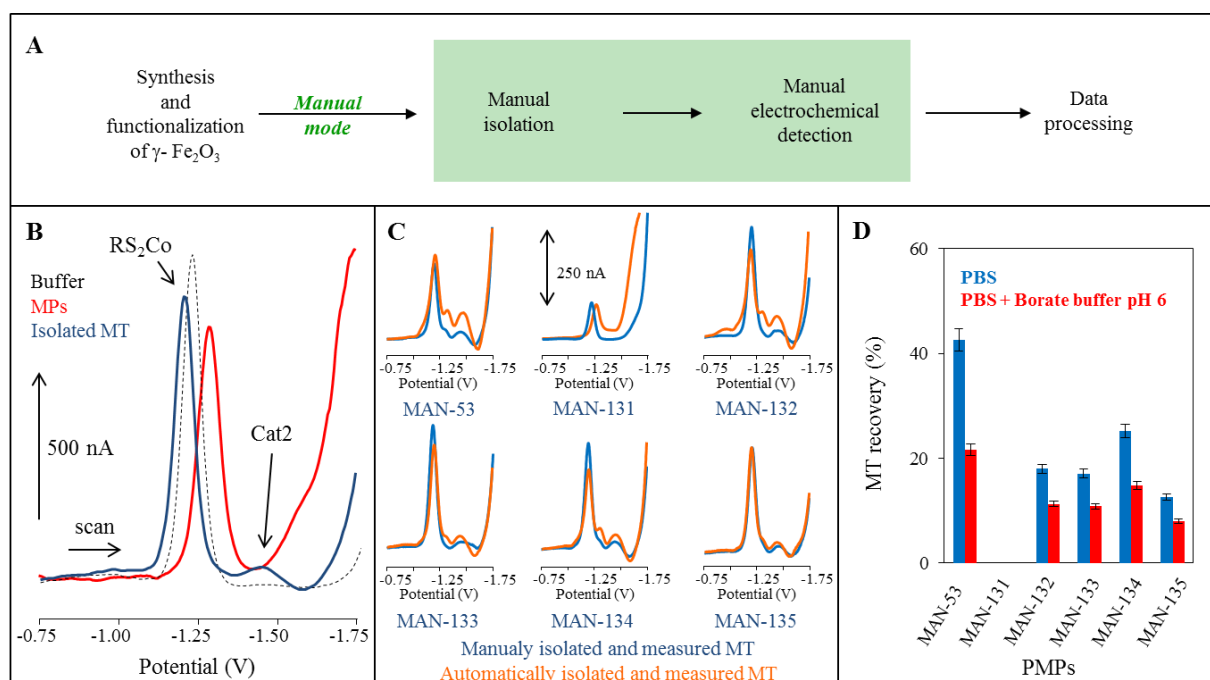
Figure 7. Scheme of manual isolation and detection of MT using functionalized magnetic particles (**A**). Typical voltammograms of isolated MT in Brdicka solution (blue line), Brdicka solution itself (black dashed line) and magnetic particles itself (red line) with highlighted peaks (RS$_2$Co and Cat2) (**B**). Comparison of typical voltammograms obtained after the manual (blue lines) and automated (orange lines) mode of the isolation and detection of MT sample (**C**). Influence of washing buffer composition on the obtained relative recovery of MT using six various MPs (MAN-53, MAN 131–135) (**D**).

3.5 Optimization of isolation procedure

The whole isolation process was optimized in three different ways. First, the effects of the isolation buffers were studied: two different buffers (PBS with 200 mM borate buffer pH = 6.0 and PBS itself) were compared. As shown in Fig. 7D, the MT recovery was found to be higher (about 36.4% – 49.3%) when PBS alone was employed. The basic difference between the buffers is the pH which may fundamentally influence the isoelectric behavior of MT and the coverage of the particles and thus their overall mutual interaction which results in the yield the isolation procedure. The second optimized parameter was type of isolation and detection (manual/automated). The MT recoveries for both types of isolation were compared. The scheme of the automated isolation and detection of MT using the functionalized PMPs is shown in Fig. 8A. Fig. 8C shows that the automated isolation and detection procedure provided higher recoveries (27.5% – 33.3%) of MT than that of the manual method. This result showed somehow a contrast to the correlation of the calibration curves in which the manual detection seemed to be much more sensitive than the automatic method (Fig. 8B). The saturation curve of the most successful PMPs (MAN-53) with the inserted detail of the Cat2 peaks of real voltammograms are shown in Fig. 8D.

In the third step of the optimization process, the type of the materials was studied to be used as an isolation platform for the fabrication of the PMPs. MAN-53 and MAN-134 showed an overlap of more than 30% in the isolation success rate. Based on the characterization using DLS, the best MAN-53 showed the smallest size (32 nm) and relatively high ζ-potential (−29.5 mV, pH = 7.0) indicating a good stability with a large surface area. The second most suitable PMPs were MAN-134. The ζ-potential (0.9 mV, pH = 6.7) exhibited the instability of this particle which has relatively big particle size (459 nm). For the fabrication of these two particles, $HAuCl_4$ and poly(4-styrenesulfonic acid) were used, because both of these materials were used previously for bioseparation [47] or particles stabilization [48]. MAN-132 and MAN-133 showed significant similarities within the results of the MT recovery. Similarities can be seen between the characterization (SEM and DLS) of both the materials which are significant for this experiment. The particle sizes (measured by DLS) were found to be 122 and 105nm for model MAN-132 and -133 respectively. The stability of both of these model was found to be very low (ζ-potential 0.56 mV, pH = 7.4, by model MAN-132 and ζ-potential −0.4 mV, pH = 7.3, by model MAN-133). In comparison with model MAN-132 and -133, the model MAN-135 showed a lower MT recovery. Although the particle size (105 nm) MAN-135 was very similar to that of MAN-132 and -133 and had relatively good stability (ζ-potential −13.6 mV, pH = 7.0), this material did not meet the expectations.

According to the obtained results, the MAN-131 PMPs were not suitable for the isolation of MT by the suggested method because the final product was not electrochemically detectable (Fig. 7C). This material exhibited a relatively high stability (ζ-potential 14.5 mV, pH = 8.7), although this could be due to a secondary aggregation (of size 2669 nm) of the primary PMPs which was 26 times higher in comparison with the most successful MAN-53.
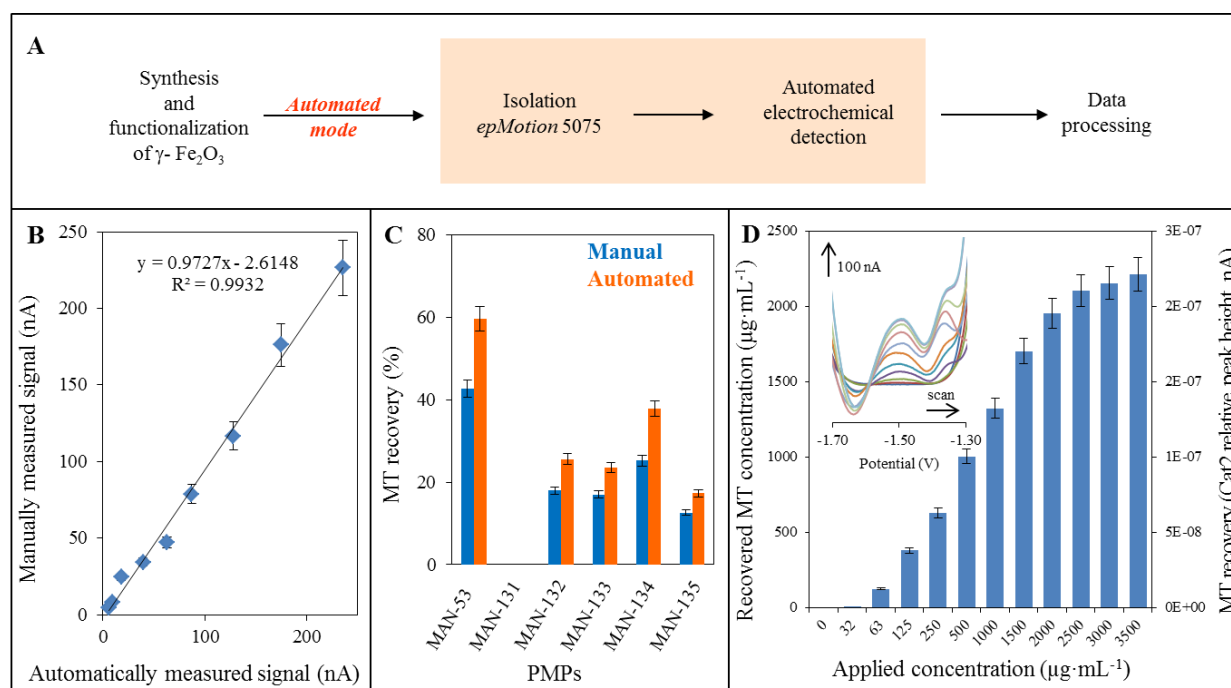
Figure 8. Scheme of automated isolation and detection of MT using functionalized PMPs (**A**). Correlation of signals (nA) of calibration of MT measured in manual and automatic mode (**B**). Influence of mode of isolation and detection on obtained relative recovery of MT using six various PMPs (MAN-53, MAN 131–135) (**C**). Saturation curve of the most successfully PMPs (MAN-53), the detail of the Cat2 peaks from interleaved real voltammograms are shown in the inset (**D**).

3.6 Validation of manual and automated procedure on real samples

In this study, a comprehensive description of manual and automated procedures to isolate and detect MT was shown. Finally both of the methods were validated for real serum samples. The isolation of MT from Wistar rat serum was carried out using the best PMPs (MAN-53). As shown in Table 2, the automated procedure provided higher recoveries of MT than that of manual procedure from all of the rat serum samples. If we compare the total time, consumed during the sample processing, the automated procedure (50min) was found to be four times faster than the manual procedure (210 min) (Table 2). These results suggested that the modified PMPs coupled with automated isolation and detection procedure can be applied

efficiently to isolate MT from various biological samples for the characterization of various pathological states including head and neck cancer.

MT	Automated isolation protocol		Manual isolation	
	Concentration ($\mu g \cdot mL^{-1}$)	Recovery (%)	Concentration ($\mu g \cdot mL^{-1}$)	Recovery (%)
1	70.9	28.9	51.9	21.2
2	69.3	20.0	47.6	13.8
3	47.5	15.6	36.3	11.9
4	52.5	14.0	45.2	12.1
Total time consumed	50 min		210 min	

Table 2. The comparison of the isolation and detection efficiency between automated and manual procedure. The isolation of MT was in both protocols carried out from Wistar rat serum using the best PMPs (MAN-53). The recoveries (%) are recalculated to total metallothionein amount prior own isolation.

4. CONCLUSIONS

The low fabrication cost and easy manipulation make the paramagnetic particles a unique material which attracts attention in various fields of science. In this study, we described the optimization of a bead-based isolation of MTs coupled with an electrochemical detection. Prior to the isolation and detection process, the rabbit liver MT was characterized by MALDI-TOF MS using DHB as a suitable matrix which showed a higher intensity of the signal than that of other matrices. Finally the rabbit liver MT was isolated using a functionalized maghemite based particles by a fully automated procedure for the electrochemical determination. A large number of samples can be handled conveniently by the automated procedure which was found to be four times faster than the manual procedure. This method was also successfully applied to isolate MTs from Wistar rat serum. The suggested procedure can also be used for the detection of other important biomolecules. Overall, our approach offers a high-throughput automated sample preparation system for the determination of MT. We anticipate that this simple and cost-effective procedure could be helpful to estimate the MT serum levels in cancer patients before and during their treatment which should allow to specify their clinical outcomes linked with possible development of MT-related chemoresistance.

Conflict of interest

The authors have declared no conflict of interest.

Acknowledgements

References

[1] M. Raudenska, J. Gumulec, O. Podlaha, M. Sztalmachova, P. Babula, T. Eckschlager, V. Adam, R. Kizekb, M. Masarik, Metallomics 6 (2014) 55.

[2] B. Ruttkay-Nedecky, L. Nejdl, J. Gumulec, O. Zitka, M. Masarik, T. Eckschlager, M. Stiborova, V. Adam, R. Kizek, Int. J. Mol. Sci. 14 (2013) 6044.

[3] M. Zalewska, J. Trefon, H. Milnerowicz, Proteomics 14 (2014) 1343.

[4] H. Skutkova, P. Babula, M. Stiborova, T. Eckschlager, L. Trnkova, I. Provaznik, J. Hubalek, R. Kizek, V. Adam, Int. J. Electrochem. Sci. 7 (2012) 12415.

[5] P. Babula, M. Masarik, V. Adam, T. Eckschlager, M. Stiborova, L. Trnkova, H. Skutkova, I. Provaznik, J. Hubalek, R. Kizek, Metallomics 4 (2012) 739.

[6] S. Krizkova, I. Fabrik, V. Adam, P. Hrabeta, T. Eckschlager, R. Kizek, Bratisl. Med. J. 110 (2009) 93.

[7] S. Krizkova, M. Ryvolova, J. Hrabeta, V. Adam, M. Stiborova, T. Eckschlager, R. Kizek, Drug Metab. Rev. 44 (2012) 287.

[8] P.E. Baurand, V. Pedrini-Martha, A. de Vaufleury, M. Niederwanger, N. Capelli, R. Scheifler, R. Dallinger, PLoS One 10 (2015) 1.

[9] K. Kowalska, A.B.M. Zalewska, H. Milnerowicz, J. Trace Elem. Med. Biol. 29 (2015) 99.

[10] P.I. Oteiza, Free Radic. Biol. Med. 53 (2012) 1748.

[11] C. Cassier-Chauvat, F. Chauvat, Int. J. Mol. Sci. 16 (2015) 871.

[12] A. Krzeslak, E. Forma, P. Jozwiak, A. Szymczyk, B. Smolarz, H. Romanowicz-Makowska, W. Rozanski, M. Brys, Clin. Exper. Med. 14 (2014) 107.

[13] J. Gumulec, J. Balvan, M. Sztalmachova, M. Raudenska, V. Dvorakova, L. Knopfova, H. Polanska, K. Hudcova, B. Ruttkay-Nedecky, P. Babula, V. Adam, R. Kizek, M. Stiborova, M. Masarik, Int. J. Oncol. 44 (2014) 923.

[14] J. Gumulec, M. Raudenska, V. Adam, R. Kizek, M. Masarik, PLoS One 9 (2014) 1.

[15] V. Adam, R. Kizek, Expert Rev. Proteomics 10 (2013) 211.

[16] T. Endo, M. Yoshikawa, M. Ebara, K. Kato, M. Sunaga, H. Fukuda, A. Hayasaka, F. Kondo, N. Sugiura, H. Saisho, J. Gastroenterol. 39 (2004) 1196.

[17] L. Krejcova, I. Fabrik, D. Hynek, S. Krizkova, J. Gumulec, M. Ryvolova, V. Adam, P. Babula, L. Trnkova, M. Stiborova, J. Hubalek, M. Masarik, H. Binkova, T. Eckschlager, R. Kizek, Int. J. Electrochem. Sci. 7 (2012) 1767.

[18] M. Namdarghanbari, W. Wobig, S. Krezoski, N.M. Tabatabai, D.H. Petering, J. Biol. Inorg. Chem. 16 (2011) 1087.

[19] Y. Fujiwara, M. Satoh, Curr. Pharm. Biotechnol. 14 (2013) 394.

[20] V. Adam, J. Baloun, I. Fabrik, L. Trnkova, R. Kizek, Sensors 8 (2008) 2293.

[21] V. Adam, J. Petrlova, J. Wang, T. Eckschlager, L. Trnkova, R. Kizek, PLoS One 5 (2010) 1.

[22] A. Prange, D. Schaumloffel, Anal. Bioanal. Chem. 373 (2002) 441.

[23] M. Ryvolova, S. Krizkova, V. Adam, M. Beklova, L. Trnkova, J. Hubalek, R. Kizek, Curr. Anal. Chem. 7 (2011) 243.

[24] P.E. Olsson, C. Hogstrand, Journal of Chromatography 402 (1987) 293.

[25] E. Bramanti, C. Lomonte, A. Galli, M. Onor, R. Zamboni, G. Raspi, A. D'Ulivo, J. Chromatogr. A 1054 (2004) 285.

[26] K. Nomiyama, H. Nomiyama, Journal of Chromatography 228 (1982) 285.

[27] K. Nostelbacher, M. Kirchgessner, G.I. Stangl, Journal of Chromatography B 744 (2000) 273.

[28] J. Alhama, A. Romero-Ruiz, J. Lopez-Barea, J. Chromatogr. A 1107 (2006) 52.

[29] H.G. Infante, K. Van Campenhout, R. Blust, F.C. Adams, J. Chromatogr. A 1121 (2006) 184.

[30] B. Tariba, T. Zivkovic, N. Krasnici, V.F. Marijic, M. Erk, M. Gamulin, M. Grgic, A. Pizent, Cancer Chemother. Pharmacol. 75 (2015) 813.

[31] S. Skalickova, O. Zitka, L. Nejdl, S. Krizkova, J. Sochor, L. Janu, M. Ryvolova, D. Hynek, J. Zidkova, V. Zidek, V. Adam, R. Kizek, Chromatographia 76 (2013) 345.

[32] M.A.M. Rodrigo, O. Zitka, S. Krizkova, A. Moulick, V. Adam, R. Kizek, Journal of Pharmaceutical and Biomedical Analysis 95 (2014) 245.

[33] R. Wang, D.A. Sens, A. Albrecht, S. Garrett, S. Somji, M.A. Sens, X. Lu, Analytical Chemistry 79 (2007) 4433.

[34] S. Krizkova, M. Ryvolova, J. Gumulec, M. Masarik, V. Adam, P. Majzlik, J. Hubalek, I. Provaznik, R. Kizek, Electrophoresis 32 (2011) 1952.

[35] L. Nejdl, J. Kudr, K. Cihalova, D. Chudobova, M. Zurek, L. Zalud, L. Kopecny, F. Burian, B. Ruttkay-Nedecky, S. Krizkova, M. Konecna, D. Hynek, P. Kopel, J. Prasek, V. Adam, R. Kizek, Electrophoresis 35 (2014) 2333.

[36] J. Kudr, L. Richtera, L. Nejdl, I. Blazkova, V. Milosavljevic, Z. Moravec, D. Wawrzak, P. Kopel, B. Ruttkay-Nedecky, V. Adam, R. Kizek, Int. J. Electrochem. Sci. 10 (2015) 8243.

[37] M. Usula, F. Mocci, F.C. Marincola, S. Porcedda, L. Gontrani, R. Caminiti, Journal of Chemical Physics 140 (2014).

[38] A.K. Gupta, M. Gupta, Biomaterials 26 (2005) 3995.

[39] D. Huska, V. Adam, P. Babula, L. Trnkova, J. Hubalek, J. Zehnalek, L. Havel, R. Kizek, Microchim. Acta 173 (2011) 189.

[40] V. Adam, D. Huska, J. Hubalek, R. Kizek, Microfluid. Nanofluid. 8 (2010) 329.

[41] M. Erk, B. Raspor, J. Electroanal. Chem. 502 (2001) 174.

[42] K. Tmejova, D. Hynek, P. Kopel, J. Gumulec, S. Krizkova, R. Guran, Z. Heger, M. Kalina, M. Vaculovicova, V. Adam, R. Kizek, Colloids and surfaces. B, Biointerfaces 134 (2015) 262.

[43] D. Hynek, S. Krizkova, L. Krejcova, J. Gumulec, M. Ryvolova, N. Cernei, M. Masarik, V. Adam, L. Trnkova, M. Stiborova, T. Eckschlager, J. Hubalek, R. Kizek, Int. J. Electrochem. Sci. 7 (2012) 1749.

[44] L. Nejdl, H.V. Nguyen, L. Richtera, S. Krizkova, R. Guran, M. Masarik, D. Hynek, Z. Heger, K. Lundberg, K. Erikson, V. Adam, R. Kizek, Electrophoresis 36 (2015) 1894.

[45] K. Tmejova, D. Hynek, P. Kopel, J. Gumulec, S. Krizkova, R. Guran, Z. Heger, M. Kalina, M. Vaculovicova, V. Adam, R. Kizek, Colloid Surf. B-Biointerfaces 134 (2015) 262.

[46] Y. Xue, X. Li, H. Li, W. Zhang, Nature Communications 5 (2014).

[47] F. Bao, J.L. Yao, R.A. Gu, Langmuir 25 (2009) 10782.

[48] S. Karahan, S. Ozkar, Int. J. Hydrog. Energy 40 (2015) 2255.

5.2.2. Reseach IV. Experimetal Chapter: Bacterial expression systems for heterologous mammalian MTs production and characterization by MALDI-TOF MS.

In this experimental chapter, a genetic approach was undertaken to investigate the characterization of mammaliam MTs. Such bacterial cultures can be used as "factories" for the synthesis of valuable eukaryotic proteins that are otherwise difficult to obtain. When bacteria are used to produce a eukaryotic protein, it is desirable to design the system so as to produce as large an amount of the protein as possible. There are several such systems for overproducing foreign proteins in *E. coli*. A constructed expression plasmid, pRSET-B, in which human MT3 and MT-2A genes were inserted downstream of a promoter, was used to transform *Escherichia coli* BL21 (DE3) strain. MTs were successfully expressed in *E. coli*. MT2 protein was directly isolated from rabbit liver by FPLC. Therefore, we show an optimal condition and fast method for characterization the MTs from different mammalian MTs isoforms by MALDI-TOF MS. These initial *in vitro* results have provided motivation to continue these studies for characterization of mammalian isoforms MTs.

5.2.2.1. Isolation and expression of different mammalians MTs, heterologously synthesized in *E. coli*.

Aligned amino acid sequences are listed in **Figure 10.A** to express the similarity in amino acid composition in human and rabbit. Differences of constituent forms come mainly from post-translational modifications, type of incorporated metal ion and speed of degradation. Despite the physicochemical similarity of the forms, their roles and occurrence in tissues vary significantly [195]. The *hMT2A* gen was identified in the NCBI database (NCBI Reference Sequence: NM_005953.3). Isolation of the *hMT2A* gen was used for PCR amplification of DNA from human blood samples (healthy patients)(**Fig.10.B**). The full-length clones of *hMT2A* gene were obtained by PCR

amplification of DNA, using a set of primers flanking the complete open reading frame from 5´ and 3´ UTR. (5´-CAACCTGTCCCGACTCTAGC-3´ (hMT2Afw) and 5´-TTGTGGAAGTCGCGTTCTTT-3´ (hMT2Arev)). PCR products were cloned in the pGEM-T vector and sequenced (Promega, USA). The orientation of the *hMT2A* sequence isolated from the blood samples within the cloning vector was properly checked by sequencing. For expression of *hMT2A* in bacteria was subcloned into pRSET-B vector (**Fig.10.C**). The chemical transformation protocol was performed following the instructions of New England Biolabs, using as host BL21 (DE3) pLysS Chemically Competent *E. coli* strain (for high level expression of recombinant protein). To obtain pRSET-hMT2A, the full-length *hMT2A* was isolated from the pGEM-T vector by digestion with restriction enzyme EcoRI and ligated in into the EcoRI-digested shuttle vector pRSET-B (**Fig.10.C**). The pRSET-B contains n-terminal polyhistidine tag (6xHis-tag), to permits purification of recombinant fusion protein on metal-chelating resins. All plasmids were amplified by transformation of *E. coli* following standard procedures and purified by using the Qiagen Miniprep Kit (Qiagen, Maryland, USA). The all positives transformants were confirmed by PCR screening.

The positive transformants of human MTs (hMT2 and hMT3) were grown in LB (Luria-Bertani) broth with 50 µg/ml ampicillin shaking at 37°C overnight. The next day, the culture was grown to 0.1 of OD 600nm. When the culture reached the exponential fase (0.4-0.6) were added IPTG to a final concentration of 1 mM and continued to grow the cells during 4 hours.

The pellet was frozen at -20°C and then, was resuspended, with 20 mM phosphate buffer at neutral pH. The method of cell lysis was carried out by freeze-thaw cycles. The lysate was frozen in liquid nitrogen and was thawed at 42°C (was repeated this freeze-thaw two to three additional times). The isolation protocol was performed

following the instructions of pRSET A, B, and C for high-level expression of recombinant proteins in *E. coli* (Invitrogen, USA). The protein fraction was harvested by centrifugation during 10 minutes at 4000 rpm at 4°C. The purification of MTs was by FPLC [193].
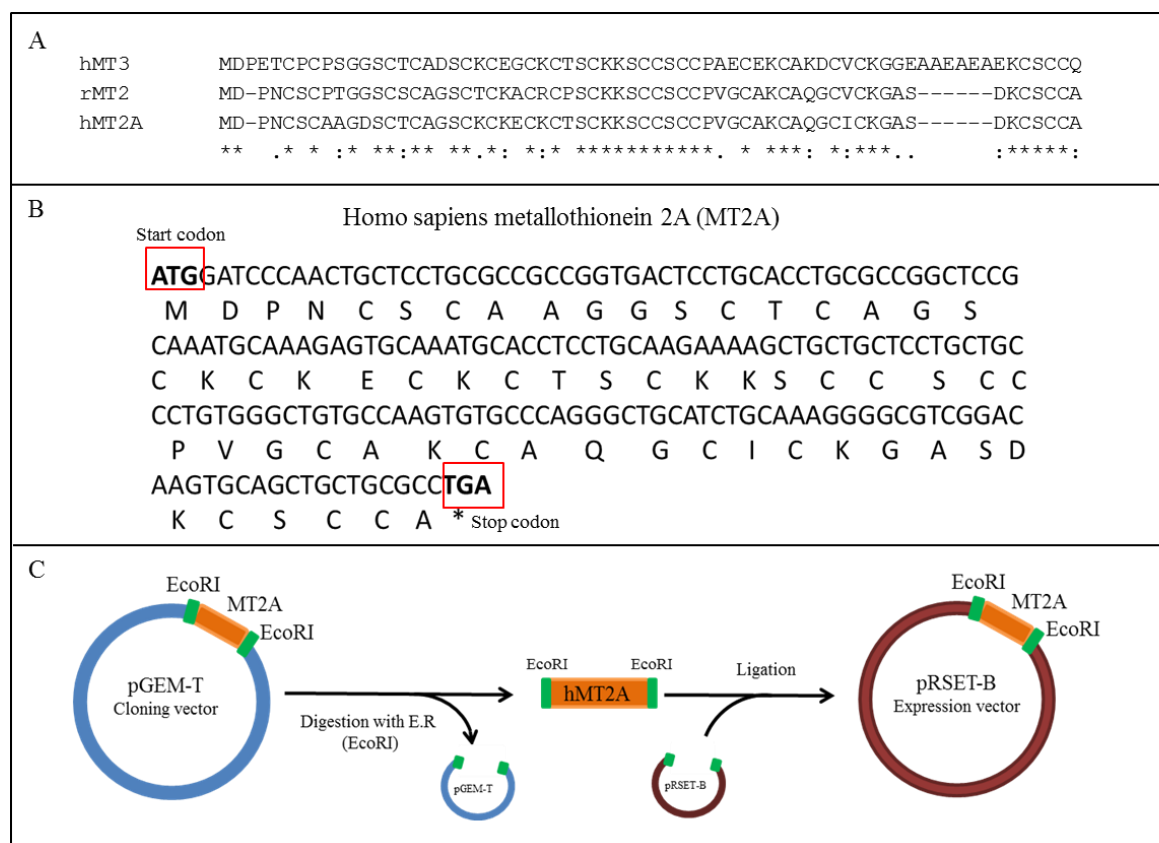
Figure 10: Alignment of amino acid sequences of hMT3, rMT2 and hMT2A isoforms was performed using Multiple sequence alignment ClustalW2 algorithm available at EBI (http://www.ebi.ac.uk/Tools/clustalw2/) (**A**). Nucleotide and amino acid sequences of human metallothionein 2A (*hMT2A*) were cloned in pRSET-B. Vector pRSET is control vector expressing β-galactosidase, which is fused to an *N*-terminal peptide containing the Xpress peptide, 6× His tag and an enterokinase recognition site (**B**). Scheme of subcloning strategy for *hMT2A* from pGEM-T cloning vector to pRSET-B expression vector. EcoRI was the restriction enzyme used for isolation of the full-length gene from pGEM-T cloning vector (**C**). The chemical transformation protocol was performed following the instructions of New England Biolabs, using as host BL21(DE3)pLysS chemically competent *Escherichia coli* strain (for high level expression of recombinant protein). To obtain pRSET-hMT2A, the full-length hMT2A was isolated from the pGEM-T vector by digestion with restriction enzyme EcoRI and ligated in into the EcoRI-digested shuttle vector pRSET-B. The pRSET-B contains N-terminal polyhistidine tag (6× His-tag), to permits purification of recombinant fusion protein on metal-chelating resins. All plasmids were amplified by transformation of *E.*

coli following standard procedures and purified by using the Qiagen Miniprep Kit (Qiagen, MD, USA). All positives transformants were confirmed by PCR screening (data not shown). The positive transformants of human MTs were grown in LB (Luria-Bertani) broth with 50 µg·mL^{-1} ampicillin and 35 µg·mL^{-1} chloramphenicol. The isolation protocol was performed following the instructions of pRSET A, B, and C for high-level expression of recombinant proteins in *E. coli* (Invitrogen, Waltham, MA, USA).

5.2.2.2. Characterization of MTs by MALDI-TOF MS.

The matrix consists of small organic compounds, which show strong resonance absorption at the applied laser wavelength. In the most of the studies reviewed, 2,5-dihydroxybenzoic acid (2,5-DHB) and α-cyano-4-hydroxycinnamic acid (HCCA) were the constituents of matrix used for appropriate determination of MTs [101, 183]. In our study, 2.5-DHB showed high increased of signal intensity (a.u) than HCCA when increased the concentration of rMT2 (**Fig. 11. A.1**). Other novel result was that 2.5-DHB removed the background from other compounds in interaction with the matrix and producing interference in the signal of spectra (**Fig. 11. A.2 and A.3**).

To verify that MTs were expressed in bacteria correctly, we analyzed it by MALDI-TOF. It is evident that Apo-MTs were not found, all MTs were expressed in heterologous organisms, so that they appear to form chelation or bidding to other proteins, metals or compounds from the bacteria, culture medium and buffers. The main observed signals for MTs shown in (**Fig. 11**) were assigned as follows: [rMT2]$^+$ (m/z 6210.94) (**Fig. 11.A.1**), [6xHis-tag-hMT2A]$^+$ (m/z 7278.29) (**Fig. 11.B**) (correspond to matrix cluster with 6 His-tag, the hMT2A protein have an added 1 kDa of molecular weight) and [hMT3]$^+$ (m/z 6907.37) (**Fig. 11.C**). Data included in this experimental chapter highlight the potential of spectroscopic strategies as MALDI-TOF MS, for monitoring structural differences among MTs.
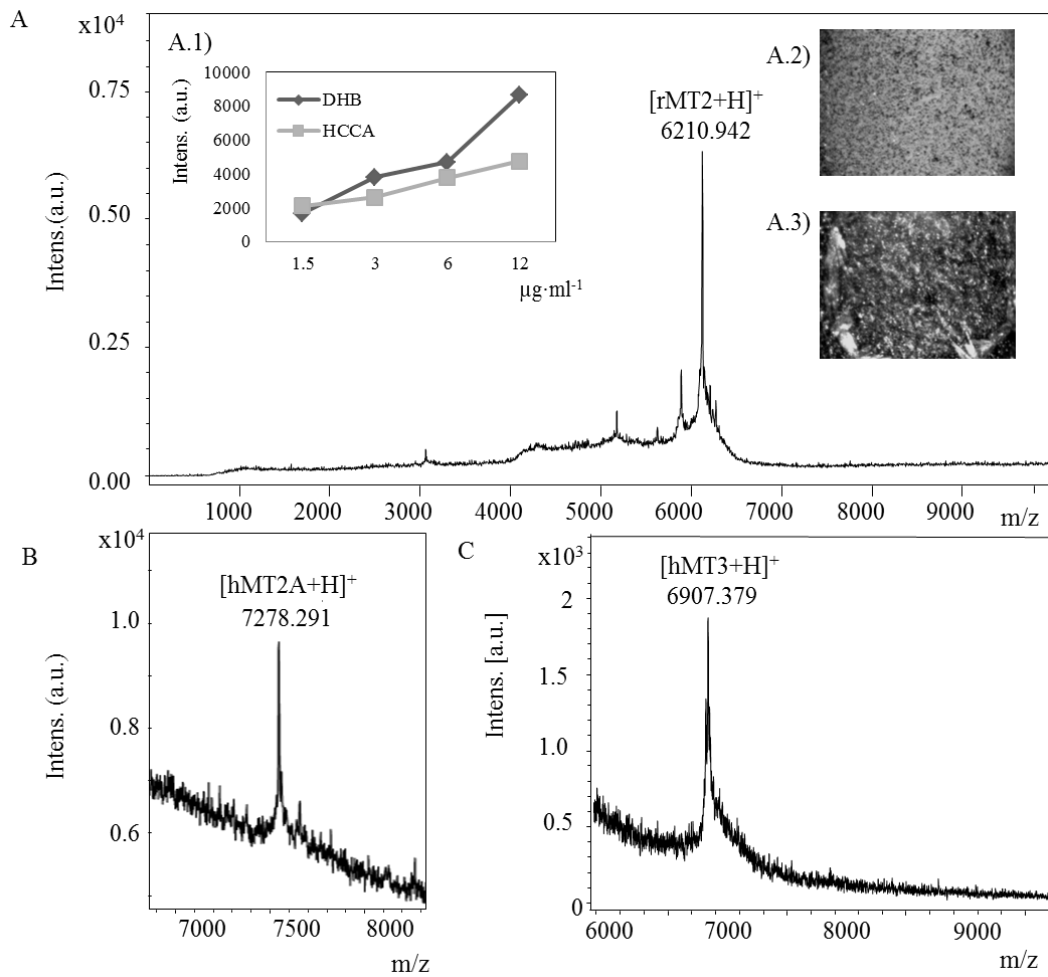
Figure 11: (**A.1**) Spectrum of rMT2 liver measured by MALDI-TOF MS with HCCA matrix and graphs of signal intensity of different concentrations of rMT2 in DHB and HCCA matrixes. Photo of the MTs crystals on a target plate using (**A.2**) DHB and (**A.3**) HCCA matrix. (**B**) Demonstrates spectrum of hMT2A with 6× His-tag and (**C**) hMT3 measured by using MALDI-TOF MS with DHB matrix prepared in TA30 at a maximum energy of 43.2 µJ with repetition rate 2000 Hz.

6. Conclusion

The plants and animals have adapted numerous ways to maintain metal homeostasis while mitigating detrimental effects of excess metals ions, including MTs and PCs. MTs constitute a very wide family of ubiquitous proteins with features that are exceptional from the perspectives both of biology and coordination chemistry. If compared with all other metalloproteins, MTs are wholly unconventional because of their small size, their extremely high thiolate sulfur and metal content. In this work for, as a first step, the optimal condition for characterization and indentification tiols (PCs and MTs) and metal-thiols complexes by MALDI-TOF MS was investigated. Subsequently, model of complex between Cd^{+2} ion and one molecules of PC2 was described. Studying of complexes among proteins and metals are of great interest for numerous branches. The obtained data show that MALDI-TOF MS was a reliable and fast method for the determination of these complexes. Also, IEC and the FIA coupled with electrochemical detection Coulochem III or/and Coularray can be other method for detemination Cd-PC2 complexes. These methods have been demonstrated to be ideal and promising techniques for screening and characterizing *in vitro* peptide-metal complexes. It was demonstrated that theses techniques had the ability to identify the formation of Cd-PC2 complex.

The optimal condition for characterization rabbit liver MTs by MALDI-TOF was determinated. The optimization of bead-based isolation of MTs terminated by electrochemical detection was investigated. This fully automated procedure could be used for detection of other specific emergency biomolecules also. Rabbit liver MT was isolated using functionalized maghemite particles-based material in fully automated implementation for electrochemical determination of a large number of samples in one assay. Data presented in this work highlighted the potential of MALDI-TOF MS to be used for monitoring differences isoforms of mammalian MTs. In particular, the MT3 and MT2A genes were isolated from human cells. The human MT2A and MT3 genes were expressed in heterologous organisms (*Escherichia coli*) by cloning. The present study demonstrates analytical approaches of employing MALDI-TOF/TOF MS for characterization mammalians MTs and this method proves to have advantages over other methods currently used, namely in terms of sensitivity, simplicity and analysis time.

7.   Abbreviations

2-DGE: two dimensional (2-D) gel electrophoresis
2-5-DHB: 2-5-dihydrobenzoic acid
AdTS-DPV: adsorptive stripping differential pulse voltammetry
BAX: essential regulators of proapoptotic signaling
CD: circular dichroism
CE-ESI-TOF-MS: capillary electrophoresis-Electrospray ionization-Time of Flight mass spectrometry
CR-EAE: chronic relapsing experimental autoimmune encephalomyelitis
DD: drop dry
DL: drop layer
DNA: deoxyribonucleic acid
DO: density optical
ELISA: enzyme-linked immunosorbent assay
EPR: electron paramagnetic resonance
ESI: electrospray ionization
FIA: flow injection analysis
FPLC: fast protein liquid chromatography
GREs: glucocorticoid response element
GSH: reduced glutathione
GSSH: oxidized glutathione
HCCA: α-cyano-4-hydroxycinnamic acid
HDVs: hydrodynamic voltammogram
HM: heavy metal
HMDE: hanging mercury drop electrode
HPLC: high-performance liquid chromatography
ICP MS: inductively coupled plasma mass spectrometry
IEC: ion exchange chromatography
IPTG: isopropyl β-D-1-thiogalactopyranoside
LB: Luria-Bertani medium
MALDI-TOF: matrix assisted laser desorption/ionization-time of flight mass spectrometric
mRNA: messenger ribonucleic acid
MREs: metal-responsive elements
MRM: multiple Reaction Monitoring
MTs: metallothioneins
MTF: metal-responsive transcription factor
NADPH: nicotinamide adenine dinucleotide phosphate
NO: nitric Oxide
NRAMP: natural resistance associated macrophage protein
PCR: polymerase chain reaction
PCs: phytochelatins
PMF: peptide mass fingerprinting
q-RT-PCR: quantitate real time polymerase chain reaction
RIA: radioimmunoassay
ROS: reactive oxygen specie
SDS-PAGE: sodium dodecyl sulfate polyacrylamide gel electrophoresis

siRNA: small interfering RNA
SNCLC: non-small-cell lung carcinoma
SOC: super optimal broth
TA30: (30:70 [*v/v*] acetonitrile : TFA 0.1% in water)
TFA: trifluoroacetic acid
TL: thin layer
TP-Pt(II): terpyridine platinum(II)
UPLC: ultra performance liquid chromatography
UV: ultraviolent

8. Literature

[1]   G. Wu, H. Kang, X. Zhang, H. Shao, L. Chu and C. Ruan, *Journal of Hazardous Materials*, **2010**, *174*, 1.
[2]   Y. N. Vodyanitskii, *Eurasian Soil Science*, **2013**, *46*, 793.
[3]   W.-y. Shi, H.-b. Shao, H. Li, M.-a. Shao and S. Du, *Journal of Hazardous Materials*, **2009**, *170*, 1.
[4]   S. S. Sharma and K.-J. Dietz, *Trends in Plant Science*, **2009**, *14*, 43.
[5]   S. K. Yadav, *South African Journal of Botany*, **2010**, *76*, 167.
[6]   A. Emamverdian, Y. Ding, F. Mokhberdoran and Y. Xie, *TheScientificWorldJournal*, **2015**, *2015*, 756120.
[7]   G. K. Harris and X. Shi, *Mutation Research-Fundamental and Molecular Mechanisms of Mutagenesis*, **2003**, *533*, 183.
[8]   C. Cobbett and P. Goldsbrough, *Annual Review of Plant Biology*, **2002**, *53*, 159.
[9]   P. A. Rea, *Physiologia Plantarum*, **2012**, *145*, 154.
[10]   D. G. Mendoza-Cozatl, E. Butko, F. Springer, J. W. Torpey, E. A. Komives, J. Kehr and J. I. Schroeder, *Plant Journal*, **2008**, *54*, 249.
[11]   W. E. Rauser, *Cell Biochemistry and Biophysics*, **1999**, *31*, 19.
[12]   M. H. Zenk, *Gene*, **1996**, *179*, 21.
[13]   M. Pivato, M. Fabrega-Prats and A. Masi, *Archives of Biochemistry and Biophysics*, **2014**, *560*, 83.
[14]   S. Clemens, E. J. Kim, D. Neumann and J. I. Schroeder, *Embo Journal*, **1999**, *18*, 3325.
[15]   A. Bolchi, R. Ruotolo, G. Marchini, E. Vurro, L. S. di Toppi, A. Kohler, E. Tisserant, F. Martin and S. Ottonello, *Fungal Genetics and Biology*, **2011**, *48*, 573.
[16]   O. K. Vatamaniuk, E. A. Bucher, J. T. Ward and P. A. Rea, *Journal of Biological Chemistry*, **2001**, *276*, 20817.
[17]   F. Brulle, C. Cocquerelle, A. N. Wamalah, A. J. Morgan, P. Kille, A. Lepretre and F. Vandenbuicke, *Ecotoxicology and Environmental Safety*, **2008**, *71*, 47.
[18]   D. Ray and D. L. Williams, *Plos Neglected Tropical Diseases*, **2011**, *5*.
[19]   R. Elran, M. Raam, R. Kraus, V. Brekhman, N. Sher, I. Plaschkes, V. Chalifa-Caspi and T. Lotan, *Molecular Ecology*, **2014**, *23*, 4722.
[20]   N. Polak, D. S. Read, K. Jurkschat, M. Matzke, F. J. Kelly, D. J. Spurgeon and S. R. Stuerzenbaum, *Comparative Biochemistry and Physiology C-Toxicology & Pharmacology*, **2014**, *160*, 75.
[21]   C. Rigouin, J. J. Vermeire, E. Nylin and D. L. Williams, *Molecular and Biochemical Parasitology*, **2013**, *191*, 1.
[22]   M. S. Schwartz, J. L. Benci, D. S. Selote, A. K. Sharma, A. G. Y. Chen, H. Dang, H. Fares and O. K. Vatamaniuk, *Plos One*, **2010**, *5*.
[23]   N. A. Anjum, M. Hasanuzzaman, M. A. Hossein, P. Thangavel, A. Roychoudhury, S. S. Gill, M. A. M. Rodrigo, V. Adam, M. Fujita, R. Kizek, A. C. Duarte, E. Pereira and I. Ahmed, *Frontiers in Plant Science*, **2015**, *6*.
[24]   J. Yoon, X. Cao, Q. Zhou and L. Q. Ma, *Science of the Total Environment*, **2006**, *368*, 456.
[25]   S. J. S. Flora, M. Mittal and A. Mehta, *Indian Journal of Medical Research*, **2008**, *128*, 501.
[26]   N. Rascio and F. Navari-Izzo, *Plant Science*, **2011**, *180*, 169.
[27]   A. Raab, J. Feldmann and A. A. Meharg, *Plant Physiology*, **2004**, *134*, 1113.
[28]   H. Bashir, M. M. Ibrahim, R. Bagheri, J. Ahmad, I. A. Arif, M. A. Baig and M. I. Qureshi, *Aob Plants*, **2015**, *7*, LV1.

[29]   D. K. Gupta, H. G. Huang and F. J. Corpas, *Environmental Science and Pollution Research*, **2013**, *20*, 2150.

[30]   Y.-O. Kim, S. Jung, K. Kim and H.-J. Bae, *Plant Physiology and Biochemistry*, **2013**, *64*, 25.

[31]   M. A. Pagani, M. Tomas, J. Carrillo, R. Bofill, M. Capdevila, S. Atrian and C. S. Andreo, *Journal of Inorganic Biochemistry*, **2012**, *117*, 306.

[32]   K. Hazama, S. Nagata, T. Fujimori, S. Yanagisawa and T. Yoneyama, *Physiologia Plantarum*, **2015**, *154*, 243.

[33]   A. V. Castro, A.-A. F. de Almeida, C. P. Pirovani, G. S. M. Reis, N. M. Almeida and P. A. O. Mangabeira, *Ecotoxicology and Environmental Safety*, **2015**, *115*, 174.

[34]   B. D. Lee and S. Hwang, *Plant Biotechnology Reports*, **2015**, *9*, 107.

[35]   F. Degola, M. De Benedictis, A. Petraglia, A. Massimi, L. Fattorini, S. Sorbo, A. Basile and L. S. di Toppi, *Plant and Cell Physiology*, **2014**, *55*, 1884.

[36]   S. Fischer, T. Kuehnlenz, M. Thieme, H. Schmidt and S. Clemens, *Environmental Science & Technology*, **2014**, *48*, 7552.

[37]   J. D. Garcia, D. G. Mendoza-Cozatl and R. Moreno-Sanchez, *Protein Science*, **2014**, *23*, 185.

[38]   T. Kuehlenz, H. Schmidt, S. Uraguchi and S. Clemens, *Journal of Experimental Botany*, **2014**, *65*, 4241.

[39]   M. A. M. Rodrigo, in A. K. Shanker (Editor), Abiotic and Biotic Stress in Plants - Recent Advances and Future Perspectives, 2016.

[40]   D. Gonzalez-Mendoza, A. Q. Moreno and O. Zapata-Perez, *Aquatic Toxicology*, **2007**, *83*, 306.

[41]   J. Freeman, J. Gustin and D. Salt, *Plant Biology (Rockville)*, **2005**, *2005*, 111.

[42]   H. Schat, M. Llugany, R. Vooijs, J. Hartley-Whitaker and P. M. Bleeker, *Journal of Experimental Botany*, **2002**, *53*, 2381.

[43]   L. Zagorchev, C. E. Seal, I. Kranner and M. Odjakova, *International Journal of Molecular Sciences*, **2013**, *14*, 7405.

[44]   S. Mishra, S. Srivastava, R. D. Tripathi, R. Govindarajan, S. V. Kuriakose and M. N. V. Prasad, *Plant Physiology and Biochemistry*, **2006**, *44*, 25.

[45]   M. Jozefczak, E. Keunen, H. Schat, M. Bliek, L. E. Hernandez, R. Carleer, T. Remans, S. Bohler, J. Vangronsveld and A. Cuypers, *Plant Physiology and Biochemistry*, **2014**, *83*, 1.

[46]   Y. J. Li, O. P. Dhankher, L. Carreira, D. Lee, A. Chen, J. I. Schroeder, R. S. Balish and R. B. Meagher, *Plant and Cell Physiology*, **2004**, *45*, 1787.

[47]   M. F. Lopez-Climent, V. Arbona, R. M. Perez-Clemente, S. I. Zandalinas and A. Gomez-Cadenas, *Plant Biology*, **2014**, *16*, 79.

[48]   J. P. Stolt, F. E. C. Sneller, T. Bryngelsson, T. Lundborg and H. Schat, *Environmental and Experimental Botany*, **2003**, *49*, 21.

[49]   M. Liebeke, I. Garcia-Perez, C. J. Anderson, A. J. Lawlor, M. H. Bennett, C. A. Morris, P. Kille, C. Svendsen, D. J. Spurgeon and J. G. Bundy, *Plos One*, **2013**, *8*.

[50]   J. G. Bundy, P. Kille, M. Liebeke and D. J. Spurgeon, *Environmental Science & Technology*, **2014**, *48*, 885.

[51]   Y. Cui, S. J. McBride, W. A. Boyd, S. Alper and J. H. Freedman, *Genome Biology*, **2007**, *8*.

[52]   J. Hall, K. L. Haas and J. H. Freedman, *Toxicological Sciences*, **2012**, *128*, 418.

[53]   O. K. Vatamaniuk, E. A. Bucher, M. V. Sundaram and P. A. Rea, *Journal of Biological Chemistry*, **2005**, *280*, 23684.

[54]   B. A. Wood and J. Feldmann, *Analytical and Bioanalytical Chemistry*, **2012**, *402*, 3299.

[55]   X. H. Ju, S. R. Tang, Y. Jia, J. K. Guo, Y. Z. Ding, Z. G. Song and Y. J. Zhao, *Journal of Chromatography B-Analytical Technologies in the Biomedical and Life Sciences*, **2011**, *879*, 1717.
[56]   S. K. Kawakami, M. Gledhill and E. P. Achterberg, *Trac-Trends in Analytical Chemistry*, **2006**, *25*, 133.
[57]   V. Vacchina, H. Chassaigne, M. Oven, M. H. Zenk and R. Lobinski, *Analyst*, **1999**, *124*, 1425.
[58]   D. Baralkiewicz, M. Kozka, A. Piechalak, B. Tomaszewska and P. Sobczak, *Talanta*, **2009**, *79*, 493.
[59]   A. Braeutigam, D. Wesenberg, H. Preud'homme and D. Schaumloeffel, *Analytical and Bioanalytical Chemistry*, **2010**, *398*, 877.
[60]   M. A. M. Rodrigo, N. Cernei, M. Kominkova, O. Zitka, M. Beklova, J. Zehnalek, R. Kizek and V. Adam, *International Journal of Environmental Research and Public Health*, **2013**, *10*, 1304.
[61]   M. A. M. Rodrigo, O. Zitka, M. Kominkova, V. Adam, M. Beklova and R. Kizek, *International Journal of Electrochemical Science*, **2013**, *8*, 4409.
[62]   O. Zitka, H. Skutkova, O. Krystofova, P. Sobrova, V. Adam, J. Zehnalek, L. Havel, M. Beklova, J. Hubalek, I. Provaznik and R. Kizek, *International Journal of Electrochemical Science*, **2011**, *6*, 1367.
[63]   O. Zitka, K. Stejskal, A. Kleckerova, V. Adam, M. Beklova, A. Horna, V. Supalkova, L. Havel and R. Kizek, *Chemicke Listy*, **2007**, *101*, 225.
[64]   J. Skladanka, V. Adam, O. Zitka, O. Krystofova, M. Beklova, R. Kizek, Z. Havlicek, P. Slama and A. Nawrath, *International Journal of Environmental Research and Public Health*, **2012**, *9*, 3789.
[65]   R. Nakazawa, H. Kato, Y. Kameda and H. Takenaga, *Biologia Plantarum*, **2002**, *45*, 311.
[66]   S. Ogawa, T. Yoshidomi, T. Shirabe and E. Yoshimura, *Journal of Inorganic Biochemistry*, **2010**, *104*, 442.
[67]   H. Mikulaskova, M. A. R. Merlos, O. Zitka, M. Kominkova, D. Hynek, V. Adam, M. Beklova and R. Kizek, *International Journal of Electrochemical Science*, **2013**, *8*, 4505.
[68]   L. Xu, Y. Wang, L. L. Zhai, Y. Y. Xu, L. J. Wang, X. W. Zhu, Y. Q. Gong, R. G. Yu, C. Limera and L. W. Liu, *Journal of Experimental Botany*, **2013**, *64*, 4271.
[69]   F. Amaro, R. Ruotolo, A. Martin-Gonzalez, A. Faccini, S. Ottonello and J. C. Gutierrez, *Comparative Biochemistry and Physiology C-Toxicology & Pharmacology*, **2009**, *149*, 598.
[70]   F. Liu, S. H. Kang, Y.-I. Lee, Y.-h. Choa, A. Mulchandani, N. V. Myung and W. Chen, *Applied Physics Letters*, **2010**, *97*.
[71]   S. A. Kumar, M. K. Abyaneh, S. W. Gosavi, S. K. Kulkarni, A. Ahmad and M. I. Khan, *Biotechnology and Applied Biochemistry*, **2007**, *47*, 191.
[72]   N. Krumov, I. Perner-Nochta, S. Oder, V. Gotchev, A. Angelov and C. Posten, *Chemical Engineering & Technology*, **2009**, *32*, 1026.
[73]   E. M. Gioacchino Scarano, *Plant Science*, **2003**, *165: 803-810.*
[74]   E. Morelli, B. H. Cruz, S. Somovigo and G. Scarano, *Plant Science*, **2002**, *163*, 807.
[75]   N. Krumov, S. Oder, I. Perner-Nochta, A. Angelov and C. Posten, *Journal of Biotechnology*, **2007**, *132*, 481.
[76]   B. Nowack, C. Brouwer, R. E. Geertsma, E. H. W. Heugens, B. L. Ross, M.-C. Toufektsian, S. W. P. Wijnhoven and R. J. Aitken, *Nanotoxicology*, **2013**, *7*, 1152.

[77]   N. Polak, D. S. Read, K. Jurkschat, M. Matzke, F. J. Kelly, D. J. Spurgeon and S. R. Sturzenbaum, *Comparative Biochemistry and Physiology C-Toxicology & Pharmacology*, **2014**, *160*, 75.

[78]   O. Krystofova, J. Sochor, O. Zitka, P. Babula, V. Kudrle, V. Adam and R. Kizek, *International Journal of Environmental Research and Public Health*, **2013**, *10*, 47.

[79]   J. H. Kagi and B. L. Vallee, *The Journal of biological chemistry*, **1961**, *236*, 2435.

[80]   J. H. R. Kagi, *Federation Proceedings*, **1960**, *19*, 340.

[81]   J. H. R. Kagi and B. L. Vallee, *Journal of Biological Chemistry*, **1960**, *235*, 3460.

[82]   M. Margoshes and B. L. Vallee, *Journal of the American Chemical Society*, **1957**, *79*, 4813.

[83]   A. Torreggiani and A. Tinti, *Metallomics*, **2010**, *2*, 246.

[84]   P. Babula, M. Masarik, V. Adam, T. Eckschlager, M. Stiborova, L. Trnkova, H. Skutkova, I. Provaznik, J. Hubalek and R. Kizek, *Metallomics*, **2012**, *4*, 739.

[85]   N. Thirumoorthy, K. T. M. Kumar, A. S. Sundar, L. Panayappan and M. Chatterjee, *World Journal of Gastroenterology*, **2007**, *13*, 993.

[86]   M. Ryvolova, S. Krizkova, V. Adam, M. Beklova, L. Trnkova, J. Hubalek and R. Kizek, *Current Analytical Chemistry*, **2011**, *7*, 243.

[87]   R. Nath, R. Kambadur, S. Gulati, V. K. Paliwal and M. Sharma, *Crc Critical Reviews in Food Science and Nutrition*, **1988**, *27*, 41.

[88]   H. Skutkova, P. Babula, M. Stiborova, T. Eckschlager, L. Trnkova, I. Provaznik, J. Hubalek, R. Kizek and V. Adam, *International Journal of Electrochemical Science*, **2012**, *7*, 12415.

[89]   K. Ghoshal and S. T. Jacob, *Progress in Nucleic Acid Research and Molecular Biology, Vol 66*, **2001**, *66*, 357.

[90]   M. Vasak and G. Meloni, *Journal of Biological Inorganic Chemistry*, **2011**, *16*, 1067.

[91]   E. Hijova, *Bratislavske lekarske listy*, **2004**, *105*, 230.

[92]   K. Kita, N. Miura, M. Yoshida, K. Yamazaki, T. Ohkubo, Y. Imai and A. Naganuma, *Human Genetics*, **2006**, *120*, 553.

[93]   W. A. Solis, N. L. Childs, D. W. Nebert and T. P. Dalton, *Abstracts of the General Meeting of the American Society for Microbiology*, **2001**, *101*, 731.

[94]   G. K. Andrews, *Biochemical Pharmacology*, **2000**, *59*, 95.

[95]   R. Heuchel, F. Radtke and W. Schaffner, Transcriptional regulation by heavy metals, exemplified at the metallothionein genes, 1995.

[96]   A. L. Albrecht, R. K. Singh, S. Somji, M. A. Sens, D. A. Sens and S. H. Garrett, *Journal of Applied Toxicology*, **2008**, *28*, 283.

[97]   C. Howells, A. K. West and R. S. Chung, *Febs Journal*, **2010**, *277*, 2931.

[98]   S. Takahashi, *Journal of Hematology & Oncology*, **2012**, *5*.

[99]   M. Knipp, *Current Medicinal Chemistry*, **2009**, *16*, 522.

[100] C. Wuelfing, H. van Ahlen, E. Eltze, H. Piechota, L. Hertle and K.-W. Schmid, *World Journal of Urology*, **2007**, *25*, 199.

[101] G. Zhang, W. Hu, Z. Du, S. Lv, W. Zheng, Q. Luo, X. Li, K. Wu, Y. Han and F. Wang, *International Journal of Mass Spectrometry*, **2011**, *307*, 79.

[102] A. Zamirska, L. Matusiak, P. Dziegiel, G. Szybejko-Machaj and J. C. Szepietowski, *Pathology & Oncology Research*, **2012**, *18*, 849.

[103]   G. Ohshio, T. Imamura, N. Okada, Z. H. Wang, K. Yamaki, T. Kyogoku, H. Suwa, H. Yamabe and M. Imamura, *Journal of Cancer Research and Clinical Oncology*, **1996**, *122*, 351.

[104]   M. Sliwinska-Mosson, H. Milnerowicz, J. Rabczynski and S. Milnerowicz, *Archivum Immunologiae Et Therapiae Experimentalis*, **2009**, *57*, 295.

[105]   S. V. Cardoso, J. B. Silveira-Junior, V. D. C. Machado, A. M. Batista De-Paula, A. M. Loyola and M. C. Ferreira De Aguiar, *Anticancer Research*, **2009**, *29*, 1189.

[106]   Y. Hishikawa, T. Koji, D. K. Dhar, S. Kinugasa, M. Yamaguchi and N. Nagasue, *British Journal of Cancer*, **1999**, *81*, 712.

[107]   G. Weinlich, K. Eisendle, E. Hassler, M. Baltaci, P. O. Fritsch and B. Zelger, *British Journal of Cancer*, **2006**, *94*, 835.

[108]   M. G. Joseph, D. Banerjee, W. Kocha, R. Feld, L. W. Stitt and M. G. Cherian, *Cancer*, **2001**, *92*, 836.

[109]   B. Peng, Y. Gu, Y. Xiong, G. Zheng and Z. He, *Plos One*, **2012**, *7*.

[110]   M. Mita, M. Satoh, A. Shimada, S. Azuma, S. Himeno and S. Hara, *Journal of Toxicological Sciences*, **2012**, *37*, 1261.

[111]   H. Ozer, G. Yenicesu, S. Arici, M. Cetin, E. Tuncer and A. Cetin, *Diagnostic Pathology*, **2012**, *7*.

[112]   D. Duval, M. Trouillas, C. Thibault, D. Dembele, F. Diemunsch, B. Reinhardt, A. L. Mertz, A. Dierich and H. Bouf, *Cell Death and Differentiation*, **2006**, *13*, 564.

[113]   P. M. Bagheri, M. T. Rahman, S. Van Soest and M. De Ley, *Journal of Trace Elements in Medicine and Biology*, **2009**, *23*, 124.

[114]   P. M. Bagheri and M. De Ley, *Cell Biology International*, **2011**, *35*, 39.

[115]   A. B. Abdel-Mageed, F. S. Zhao, B. J. Rider and K. C. Agrawal, *Experimental Biology and Medicine*, **2003**, *228*, 1033.

[116]   M. G. Cherian, A. Jayasurya and B.-H. Bay, *Mutation Research-Fundamental and Molecular Mechanisms of Mutagenesis*, **2003**, *533*, 201.

[117]   R. X. Jin, J. X. Huang, P. H. Tan and B. H. Bay, *Pathology & Oncology Research*, **2004**, *10*, 74.

[118]   B. Werynska, B. Pula, B. Muszczynska-Bernhard, A. Gomulkiewicz, A. Piotrowska, R. Prus, M. Podhorska-Okolow, R. Jankowska and P. Dziegiel, *Experimental and Molecular Pathology*, **2013**, *94*, 301.

[119]   J. E. Peixoto-Santos, O. Y. Galvis-Alonso, T. R. Velasco, L. Kandratavicius, J. A. Assirati, C. G. Carlotti, R. C. Scandiuzzi, L. N. Serafini and J. P. Leite, *Plos One*, **2012**, *7*.

[120]   H. Jakovac, D. Grebic, M. Tota, V. Barac-Latas, I. Mrakovcic-Sutic, C. Milin and B. Radosevic-Stasic, *Histology and Histopathology*, **2011**, *26*, 233.

[121]   B. Ruttkay-Nedecky, L. Nejdl, J. Gumulec, O. Zitka, M. Masarik, T. Eckschlager, M. Stiborova, V. Adam and R. Kizek, *International Journal of Molecular Sciences*, **2013**, *14*, 6044.

[122]   N. Chiaverini and M. De Ley, *Free Radical Research*, **2010**, *44*, 605.

[123]   L. Cai, J. B. Klein and Y. J. Kang, *Journal of Biological Chemistry*, **2000**, *275*, 38957.

[124]   M. B. Iszard, J. Liu and C. D. Klassen, *Toxicology*, **1995**, *104*, 25.

[125]   M. Satoh, Y. Kondo, M. Mita, I. Nakagawa, A. Naganuma and N. Imura, *Cancer Research*, **1993**, *53*, 4767.

[126]   A. R. Quesada, R. W. Byrnes, S. O. Krezoski and D. H. Petering, *Archives of Biochemistry and Biophysics*, **1996**, *334*, 241.

[127]   H. Wu, S. S. Zhou, L. L. Kong, J. Chen, W. K. Feng, J. Cai, L. N. Miao and Y. Tan, *Toxicology Letters*, **2015**, *232*, 340.

[128]   Y. Ogra, S. Onishi, A. Kajiwara, A. Hara and K. T. Suzuki, *Journal of Health Science*, **2008**, *54*, 339.

[129]   L. Cai, J. X. Wang, Y. Li, X. H. Sun, L. P. Wang, Z. X. Zhou and Y. J. Kang, *Diabetes*, **2005**, *54*, 1829.

[130]   W. Maret, *Journal of Chromatography B-Analytical Technologies in the Biomedical and Life Sciences*, **2009**, *877*, 3378.

[131]   N. Thirumoorthy, A. S. Sunder, K. T. M. Kumar, M. S. Kumar, G. N. K. Ganesh and M. Chatterjee, *World Journal of Surgical Oncology*, **2011**, *9*.

[132]   M. O. Pedersen, A. Larsen, M. Stoltenberg and M. Penkowa, *Progress in Histochemistry and Cytochemistry*, **2009**, *44*, 1.

[133]   R. S. Chung, M. Penkowa, J. Dittmann, C. E. King, C. Bartlett, J. W. Asmussen, J. Hidalgo, J. Carrasco, Y. K. J. Leung, A. K. Walker, S. J. Fung, S. A. Dunlop, M. Fitzgerald, L. D. Beazley, M. I. Chuah, J. C. Vickers and A. K. West, *Journal of Biological Chemistry*, **2008**, *283*, 15349.

[134]   M. Zalewska, J. Trefon and H. Milnerowicz, *Proteomics*, **2014**, *14*, 1343.

[135]   C. A. Sogawa, M. Asanuma, N. Sogawa, I. Miyazaki, T. Nakanishi, H. Furuta and N. Ogawa, *Acta Medica Okayama*, **2001**, *55*, 1.

[136]   J. Hidalgo, *Environmental health and preventive medicine*, **2004**, *9*, 87.

[137]   K. J. Barnham, C. L. Masters and A. I. Bush, *Nature Reviews Drug Discovery*, **2004**, *3*, 205.

[138]   K. J. Barnham, R. Cappai, K. Beyreuther, C. L. Masters and A. F. Hill, *Trends in Biochemical Sciences*, **2006**, *31*, 465.

[139]   K.-i. Inoue, H. Takano, A. Shimada and M. Satoh, *Mediators of inflammation*, **2009**, *2009*, 101659.

[140]   H. Miyazaki, N. Oka, A. Koga, H. Ohmura, T. Ueda and T. Imaizumi, *Hypertension Research*, **2006**, *29*, 1029.

[141]   P. Coyle, J. C. Philcox, L. C. Carey and A. M. Rofe, *Cellular and Molecular Life Sciences*, **2002**, *59*, 627.

[142]   P. Athanassiadou, A. Bantis, M. Gonidi, P. Athanassiades, E. Agelonidou, D. Grapsa, P. Nikolopoulou and E. Patsouris, *Tumori*, **2007**, *93*, 189.

[143]   S. Bolognin, B. Cozzi, P. Zambenedetti and P. Zatta, *Journal of Alzheimers Disease*, **2014**, *41*, 29.

[144]   P. Adam, S. Krizkova, Z. Heger, P. Babula, V. Pekarik, M. Vaculovicova, C. M. Gomes, R. Kizek and V. Adam, *Journal of Alzheimers Disease*, **2016**, *51*, 637.

[145]   K. Terpe, *Applied Microbiology and Biotechnology*, **2006**, *72*, 211.

[146]   T. Makino, G. Skretas and G. Georgiou, *Microbial Cell Factories*, **2011**, *10*.

[147]   G. L. Rosano and E. A. Ceccarelli, *Frontiers in Microbiology*, **2014**, *5*.

[148]   F. Odawara, M. Kurasaki, M. Suzukikurasaki, S. Oikawa, T. Emoto, F. Yamasaki, A. R. L. Arias and Y. Kojima, *Journal of Biochemistry*, **1995**, *118*, 1131.

[149]   V. Adam, D. Chudobova, K. Tmejova, K. Cihalova, S. Krizkova, R. Guran, M. Kominkova, M. Zurek, M. Kremplova, A. M. J. Jimenez, M. Konecna, D. Hynek, V. Pekarik and R. Kizek, *Electrochimica Acta*, **2014**, *140*, 11.

[150]   M. J. Stillman, *Coordination Chemistry Reviews*, **1995**, *144*, 461.

[151]   K. E. R. Duncan, C. W. Kirby and M. J. Stillman, *Febs Journal*, **2008**, *275*, 2227.

[152]   E. Gottschalg, N. E. Moore, A. K. Ryan, L. C. Travis, R. C. Waller, S. Pratt, M. Atmaca, C. N. Kind and J. R. Fry, *Chemico-Biological Interactions*, **2006**, *161*, 251.

[153]   C. Ferrario, P. Lavagni, M. Gariboldi, C. Miranda, M. Losa, L. Cleris, F. Formelli, S. Pilotti, M. A. Pierotti and A. Greco, *Laboratory Investigation*, **2008**, *88*, 474.

[154] S.-S. Lee, S.-F. Yang, Y.-C. Ho, C.-H. Tsai and Y.-C. Chang, *Oral Oncology*, **2008**, *44*, 180.

[155] H. Wei, M. M. Desouki, S. Lin, D. Xiao, R. B. Franklin and P. Feng, *Molecular Cancer*, **2008**, *7*.

[156] F. Sellrie, A. Warsinke and B. Micheel, *Analytical and Bioanalytical Chemistry*, **2006**, *386*, 206.

[157] C. Vicente-Sanchez, J. Edigo, P. D. Sanchez-Gonzalez, F. Perez-Barriocanal, J. M. Lopez-Novoa and A. I. Morales, *Food and Chemical Toxicology*, **2008**, *46*, 2279.

[158] M. Casadei, T. Persichini, F. Polticelli, G. Musci and M. Colasanti, *Experimental Gerontology*, **2008**, *43*, 415.

[159] S. Krizkova, V. Adam, T. Eckschlager and R. Kizek, *Electrophoresis*, **2009**, *30*, 3726.

[160] J. Lu, T. Y. Jin, G. Nordberg and M. Nordberg, *Cell Stress & Chaperones*, **2001**, *6*, 97.

[161] L. Quiros, B. Pina, M. Sole, J. Blasco, M. Angel Lopez, M. C. Riva, D. Barcelo and D. Raldua, *Chemosphere*, **2007**, *67*, 1144.

[162] S. Fonfara, A. Kakuschke, T. Rosenberger, U. Siebert and A. Prange, *Marine Biology*, **2008**, *155*, 337.

[163] D. Egli, J. Domenach, A. Selvaraj, K. Balamurugan, H. Q. Hua, M. Capdevila, O. Georgiev, W. Schaffner and S. Atrian, *Genes to Cells*, **2006**, *11*, 647.

[164] H. Shen, H. Qin and J. Guo, *Nutrition Research*, **2008**, *28*, 406.

[165] S. Swierzcek, R. A. Abuknesha, I. Chivers, I. Baranovska, P. Cunningham and R. G. Price, *Biomarkers*, **2004**, *9*, 331.

[166] X. Y. Ren, Y. Zhou, H. P. Zhang, W. H. Feng and B. H. Jiao, *Reproductive Toxicology*, **2003**, *17*, 219.

[167] P. C. Borges, Jr., R. I. M. A. Ribeiro, S. V. Cardoso, A. L. C. Berbet, A. Rocha, F. S. Espindola and A. M. Loyola, *Applied Immunohistochemistry & Molecular Morphology*, **2007**, *15*, 165.

[168] L. Wicherek, M. Dutsch-Wicherek, K. Galazka, T. Banas, T. Popiela, A. Lazar and B. Kleinrok-Podsiadlo, *Reproductive Biology and Endocrinology*, **2006**, *4*.

[169] T. J. Popiela, L. Rudnicka-Sosin, M. Dutsch-Wicherek, M. Klimek, P. Basta, K. Galazka and L. Wicherek, *Neuroendocrinology Letters*, **2006**, *27*, 786.

[170] F. Otsuka, M. Komatsu-Okugaito, S. Koizumi and M. Ohsawa, *Industrial Health*, **2006**, *44*, 674.

[171] T. W. M. Fan, A. N. Lane and R. M. Higashi, *Phytochemical Analysis*, **2004**, *15*, 175.

[172] T. Kawata, S. Nakamura, A. Nakayama, H. Fukuda, M. Ebara, T. Nagamine, T. Minami and H. Sakurai, *Biological & Pharmaceutical Bulletin*, **2006**, *29*, 403.

[173] S. Krizkova, V. Adam and R. Kizek, *Electrophoresis*, **2009**, *30*, 4029.

[174] N. Miura and S. Koizumi, *Yakugaku Zasshi-Journal of the Pharmaceutical Society of Japan*, **2007**, *127*, 665.

[175] J. Petrlova, S. Krizkova, O. Zitka, J. Hubalek, R. Prusa, V. Adam, J. Wang, M. Beklova, B. Sures and R. Kizek, *Sensors and Actuators B-Chemical*, **2007**, *127*, 112.

[176] D. Huska, S. Krizkova, M. Beklova, L. Havel, J. Zehnalek, V. Diopan, V. Adam, L. Zeman, P. Babula and R. Kizek, *Sensors*, **2008**, *8*, 1039.

[177] R. Kizek, L. Trnkova and E. Palecek, *Analytical Chemistry*, **2001**, *73*, 4801.

[178] L. Trnkova, S. Krizkova, V. Adam, J. Hubalek and R. Kizek, *Biosensors & Bioelectronics*, **2011**, *26*, 2201.

[179] B. Andon, J. Barbosa and V. Sanz-Nebot, *Electrophoresis*, **2006**, *27*, 3661.

[180]   R. Zhao, J. G. Ji, H. S. Yuan, H. S. Guan and B. G. Ru, *Chemical Journal of Chinese Universities-Chinese*, **2002**, *23*, 1086.

[181]   C. Y. Chen, J. H. Jia, M. X. Zhang, Y. S. Meng, D. X. Kong, X. L. Pan and X. P. Yu, *Chinese Journal of Physiology*, **2005**, *48*, 230.

[182]   Y. Zhang, L. Li, P. Yang and H. Lu, *Analytical Methods*, **2012**, *4*, 2622.

[183]   R. Wang, D. A. Sens, A. Albrecht, S. Garrett, S. Somji, M. A. Sens and X. Lu, *Analytical Chemistry*, **2007**, *79*, 4433.

[184]   O. Zitka, J. Kukacka, S. Krizkova, D. Huska, V. Adam, M. Masarik, R. Prusa and R. Kizek, *Current Medicinal Chemistry*, **2010**, *17*, 3751.

[185]   Y.-C. Lo, W.-C. Su, T.-P. Ko, N.-C. Wang and A. H. J. Wang, *Journal of Biomolecular Structure & Dynamics*, **2011**, *29*, 267.

[186]   R. Y. Wang, D. A. Sens, A. Albrecht, S. Garrett, S. Somji, M. A. Sens and X. N. Lu, *Analytical Chemistry*, **2007**, *79*, 4433.

[187]   G. X. Zhang, W. B. Hu, Z. F. Du, S. Lv, W. Zheng, Q. Luo, X. C. Li, K. Wu, Y. M. Han and F. Y. Wang, *International Journal of Mass Spectrometry*, **2011**, *307*, 79.

[188]   I. P. Smirnov, X. Zhu, T. Taylor, Y. Huang, P. Ross, I. A. Papayanopoulos, S. A. Martin and D. J. Pappin, *Analytical Chemistry*, **2004**, *76*, 2958.

[189]   X. Zhu and I. A. Papayannopoulos, *Journal of biomolecular techniques : JBT*, **2003**, *14*, 298.

[190]   E. Szajli, T. Feher and K. F. Medzihradszky, *Molecular & Cellular Proteomics*, **2008**, *7*, 2410.

[191]   O. A. Mirgorodskaya, Y. P. Kozmin, M. I. Titov, R. Korner, C. P. Sonksen and P. Roepstorff, *Rapid Communications in Mass Spectrometry*, **2000**, *14*, 1226.

[192]   K. M. Park, Y. J. Bae, S. H. Ahn and M. S. Kim, *Analytical Chemistry*, **2012**, *84*, 10332.

[193]   S. Skalickova, O. Zitka, L. Nejdl, S. Krizkova, J. Sochor, L. Janu, M. Ryvolova, D. Hynek, J. Zidkova, V. Zidek, V. Adam and R. Kizek, *Chromatographia*, **2013**, *76*, 345.

[194]   C. Wong, *Biotechniques*, **2000**, *29*, 544.

[195]   M. Ryvolova, D. Hynek, H. Skutkova, V. Adam, I. Provaznik and R. Kizek, *Electrophoresis*, **2012**, *33*, 270.